UNIVERSITÉ DU QUÉBEC À MONTRÉAL

PALYNOLOGIE DE LA TERRE DE BAFFIN ET DU GROENLAND : APPROCHES MÉTHODOLOGIQUES ET RECONSTITUTIONS CLIMATIQUES DU DERNIER INTERGLACIAIRE ET DE L'HOLOCÈNE

THÈSE
PRÉSENTÉE
COMME EXIGENCE PARTIELLE
DU DOCTORAT EN SCIENCES DE L'ENVIRONNEMENT

PAR
BIANCA FRÉCHETTE

AVRIL 2007

REMERCIEMENTS

Je remercie sincèrement mes directeurs de recherche, Madame Anne de Vernal, professeur au département des Sciences de la Terre et de l'Atmosphère et membre du GEOTOP de l'université du Québec à Montréal et Monsieur Gifford Miller, professeur au Department of Geological Sciences et membre de l'INSTAAR de l'University of Colorado. Je remercie Anne de Vernal pour avoir bien voulu diriger mes recherches et pour avoir respecté mon rythme. Je la remercie tout particulièrement pour m'avoir encouragée à me dépasser et à avoir une vision davantage globale de mes résultats. I thank Gifford Miller for his confidence on my pollen work on Baffin Island and Greenland lacustrine sediment cores since more than ten years and to have let me use these samples to undertake this research project. I also thank him for his encouragements throughout all these years.

J'adresse également de sincères remerciements à Monsieur Pierre Richard, de l'Université de Montréal et à Monsieur Alexander Wolfe de l'University of Alberta. Ces deux collègues de recherche sont responsables de mon aventure en palynologie arctique. Le premier m'y a initiée il y a une quinzaine d'années et m'a transmis son souci du détail. Le second, lors d'un séjour post-doctoral au laboratoire de Pierre Richard, m'a mis en contact avec les sédiments de la Terre de Baffin. Alexander Wolfe m'a surtout grandement encouragée à entreprendre ce doctorat et s'est toujours montré très enthousiaste pour tous mes résultats.

Du GEOTOP de l'UQÀM, je remercie Maryse Henry, pour son aide lors de mes premières reconstitutions climatiques et pour sa très grande disponibilité, les étudiants du groupe de recherche de Madame Anne de Vernal et de Monsieur Claude Hillaire-Marcel pour leur soutien et Taoufik Radi, Chantal Gosselin et Josée Savard pour avoir résolus tous mes problèmes informatiques.

Du Laboratoire Jacques-Rousseau de l'université de Montréal, je remercie Nicole Morasse pour m'avoir aidée lors de l'analyse pollinique des sédiments et Alayn Larouche pour avoir pris le temps de répondre à mes nombreuses questions à propos du logiciel TILIA.

Je remercie Monsieur Bent Fredskild du Botanical Museum de l'University of Copenhagen et Monsieur Michael W. Kerwin du Department of Geography de l'University of Denver pour m'avoir transmis leurs données polliniques modernes du Groenland et de la Terre de Baffin.

Je remercie toutes les interprètes qui ont travaillé avec moi. Plus particulièrement Monique Rocheleau, Lyne Larivière, Micheline Bernard et Anne Simard. Je remercie Rachel Jones, qui a corrigé ma première rédaction anglaise et qui a bien voulu prendre le temps de m'expliquer mes nombreuses erreurs. Je remercie enfin toutes les personnes qui ont partagé le bureau avec moi tout au long de ces années pour leur encouragement et tous les petits services téléphoniques qu'ils m'ont rendus.

À titre plus personnel, je remercie ma mère Yolande Lieutenant, mon père Yvon, ma sœur Virginie et son copain Kevin Lapalme et ma colocataire de plusieurs années, Marie Josée Bouffard pour leur soutien et leur encouragement.

J'ai bénéficié pour ce travail de recherche d'un soutien financier de la part du Fonds québécois de la recherche sur la nature et les technologies (FQRNT), du GEOTOP, de l'UQAM et des fonds de recherche de ma directrice Madame Anne de Vernal. Merci beaucoup Anne !

Les paroles qui suivent ne sont pas de moi. Je les ai notées il y a quelques années. Mais malheureusement, je n'ai pas pris en note leur auteur. Elles m'avaient touchée par leur simplicité. Mais surtout, elles traduisent très bien la façon dont je vois les sciences naturelles en général et la recherche en particulier.

On commence à mieux voir ce que la nature nous cache. On parvient à comprendre ce qui se passe. C'est la vraie découverte, c'est de là que viennent notre inspiration et nos questions. Car les découvertes, en définitive, sont là. Elles existent, devant nous. C'est qu'on ne les voit pas tout de suite.

AVANT-PROPOS

Les chapitres de la thèse ont été rédigés pour publication dans des revues scientifiques. La mise en forme des chapitres est adaptée à celle des revues. On trouvera le style un peu différent et des répétitions de certaines références bibliographiques d'un chapitre à un autre. La numérotation des figures et des tableaux n'a pas été modifiée. Il y a donc répétition des numéros des figures et des tableaux. Une liste des figures et des tableaux, par chapitre, a été faite afin de permettre au lecteur de s'y retrouver. Les trois chapitres ont été écrits en collaboration avec mes directeurs de thèse et autres collègues de recherche. J'ai bénéficié des nombreuses discussions avec chacun d'eux. Je porte néanmoins la responsabilité du développement de la méthodologie et de la première rédaction des articles. Je suis également responsable de l'analyse pollinique des échantillons fossiles et de leur interprétation paléoenvironnementale (végétation et climat).

Le chapitre I présente la base de données et deux exemples de reconstitutions paléoclimatiques de sédiments holocènes de la côte est de la Terre de Baffin. Ce chapitre a été écrit avec la collaboration de Anne de Vernal, Joël Guiot, Alexander P. Wolfe, Gifford H. Miller, Bent Fredskild, Micheal W. Kerwin, Pierre J.H. Richard et Konrad Gajewski et soumis le 4 avril 2006 à la revue scientifique *Quaternary Science Reviews*. Il a été accepté sous réserve de modifications. Les données polliniques modernes utilisées proviennent du Laboratory for Paleoclimatology and Climatology (K. Gajewski), du Laboratoire Jacques-Rousseau (P.J.H. Richard) et de contributions personnelles (M. Kerwin et B. Fredskild). Je suis responsable de la compilation des données polliniques et climatiques modernes, des traitements statistiques qui ont permis de mieux cerner la relation pollen – climat et du développement de fonctions de transfert nécessaires aux reconstitutions paléoclimatiques.

Le chapitre II présente un exemple d'application des fonctions de transfert aux sédiments du dernier interglaciaire de la péninsule de Cumberland de la Terre de Baffin. Ce chapitre a été écrit avec Alexander P. Wolfe, Gifford H. Miller, Pierre J.H. Richard et Anne de Vernal. Le texte de chapitre est publié dans la revue scientifique *Palaeogeography, Palaeoclimatology, Palaeoecology* 236 (2006), 91-106. G.H. Miller et A.P. Wolfe ont procédé à l'échantillonnage et ont établi le cadre stratigraphique et chronologique. Ma contribution concerne l'analyse pollinique, les traitements statistiques et l'interprétation des résultats. Les reconstitutions de la température estivale du dernier interglaciaire présentées dans cet article ont par la suite été utilisées dans le cadre d'une synthèse circum-arctique (CAPE Last Interglacial Project Members, *Quaternary Science Reviews* 25 (2006), 1383-1400), puis comparées aux données reconstituées par simulation numérique (Community Climate System Model [CCSM]) (Otto-Bliesner, B.L., Marshall, S.J., Overpeck, J.T., Miller, G.H., Hu, A. et CAPE Last Interglacial Project Members, *Science* 311 (2006), 1751-1753).

Le chapitre III présente une comparaison entre les changements climatiques des dernières 7000 années sur la Terre de Baffin et au Groenland, et les conditions des masses d'eau de surface de la mer du Labrador et de l'Atlantique central pour la même période. Nos collègues de l'INSTAAR (University of Colorado) sont responsables de l'échantillonnage des sédiments de la Terre de Baffin et du Groenland et des datations au radiocarbone des sédiments lacustres. Je suis responsable des modèles chronologiques, de l'analyse pollinique et statistique et de l'interprétation des résultats. A. de Vernal a fourni les résultats de l'analyse des dinokystes et des reconstitutions paléocéanographiques. Ce chapitre est en préparation et nous envisageons de la soumettre cet automne à la revue scientifique *Science*.

LISTE DE FIGURES

CHAPITRE III

LISTE DES TABLEAUX

CHAPITRE II

CHAPITRE III

RÉSUMÉ GÉNÉRAL

La première partie de ce travail présente une base de données polliniques et climatiques actuelles du Canada (>50°N) et du Groenland. Cette base de données comprend 400 échantillons de sédiments lacustres de surface et 34 taxons polliniques (13 taxons ligneux et 21 taxons herbacés). Des ordinations multidimensionnelles, notamment une analyse factorielle des correspondances (CA) et une analyse canonique des correspondances (CCA) à partir des données polliniques et climatiques, ont permis de définir les relations entre les assemblages polliniques et le climat. Les ordinations ont mis en évidence le lien étroit existant entre les assemblages polliniques et la température de juillet (r = -0,86) et ont révélé l'ambiguïté de la relation entre les assemblages polliniques et les températures de janvier et annuelle et la précipitation annuelle. Deux techniques ont été développées pour reconstituer les paléoclimats : la méthode des meilleurs analogues modernes (BMA) et une régression issue d'une analyse factorielle des correspondances (CA). Les deux techniques de reconstitutions ont été appliquées aux assemblages polliniques du dernier interglaciaire et de l'Holocène de la Terre de Baffin et du Groenland. Des tests de validation ont indiqué une erreur d'estimation (RMSE) de la température de juillet de ±1,02°C avec la technique BMA et de ±1,98°C avec la régression découlant de CA. Sur la Terre de Baffin et au Groenland la variabilité interannuelle de la température de juillet est actuellement de ±1,7-1,8°C. Les erreurs d'estimation de la température de juillet sont acceptables et les valeurs reconstruites présentées dans ce travail sont réalistes. Cependant, les techniques développées n'autorisent pas la reconstitution quantitative de la température de janvier et de la précipitation annuelle sur la Terre de Baffin et au Groenland. Néanmoins, il est possible d'estimer semi-quantitativement leur variation à l'aide de l'analyse factorielle de correspondances (CA).

La seconde partie présente une reconstitution de la végétation et du climat de l'Holocène et du dernier interglaciaire sur la péninsule de Cumberland de la Terre de Baffin. Les séquences sédimentaires étudiées proviennent de trois lacs. L'analyse pollinique des ces séquences a d'abord montré que les sédiments interglaciaires affichent de très fortes concentrations polliniques et une représentation élevée du pollen d'arbustes (*Betula* et *Alnus*) par rapport aux sédiments holocènes. Les assemblages polliniques du dernier interglaciaire sont comparables aux spectres actuels du sud-ouest du Groenland. Les résultats révèlent que lors du dernier interglaciaire la côte est de la Terre de Baffin abritait une végétation dense de toundra arbustive alors qu'aujourd'hui une toundra herbacée clairsemée occupe les sols de la région. L'application des techniques de reconstitutions paléoclimatiques a ensuite montré que la température estivale du dernier interglaciaire était de 4 à 5°C plus

élevée qu'actuellement sur la côte est de la Terre de Baffin et sans doute également plus chaude que celle de l'Holocène. La température de janvier était également plus chaude que l'actuelle et les précipitations annuelles plus abondantes. Le climat du dernier interglaciaire était davantage océanique que celui de l'Holocène.

Finalement, la dernière partie de ce travail présente une reconstitution du climat de part et d'autre de la baie de Baffin. À partir de relevés polliniques de séquences sédimentaires lacustres, nous montrons qu'au cours des dernières 7000 années, le refroidissement estival fut davantage prononcé sur la côte sud-ouest du Groenland (3,0-3,5°C) que sur la côte est de la Terre de Baffin (0,5-1,0°C). Ce régionalisme dans l'évolution du climat de cette période est cohérent avec les relevés marins. En effet, la température estivale des masses d'eau de surface a très peu changé dans le secteur ouest de la mer du Labrador alors qu'au large, dans la région de la Ride de Reykjanes, un refroidissement de plus de 6°C a été enregistré. Ce contraste climatique d'ouest en est ainsi que la diminution de son intensité de l'Holocène moyen à l'Holocène supérieur suggèrent une diminution de l'influence du flux d'eau chaude nord Atlantique sur les conditions hydro-climatiques du sud du Groenland, alors que la Terre de Baffin et les marges est canadiennes seraient vraisemblablement demeurées sous l'influence des courants froids de Baffin et du Labrador. Les résultats soulignent l'étroit lien entre la circulation océanique de surface et le climat atmosphérique des marges est canadiennes et du Groenland. Par ailleurs, l'abondance du pollen de *Betula* dans les sédiments de la Terre de Baffin et du Groenland depuis ca. 5000 ans BP suggère une augmentation de la température de janvier et des précipitations annuelles durant l'Holocène supérieur. Ce changement d'humidité suggère un changement de régime climatique, plus particulièrement une influence grandissante de l'océan sur le climat côtier de la Terre de Baffin et du Groenland.

Mots-clés : palynologie, reconstitution climatique, Holocène, dernier interglaciaire, région arctique.

TABLE DES MATIÈRES

Page

INTRODUCTION GÉNÉRALE

Dans une perspective d'augmentation continue du CO_2 atmosphérique et autres gaz à effet de serre les changements climatiques affecteront en particulier les milieux arctiques (Overpeck et al., 1997 ; Holland et Bitz, 2003 ; Arctic Climate Impact Assessment, 2005). Même si certains doutes subsistent (Serreze et Francis, 2006) et que les simulations climatiques nécessitent d'être corroborées (Foley, 2005), l'accélération du réchauffement dans la région arctique apparaît de plus en plus vraisemblable (Chapin et al., 2005 ; CAPE Last Interglacial Project Members, 2006) et ce, notamment en raison de l'importance de l'albedo du territoire sur le climat polaire (Chapin et al., 2005 ; Foley, 2005 ; Serreze et Francis, 2006). Effectivement, une diminution de l'étendue de la glace de mer dans l'océan Arctique (Serreze et Francis, 2006), une réduction du couvert du neige, un remplacement des plantes herbacées par des arbustes ainsi qu'une migration de la limite septentrionale de la forêt boréale (Chapin et al., 2005) pourraient amplifier le réchauffement de la région arctique en diminuant l'albedo. Il apparaît évident que les processus d'action et de rétroaction impliqués dans un changement climatique sont complexes. Le système climatique est un énorme réservoir dans lequel de la matière, de l'énergie et de la quantité de mouvement sont emmagasinées, continuellement transformées et inégalement redistribuées (Berger, 1983).

Nous croyons que la végétation à la frontière des zones bioclimatiques est susceptible de réagir plus fortement à un changement climatique, car il s'agit de régions où un faible changement climatique engendre parfois un changement important dans la végétation (Barbour et al., 1998). Il nous semble essentiel de comprendre la végétation et le climat du passé, et les mécanismes qui régissent leur évolution, afin d'envisager le plus objectivement possible les conséquences de changements climatiques sur la végétation parce que l'équilibre entre la végétation et le climat est complexe (Prentice, 1986 ; Ritchie, 1986 ; Webb, 1986). Outre le climat, plusieurs

agents peuvent être la cause d'un changement de végétation : par exemple la succession, la migration, l'évolution, la compétition entre espèces et les conditions édaphiques locales (Webb, 1986). Il est très difficile d'identifier un seul responsable. Par ailleurs, des seuils écologiques peuvent être franchis lors de changements climatiques et engendrer une modification de la végétation tout à fait inattendue et même irréversible (e.g. Maslin, 2004).

La réponse de la végétation à un changement climatique peut-être étudiée rétrospectivement en analysant les assemblages polliniques fossiles de séquences sédimentaires lacustres. Malgré de récentes synthèses paléoenvironnementales (e.g. CAPE Project Members, 2001 ; Bigelow et al., 2003 ; Kaufman et al., 2004), le caractère exact des changements de végétation en relation aux variations naturelles du climat demeurr mal connu dans l'Arctique en général et dans l'archipel de l'Arctique canadien en particulier parce qu'il a été peu étudié. En effet, dans la littérature concernant l'archipel de l'Arctique canadien, il existe peu d'enregistrements sporopolliniques présentant une résolution chronologique suffisante permettant de bien cerner la dynamique de l'environnement à long et moyen terme. Les principaux travaux abordant ce sujet sont ceux de Boulton et al. (1976), Davis, (1980), Mode (1980), Hyvärinen (1985), Short et al. (1985), Gajewski (1995), Gajewski et al. (1995), Gajewski et al. (2000), Wolfe et al. (2000) et Gajewski et Frappier (2001).

Objectifs de la thèse

En se basant sur le potentiel paléoenvironnemental (végétation et climat) des grains de pollen et des spores contenus dans les sédiments lacustres arctiques (Gajewski et MacDonald, 2004), la présente thèse vise dans un premier temps à bien décrire la relation entre les assemblages polliniques modernes et les conditions climatiques actuelles. La reconnaissance d'un lien entre les assemblages polliniques et le climat est essentielle aux reconstitutions climatiques, car sans relation précise nous ne

pourrions reconstituer les anciens climats. De plus, l'étude approfondie des données modernes facilitera l'interprétation des assemblages polliniques fossiles en termes de paléovégétations ainsi que le développement des fonctions de transfert destinées à transcrire les assemblages fossiles en termes de paléoclimats (température et précipitation). Les fonctions de transfert seront ensuite appliquées aux assemblages polliniques holocènes et à ceux du dernier interglaciaire, de la Terre de Baffin et du Groenland.

Le dernier interglaciaire est une période à climat plus chaud que l'actuel et constitue de ce fait une période propice à l'étude de changements climatiques (e.g. CAPE Last Interglacial Project Members, 2006). La présente thèse vise dans un second temps à reconstituer le climat du dernier interglaciaire sur la Terre de Baffin. La comparaison du réchauffement interglaciaire sur la Terre de Baffin avec celui d'autres sites des hautes latitudes de l'Hémisphère nord permettra de situer la Terre de Baffin dans une perspective circum-arctique. Par la suite, la reconstitution de la végétation interglaciaire et sa comparaison avec celle de l'Holocène permettra de préciser l'étendue de la toundra herbacée et arbustive sur la Terre de Baffin lors du dernier interglaciaire.

Récemment, une synthèse paléocéanographique, basée sur les assemblages de kystes de dinoflagellés, a montré l'existence d'un régionalisme dans l'évolution des conditions hydrographiques des masses d'eau de surface du nord-ouest de l'Atlantique nord, au cours de l'Holocène (de Vernal et Hillaire-Marcel, 2006). Ce régionalisme est marqué par une évolution climatique contrastée entre les marges est canadiennes et les environnements plus océaniques de l'Atlantique central. La présente thèse vise dans un dernier temps à vérifier l'existence éventuelle d'un tel régionalisme dans l'évolution du climat terrestre au cours de l'Holocène. À partir de relevés polliniques de la côte est de la Terre de Baffin et de la côte sud, sud-ouest du Groenland, nous vérifierons si le climat terrestre a évolué de façon uniforme ou pas à

travers la baie de Baffin et le détroit de Davis. Cette comparaison permettra de définir les liens entre la variabilié du climat atmosphérique et océanique aux latitudes subpolaires de l'Atlantique nord. Finalement, il est bon de souligner que comparativement à plusieurs études paléoclimatiques ayant précisés de tels liens (e.g. Chapman et Shakleton, 2000 ; Jiang et al., 2002 ; Moreno et al., 2005), nous utiliserons pour notre comparaison des données climatiques indirectes de même nature, i.e. des 'proxies' de nature biologique et livrant des microfossiles à membrane organique, soit des palynomorphes tels les kystes de dinoflagellés et les grains de pollens.

Contexte paléoclimatique des périodes à l'étude

La dernière période interglaciaire *sensu lato* (ca. 75 000-130 000 ans BP ; stade isotopique marin 5 ; MIS 5) est considérée comme une période à climat relativement chaud. En fait, il s'agit du seul moment au cours des dernières 250 000 années où les températures moyennes planétaires étaient de 0 à 2°C plus chaudes que les actuelles (e.g. CLIMAP Project Members, 1984). C'est dans la région circum-arctique que le réchauffement fut le plus important. En effet, lors de l'époque la plus chaude du dernier interglaciaire, i.e. le dernier interglaciaire *sensu stricto* (ca. 115 000-130 000 ans BP, i.e. MIS 5e), les températures estivales y étaient sans doute de 4 à 5°C plus chaudes qu'à l'actuel (e.g. NGRIP Members, 2004 ; CAPE Last Interglacial Project Members, 2006). Les températures comparativement plus élevées qu'ailleurs dans la région circum-arctique s'expliquent entre autres par une forte insolation estivale lors du dernier interglaciaire et sans doute par d'autres mécanismes de rétroaction positive sur le climat, principalement ceux affectant l'albedo, soit une moindre étendue de glace de mer dans l'océan Arctique, une réduction du volume de la calotte groenlandaise (Otto-Bliesner et al., 2006 ; Overpeck et al., 2006) et des autres glaciers continentaux de l'Hémisphère Nord, et une limite plus septentrionale de la

forêt boréale (CAPE Last Interglacial Project Members, 2006), d'après le pollen et les macrorestes végétaux.

L'Holocène (11 500 ans BP à aujourd'hui) représente l'interglaciaire actuel. Son évolution climatique générale se résume comme suit : un réchauffement lors de l'Holocène inférieur, suivi d'une période à climat relativement chaud lors de l'Holocène moyen (ca. 9000 à 5000 ans BP), et finalement un refroidissement à l'Holocène supérieur. Le concept de son uniformité climatique à travers le temps et l'espace, jadis accepté, est dorénavant remis en question. En effet, il ressort de récentes études paléoclimatiques que le climat holocène évolua différemment au sein de la région circum-arctique. Un régionalisme du climat holocène est donc observé et il s'illustre notamment par l'asynchronisme du maximum thermique et l'inégalité de l'ampleur du refroidissement (e.g. Andersen et al., 2004 ; Fréchette, 2004 ; Kaufman et al., 2004 ; de Vernal et Hillaire-Marcel, 2006 ; Kaplan et Wolfe, 2006).

La forte insolation estivale du début de l'Holocène est la principale cause du réchauffement du climat. À l'Holocène inférieur, l'énergie solaire de juin et juillet était de 40-50 Watts/m^2 plus forte que l'actuelle et celle de septembre et d'octobre, de 40-50 Watts/m^2 plus faible au 60°N de latitude (Berger et Loutre, 1991). Depuis 11 500 ans BP il y a un affaiblissement de l'insolation estivale concomittant à une intensification de l'insolation hivernale. Le déficit d'insolation qui caractérisait l'hiver à 11 500 ans BP, se déplace peu à peu sur l'été avec les années. L'affaiblissement de l'insolation estivale depuis ca. 7000 ans BP est considéré comme étant un important mécanisme du refroidissement holocène. Le régionalisme du climat holocène de la région circum-arctique s'explique par des mécanismes de rétroaction provenant de la cryosphère, de l'hydrosphère et de la biosphère (e.g. Kaufman et al., 2004). Les mécanismes de rétroaction par les courants océaniques de surface, comme par exemple un changement de leur intensité, sont tout particulièrement importants pour la compréhension de la dynamique du système

climatique holocène des latitudes subpolaires de l'Atlantique nord et des terres adjacentes (e.g. de Vernal et Hillaire-Marcel, 2006).

Contexte bioclimatique des sites à l'étude

Les sites étudiés proviennent de la péninsule de Cumberland, sur la Terre de Baffin (lacs, Amarok, Fog, Brother-of-Fog et Akvaqiak), et de la région du fjord de Kobberminebugt, au sud du Groenland (lac Qipisarqo) (Figure 1). Ils sont tous en région côtière. Le lac Amarok est légèrement au nord du fjord de Pangnirtung, au sud-ouest de la péninsule de Cumberland. Il est situé dans la zone bioclimatique du moyen arctique (Young, 1971). De par son altitude (848 m asl), sa végétation locale est très clairsemée, et principalement composée de *Cassiope tetragona*, de *Salix* prostrés, et de lichens. *Betula* est absent de la flore locale. Les lacs Fog et Brother-of-Fog, distants d'une quinzaine de kilomètres, sont situés sur la côte est de la péninsule de Cumberland. La végétation à proximité de ces deux sites est une toundra herbacée, typique de la zone bioclimatique du moyen arctique. Le couvert végétal est clairsemé et les quelques plantes ligneuses présentes y sont prostrées. Les éricales sont abondantes, spécialement *Cassiope tetragona* et *Empetrum nigrum*. *Betula* est aussi absent de la végétation locale. Le lac Akvaqiak est situé à la tête du fjord de Kangert, 60 km au sud sud-ouest des lacs Fog et Brother-of-Fog. La végétation locale est une toundra arbustive. Des populations isolées et luxuriantes de bouleaux arbustifs (*Betula glandulosa*) tapissent le fond de la vallée. La végétation des environs du lac Akvaqiak est caractéristique de la zone bioclimatique du bas arctique. *Alnus* est absent de la flore de la Terre de Baffin. Le lac Qipisarqo, au Groenland, est aussi localisé dans la zone bioclimatique du bas arctique. La végétation locale est une toundra arbustive modérément luxuriante dominée par le bouleau arbustif (*Betula glandulosa*) et les éricales (*Cassiope*, *Empetrum*, *Vaccinium*). Bien que les aulnes (*Alnus crispa*) soient absents localement, ils sont présents à la tête des fjords de la région (Kaplan et al., 2002).

Le climat de la région à l'étude n'est pas uniforme. Sur une base annuelle, le climat de la côte est de la Terre de Baffin est substantiellement différent de celui de la côte ouest du Groenland pour une même latitude (Tableau 1). En effet, entre les latitudes 65 et 70°N, la température moyenne annuelle de l'est de la Terre de Baffin est de -11,6°C (écart annuel de 29,4°C) (Environnement Canada, 2004) alors que celle de l'ouest du Groenland est de -3,5°C (écart annuel de 18,5°C) (Cappelen et al., 2001). Au sud du 65°N, au Groenland, la température moyenne annuelle est de -0,9°C (écart annuel de 12,9°C) (Cappelen et al., 2001). Cet important contraste climatique observé de part et d'autre de la baie de Baffin et du détroit de Davis s'explique principalement par la circulation océanique de surface. Un écoulement d'eau de surface froide et de faible salinité, en provenance de l'océan Arctique (le courant de Baffin [BLC]), contrôle le climat de la côte est de la Terre de Baffin alors que l'ouest du Groenland est plutôt influencé par les eaux relativement chaudes et salées du courant ouest groenlandais [WGC], lequel est le résultat du mélange des eaux froides du courant est groenlandais [EGC] et des eaux chaudes de la dérive Nord Atlantique [NAD] (Figure 1).

Les précipitations moyennes annuelles enregistrées à travers la région de la baie de Baffin et du détroit de Davis sont fortement liées au couvert de glace de mer. Au sud du 64°N de latitude le long de la côte ouest groenlandaise, l'eau est parfois libre de glace tout au long de l'année alors que cette situation n'est observée qu'au sud du 49°N le long des marges est canadiennes (Williams et Bradley, 1985). Certaines années, il arrive que les eaux bordant la péninsule de Cumberland soient toujours englacées à la fin de l'été. La précipitation moyenne annuelle augmente significativement au sud sud-ouest du Groenland (au sud du 62°N) (>800 mm), là où les eaux ne sont presque jamais englacées (Tableau 1). Sur la côte est de la Terre de Baffin, les plus importantes précipitations annuelles sont observées à Cape Dyer A (663 mm), un endroit où il y a localement de grands plans d'eau libres de glace durant

plusieurs mois (Williams et Bradley, 1985). Ailleurs, la précipitation moyenne annuelle n'atteint pas 400 mm.

Organisation de la thèse

La reconnaissance du potentiel paléoenvironnemental (paléovégétation et paléoclimat) des assemblages polliniques des sédiments lacustres de la région Arctique, demande une étude approfondie de la relation entre les assemblages polliniques et le climat. L'étude de la relation pollen – climat est tout particulièrement essentielle aux reconstitutions climatiques, car sans lien précis nous ne pourrions reconstituer les anciens climats. C'est dans l'objectif de mieux cerner la relation pollen – climat que nous avons compilé une base de données polliniques modernes de 400 sites provenant du Canada (>50°N de latitude) et du Groenland.

Le chapitre I présente la base données. Le texte est rédigé en anglais. Nous présentons tout d'abord les résultats de l'analyse de la relation entre les assemblages polliniques modernes et les paramètres climatiques (température de janvier, de juillet, annuelle, et précipitation annuelle). Cette étude la relation pollen - climat a été faite à l'aide d'analyses multidimensionnelles. Deux techniques de reconstitution climatique sont par la suite présentées. Il s'agit de la méthode des meilleurs analogues modernes et celle d'une régression issue d'une analyse factorielle des correspondances. Ces deux techniques sont ensuite appliquées à deux séquences de sédiments holocènes. Les deux sites servant d'exemple sont localisés sur la côte est de la péninsule de Cumberland, à proximité de la frontière entre les zones bioclimatiques du bas et du moyen arctique. Ces deux sites ont permis de tester les deux techniques de reconstitution et d'identifier les limites propres à chacune.

Le chapitre II présente la reconstitution climatique de sédiments holocènes et du dernier interglaciaire de la péninsule de Cumberland, sur la Terre de Baffin, ainsi

qu'une reconstitution des anciennes végétations de ces périodes. Le texte est rédigé en anglais. La reconstitution quantitative de la température estivale a permis de situer le réchauffement du dernier interglaciaire de la côte est de la Terre de Baffin dans une perspective subpolaire (CAPE Last Interglacial Project Members, 2006). La reconstitution de la végétation interglaciaire et sa comparaison avec celle de l'Holocène a permis de suggérer une limite de la toundra arbustive, sur la côte est de la Terre de Baffin, davantage septentrionale lors du dernier interglaciaire que lors de l'Holocène.

Le chapitre III présente une reconstitution de la température estivale sur la côte est de la Terre de Baffin et la côte sud, sud-ouest du Groenland, suivie d'une reconstitution de la température estivale des masses d'eau de surface du talus du Labrador et de l'Atlantique central. Le texte est rédigé en anglais. La comparaison des résultats a permis de montrer que le climat, depuis 7000 ans BP, évolua différemment le long des marges est canadiennes que plus au large, en Atlantique central et au Groenland. La circulation océanique peut expliquer le régionalisme du climat observé à travers le secteur nord-ouest de l'Atlantique nord, depuis 7000 ans BP (de Vernal et Hillaire-Marcel, 2006). Le chapitre III comporte deux parties. La première partie traite des résultats principaux de l'étude alors que la seconde présente des informations supplémentaires. Ces informations supplémentaires sont nécessaires à la compréhension et à l'évaluation critique des résultats principaux.

La thèse comporte 4 annexes. L'Annexe A est présentée sur un CD et comporte les données modernes (pollen et climat) nécessaires aux reconstitutions climatiques. L'Annexe B présente les diagrammes polliniques complets des sites à l'étude et l'Annexe C, leur chronologie. Finalement l'Annexe D est une copie de l'article des membres de CAPE Last Interglacial Project publié en 2006 dans *Quaternary Science Reviews*. Le texte des annexes est rédigé en anglais.

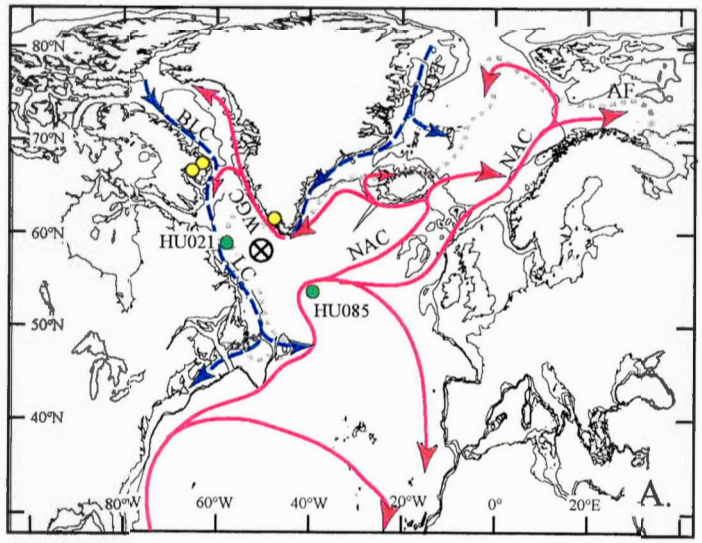

Figure 1A. Circulation océanographique de surface de l'Atlantique nord (Meinck, 2002). Les courants chauds sont illustrés en rouge et les courants froids en bleu.
NAC: dérive Nord Atlantique, LC: courant du Labrador, EGC: courant est groenlandais, WGC: courant ouest groenlandais, BLC: courant de Baffin, AF: front arctique. Les sites terrestres à l'étude sont illustrés par des cercles jaunes et les sites marins par des cercles de couleur verte. Une localisation plus précise des sites terrestres à l'étude est donnée aux figures 1B et 1C. Le cercle avec une croix représente le site de formation d'eau profonde du Labrador.
HU021: carotte HU84-030-021TWC,
HU085: carotte HU-91-045-085TWC.

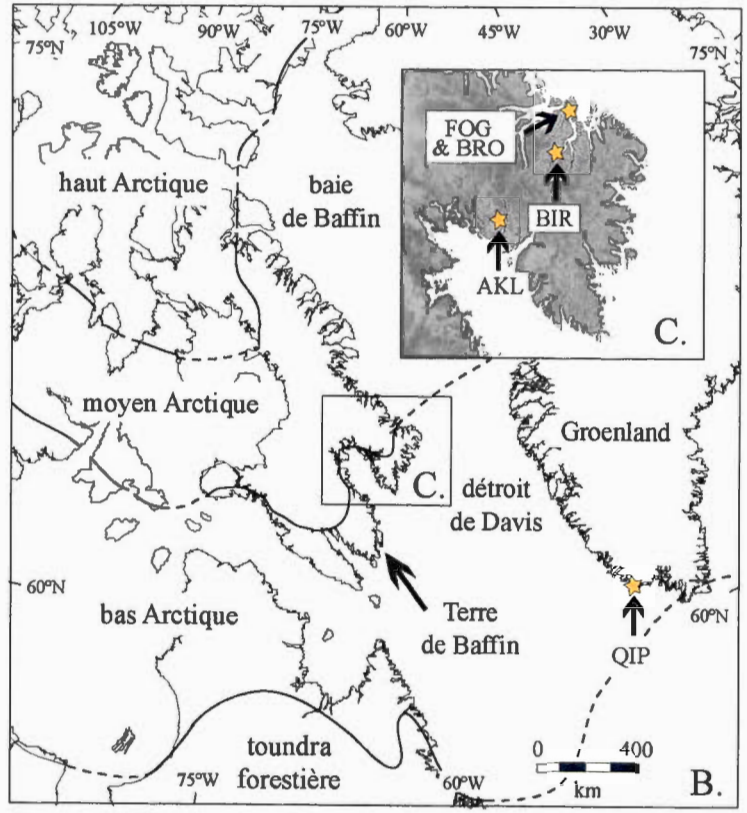

Figure 1B. Distribution des zones bioclimatiques dans la région à l'étude (Young, 1971) et localisation des sites terrestres étudiés. C. Agrandissement de la péninsule de Cumberland de la terre de Baffin.
FOG: lac Fog, BRO: lac Brother-of-Fog, BIR: lac Akvaqiak, AKL: lac Amarok, QIP: lac Qipisarqo.

Tableau 1. Données des stations climatiques de la côte est de la Terre de Baffin (Environnement Canada, 2004) et de la côte ouest du Groenland (Cappelen et al., 2001). Dans chacune des régions, les stations sont ordonnées en ordre décroissant de latitude nord. Pour les stations de la Terre de Baffin, les normales climatiques des périodes 1961-1990 et 1971-2000 sont indiquées.

Nom de la Station	Lat. Nord	Long. Ouest	Alt. m asl	T janv. °C	T juil. °C	T ann. °C	P ann. mm
Terre de Baffin							
Pond Inlet*	72° 40'	77° 58'	55	-32,4	6.0	-15,1	191
Clyde A*	70° 29'	68° 31'	27	-28,1	4,4	-12,8	233
Clyde A**	70° 29'	68° 31'	25	-26,9	4,2	-12,4	226
Cape Hooper*	68° 28'	66° 49'	390	-25,5	4,1	-12.0	282
Cape Hooper**	68° 28'	66° 48'	401	-25,1	4,2	-11,8	224
Fox Five[1]*	67° 32'	63° 47'	584	-24,8	4,4	-11,8	262
Broughton Island**	67° 32'	63° 47'	587	-24,2	4,4	-11,5	279
Cape Dyer A*	66° 34'	61° 37'	393	-24,2	5,3	-11.0	603
Cape Dyer A**	66° 35'	61° 37'	393	-23,2	5,1	-10,5	636
Groenland							
Pituffik**	76° 32'	68° 45'	77	-23,3	4,5	-11,1	127
Upernavik**	72° 47'	56° 10'	120	-17.0	5,2	-7,2	n.d.
Ilulissat**	69° 13'	51° 03'	39	-12,7	8,3	-3,9	266
Aasiaat**	68° 42'	52° 45'	43	-13,4	5,7	-4,9	304
Sisimiut**	66° 55'	53° 40'	12	-12,8	6,3	-3,9	383
Maniitsoq**	65° 24'	52° 52'	25	-7,6	7,3	-1,3	667
Nuuk**	64° 10'	51° 45'	80	-7,4	6,5	-1,4	752
Paamiut**	62° 00'	49° 40'	13	-6,6	5,6	-0,8	874
Qaqortoq**	60° 43'	46° 03'	32	-5,5	7,2	0,6	858
Prins Christian Sund**	60° 03'	43° 10'	88	-4,1	6,5	0,7	2474

[1] Anciennement Broughton Island

* Années de calcul (1971-2000)

** Années de calcul (1961-1990)

CHAPITRE I

QUANTITATIVE PALEOCLIMATE RECONSTRUCTION IN THE CANADIAN ARCTIC FROM POLLEN ASSEMBLAGES PRESERVED IN LAKE SEDIMENTS: METHODOLOGY AND APPLICATION TO HOLOCENE SEQUENCES FROM EASTERN BAFFIN ISLAND

Bianca Fréchette[a], Anne de Vernal[a], Joël Guiot[b], Alexander P. Wolfe[c], Gifford H. Miller[d], Bent Fredskild[e], Micheal W. Kerwin[f], Pierre J.H. Richard[g], Konrad Gajewski[h]

[a] GEOTOP, Université du Québec à Montréal, P.O. Box 8888, Succ. Centre-Ville, Montréal, QC H3C 3P8, Canada

[b] CNRS-CEREGE, B.P. 80, 13545 Aix en Provence, Cedex 4, France

[c] Department of Earth and Atmospheric Sciences, University of Alberta, Edmonton, AB T6G 2E3, Canada

[d] INSTAAR and Department of Geological Sciences, University of Colorado, Boulder, CO 80309-0450, USA

[e] Greenland Botanical Survey, Botanical Museum, University of Copenhagen, Gothersgade 130, DK-1123 Copenhagen, Denmark

[f] Department of Geography, University of Denver, 2050 E Iliff Ave, Denver, CO 80208, USA

[g] Département de géographie, Université de Montréal, P.O. Box 6128, Succ. Centre-Ville, Montréal, QC H3C 3J7, Canada

[h] Department of Geography, University of Ottawa, 60 University, Ottawa, ON, K1N 6N5, Canada

Accepté sous réserve de modifications par la revue scientifique

Quaternary Science Reviews

Résumé

Cette étude présente une compilation de données polliniques et climatiques actuelles de 400 sites de surface du Canada et du Groenland. Ces échantillons polliniques proviennent de sédiments lacustres. Les sites sont répartis de la forêt boréale à la toundra du haut arctique et représentent une gamme de la température allant de 3,5 à 18,2°C en juillet et de -36,8 à -4,1°C en janvier, et une précipitation moyenne annuelle s'étalant de 81 à 2470 mm. Pour les données polliniques, 34 principaux taxons ont été retenus (13 taxons ligneux, 21 taxons herbacés). Des ordinations multidimensionnelles, notamment une analyse factorielle des correspondances (CA) et une analyse canonique des correspondances (CCA) à partir des données polliniques et climatiques, montrent que la température de juillet rend compte de 62,1% de la variance des assemblages polliniques et que les températures de janvier et annuelle rendent compte de 25,9% et 11,9% de la variance, respectivement. Les CA et CCA font ainsi ressortir le lien étroit existant entre les assemblages polliniques et la température de juillet (r = -0,86). Deux techniques ont été développées pour reconstituer les paléoclimats : la méthode des meilleurs analogues modernes (BMA) et une régression découlant d'une analyse factorielle des correspondances (CA). Des tests de validation indiquent une erreur d'estimation (RMSE) de la température de juillet de ±1,02°C avec la technique BMA et de ±1,98°C avec la régression issue de CA. Finalement, ces techniques de reconstitutions paléoclimatiques sont appliquées à deux séquences de sédiments lacustres holocènes de la péninsule de Cumberland sur la Terre de Baffin dans l'Arctique canadien. Malgré quelques différences locales, les résultats sont régionalement cohérents. Ils montrent une diminution progressive de la température de juillet de 0,5-1,0°C depuis 8000-6000 ans BP. Ce refroidissement est compatible avec le déclin de l'insolation estivale holocène. Par ailleurs, les résultats indiquent une augmentation de la précipitation moyenne annuelle lors de l'Holocène supérieur. Cette augmentation des précipitations suggère un changement de régime climatique, plus particulièrement une influence grandissante de l'océan sur le climat côtier de la Terre de Baffin.

Abstract

This study presents a modern pollen and climate database including 400 sites of surface lake-sediment pollen assemblages and corresponding temperature and precipitation estimates. The study area covers from the boreal forest to the high arctic phytogeographical zones of Canada and Greenland. The database captures modern climates ranging from 3.5 to 18.2°C and from -36.8 to -4.1°C for mean July and January air temperatures, respectively, and 81 to 2470 mm for mean annual precipitation. Pollen data include the 34 most common vascular taxa of the boreal forest to Arctic zones (13 woody plant and 21 herb taxa). Multivariate ordinations using correspondence analysis (CA) and canonical correspondence analysis (CCA) with both pollen and climate data reveal that July air temperature accounts for 62.1% of the variance, whereas January and mean annual air temperatures account for an additional 25.9% and 11.9% of the variance, respectively. CA and CCA thus demonstrate an exceptionally robust relationship between pollen assemblages and July air temperature (r = -0.86). Two approaches were developed for quantitative paleoclimate reconstructions: the best modern analogue (BMA) method and correspondence analysis (CA) regression. Validation tests indicate a root mean square error (RMSE) for July air temperature of ±1.02°C with the BMA technique, and ±1.98°C for CA regression. Two examples of paleoclimatic applications are presented for Holocene lake sediments from northern Cumberland Peninsula, Baffin Island, Arctic Canada. Despite local differences, the results are regionally coherent, showing a progressive 0.5-1°C decrease of July air temperature since 8000-6000 cal. years BP, consistent with declining summer insolation. The results further document late-Holocene increase of mean annual precipitation, suggesting gradual enhancement of the oceanic influence on climate.

Keywords: modern pollen; climate; Canadian Arctic; Greenland; Holocene; paleoclimate reconstruction

1.1. Introduction

In the Arctic, areas situated at sensitive ecotonal boundaries, such as the Low and Middle Arctic bioclimatic zones, are of particular botanical relevance because small climate changes may induce relatively large vegetational changes (Barbour et al., 1998). The understanding of oceanic, cryospheric, and vegetational feedbacks within the Arctic climate system relies largely on the analysis of continental scale paleoclimate simulations (e.g., Wohlfahrt et al., 2004 and references therein). However, unlike the Boreal forest, Arctic vegetation community structure is typically characterized by elevated diversity and pronounced topoclimatic heterogeneity at local to regional scales, which mandate examinations at the finest spatial scale possible. The understanding of Arctic vegetation dynamics remains hampered by a lack of long-term information concerning long-term vegetation-climate relationships. From this point of view, pollen grains preserved in lake sediments are particularly useful for reconstructing both vegetation and climate.

Pollen-based Holocene climate history of western Canadian Arctic and Alaska (Anderson et al., 1989; Bigelow et al., 2003; Kaplan et al., 2003), Scandinavia (Seppä and Birks, 2001, 2002) and northern Eurasia (Andreev et al., 2003, 2004a,b,c, 2005) is well documented. However, few quantitative climate reconstructions from pollen records are available for the eastern Canadian Arctic (Kerwin et al., 2004; Fréchette et al., 2006). It is in this context that we compiled a modern pollen database including 400 lake sediment samples from northwestern Canada, northern Québec, the Canadian Arctic Archipelago and Greenland (Fig. 1A). The aim is to first develop a paleoclimatic inference tool for the eastern Canadian Arctic and Greenland, following detailed standardization and harmonization of pollen taxonomy, a range of exploratory and explanatory multivariate analyses, and extensive assessment of modern pollen-climate relationships. Details on the relationship between pollen and

vegetation is presented elsewhere (Kerwin et al., submitted). Second, we present two applications of this tool to Holocene lake sediments from sites near the Low-Middle Arctic ecotonal boundary on Cumberland Peninsula, eastern Baffin Island. Our focus on lake sediments, with respect to both modern and fossil pollen assemblages, avoids problems associated with differential pollen representation between lake sediments and other terrestrial repositories, such as moss polsters and soils. This approach is further guided by the the general suitability and great promise of lake sediments for the study of high-latitude environmental change (Pienitz et al,, 2004).

1.2. Methodology

1.2.1. Modern pollen database

The 400 modern pollen assemblages compiled here originate from several sources, including the Canadian Pollen Database (http://www.lpc.uottawa.ca/data/cpd/index.html), the Base de Données Polliniques et Macrofossiles du Québec (BDPMQ) (http://www.geog.umontreal.ca/palyno), and new data from two of us (M.W. Kerwin and B. Fredskild). Additional pollen data have been published previously over more than three decades (Fredskild, 1973; Ritchie, 1974; Richard, 1979, 1981; Fredskild, 1983, 1985; MacDonald and Ritchie, 1986; Ritchie et al., 1987; Gajewski, 1991; Richard et al., 1991; Sandgren and Fredskild, 1991; Fredskild, 1992; Kerwin, 2000; Gajewski, 2002; Kerwin et al., 2004, Kerwin et al., submitted). The 400 lake sites are now part of the larger (but less exclusive in terms of sample type) North America-Greenland database (n = 4634 samples) of Whitmore et al. (2005), with the exception of 11 Greenland samples that have subsequently been added in the present effort The source of all pollen assemblages is given in Appendix A.

These 400 sites have been grouped according to their geographical location: Western Canada (WC-1; $n = 47$, WC-2; $n = 73$, WC-3; $n = 38$), James Bay (JB; $n = 18$), Northern Québec (NQ; $n = 51$), Fort Chimo-Diana Bay (FCD; $n = 25$), Baffin Island (B; $n = 67$), the Canadian Arctic Archipelago (A; $n = 23$) and Greenland (G; $n = 58$). They are thus representative of twelve distinct floristic zones (Fig. 2), more broadly representing the grassland-boreal-subarctic (WC-1, WC-2, JB, NQ, FCD) and Arctic (WC-3, G, B, A) vegetation zones of North America and Greenland.

1.2.1.1. Selection of pollen taxa for inclusion in the database

The initial pollen relative frequency matrix contains 400 sites and 159 taxa (Appendix A) prior to pruning. However, 89% of this matrix comprises zero values, with the number of taxa per site ranging from 8 to 29, and the number of occurences per taxon varying from 1 to 398. Simplification and rationalization of the data matrix was deemed necessary prior to numerical analysis, and was undertaken as described below, following several lines of ecological and statistical reasoning.

The assumption that most of the pollen observed in a sample was produced by plants living in proximity to the lake underlies the use of pollen data for paleoclimatic reconstruction. However, wind-blown long-distance pollen grains produced by boreal forest trees and shrubs often occur in appreciable numbers in arctic lake sediments (Ritchie et al., 1987; Gajewski et al., 1995; Gajewski, 2002). Their proportions are a function of distance from the source vegetation and wind direction and speed during pollination season, but also of the degree of dilution by pollen produced locally and regionally by herbs and shrubs (Bourgeois et al., 2001). One appraoch is to simply omit boreal taxa from the pollen sum, but this practice remains problematic because percentages of local taxa increase commensurately when the assumed long-distance component is excluded. Moreover, any climatic information provided by long-distance pollen transport is lost, for example pertaining to southerly

atmospheric flow (Nichols et al., 1978; Calcote, 2003; Jackson and Williams, 2004; Fréchette et al., 2006). Therefore, 7 boreal tree and shrub taxa (*Abies*, *Larix*, *Picea*, *Pinus*, *Populus*, *Myrica*, *Shepherdia*) and 2 herb taxa (*Ambrosia*, Chenopodiaceae) exotic to the tundra biome in arctic Canada and Greenland were retained in the finalized modern database (see Table 1).

As pollen counts were performed in various laboratories by different analysts, problems arising from inconsistent taxonomy and nomenclature may arise (Birks, 1995). For example, the inclusion of pteridophyte spores in the modern database was also considered. However, the common designation of 'pteridophyta' at some sites in WC includes taxa of exceedingly broad ecological and climatic affinities. Without further taxonomic scrutiny this taxon is unlikely ecologically or climatically relevant, and was thus excluded from the sum. Further taxonomic concerns were raised with respect to *Picea*, *Pinus*, and *Alnus*, which were only identified at the species level at some sites in NQ, FCD, JB, A, and WC. Similarly, the differentiation of Ericales tetrads at the genus level was only occasionally reported from some sites of A, G and WC. Therefore, among the 159 pollen taxa counted and reported by the different authors, we reclassified several taxa to the highest consistent taxon, thereby ensuring a fully standardized and unambiguous taxonomy. A new total of 63 taxa remained after this harmonization (Appendix A). Thereafter, we excluded all taxa that did not occur at least twice with a minimum relative frequency of 1% in the 400 samples. This additional filtering of rare (and occasionally taxonomically uncertain) taxa produced 34 spermatophyte taxa that represent the finalized modern database (Table 1). In this 400 x 34 matrix, only 56% of cells correspond to zero-value, as 33% reduction. The new number of taxa per sample varies from 8 to 24, and the reduced sum used for calculation of relative frequencies ranges between 62 and 2733 grains per site, with a mean of 492 ± 250.

1.2.1.2. Climate of the modern pollen sites

Among the difficulties in developing a modern pollen database for paleoclimatic reconstruction is the estimation of corresponding climate parameters for sites, a problem that is exacerbated in the Arctic where meterorological stations are few and climate data quality is variable. For this study, climate parameters (annual, July and January air temperatures and annual precipitation) were estimated from weighted-averages of the closest meteorological stations, derived using 3Pbase software (Guiot and Goeury, 1996). A 10° radius of latitude and longitude was used for these interpolations, involving data from 400 meteorological stations in Canada (Alberta, $n = 146$; Yukon, $n = 19$; NWT and Nunavut, $n = 52$; Ontario, $n = 68$; Newfoundland , $n = 12$; Québec, $n = 79$) and Greenland, $n = 24$ (Environment Canada, 2004; Cappelen et al., 2001). The climate data derived from 30 year normals from 1971 to 2000 for the majority of stations (361 sites, 90% of sites), and 1961 to 1990 for the remaining 39 stations with either discontinued or unavailable measurements. Because bioclimatic parameters such as the annual sum of daily temperatures above 0°C (GDD0) and 5°C (GDD5), were not available from Greenland, these parameters are not included.

The modern climate parameter values, c_o, at a given lake, o, have been estimated from the weighted-average of all the meteorological stations, k, within a distance, d_{ok}, less than R (10°) from the lake (Guiot, 1987), following the equations below, where x_k, y_k and c_k represent the longitude, latitude, and climate data at each meteorological station, $k = 1$ to m ($m = 400$):

$$c_o = (\Sigma_k c_k / d_{ok}^2) / \Sigma_k 1 / d_{ok}^2)$$

and

$$d_{ok}^2 = (x_o - x_k)^2 + (y_o - y_k)^2.$$

The reliability of this approach has been tested by comparisons of observed and estimated values for each meteorological station. The root-mean-squared error (RMSE: the square root of the mean of the squared differences between observed and estimated data) is ±1.31°C ($r = 0.98$) for annual air temperature, ±1.23°C ($r = 0.96$) for July air temperature, ±2.19°C ($r = 0.95$) for January air temperatures, and ±119.13 mm ($r = 0.93$) for mean annual precipitation (Fig. 3A).

1.2.2. Numerical analyses

Pollen-climate relationships were explored statistically, in order to model the biological response of the 400 x 34 pollen matrix to an environmental predictor matrix of 400 x 7 parameters reflecting either the interpolated meterological data (mean annual, July, and January air temperatures, mean annual precipitation), or site variables likely to covary with local climatic conditions (latitude, longitude and altitude).

1.2.2.1. Ordination

Detrended correspondence analysis (DCA) with detrending by segments was first used to estimate the compositional gradient lengths of the first few DCA axes in the modern pollen data (Gauch, 1982; ter Braak and Prentice, 1988; Birks, 1995). The gradient length of DCA axis 1 is 2.58 standard deviation units, which indicates the preferred use of unimodal response models of pollen-environmental gradients: correspondence analysis (CA) and canonical correspondence analyses (CCA). CA was used to detect major floristic gradients within the 400 modern pollen assemblages, and CCA was therafter applied to evaluate the environnmental data's explanatory skill with respect to the biotic response encapsulated in the pollen assemblages. Forward-selection in CCA was applied to assess the explanatory power of environmental variables (ter Braak and Verdonschot, 1995; ter Braak and

Šmilauer, 1998), and the significance was established with 999 unrestricted Monte-Carlo permutations with the application of a Bonferroni correction to the reported *p*-values (Legendre and Legendre, 1998, Birks et al., 2004). The CCA results were also compared to those of the unconstrained (CA) ordination to verify that environmental variables used in the CCA retain the major floristic gradients suggested by CA in absence of *a priori* environmental contraints. For all of these ordinations (DCA, CA, and CCA) the frequencies of the 34 pollen taxa were first square-root transformed to downweight the most abundant taxa and upweight rare taxa. This transformation is deemed necessary because many arctic plants, notably herbaceous taxa, are sytematically under-represented due to low pollen production, whereas others, such as shrub *Alnus* and *Betula* are often ubiquitous. All ordinations were performed with CANOCO version 4.0 (ter Braak and Šmilauer, 1998).

1.2.2.1. Best modern analogues

The best modern analogue method (BMA) (also known as the modern analogue technique, MAT), assumes that a fossil pollen assemblage of similar composition to a modern counterpart has been produced by similar vegetation and consequently reflects a similar prevailing climate (Overpeck et al., 1985; Anderson et al., 1989; Guiot et al., 1989; Guiot, 1990; Andreev et al., 2003, 2004c; Jackson and Williams, 2004; Kerwin et al., 2004; Sawada et al., 2004). Similarity between fossil and modern assemblages is based on the squared chord distance (SCD) dissimilarity metric (Birks, 1977; Prentice, 1980; Overpeck et al., 1985; Gavin et al., 2003). SCD (d^2) between the fossil (t) and modern (i) assemblages is calculated from differences in pollen relative frequencies (p), for each taxon ($j = 1$ to m) ($m = 34$) as follows:

$$d_{it}^2 = \Sigma_j((p_{ij})^{1/2} - (p_{tj})^{1/2})^2,$$

which can be rewritten as

$$d_{it}^2 = 2 - 2\Sigma_j(p_{ij}p_{tj})^{1/2}.$$

Both Krzanowski (1971) and Goodman (1972) provide further discussion of this dissimilarity measure. Values of SCD vary between zero and 2 (the upper limit occurs when the product $p_{ij}p_{tj}$ is always zero, implying that no taxon occurs simultaneously in both assemblages), so that larger values indicate greater dissimilarity.

The reconstructed climate from a fossil assemblage t (r_t), indexed by the climate of the modern assemblage i (c_i), where i varies from 1 to s (s = number of analogues), from which the distance is d_{ti}, is given by:

$$r_t = (\Sigma_i c_i/d_{ti}^2)/ \Sigma_i(1/d_{ti}^2).$$

If the SCD of the closest analogues remains higher than a consistently adopted threshold, no reconstruction can be made (Guiot et al., 1989). The number of analogues (s) selected for paleoclimate interpolation is somewhat arbitrary. In general, 5 to 10 modern analogues are used. For example, Andreev et al. (2003, 2004b, 2005) used 10 when applying 1110-1310 modern assemblage, and 39-77 taxa, Andreev et al. (2004c) used 8 for 1106 modern assemblages and 77 taxa, Kerwin et al. (2004) used 10 for 275 modern assemblages and 11-12 taxa, and Sawada et al. (2004) used 10 for 4590 modern assemblages and 89 taxa. Our most recent efforts on Baffin Island, which address primarily sediments of last interglacial age (Fréchette et al., 2006) employ a lower value of $s = 5$ with respect to the current 400 modern assemblages and 34 taxa. Thus, for consistency, here we use 5 analogues, which further limits the risk of excessive heterogeneity within the modern analogues retained for paleoclimatic reconstruction. All BMA reconstructions were performed with the 3Pbase software (Guiot and Goeury, 1996).

1.2.3. Fossil pollen sites

Fog Lake (67°11'N, 63°15'W, 460 m a.s.l., 170 m long and 140 m wide, 9.5 m water depth at the coring site) and Akvaqiak Lake, 50 km to the west (66°47'N, 63°57'W, 17 m a.s.l., 400 m long and 200 m wide, 13 m water depth at the coring site), are typical small non-glacial lakes in the Padle Fiord-Merchants Bay region of northern Cumberland Peninsula, eastern Baffin Island, Nunavut (Fig. 1B). These sites were selected for analysis because of considerable prior study in the region, and the relatively secure chronologies based on numerous accelerator mass spectrometry (AMS) ^{14}C dates. The Fog Lake sediment record has been investigated from several perspectives, including a pre-Holocene sequence that is considered in detail elsewhere (Steig et al., 1998; Wolfe et al., 2000; Miller et al., 2002; Wolfe et al., 2004; Francis et al., 2006; Fréchette et al., 2006). Local vegetation is typical of the Middle Arctic Zone (Young, 1971), with a sparse vascular plant cover and few woody taxa. At Akvaqiak Lake, at the head of Padle Fiord, the vegetation is considerably denser due to an ameliorated local climate and low elevation, such that outlier populations of prostrate dwarf birch (*Betula nana*, *B. glandulosa*) are abundant surrounding the lake. Green alder (*Alnus crispa*) does not occur on Baffin Island today, nor does it appear to have grown in the area at any time during the Holocene. The modern climate at both sites was estimated by interpolation, identically to the modern sites. At Qikiqtarjuaq (Broughton Island), the nearest climate station 40 km northwest of Padle Fiord, mean annual temperature is -11.5°C (summer mean (JJA): 2.3°C; winter (DJF): -23.5°C), and mean annual precipitation is 280 mm a^{-1} (85% as snow). However, precipitation increases markedly eastward, producing over 600 mm a^{-1} at Cape Dyer, 100 km east of the lakes on the outer coast. Depth of snow cover is likely critical to the survival of *Betula* at the heads of Padle and Kangert fiords (cf Fredskild, 1991).

1.2.3.1. Sediment coring and chronology

The two cores were obtained in May 1996 (Fog) and 1998 (Akvaqiak) through lake ice using a sledge-mounted percussion coring system (7 cm diameter) capable of penetrating dense inorganic sediments (Nesje, 1992). This study is limited to the Holocene section from Fog Lake, captured in the upper 50 cm of core. The 90 cm core from Akvaqiak Lake is entirely post-glacial in age. These sediment records do not capture recent vegetational changes associated with post-Little Ice Age warming as the uppermost sediments are lost when coring. Instead, we focus on palynological changes that encompass the time between the "Holocene thermal maximum" and the Little Ice Age (LIA) (ca. 1600 to 1900 AD) (Grove, 1988; Koerner and Fisher, 1990). The original chronology of Fog Lake (Wolfe et al., 2000) has been supplemented by two additional AMS ^{14}C dates reported here (Table 2). Dates were obtained on bryophyte macrofossils (*Warnstorfia exannulata* leaves and stems), chitin from chironomid head capsules, and humic acid extracts. Although aquatic bryophytes appear reliable for AMS ^{14}C dating in this region, implying full equilibration of lake waters with respect to atmospheric CO_2 (Miller et al., 1999), humic acids are far more problematic when ancient (i.e., last interglacial) dissolved organic carbon are present in the catchment, as is the case with many Baffin Island lakes (Wolfe et al., 2004). Paired macrofossil and humic acid dates have been obtained at one level in the Fog Lake core and three levels in the Akvaqiak Lake core, producing humic acid ages that are universally older than adjacent macrofossils. This has led to the application of corrections of 170 and 537 years in Fog and Akvaqiak lakes, respectively, that are subtracted from all humic acid ages prior to age model development. All resulting corrected (humic acid) and uncorrected (bryophyte and chitin) dates have been calibrated to calendar years using the CALIB (Stuiver and Reimer, 1993) updated with the Intcal98 dataset (Stuiver et al., 1998).

1.2.3.2. Pollen-based Holocene climate reconstructions

The cores were subsampled at 0.5 to 3 cm intervals for fossil pollen analysis, resulting in 22 and 30 samples from the Fog and Akvaqiak lake cores, respectively. Standard pollen preparation techniques, including dispersion with KOH, digestion with HF and HCl, and acetolysis (Faegri and Iversen, 1975), were applied to 2.0 cm^3 samples of fresh (wet) sediment. Residues were stained with fuschin, mounted in glycerine, and examined microscopically at 400x and 1000x. Pollen and spores were identified using the taxonomic keys of Richard (1970), McAndrews et al. (1973) and Moore et al. (1991), as well as reference to the modern pollen collection archived at the Laboratoire Jacques-Rousseau, Université de Montréal. Pollen concentrations (grains.cm^{-3} of wet sediment) were determined by spiking with *Eucalyptus* pollen grains prior to processing (Benninghoff, 1962).

The pollen sum used for computing relative frequencies from the fossil assemblages includes the same 34 pollen types contained in the modern databse (Table 1). These sums average 512 ± 17 grains for Fog Lake, and 547 ± 41 grains for Akvaqiak Lake. However, the palynomorph concentrations are reported for both total spermatophyte pollen, as well as all pteridophyte spores (grains.cm^{-3}).

To assess stratigraphic changes in pollen assemblages we first calculated the squared chord distance (SCD) between adjacent pollen spectra in both records. These SCD values approximate the magnitude of between-sample vegetation change, but are also influenced by the time elapsed between deposition of consecutive samples analyzed. In order to normalize for this temporal component, we applied the age models from both lakes to calculate between-sample rates of change (ROC) (Jacobson et al., 1987; Grimm and Jacobson, 1992), which are equal to between-sample SCD divided by the time interval separating adjacent samples. ROC (SCD $year^{-1}$) is an important variable for identifying periods of accelerated vegetation change, as well as patterns

that may be expressed regionally to enalbe correlation (Grimm and Jacobson, 1992; Shuman et al., 2005). These calculations are based on the 34 principal pollen taxa only, and were performed using the program Progiciel R (version 4) of Legendre and Legendre (1998), available from http://www.bio.umontreal.ca/casgrain/fr/labo/R/index.html.

1.3. Results I: the modern pollen database

1.3.1. Modern climate of the reference sites

The modern database encompasses environmental gradients ranging from -19.5 to 5.1°C for annual temperature (mean: -6.3 ± 5.9°C), 3.5 to 18.2°C for July temperature (mean: 10.3 ± 3.9°C), -36.8 to -4.1°C of January temperatures (mean: -21.9 ± 8.0°C), and 81 to 2470 mm for annual precipitation (mean: 498 ± 391 mm). These data are summarized in Table 3 and Fig. 4. To assess regional differences, the 400 sites have been subdivided in Fig. 4 according to geographic location: North American sites west of longitude 110°W (WC-1, WC-2, WC-3), North American sites east of longitude 110°W (A, B, FCD, NQ, JB), and sites from Greenland (G).

1.3.2. Palynological signature of the reference sites

The palynological signatures of the 400 reference sites are portrayed in Fig. 5 as the relative frequencies of the 34 principal taxa ordered according to their first axis CCA scores and ordered latitudinally within each region. Latitudinal patterns are clearly expressed by some boreal tree taxa (*Picea* and *Pinus*), as well as for alder (*Alnus*). Saxifragaceae and *Oxyria/Rumex* contain additional latitudinal structure within the mid- to high-arctic zones. Conversely, representations of the dominant arctic shrub and herb taxa (Ericales, *Salix*, Cyperaceae, Poaceae) and *Betula* lack such obvious latitudinal trends.

1.3.3. Major floristic gradient in relation with environment variables

CA ordination reveals the major floristic gradient among the 400 modern pollen assemblages. The first CA axis accounts for 24.1% of total variance and has an eigenvalue ($\lambda_1 = 0.242$) twice that of the second CA axis ($\lambda_2 = 0.122$) (Table 4). CA axis 1 sample scores preserve a clear latitudinal trend both between and within each subregion (Fig. 6A, B). These scores have a significant negative correlation with July air temperature ($r = -0.86$) (Fig. 6C). Sites from herb and shrub tundra vegetation zones of the Arctic (A, B, G, WC-3) have positive scores on CA axis 1, whereas sites from grassland-boreal-subarctic zones (JB, NQ, FCD, WC-1, WC-2) have negative scores. The relationship between CA axis 1 assemblage scores and July air temperatures (Fig. 6C) indicates that pollen sensitively captures the climatic distinction between subarctic and arctic vegetational zones, which broadly coincides with July air temperatures near 10°C (Koeppen, 1936; Young, 1971; Bonan et al., 1992; Foley et al., 1994; Pielke and Vidale, 1995).

The CCA constraining the 400 pollen assemblages to the 7 environmental variables aims to pinpoint those environmental variables that maximize the floristic gradients identified by CA, whereas subsequent forward selection (*sensu* ter Braak and Verdonschot, 1995) confirms that July air temperature is the most significant environmental predictor, followed by January air temperature (Table 5). The three temperature variables collectively account for 65.3% of the variation within the pollen assemblage data, whereas annual precipitation only accounts for 4.5% of the total floristic variance. At the 95% level ($p = 0.05$), all seven environmental variables are significant predictors of the composition of pollen assemblages.

The first three canonical axes collectively explain 32.0% of the variance in the pollen data alone, and 85.2% of the variance in the weighted-averages of the pollen taxa constrains to environment (Table 4). The second and the third CCA axes have similar eigenvalues that are both statistically significant. Close correspondence between the eigenvalues of CA and CCA ordinations indicates that the dominant gradient in pollen assemblage composition is captured both in the absence (CA) and the presence (CCA) of the environmental constraints imposed by the 7 variables (Birks et al., 2004). Thus, CCA axis 1 captures the gradients of both July air temperature (r = -0.93) and latitude (r = 0.73), whereas axis 2 is correlated with annual precipitation (r = -0.81) and January air temperature (r = -0.80), and axis 3 captures mainly a gradient of altitude (r = 0.72) and to some extent January air temperature (r = 0.50) (Table 6). CCA ordination biplots also illustrate the separation of pollen assemblages among floristic zones (Fig. 7A, C), which is maximized along axis 1, corresponding to the July air temperature gradient intially revealed by CA.

By projecting taxon scores onto the vector of July air temperature, three distinct groupings are observed (Fig. 7B, D). This ranking of taxa approximates the weighted-averages of individual pollen taxa with respect to July air temperature (Jongman et al., 1987; Legendre and Legendre, 1998). A first group is characterized by strongly negative CCA axis 1 scores and includes the most thermophilous taxa such as *Larix* (PLAR), *Abies* (PABI), *Myrica* (MMYR), Chenopodiaceae (CHEN), *Picea* (PPIC), *Pinus* (PPIN), *Populus* (SPOP) and *Shepherdia* (ESHE). A second group with strongly positive scores includes the taxa most common in the coldest environments of the mid- to high-arctic zones: Papaveraceae (PPAV), *Dryas* (RDRY), Saxifragaceae (SAXI), *Oxyria/Rumex* (POXR), Scrophulariaceae (SCRO), Polygonaceae (POLY), Caryophyllaceae (CARY), Brassicaceae (BRAS), Fabaceae (FABA), Ranunculaceae (RANU) and *Salix* (SSAL). A third group of taxa are generally more abundant in surface sediments from subarctic and low arctic zones, but are also encountered in samples spanning the full gradient from boreal to high

arctic (Fig. 5). This group therefore has somewhat dimished ecological specificity with respect to the parameterized environmental gradients, and includes *Betula* (BBET), *Artemisia* (CART), *Alnus* (BALN), Tubuliflorae-Liguliflorae (TULI), *Ambrosia* (CAMB), Cupressaceae (CUPR), Rosaceae (ROSA), Cyperaceae (CYPE), Poaceae (POAC), Onagraceae (ONAG) and *Plantago* (PPLA).

1.4. Results II: best modern analogues

1.4.1. Threshold values of the SCD

An absolutely critical consideration with the BMA method is selecting the threshold value beyond which dissimilarity is too high for a reliable analogue to be assigned. Yet the definition of this threshold often appears somewhat arbitrary. Moreover, the selected threshold value may not universally prevent errors arising from false apparent similarity or dissimilarity (i.e. false positive or false negative errors, respectively analogous to Type I and Type II errors in statistical hypothesis testing) (Jackson and Williams, 2004; Wahl, 2004). In previous BMA studies (Overpeck et al., 1985; Anderson et al., 1989; Calcote, 1998), SCD thresholds were determined from comparisons between modern pollen assemblages and their corresponding vegetation types, in order to ascertain SDC values that define boundaries between analogue and non-analogue situations. This often resulted in relatively low SCD thresholds values, which reduce the chance of generatings false positive errors when choosing modern analogues. For example, Overpeck et al. (1985), using 1618 modern sites (lake and bog surface sediments, and moss polsters) and 15 (14 woody plants, 1 herb) or 40 taxa (32 woody plants, 8 herbs), showed that assemblages with SCD ≤ 0.12 can be considered reliable analogues, but SCD of 0.15 remain applicable if the number of analogues decreases. Anderson et al. (1989), using 303 modern lake-sediment sites and and 25 taxa (15 woody plants, 10 herbs), proposed SCD thresholds of 0.095, 0.185 and 0.400 to identify 'good analogues', 'analogues' and

'possible analogues', respectively. Calcote (1998), using 66 modern forest hollow sites and 13 woody plant taxa, suggested that SCD ≤ 0.05 indicates the presence of acceptable analogues. More recently, Jackson and Williams (2004) and Wahl (2004) have stressed the importance of considering the risk of failing to correctly identify pollen assemblages from similar vegetation (false negative error). Typically, this results in the need for higher SCD threshold values. Wahl (2004) has shown that an SCD threshold of 0.225 was appropriate for his database comprising 41 surface soil samples (13 taxa including 8 woody plants, 4 herbs and a collective category including pteridophyte spores, unidentifiable and unknown pollen grains). At the continental scale, an even higher threshold SCD of 0.30 may be warranted (Sawada et al., 2004). In this case, the threshold SCD was determined by plotting the frequency distribution of SCD values obtained from the first best modern analogue for each of the 4590 modern pollen assemblages (89 taxa including 49 woody plants, 30 herbs, 9 pteridophyte and 1 bryophyte). The upshot is that studies comparing within-biome pollen assemblages require smaller threshold SCD values than those involving more than one plant biome (Gavin et al., 2003; Oswald et al., 2003; Sawada et al., 2004). Furthermore, the SCD threshold itself may become biome-specific, as suggested by considerations of information-statistic indices (Waelbroeck et al., 1998) applied to continent-scale compilations of pollen assemblage data (Whitmore et al., 2005).

In order to address these issues in the present investigation, we calculated SCD between all pairs (i.e. 79,800) of the 400 modern pollen assemblages (34 taxa). Thereafter, we plot the frequency distribution of SCD values between pairs to illustrate dissimilarities between (1) all 400 sites (2) sites from grassland-boreal-subarctic zones, and (3) sites from arctic tundra zones (Fig. 8B, E, H). Because these pair-wise SCD values were calculated among pollen assemblages originating from differing vegetation types, they are representative of the between-biome dissimilarity. In parallel, we plotted the frequency distribution of SCD values of the first best analogue for the same three broad subsets of sites (Fig. 8C, F, I). Since the first best

analogue is more likely to originate from the same vegetation type as the corresponding pollen assemblage, these SCD values are representative of within-biome dissimilarity. The results demonstrate that SCD from the grassland-boreal-subarctic zones are generally lower than those from arctic tundra vegetation zones (Fig. 8E, H). Likewise, SCD values of the first best analogue are lower in the grassland-boreal-subarctic zones than for arctic tundra zones (Fig. 8F, I). Furthermore, the frequency distribution of SCD values of the best analogue of sites from the grassland-boreal-subarctic zones preserve skewness and kurtosis (Fig. 8F), whereas the distribution is closer to normal for the arctic vegetation zone (Fig. 8I). The higher modal SCD values for arctic zones, and their more normal distribution cannot be explained by a larger range of July air temperature or other climate variables (Table 3), nor by a lower density of sites (Fig. 1A). From these result, we conservatively suggest that high SCD threshold values are most appropriate for BMA-based climate reconstructions from fossil pollen assemblages from arctic lake sediments. Such thresholds reduce the probability of generating false-negative errors, such as the omission of contrasting pollen assemblages originating from sites experiencing similar climate and therefore representing viable analogues. Conversely, low SCD thresholds are likely to remain appropriate when considering fossil assemblages from the warmer subarctic portion of the temperature gradient.

The SCD threshold objectively obtained from the 3Pbase program is based on a Monte Carlo simulation of the modern assemblage data (this way to proceed has the advantage to take into account the number of taxa which has a positive effect on the value of the threshold), whereby i modern spectra are randomly extracted with replacement from i selected modern spectra, and the best-fit spectrum from that group is obtained (Guiot et al., 1989; Guiot, 1990). This is repeated s times, providing s best analogues from which confidence intervals are calculated. The mean SCD obtained in this way, generated between randomly-selected pairs from within the modern assemblage data, is 0.62 ± 0.31. The mean minus standard deviation provides

the SCD threshold, that is, 0.31. When comparing to the frequency distribution of SCD values from arctic vegetation zones (Fig. 8H, I), the SCD threshold of 0.31 seems entirely adequate for quantitative paleoclimate reconstructions from fossil pollen asssembalges from lake sediments in arctic Canada and Greenland.

1.4.2. Robustness of quantitative climate inferences

Validation tests using the 5 best modern analogues (s) demonstrate that the BMA method reconstructs modern climate variables in the Arctic with reasonable accuracy, for both the climate station (Fig. 3C) and lake sediment (Fig. 3D) localities. Ideally, these validations approach 1:1 linear relationships between inferred and observed values, as assessed by the slope and the correlation coefficient (r), as well as the lowest variability measured by the RMSE for each climate parameter (de Vernal et al., 2001; Muller et al., 2003; Sawada et al., 2004). Correlation coefficients suggest that July, annual and January air temperatures can be reconstructed with high degress of confidence ($r = 0.97$, 0.95 and 0.93, respectively). Annual precipitation was also reconstructed with accuracy ($r = 0.86$). These degrees of correlation and RMSE justify the choice to include pollen grains derived from both local, regional, and long-distance sources. The degree of accuracy of July air temperature predicitons is better in the Arctic relative to grassland-boreal-subarctic zones (RMSE of 0.84 and 1.15°C, respectively). Conversely, the other climate parameters are more accurately reconstructed south of the arctic tundra zones. Different precipitation and winter temperature regimes among arctic sites, notably between Greenland and the Canadian Arctic Archipelago, explain this phenomenon (Fig. 4).

1.4.3. Evaluating the potential effects of spatial autocorrelation in BMA reconstructions

Recently, Telford et al. (2004) and Telford and Birks (2005) stressed that the reliability of the BMA method may be overestimated because of spatial autocorrelation. Indeed, spatial autocorrelation may distort the performance of certain calculations, such as that of standard statistical tests (e.g. r value and RMSE) (Legendre, 1993). With the aim of assessing this potential problem, we removed sites from the modern reference database (N). We first retained three sites of every four sites ($N = 300$), then one site of every two sites ($N = 200$) and finally only one of every four sites ($N = 100$) from the original latitudinal ordering, and recalculated BMA estimates of the four most significant climate parameters. In the last way ($N = 100$), the closeness, geographically and climatologically, among sites comprising the training set is reduced, as is the potential for statistical artifacts of autocorrelation. Comparable results were found for the $N = 100$, 200, 300 and 400 reference samples (Table 7). Thus, if we take into account that we are in a very defavourable situation with a very small reference database, we may conclude that spatial autocorrelation does not affect the BMA method. Overall, the validation tests presented here prove that modern climate information is effectively registered by high-latitude pollen assemblages, and that paleoclimate reconstructions using the BMA method are methodologically and statistically robust.

1.5. Results III: Holocene climate of Baffin Island reconstructed from fossil pollen

1.5.1. Stratigraphy and palynology of the Fog and Akvaqiak lake cores

Age models for the Fog and Akvaqiak lake cores were derived from calibrated AMS ^{14}C measurements (Fig. 9). Sediment accumulation rates average 6.7 ± 2.4 cm ka^{-1} at

Fog Lake and 13.5 ± 7.2 cm ka^{-1} at Akvaqiak Lake, which are typical for unproductive Baffin Island lakes in small drainage basins (Wolfe et al., 2004). According to the available dates, organic sedimentation commenced approximately 8300 cal. years BP in both lakes. Underlying and largely inorganic sediments contain pre-Holocene organic matter (including palynomorphs) remobilized during regional deglaciation, and are not considered for quantitative climate reconstruction (Table 2). Local vegetation in the vicinities of Fog and Akvaqiak lakes are quite different despite their proximity, and this is well expressed in their respective pollen assemblages (Fig. 10). The main floristic differences concern representations of *Betula*, Cyperaceae and *Oxyria/Rumex* pollen. Akvaqiak Lake assemblages are dominated by *Betula* and Ericales, whereas boreal taxa (*Picea*, *Pinus, Artemisia*), *Oxyria/Rumex*, and other arctic herb taxa are poorly represented. Fog Lake assemblages show higher frequencies of boreal taxa, as well as relatively high representations of *Oxyria/Rumex*.

Pollen concentrations in Fog Lake sediments are about half those observed in Akvaqiak Lake. The mean pollen influx at Fog Lake is 36 ± 30 grains cm^{-2} yr^{-1} and 229 ± 177 grains cm^{-2} yr^{-1} at Akvaqiak Lake. The lower pollen influx at Fog Lake is explained by the local absence of shrub *Betula*, and the lake's more exposed position on an upland surface, that contrasts the protected valley-floor situation of Akvaqiak Lake. SCD between the uppermost pollen assemblages of the two lakes is 0.14, which is relatively high when considering their close proximity of ~50 km. Downcore, between-sample, SCD values indicate three distinct intervals of vegetation development expressed in both lakes, with transitions at ~8000, ~3000 and ~1000 cal. years BP (Fig. 10). Within-core pollen assemblage SCD values are much lower (SCD < 0.10) by comparison to regional arctic assemblages (Fig. 8H, I), which indicates that the vegetation changes associated with these Holocene pollen shifts were relatively subtle. Rate of change (ROC) calculations show that changes

centered at ~8000 and ~1000 cal. years BP were comparable in magnitude at the 2 sites, and more rapid than the one expressed at ~3000 cal. years BP (Fig. 10).

1.5.2. Compositional changes in the pollen diagrams

Visual inspection of pollen diagrams reveals three biostratigraphic zones (Fig. 10). Between ~8300 and ~8000 cal. years BP, *Betula*, *Alnus*, Ericales, and several arctic herb taxa dominate the assemblages of both sites. Pollen rain consisted of a significant component of subarctic and boreal taxa, along with local, cold environment taxa. The pollen content and ROC values suggest that the landscape supported a sparse and unstable herb tundra vegetation, readily diluted by contributions from pollen transported from the south.

From ~ 8000 to ~3200 cal. years BP, frequencies of Cyperaceae and *Alnus* rose (i.e., until ~5000 cal year BP), then declined progressively as Ericales pollen representation began to increase after ~5000 cal. years BP. The rise in Cyperaceae frequencies, and high ROC values at ~7700 cal. years BP, reflect the establishment of a middle-Holocene herb tundra vegetation. The rise of *Alnus* frequencies around 6000 cal. years BP suggests increased recruitment of long-distance pollen derived from northward expansion of alder in Nunavik, northern Québec (Richard, 1981, 1995; Gajewski et al., 1993, 1996). The decrease in Cyperaceae percentages, accompanied by the progressive increase in Ericales pollen, suggest an empoverishment of local vegetation cover and soil nutrient status, ultimately reflecting the onset of the Neoglacial on northern Cumberland Peninsula (Wolfe et al., 2000; Kerwin et al., 2004; Miller et al., 2005). An empoverishment of local vegetation trend is observed on east-central Ellesmere Island, where slight increases in pioneer herbs after ~3800 cal. years BP indicate a pronounced cooling phase (Hyvärinen, 1985), and in the central Arctic (Gajewski, 1995; Gajewski and Frappier, 2001).

The final pollen zone recognized here, post-3200 cal. years BP, is characterised by increasing ROC values, enhanced representation by Ericales, and decreased frequencies of *Alnus*, together suggesting instability of local vegetation cover. ROC values after ~3200 cal. years BP suggest that vegetation responded rapidly to the Neoglacial cooling. However, proportions of long-distance pollen do not increase during this phase, although they do increase in ice core pollen studies on Ellesmere Island (Bourgeois et al., 2000). ROC values also reveal that vegetation during the last millennium was as unstable as that of the early Holocene, in keeping with observations from elsewhere in North America (Jacobson et al., 1987; Jacobson and Grimm, 1988; Grimm and Jacobson, 1992; Shuman et al., 2005).

1.5.3. Quantitative paleoclimate reconstructions from the BMA method

Close analogues for the Fog and Akvaqiak lakes fossil pollen assembalges exist in the 400 site modern database, with at least five solutions possessing SCD values < 0.12, much lower than the prescribed threshold value of 0.31 (Fig. 11). For both sediment cores, the range of SCD values is slightly larger prior to 7000, and post-3200 cal. years BP. Although reconstructions from the uppermost pollen assemblages overestimate modern interpolated temperatures and precipitation for either site, these discrepancies fall within the range of their respective RMSE (Fig. 3), and within the ranges of interannual variability measured on eastern Cumberland Peninsula for 1971-2000 (annual air T: -11.6 ± 2.5°C; July air T: 4.6 ± 1.7°C; January air T: -24.8 ± 4.4°C, Environment Canada, 2004). Furthermore, the likelihood that pollen assemblages reflect longer time-frames than those embraced by instrumental climate normals cannot be eliminated given the low sediment accumlation rates at these sites. According to calculated sedimentation rates, the uppermost pollen assemblage at Fog Lake encompasses about two centuries from about 610 to 380 cal. years BP, and the

uppermost assemblage at Akvaqiak Lake represents almost one century from about 360 to 280 cal. years BP.

At Fog Lake, the five best modern analogues used for climatic inferences originate from Greenland (55%) and Baffin Island (45%), whereas those for Akvaqiak Lake are mainly from Greenland (85%), with some from Baffin Island (13%) and Mackenzie Delta region (WC-2; 2%).

Although the pollen stratigraphies from both lakes differ, paleoclimate reconstructions are broadly consistent (Figs. 11, 12, 13A). At both sites, reconstructed July air temperatures exhibit slight cooling trend since 8000 cal. years BP, amounting to ~1.0°C at Fog Lake and ~1.2°C at Akvaqiak Lake. At the latter site, reconstructed annual precipitation increased markedly after 5000 cal. years BP. The composition of pollen assemblages from Akvaqiak Lake, coupled to the locations of their best modern analogues (primarily southern Greenland after 5000 cal. years BP), imply that low elevations along the east coast of Cumberland Peninsula experienced progressively more oceanic climates since the mid-Holocene.

Reconstructed annual and January air temperature trends are superimposed at both Fog and Akvaqiak lakes. This is likely borne out of the strong relationship between these two climate variables in the $n = 400$ database ($r = 0.87$), which increases further when only arctic sites are considered ($r = 0.99$, Table 8). At Fog Lake, reconstructed annual and January air temperatures rise marginally during the late Holocene, but these trends are not evident in BMA estimates from Akvaqiak Lake (Fig. 11). The large range of values for these climate variables among sites selected as best modern analogues, which combine Greenland and Canada, may explain these discrepancies (Fig. 4). Thus, BMA-based reconstructions of annual and January air temperatures should be viewed cautiously as first appproximations.

1.5.4. Quantitative July temperatures reconstructed from CA regression

Following initial CA ordination of the 400-lake modern assemblages, fossil pollen data from Fog and Akvaqiak lake cores were projected passively onto the ordination space, without influencing the analysis in any other way. The linear regression equation between CA axis 1 sample scores and July air temperature (July T (°C) = 10.28 – 6.54 (CA axis 1 sample score); Fig. 6C) was applied to fossil sample scores to quantitatively reconstruct the July air temperatures, with an estimated RMSE of ±1.98°C ($r = 0.86$). CA regression thus provides simpler, but less precise, July temperature estimates than the BMA method. Fossil pollen assemblages from Fog and Akvaqiak lakes produce positive CA axis 1 scores (0.25 to 0.50) and negative axis 2 scores (-0.10 to -0.75). When compared to scores from the 400 modern assemblages, pollen from both lakes are more comparable to modern Geenland (67% for Fog Lake, 89% for Akvaqiak Lake) than to Baffin Island (33% for Fog Lake, 11% for Akvaqiak Lake).

CA regression reconstructions of July air temperature from Fog Lake depict a slight cooling trend, in the order of 0.8°C, since 8000 cal. years BP. In contrast, no significant trend is evident from Akvaqiak Lake. (Figs. 12, 13B). CA axis 2 is negatively correlated to annual precipitation and its covariable, January air temperature (Fig. 7B; Table 6). At Akvaqiak Lake the increasingly negative scores on CA axis 2 (Fig. 13E) thus suggest increased precipitation after ~5000 cal. years BP, which is entirely consistent with estimates from BMA (Figs. 11, 13D). The strong correlation between annual precipitation and winter temperature ($r = 0.76$) implies that the trends of increased late Holocene precipitation witnessed at both lakes may ultimately be the result warmer winter air temperatures, despite progressive summer cooling. This trend translates the progressive reduction in annual temperature amplitude over the course of the late Holocene (Bradley and Miller, 1972).

1.5.5. Integration of reconstructed July temperatures estimates

For both lakes, CA-based reconstructed July air temperatures are about 1.0°C warmer than those inferred by the BMA method and largely parallel, with the exception of the 8000 to 5000 cal. years BP interval at Akvaqiak Lake, where CA- and BMA reconstructions are nearly superimposed (Fig. 12). Irrespectively, the results from both techniques overlap when their respective confidence intervals are taked into account. In order to balance the contributions of both approaches, we averaged the BMA- and CA-based July air temperature reconstructions from Fog and Akvaqiak lakes individually, thus yielding "consensus" reconstructions (Figs. 12, 13C) that follow the rationales used previously (Bartlein and Whitlock, 1993; Kerwin et al., 2004). The robustness of our BMA-CA consensus approach was assessed by reconstructing modern July air temperatures for the 400 training set sites, which yielded a strong correlation between inferred and observed July temperature ($r = 0.94$), and an RMSE of ±1.30°C. The performance of the consensus model is comparable to the BMA reconstruction (r = 0.97, RMSE = 1.02°C). However, when individual lake records are merged into single, composite record (BMA-CA consensus values) (Fig. 13C), there is more agreement between Fog and Akvaqiak lakes July air temperature reconstructions than with their BMA and CA records individually (Fig. 13A, B). This agreement in the climate trend at the regional scale highlights the clear advantage of developing, implementing, and synthesizing multiple reconstruction strategies for a single variable.

1.5.6. Spatial and temporal scales of Holocene climate variability

The consensus July air temperature reconstructions from Fog and Akvaqiak lakes coherently preserve a long-term cooling trend of 0.6-0.8°C at the regional scale on northern Cumberland Peninsula since 8000 cal. years BP. This summer cooling is in

strong agreement with palynological changes indicating a gradual empoverishment of local vegetation (Fig. 10). This trend is consistent with summer insolation forcing (Berger, 1998). Regionally, summer cooling may have become exacerbated following the initiation of Neoglacial advances among local glaciers after 6000 cal. years BP (Miller et al., 2005), particularly if localized feedbacks involving prolonged snow cover were involved (Wolken et al., 2005). Superposed on this secular trend is a faint expession of mid-Holocne warming beginning ~6500 cal. years BP and lasting approximately 1000 years. This feature is evident in other pollen records from the region (Kerwin et al., 2004).

Subsequently, the long-term Holocene cooling trend is punctuated by discrete short-term warming episodes at ~6000, ~3500, ~1500, and ~500 cal. years BP, which are well-expressed at Akvaqiak Lake, and are of relatively low amplitude (±0.3-0.4°C). July air temperatures decreased by ~0.4-0.5°C between 3200 cal. years BP and the Little Ice Age, implying an acceleration of summer cooling in the late Holocene. At this time, enhanced summer cooling destabilized vegetation, as witnessed by increased pollen ROC values (Fig. 13). Dinoflagelllate cyst assemblages from northern Baffin Bay register a similar cooling after 3600 ^{14}C years, punctuated by several short-term fluctuations of sea-surface temperature (Levac et al., 2001). The replacement of Atlantic surface waters by cold, low-salinity Arctic Ocean water along the coast of eastern Baffin Island (Dyke et al., 1996; Levac et al., 2001), coupled with the steady reduction of summer insolation, likely resulted in significant sea-ice feedbacks that amplified the late Holocene summer cooling trend.

With respect to these finer scale changes, the Akvaqiak Lake pollen record appears more variable than that from Fog Lake, and this may relate to local conditions and vegetation status. For example, local vegetation cover in the vicinity of Fog Lake is discontinuous, which suppresses local pollen representation in lake sediments, while maximizing that of regional and long-distance grains that are wind-borne.

Conversely, Akvaqiak Lake's situation, a mid dense copses of shrub *Betula* and near-continuous tundra, collectively maximize the representation of local pollen grains in its sediments. We assume that these differences have persisted throughout the Holocene, implying that short-term climate oscillations of the past few millennnia have primarily impacted the structure of vegetation at the local scale of individual catchments, with minimal attendant effects on extra-local pollen rain. These and other hypotheses remain to be tested more rigourously by means of analyses at higher stratigraphic resolution.

1.6. Conclusion

The compilation of 400 modern pollen assemblages encompassing lakes from northwestern Canada, northern Québec, the Canadian Arctic Archipelago, and Greenland has allowed the development and testing of quantitative models relating arctic pollen to climate. In the course of this compilation, we noted considerable variability in pollen taxonomy and nomenclature that mandated an objective standardization of the data prior to inference model development. Despite the various difficulties inherent to high-latitude palynology, stemming principally from low or highly variable pollen production from tundra plants (Gajewski et al., 1995) and disproportionately large representation of long-distance grains, we have shown that quantitative reconstructions of Holocene summer temperature and annual precipitation trends are nonetheless tractable, enabling further inferences concerning seasonality and site-specific characteristics with regards to pollen rectruitment. Both BMA and CA regression techniques proved effective, together yielding complementary trends from two lakes with contrasting local vegetation. Different moisture and winter temperature regimes between the Greenland and Canadian Arctic Archipelago sites within the modern databae appear to limit BMA-based quantitative reconstructions for annual precipitation, January air temperature, and annual air temperature. However, estimates of these varaibles remain possible with CA

regression. The most reliable reconstructions are those of July air temperature using the average between BMA and CA regression estimates for this parameter.

Reconstructed climate and vegetation dynamics from Fog and Akvaqiak lakes indicated progressive mid- to late-Holocene cooling trend on northern Cumberland Peninsula, which is consistent with decreasing summertime insolation (Kerwin et al., 2004). Concomitant increases of annual precipitation is also registered during the late Holocene, suggesting enhanced oceanic influences at the regional scale, in close agreement with the record of local glacier readvances (Dahl and Nesje, 1996; Nesje et al., 2001). The close relationship between annual precipitation and January air temperature ($r = 0.83$) also implies that winter temperatures increased progressively during the late Holocene. Such a trend, in turn, suggests that the annual amplitude of air temperatures, or seasonality, has progressively decreased, especially since 3200 cal. years BP.

The long-term summer cooling trend since 8000 cal. years BP to the Little Ice Age is punctuated by discrete intervals of shorter-term warming that are better expressed in the Akvaqiak Lake record, which is better resolved temporally. Sites such as Fog Lake, in which extra-local pollen sources are more evident, present more complacent pollen records when quantitatively translated to climate parameters using BMA and CA regression transfer functions. These results indicate the relevance of local site characteristics in shaping both catchment vegetation dynamics and the attendant composition of lake-sediment pollen assemblages. Despite earlier cautionary notices (Gajewski et al., 1995), our results reveal promise for arctic palynology and its applications to paleoclimatic reconstruction. For example, the inference methods developed from the 400 site modern lake sediments database appear sufficiently sensitive to address the climatic significance of fine-scale changes, in both space and time, expressed by arctic pollen assemblages.

Acknowledgements

This study is a contribution to the Polar Climate Stability Network (PCSN) supported by the Canadian Foundation for Climate and Atmospheric Sciences (CFCAS). Initial funding by the Climate System History & Dynamics (CSHD) project supported by the Natural Sciences and Engineering Research Council (NSERC) of Canada is also acknowledged. Complementary support was provided by the *Fonds Québécois de la Recherche sur la Nature et les Technologies* (FQRNT) discovery grants from NSERC (BF, AdV, APW, PJHR and KG) and by National Science Foundation (NSF) grants to GHM and MWK. Extensive logistical support was provided by the Nunavut Research Institute (Nunavummi Qaujisaqtulirijikkut, Government of Nunavut, Iqaluit), and the Inuit of Qikiqtarjuaq. Special thanks are due to Maryse Henry (GEOTOP) for her help with the data analysis and Nicole Morasse (Université de Montréal) for her help with pollen analysis.

References

Anderson, P.M., Bartlein, P.J., Brubaker, L.B., Gajewski, K., Ritchie, J.C., 1989. Modern analogues of late-Quaternary pollen spectra from the western interior of North America. Journal of Biogeography 16, 573-596.

Andreev, A.A., Tarasov, P.E., Siegert, C., Ebel, T., Klimanov, V.A., Melles, M., Bobrov, A.A., Dereviagin, A.Y., Lubinski, D.J., Hubberten, H.-W., 2003. Late Pleistocene and Holocene vegetation and climate on the northern Taymyr Peninsula, Arctic Russia. Boreas 32, 484-505.

Andreev, A.A., Tarasov, P.E., Klimanov, V.A., Melles, M., Lisitsyna, O.M., Hubberten, H.-W., 2004a. Vegetation and climate changes around the Lama Lake, Taymyr Peninsula, Russia during the Late Pleistocene and Holocene. Quaternary International 122, 69-84.

Andreev, A.A., Grosse, G., Schirrmeister, L., Kuzmina, S.A., Novenko, E.Y., Bobrov, A.A., Tarasov, P.E., Ilyashuk, B.P., Kuznetsova, T.V., Krbetschek, M., Meyer, H., Kunitsky, V.V., 2004b. Late Saalian and Eemian paleoenvironmental history of the Bol'shoy Lyakhovsky Island (Laptev Sea Region, Arctic Siberia). Boreas 33, 319-348.

Andreev, A.A., Tarasov, P., Schwamborn, G., Ilyashuk, B., Ilyashuk, E., Bobrov, A., Klimanov, V., Rachold, V., Hubberten, H.-W., 2004c. Holocene paleoenvironmental records from Nikolay Lake, Lena River Delta, Arctic Russia. Palaeogeography, Palaeoclimatology, Palaeoecology 209, 197-217.

Andreev, A.A., Tarasov, P.E., Ilyashuk, B.P., Ilyashuk, E.A., Cremer, H., Hermichen, W.-D., Wischer, F., Hubberten, H.-W., 2005. Holocene environmental history recorded in Lake Lyadhej-To sediments, Polar Urals, Russia. Palaeogeography, Palaeoclimatology, Palaeoecology 223, 181-203.

Barber, D.C., Dyke, A., Hillaire-Marcel, C., Jennings, A.E., Andrews, J.T., Kerwin, M.W., Bilodeau, G., McNeely, R., Southon, J., Morehead, M.D., Gagnon, J.-M., 1999. Forcing of the cold event of 8,200 years ago by catastrophic drainage of Laurentide lakes. Nature 400, 344-348.

Barbour, M.G., Burk, J.H., Pitts, W.D., Gilliam, F.S., Schwartz, M.W., 1998. Terrestrial plant ecology. 3rd edition. Addison Wesley Longman, Inc. Menlo Park, California.

Bartlein, P.J., Whitlock, C., 1993. Paleoclimatic interpretations of the Elk Lake pollen record in Elk Lake Minnesota. In: Bradbury, J.P., Dean, W.E. (Eds.), Elk Lake Minnesota: Evidence for Rapid Climate Change in North-Central United States, Boulder, CO. Geological Society of America Special Paper 276, pp. 275-293.

Benninghoff, W.S., 1962. Calibration of pollen and spore density in sediments by addition of exotic pollen in known quantities. Pollen et Spores 4, 232-233.

Berger, A., 1988. Milankovitch theory and climate. Reviews of Geophysics 26, 624-657.

Berger, A., Loutre, M.F., 1991. Insolation values for the climate of the last 10 million years. Quaternary Science Reviews 10, 297-318.

Bigelow, N.H., Brubaker, L.B., Edwards, M.E., Harrison, S.P., Prentice, I.C., Anderson, P.M., Andreev, A.A., Bartlein, P.J., Christensen, T.R., Cramer, W., Kaplan, J.O., Lozhkin, A.V., Matveyeva, N.V., Murray, D.F., McGuire, A.D., Razzhivin, V.Y., Ritchie, J.C., Smith, B., Walker, D.A., Gajewski, K., Wolf, V., Holmqvist, B.H., Igarashi, Y., Kremenetskii, K., Paus, A., Pisaric, M.F.J., Volkova, V.S., 2003. Climate change and Arctic ecosystems: 1. Vegetation changes north of 55°N between the last glacial maximum, mid-Holocene, and present. Journal of Geophysical Research 108, doi:10.1029/2002JD002558.

Birks, H.J.B., 1977. Modern pollen rain and vegetation of the St. Elias Mountains, Yukon Territory. Canadian Journal of Botany 55, 2367-2382.

Birks, H.J.B., 1995. Quantitative palaeoenvironmental reconstructions. In Maddy, D. & J.S. Brew (eds), Statistical Modelling of Quaternary Science Data. Technical guide 5. Quaternary Research Association, Cambridge, 161-254.

Birks, H.J.B., Monteith, D.T., Rose, N.L., Jones, V.J., Peglar, S.M., 2004. Recent environmental change and atmospheric contamination on Svalbard as recorded in lake sediments – modern limnology, vegetation, and pollen deposition. Journal of Paleolimnology 31, 411-431.

Bonan, G.B., Pollard, D., Thompson, S.L., 1992. Effects of boreal forest vegetation on global climate. Nature 359, 716-718.

Bourgeois, J.C., Gajewski, K., Koerner, R.M., 2001. Spatial patterns of pollen deposition in arctic snow. Journal of Geophysical Research 106, 5255-5265.

Bourgeois, J.C., Koerner, R.M., Gajewski, K., Fisher, D.A., 2000. A Holocene ice-core pollen record from Ellesmere Island, Nunavut, Canada. Quaternary Research 54, 275-283.

Bradley, R.S., Miller, G.H., 1972. Recent climatic change and increased glacierization in the eastern Canadian Arctic. Nature 237, 385-387.

Calcote, R., 1998. Identifying forest stand types using pollen from forest hollows. The Holocene 8, 423-432.

Calcote, R., 2003. Mid-Holocene climate and the hemlock decline : the range limit of *Tsuga canadensis* in the western Great Lakes region, USA. The Holocene 13, 215-224.

Cappelen, J., Jørgensen, B., Laursen, E., Stanius, L., Thomsen, R., 2001. The observed climate of Greenland – with climatological normals, 1961-90. DMI Technical Report No. 00-18.

Dahl, O.S., Nesje, A., 1996. A new approach to calculating Holocene winter precipitation by combining glacier equilibrium-line altitudes and pine-tree limits: a case study from Hardangerjokulen, central southern Norway. The Holocene 6, 381-398.

de Vernal, A., Henry, M., Matthiessen, J., Mudie, P.J., Rochon, A., Boessenkool, K.P., Eynard, F., Grøsfjeld, K., Guiot, J., Hamel, D., Harland, R., Head, M.J., Kunz-Pirrung, M., Levac, E., Loucheur, V., Peyron, O., Pospelova, V., Radi, T., Turon, J.-L., Voronina, E., 2001. Dinoflagellate cyst assemblages as tracers of sea-surface conditions in the northern North Atlantic, Arctic and sub-Arctic seas: the new 'n = 677' data base and its application for quantitative palaeoceanographic reconstruction. Journal of Quaternary Science 16, 681-698.

Dyke, A.S., Dale, J.E., McNeely, R.N., 1996. Marine molluscs as indicators of environmental change in glaciated North America and Greenland during the last 18,000 years. Géographie physique et Quaternaire 36, 5-14.

Environment Canada, 2004. http://climate.weatheroffice.ec.gc.ca/climate_normals

Faegri, K., Iversen, J., 1975. Textbook of Pollen Analysis, 3rd Edition. Blackwell Scientific Publications, Oxford.

Fedorova, I. T., Volkova, Y. A., and Varylguin, E., 1990. World Vegetation Cover Map, pp. Global analog map of 1:80,000,000 scale in Russian polyconical projection, stored in Global Ecosystems Database Version 2.0. USDOC/NOAA National Geophysical Data Center, Boulder, CO.

Foley, J.A., Kutzbach, J.E., Coe, M.T., Levis, S., 1994. Feedbacks between climate and boreal forests during the Holocene epoch. Nature 371, 52-54.

Francis, D., Wolfe, A.P., Walker, I.R., Miller, G.H., 2006. Interglacial and Holocene temperature reconstructions based on midge remains in sediments of two

lakes from Baffin Island, Nunavut, Arctic Canada. Palaeogeography, Palaeoclimatology, Palaeoecology 236, 107-124.

Fréchette, B., Wolfe, A.P., Miller, G.H., Richard, P.J.H., de Vernal, A., 2006. Vegetation and climate of the last interglacial on Baffin Island, Arctic Canada. Palaeogeography, Palaeoclimatology, Palaeoecology 236, 91-106.

Fredskild, B., 1973. Studies in the vegetational history of Greenland. Palaeobotanical investigations of some Holocene lake and bog deposits. Meddelelser om Grønland 198 (4), 245 pp.

Fredskild, B., 1983. The Holocene vegetational development of the Godhåbsfjord area, West Greenland. Meddelelser om Grønland, Geoscience 10, 28 p.

Fredskild, B., 1985. The Holocene vegetational development of Tugtuligssuaq and Qeqertat, Northwest Greenland. Meddelelser om Grønland, Geoscience 14, 20 p.

Fredskild, B., 1991. The genus Betula in Greenland – Holocene history, present distribution and synecology. Nordic Journal of Botany 11, 393-412.

Fredskild, B., 1992. Erosion and vegetational changes in South Greenland caused by agriculture. Geografisk. Tidsskrift 92, 14-21.

Gajewski, K., 1991. Représentation pollinique actuelle à la limite des arbres au Nouveau Québec. Canadian Journal of Earth Sciences 28, 643-648.

Gajewski, K., 1995. Modern and Holocene pollen assemblages from some small Arctic lakes on Somerset Island, N.W.T., Canada. Quat. Res. 44, 228-236.

Gajewski, K., 2002. Modern pollen assemblages in lake sediments from the canadian Arctic. Arctic, Antarctarctic, and Alpine Research 34, 26-32.

Gajewski, K., Frappier, M., 2001. A Holocene lacustrine record of environmental change in northeastern Prince of Wales Island, Nunavut, Canada. Boreas 30, 285-289.

Gajewski, K., Payette, S., Ritchie, J.C., 1993. Holocene vegetation history at the boreal-forest – shrub-tundra transition in north-western Québec. J. Ecol. 81, 433-443.

Gajewski K., Garneau M., Bourgeois J.C., 1995. Paleoenvironments of the Canadian High Arctic derived from pollen and plant macrofossils: problems and potentials. Quaternary Science Reviews 14, 609-629.

Gajewski, K., Garralla, S., Milot-Roy, V., 1996. Postglacial vegetation at the northern limit of lichen woodland in northwestern Québec. Géographie physique et Quaternaire 50, 341-350.

Gauch, H.G.Jr., 1982. Multivariate analysis in community ecology. Cambridge University Press, Cambridge, 298 p.

Gavin, D.G., Oswald, W.W., Wahl, E.R., Williams, J.W., 2003. A statistical approach to evaluating distance metrics and analog assignments for pollen records. Quaternary Research 60, 356-367.

Goodman, M.M., 1972. Distance analysis in biology. Systematic Zoology 21, 174-186.

Gould, W.A., Zoltai, S.E., Raynolds, M., Walker, D.A., Maier, H., 2002. Canadian Arctic vegetation mapping. International Journal of Remote Sensing 23, 4597-4609.

Grimm, E.C., Jacobson Jr., G.L., 1992. Fossil-pollen evidence for abrupt climate changes during the past 18000 years in eastern North America. Climate Dynamics 6, 179-184.

Grove, J.M., 1988. The Little Ice Age. London: Methuen.

Guiot, J., 1987. Late Quaternary climatic change in France estimated from multivariate pollen time series. Quaternary Research 28, 100-118.

Guiot, J., 1990. Methodology of the last climatic cycle reconstruction in France from pollen data. Palaeogeography, Palaeoclimatology, Palaeoecology 80, 49-69.

Guiot, J., Goeury, C., 1996. 3Pbase – a software for statistical analysis of paleoecological and paleoclimatological data. Dendrochronologia 14, 123-135.

Guiot, J., Pons, A., de Beaulieu, J.-L., Reille, M., 1989. A 140,000-year continental climate reconstruction from two European pollen records. Nature 338, 309-313.

Hyvärinen, H., 1985. Holocene pollen stratigraphy of Baird Inlet, east-central Ellesmere Island, Arctic Canada. Boreas 14, 19-32.

Jackson, S.T., Williams, J.W., 2004. Modern analogs in Quaternary paleoecology: here today, gone yesterday, gone tomorrow? Annual Review of Earth and Planetary Sciences 32, 495-537.

Jacobson Jr., G.L., Grimm, E.C., 1988. Synchrony of rapid change in late-glacial vegetation south of the Laurentide ice sheet. Bulletin of the Buffalo Society of Natural Sciences 33, 31-38.

Jacobson Jr., G.L., Webb III, T., Grimm, E.C., 1987. Patterns and rates of vegetation change during the deglaciation of eastern North America. In: Ruddiman, W.F., Wright Jr., H.E. (Eds.), North America and Adjacent Oceans During the Last Deglaciation, vol. k-3. Geology of North America, Geological Survey of America, Boulder, pp. 277-288.

Jongman, R.H.G., Ter Braak, C.J.F., Van Tongeren, O.F.R., 1987. Data analysis in community and landscape ecology. Pudoc, Wageningen.

Kaplan, J.O., Bigelow, N.H., Prentice, I.C., Harrison, S.P., Bartlein, P.J., Christensen, T.R., Cramer, W., Matveyeva, N.V., McGuire, A.D., Murray, D.F., Razzhivin, V.Y., Smith, B., Walker, D.A., Anderson, P.M., Andreev, A.A., Brubaker, L.B., Edwards, M.E., Lozhkin, A.V., 2003. Climate change and Arctic ecosystems: 2. Modeling, paleodata-model comparisons, and future projections. Journal of Geophysical Research 108, doi:10.1029/2002JD002559.

Kerwin, M.K., 2000. Quantifying and modeling Holocene climate variability based on modern and fossil pollen records from the Eastern Canadian Arctic and subarctic. Unpublished Ph.D. thesis, University of Colorado, Boulder, U.S.A.

Kerwin, M.K., Overpeck, J.T., Webb, R.S., Anderson, K.H., 2004. Pollen-based summer temperature reconstructions for the Eastern Canadian Boreal forest, Sub-Arctic and Arctic. Quaternary Science Reviews 23, 1901-1924.

Kerwin, M.K., Overpeck, J.T., Webb, R.S., submitted. Corresponding patterns of modern lake sediment pollen and vegetation in boreal, subarctic, and Arctic regions of eastern Canada. Review of Palaeobotany and Palynology.

Koeppen, W., 1936. Das Geographische System der Klimate. In Handbuch der Klimatologie, Koeppen and R. Geiger eds. Berlin: 636 p.

Koerner, R.M., Fisher, D.A., 1990. A record of Holocene summer climate from a Canadian High Arctic ice core. Nature 343, 630-631.

Krzanowski, W.J., 1971. A comparison of some distance measures applicable to multinomial data, using a rotational fit technique. Biometrics 27, 1062-1068.

Legendre, P., 1993. Spatial autocorrelation: trouble or new paradigm? Ecology 74, 1659-1673.

Legendre, P., Legendre, L., 1998. Numerical ecology, 2nd English edition. Elsevier Science BV, Amsterdam.

Levac, E., de Vernal, A., Blake, W. Jr., 2001. Sea-surface conditions in northernmost Baffin Bay during the Holocene : palynological evidence. Journal of Quaternary Science 16, 353-363.

MacDonald, G.M., Ritchie, J.C., 1986. Modern pollen spectra from the western interior of Canada and the interpretation of late Quaternary vegetation development. New Phytologist 102, 245-268.

McAndrews, J.H., Berti, A.A., Norris, G., 1973. Key to the Quaternary pollen and spores of the great Lakes region. Life Science Miscellaneous Publications, Royal Ontario Museum, Toronto, Canada.

Miller, G.H., Mode, W.N., Wolfe, A.P., Sauer, P.E., Bennike, O., Forman, S.L., Short, S.K., Stafford Jr., T.W., 1999. Stratified interglacial lacustrine sediments from Baffin Island, Arctic Canada: chronology and paleoenvironmental implications. Quaternary Science Reviews 18, 789-810.

Miller, G.H., Wolfe, A.P., Steig, E.J., Sauer, P.E., Kaplan, M.R., Briner, J.P., 2002. The Goldilocks dilemma: big ice, little ice, or 'just-right' ice in the Eastern Canadian Arctic. Quaternary Science Reviews 21, 33-48.

Miller, G.H., Wolfe, A.P., Briner, J.P., Sauer, P.E., Nesje, A., 2005. Holocene glaciation and climate evolution of Baffin Island, Arctic Canada. Quaternary Science Reviews 24, 1703-1721.

Moore, P.D., Webb, J.A., Collinson, M.E., 1991. Pollen analysis, 2nd edition. Blackwell Scientific Publications, Oxford.

Muller, S.D., Richard, P.J.H., Guiot, J., de Beaulieu, J.-L., Fortin, D., 2003. Postglacial climate in the St. Lawrence lowlands, southern Québec : pollen and lake-level evidence. Palaeogeography, Palaeoclimatology, Palaeoecology 193, 51-72.

Nesje, A., 1992. A piston corer for lacustrine and marine sediments. Arctic Alpine Research 24, 257-259.

Nesje, A., Matthews, J.A., Dahl, S.O., Berrisford, M.S., Andersson, C., 2001. Holocene glacier fluctuations of Flatebreen and winter-precipitation changes in the Jostedalsbreen region, western Norway, based on glaciolacustrine sediment records. The Holocene 11, 267-280.

Nichols, H., Kelly, P.M., Andrews, J.T., 1978. Holocene palaeo-wind evidence from palynology in Baffin Island. Nature 273, 140-142.

Oswald, W.W., Anderson, P.M., Brubaker, L.B., Hu, F.S., Engstrom, D.R., 2003. Representation of tundra vegetation by pollen in lake sediments of northern Alaska. Journal of Biogeography 30, 521-535.

Overpeck, J.T., Webb, T., III, Prentice, I.C., 1985. Quatitative interpretation of fossil pollen spectra: dissimilarity coefficients and the method of modern analogs. Quaternary Research 23, 87-108.

Payette, S., 1983. The forest tundra and present tree-lines of the northern Québec-Labrador peninsula. Nordicana 47, 3-23.

Pielke, R.A., Vidale, P.L., 1995. The boreal forest and the polar front. Journal of Geophysical Research 100, 755-758.

Pienitz, R., Douglas, M.S.V., Smol, J.P., 2004. Long-Term Environmental Change in Arctic and Antarctic Lakes. Developments in Paleoenvironmental Research Vol. 8. Springer Verlag, Dordrecht.

Prentice, I.C., 1980. Multidimensional scaling as a research tool in Quaternary palynology: a review of theory and methods. Review of Palaeobotany and Palynology 31, 71-104.

Richard, P.J.H., 1970. Atlas pollinique des arbres et de quelques arbustes indigènes du Québec. Naturaliste Canadien 97, 1-34, 97-161, 241-306.

Richard, P.J.H., 1979. Contributions à l'histoire postglaciaire de la végétation au nord-est de la Jamésie, Nouveau-Québec. Géographie Physique et Quaternaire 33, 93-112.

Richard, P.J.H., 1981. Paléophytogéographie postglaciaire en Ungava par l'analyse pollinique. Collection Paléo-Québec 13, Université du Québec à Trois-Rivières, Trois-Rivières.

Richard, P.J.H., Bouchard, M.A., Gangloff, P., 1991. The significance of pollen-rich inorganic lake sediments in the Cratère du Nouveau-Québec area, Ungava, Canada. Boreas 20, 135-149.

Richard, P.J.H., 1995. Le couvert végétal du Québec-Labrador il y a 6000 ans BP: Essai. Géographie physique et Quaternaire 49, 117-140.

Ritchie, J.C., 1974. Modern pollen assemblages near the arctic treeline, Mackenzie Delta region, Northwest Territories. Canadian Journal of Botany 52, 381-396.

Ritchie, J.C., Hadden, K.A., Gajewski, K., 1987. Modern pollen spectra from lakes in arctic western Canada. Canadian Journal of Botany 65, 1605-1613.

Sandgren, P., Fredskild, B., 1991. Magnetic measurements as recorders of Late Holocene man-induced erosion in the interior of South Greenland. Boreas 20, 315-331.

Sawada, M., Viau, A.E., Vettoretti, G., Peltier, W.R., Gajewski, K., 2004. Comparison of North-American pollen-based temperature and global lake-status with CCCma AGCM2 output at 6ka. Quaternary Science Reviews 23, 225-244.

Seppä, H., Birks, H.J.B., 2001. July mean temperature and annual precipitation trends during the Holocene in the Fennoscandian tree-line area: pollen-based climate reconstructions. The Holocene 11, 527-539.

Seppä, H., Birks, H.J.B., 2002. Holocene climate reconstructions from the Fennoscandian tree-line area based on pollen data from Toskaljavri. Quaternary Research 57, 191-199.

Seppä, H., Cwynar, L.C., MacDonald, G.M., 2003. Post-glacial vegetation reconstruction and a possible 8200 cal. yr BP event from the low arctic continental Nunavut, Canada. Journal of Quaternary Science 18, 621-629.

Shuman, B., Bartlein, P.J., Webb III, T., 2005. The magnitudes of millennial- and orbital-scale climatic change in eastern North America during the Late Quaternary. Quaternary Science Reviews 24, 2194-2206.

Steig, E.J., Wolfe, A.P., Miller, G.H., 1998. Wisconsinan refugia and the late glacial history of eastern Baffin Island, Arctic Canada: Coupled evidence from cosmogenic isotopes and lake sediments. Geology 26, 835-838.

Stuiver, M., Grootes, P.M., Braziunas, T.F., 1995. The GISP2 18O record of the past 16,500 yrs and the role of the sun, ocean and volcanoes. Quaternary Research 44, 341-354.

Stuiver, M., Reimer, P. J., 1993. Extended 14C database and revised CALIB radiocarbon calibration program. Radiocarbon 35, 215-230.

Stuiver, M., Reimer, P.J., Bard, E., Beck, J.W., Burr, G.S., Hughen, K.A., Kromer, B., McCormac, F.G., v. d. Plicht, J., Spurk, M.,1998. INTCAL98 Radiocarbon age calibration 24,000 - 0 cal BP. Radiocarbon 40, 1041-1083.

Telford, R.J., Andersson, C., Birks, H.J.B., Juggins, S., 2004. Biases in the estimation of transfer function prediction errors. Paleoceanography 19, PA4014, doi:10.1029/2004PA001072.

Telford, R.J., Birks, H.J.B., 2005. The secret of transfert functions: problems with spatial autocorrelation in evaluating model performance. Quaternary Science Reviews 24, 2173-2179.

ter Braak, C.J.F, Prentice, I.C., 1988. A theory of gradient analysis. Advances in ecological research 18, 271-317.

ter Braak, C.J.F., Šmilauer, P., 1998. CANOCO for windows: software for Canonical Community Ordination (version 4). Microcomputer Power, Ithaca, NY, USA.

ter Braak, C.J.F., Verdonschot, P.F.M., 1995. Canonical correspondence analysis and related multivariate methods in aquatic ecology. Aquatic Sciences 57, 255-289.

Waelbroeck, C., Labeyrie, L., Duplessy, J.-C., Guiot, J., Labracherie, M., Leclaire, H., Duprat, J., 1998. Improving past sea surface temperature estimates based on planktonic faunas. Paleoceanography 13, 272-283.

Wahl, E.R., 2004. A general framework for determining cutoff values to select pollen analogs with dissimilarity metrics in the modern analog technique. Review of Palaeobotany and Palynology 128, 263-280.

Whitmore, J., Gajewski, K., Sawada, M., Williams, J.W., Shuman, B., Bartlein, P.J., Minckley, T., Viau, A.E., Webb III, T., Shafer, S., Anderson, P., Brubaker, L., 2005. Modern pollen data from North America and Greenland for multi-scale paleoenvironmental applications. Quaternary Science Reviews 24, 1828-1848.

Wohlfahrt, J., Harrison, S.P., Braconnot, P., 2004. Synergistic feedbacks between ocean and vegetation on mid- and high-latitude climates during the mid-Holocene. Climate Dynamics 22, 223-238.

Wolfe, A.P., Fréchette, B., Richard, P.J.H., Miller, G.H., Forman, S.L., 2000. Paleoecology of a >90,000-year lacustrine sequence from Fog Lake, Baffin Island, Arctic Canada. Quaternary Science Reviews 19, 1677-1699.

Wolfe, A.P., Miller, G.H., Olsen, C.A., Forman, S.L., Doran, P.T., Holmgren, S.U., 2004. Geochronology of high latitude lake sediments. In R. Pienitz, M.S.V. Douglas and J.P. Smol (Eds). Long-term Environmental Change in Arctic and Antartic Lakes. Developments in Paleoenvironmental Research, vol. 8, Springer, The Netherlands, pp 19-52.

Wolken, G.J., England, J.H., Dyke, A.S., 2005. Re-evaluating the relevance of vegetation trimlines in the Canadian Arctic as an indicator of Little Ice Age paleoenvironments. Arctic 58, 341-353.

Young, S.B., 1971. The vascular flora of St-Lawrence Island with special reference to floristic zonation in the arctic region. Contribution of the Herbarium of Harvard University 201, 11-115.

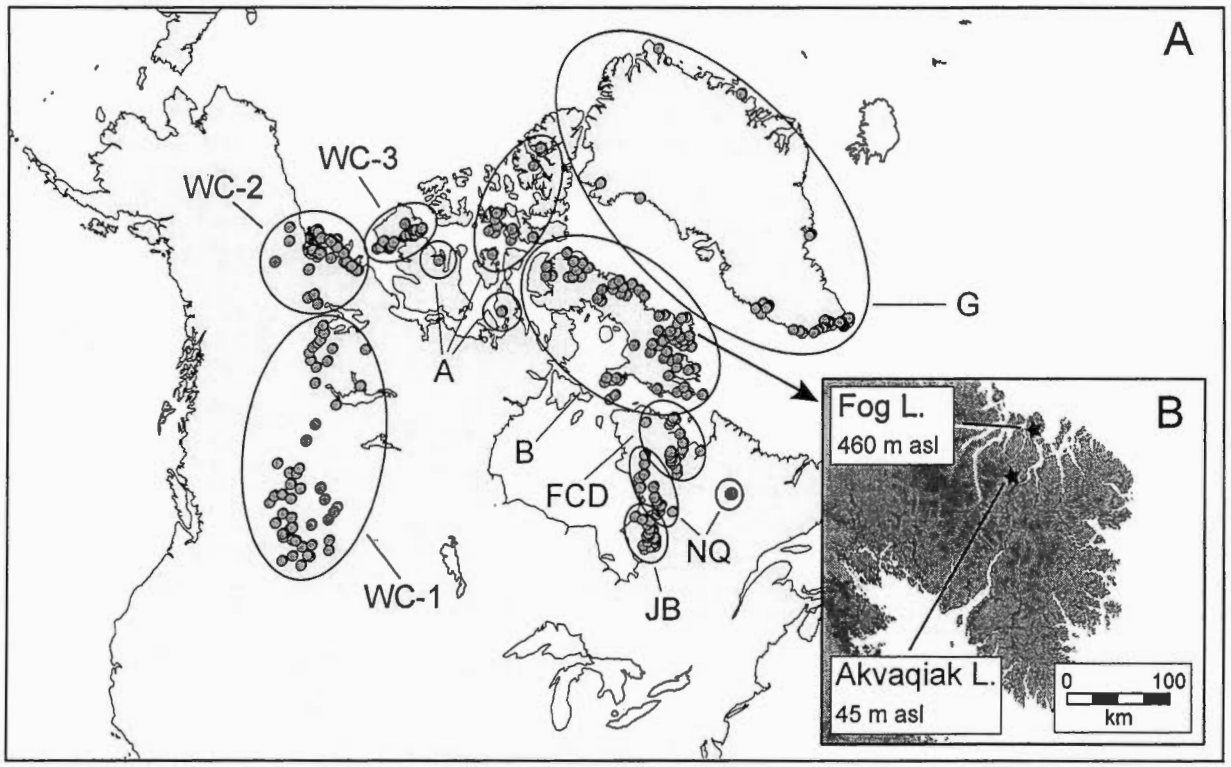

Figure 1. A. Locations of the 400 lake sediment samples used to develop the modern pollen database. The sites have been grouped in nine geographical regions: Western Canada (WC), James Bay (JB), northern Québec (NQ), Fort Chimo-Diana Bay (FCD), Baffin Island (B), Canadian Arctic Archipelago (A)

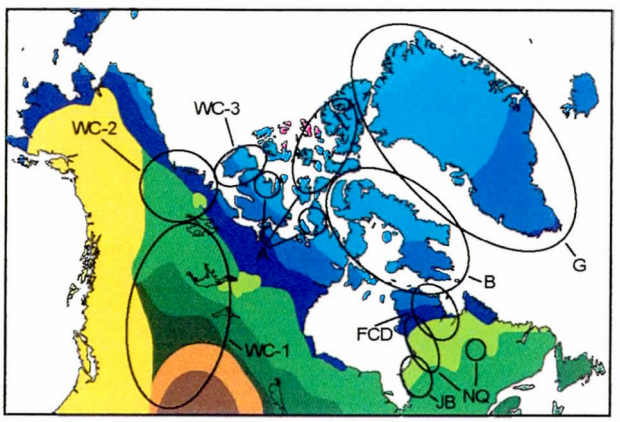

Arctic

- Rock desert : cushion forb, lichen and moss tundra
- High Arctic tundra : prostrate dwarf-shrub tundra
- Mid Arctic tundra : hemiprostrate dwarf-shrub tundra
- Low Arctic tundra : erect dwarf-shrub tundra
- Subarctic tundra : low- and high-shrub tundra

Boreal

- Forest tundra
- Northern taiga
- Central taiga
- Southern taiga

Coastal - Mountain

- Mountain vegetation

Prairies

- Parkland
- Grassland

Figure 2. Major vegetation zones of northern North America and Greenland synthesized from Young (1971), Payette (1983), Anderson et al. (1989),

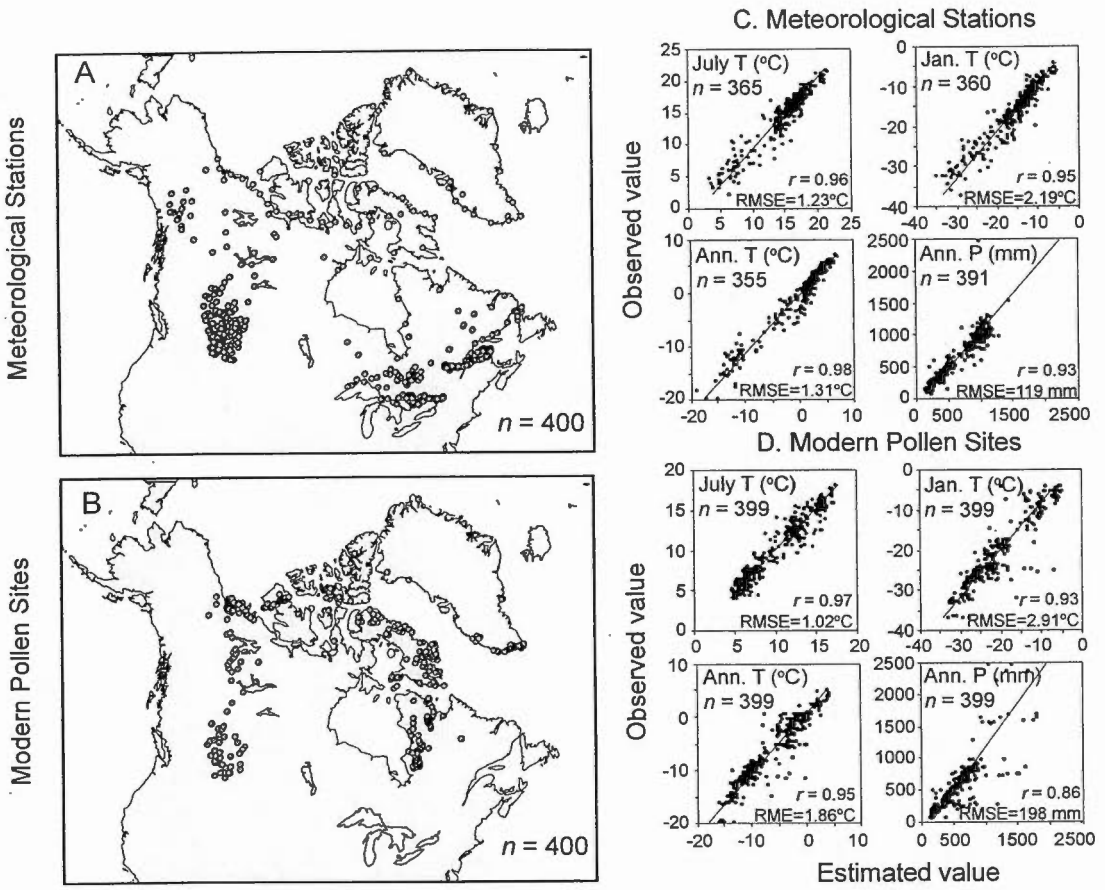

Figure 3. A. Location map of the 400 meteorological stations used for the interpolation of climate data to the modern pollen sites. B. Location map of the 400 modern pollen sites used for climate inference model development. C. Comparisons between observed and interpolated climate data for the 400 stations. The x-axis shows estimates derived from weighted-averages of all meteorological stations located within a 10° radius of latitude and longitude of each station's location. D. Comparisons between measured and pollen-inferred modern climate variable for the 400 lake sites, using the BMA model. The x-axis shows estimates from surface sediment pollen assemblages. In each case for C and D, linear correlation coefficients (r) and root mean squared errors (RMSE) provide measures of the accuracy of estimates.

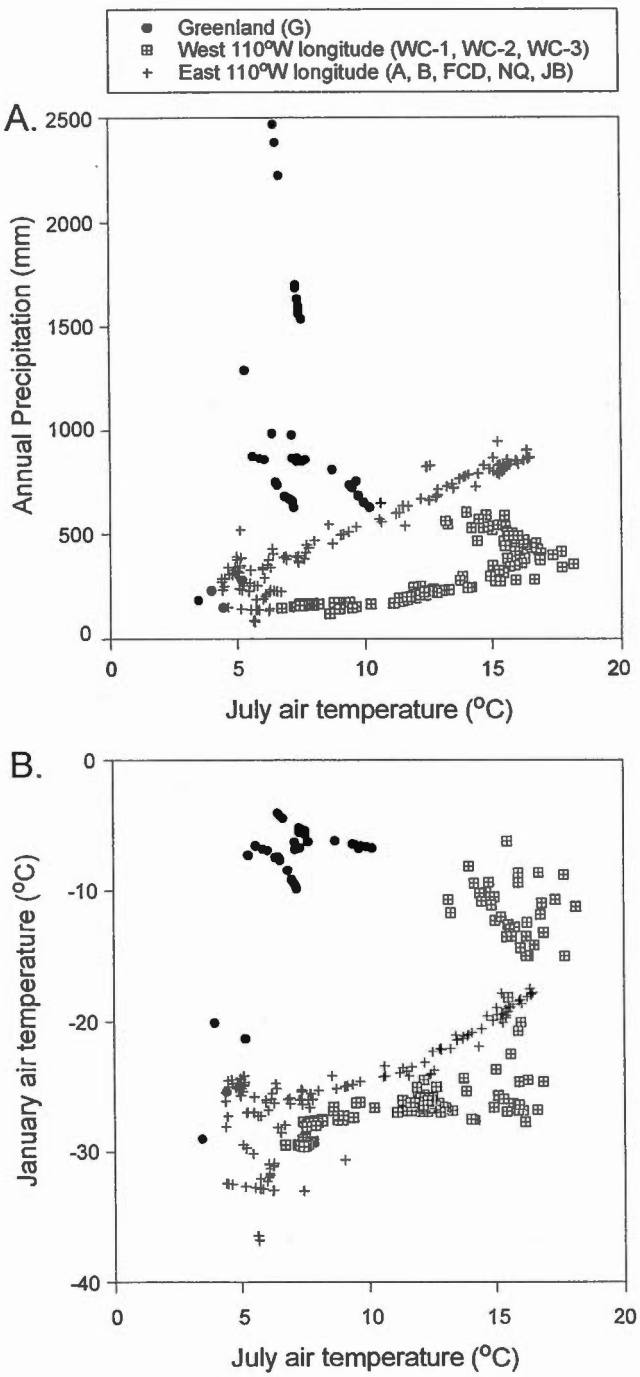

Figure 4. A. Relationship between interpolated annual precipitation and July temperature for the 400 modern lake localities. B. Relationship between interpolated January and July air temperatures for the same sites.

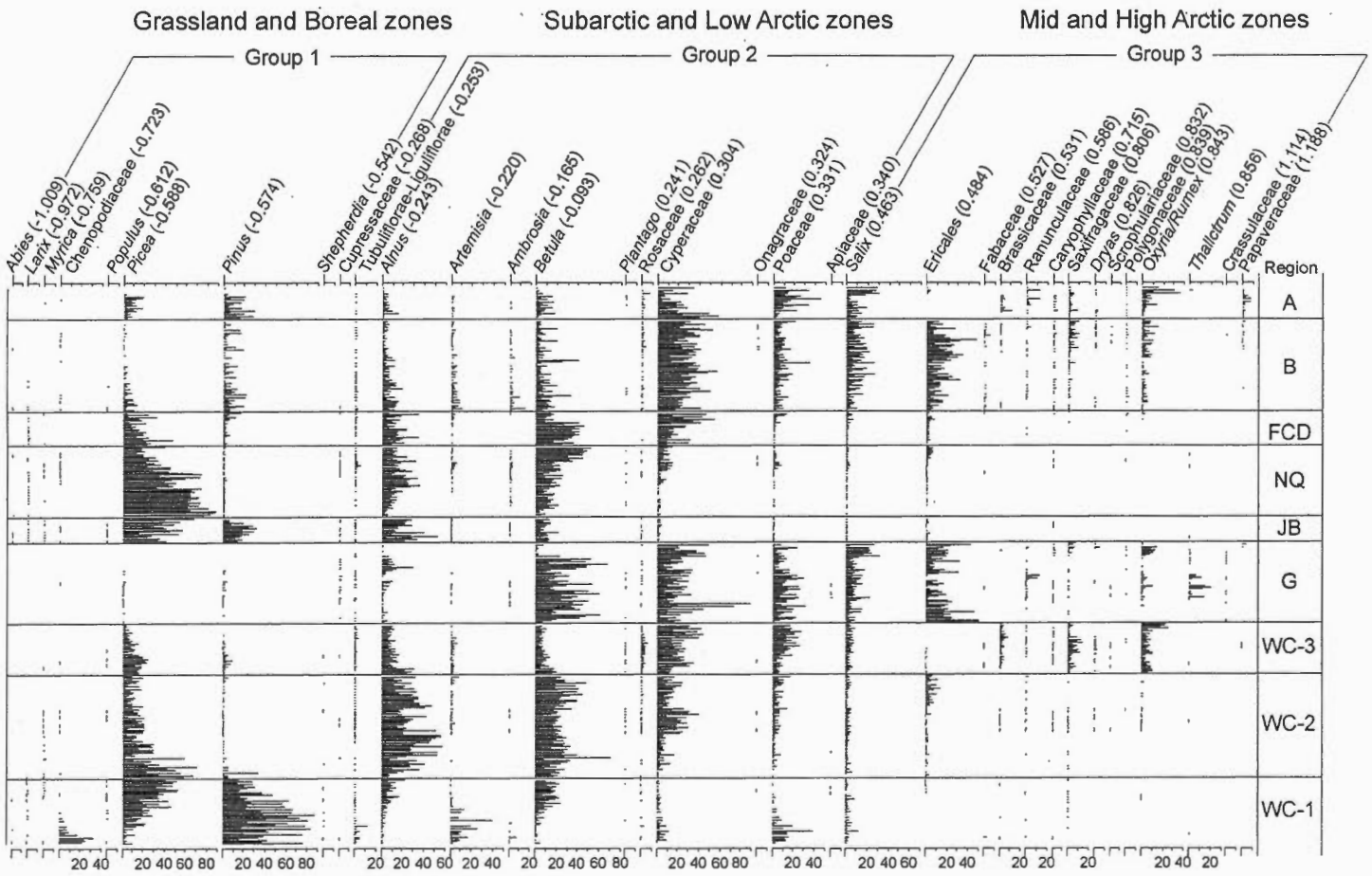

Figure 5. Relative frequencies of pollen assemblages from the 400 modern lake sediment samples, for the 34 taxa pruned and re-summed from the orginal count data, according to procedures outlined in the text. Taxa are ordered according to their scores on the primary CCA axis (Fig. 7B), which appear in brackets. In general, this ordering progresses from taxa typical of warmer (boreal) environnments on the left, to those characterizing sites that are increasingly polar to the right. Horizontal lines demarcate the various geographic regions given in Fig. 1. Within each of these regions, individual assemblages are arranged according to latitude, from low (bottom) to high (top).

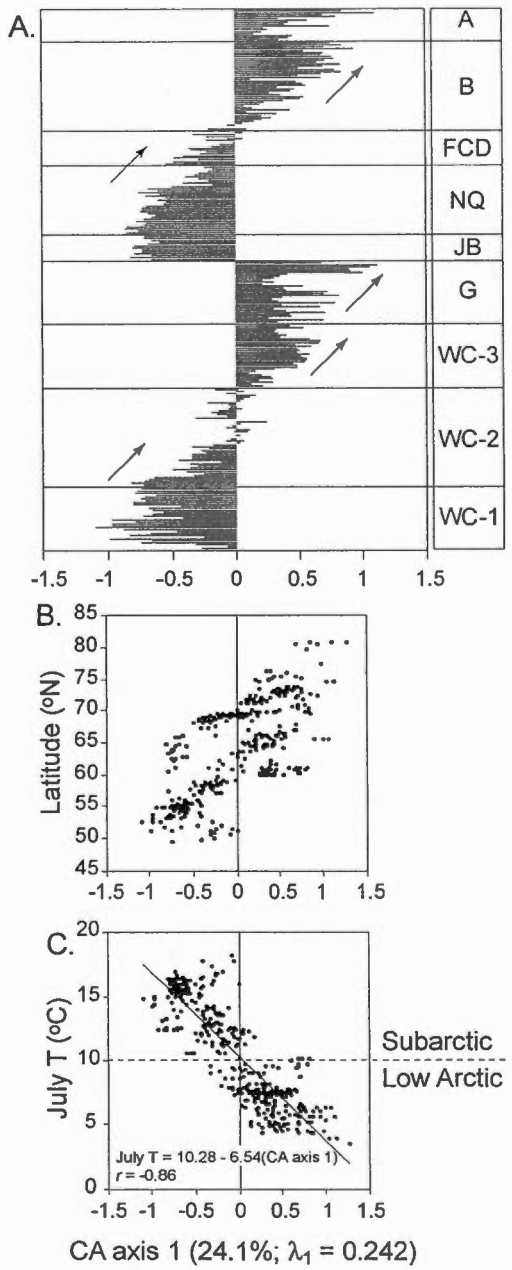

Figure 6. Correspondence analysis (CA) of the square-root transformed modern pollen assemblage frequencies. A. Plot of CA sample scores on the first axis, ordered for each region as in Fig. 5, using distance joint plot scaling (site-conditional CA joint plot, i.e. scaling type 1) for which distances between pollen sites approximate their chi-square distances. Arrows illustrate concomitant increases of CA axis 1 sample scores with latitude within each region. B. Relationship between CA axis 1 site scores and latitude. C. Plot of CA axis 1 sample scores against July air temperature (Fréchette et al., 2006). The horizontal dashed line separates subarctic (forest tundra) from low arctic (shrub tundra) sites, approximated by the 10°C July isotherm.

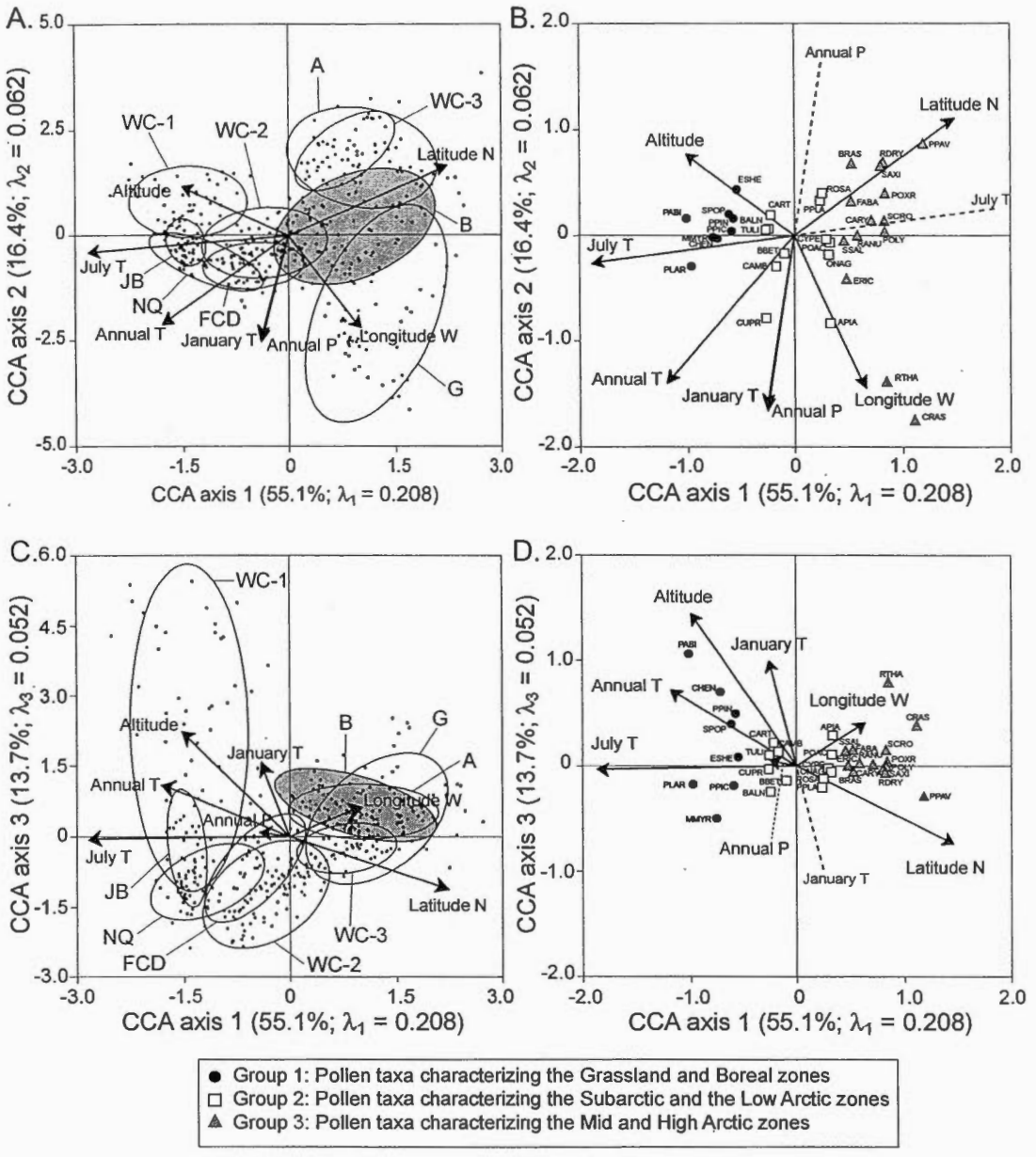

Figure 7. Canonical correspondence analysis (CCA) ordination biplots of the modern pollen assemblages, using correlation biplot scaling (taxa-conditional biplot, i.e. scaling type 2) for which distances between pollen taxa approximate their interspecific correlation. Biplots representing sites (and regions) and environmental variables (arrows) on CCA axes 1 and 2 (A) and CCA axes 1 and 3 (C). 95% ellipses encircle each region. Biplots representing species (symbols) and environmental variables (arrows) on CCA axes 1 and 2 (B) and CCA axes 1 and 3 (D). Taxon codes are given in Table 1. For clarity, the lenghts of all arrows have been multiplied by either 3 (A, C) or 2 (B, D). Note that, in A and B, January air temperature and annual precipitation gradients are nearly perfectly superimposed.

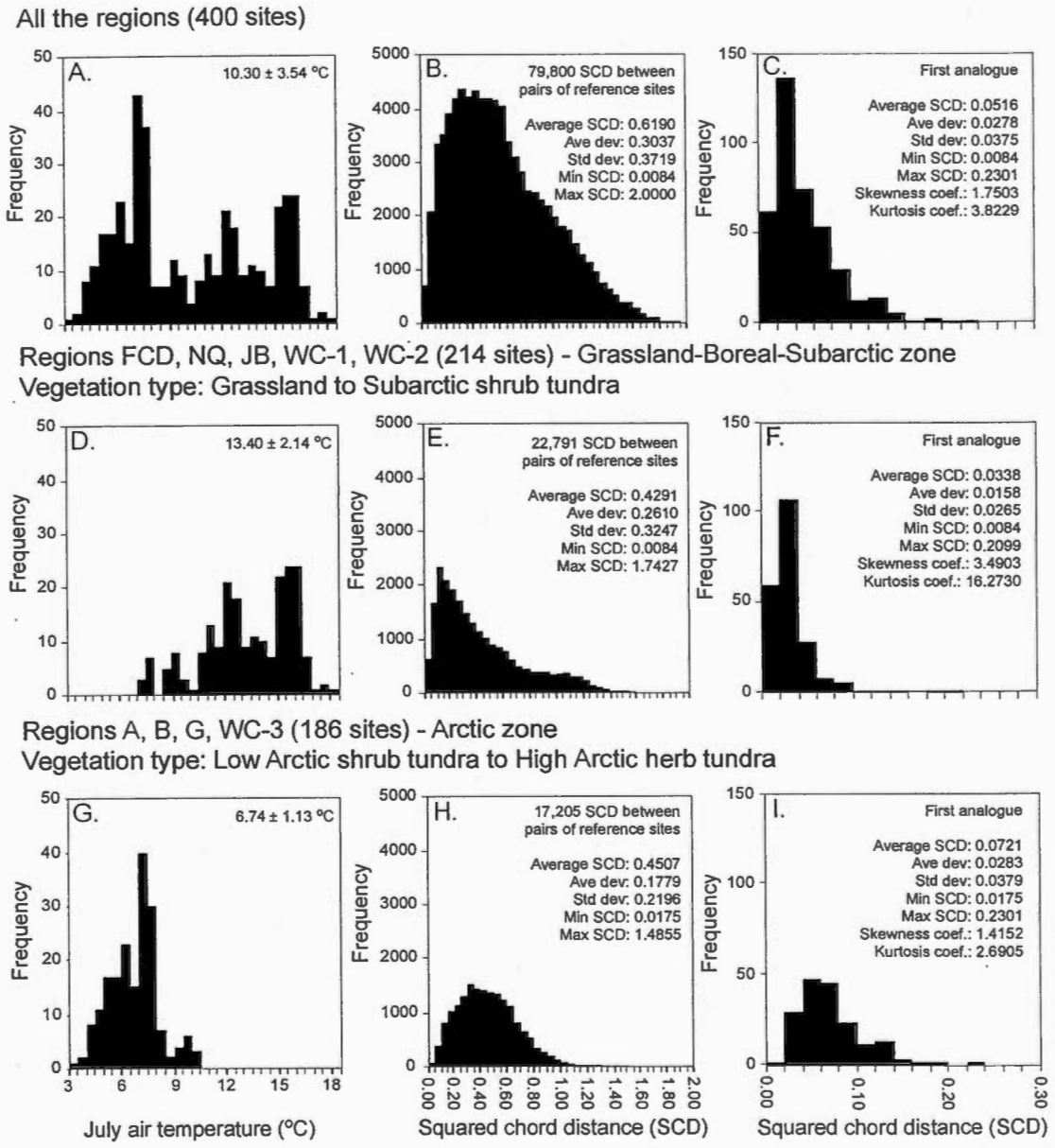

Figure 8. Relationships between vegetation type and the frequency distribution of mean July air temperature values at the 400 modern sites (A), the 214 site subset representing grassland, boreal and subarctic biomes (D), and the remaining 186 arctic (tundra) sites (G). Similar plots are shown for the frequency distributions of pair-wise SCD dissimilarities between modern pollen assemblages (0.05 increments) for each of the total (B), grassland, boreal and subarctic (E), and arctic (H) subsets of the data. Between-biome differences underly the contrasting shapes of the curves in E and H. Finally, frequency distributions of SCD for the first (closest) analogue (0.02 increments) are illustrated for all sites (C) as well as grassland, boreal and subarctic sites (F) and those from low to high artic tundra (I).

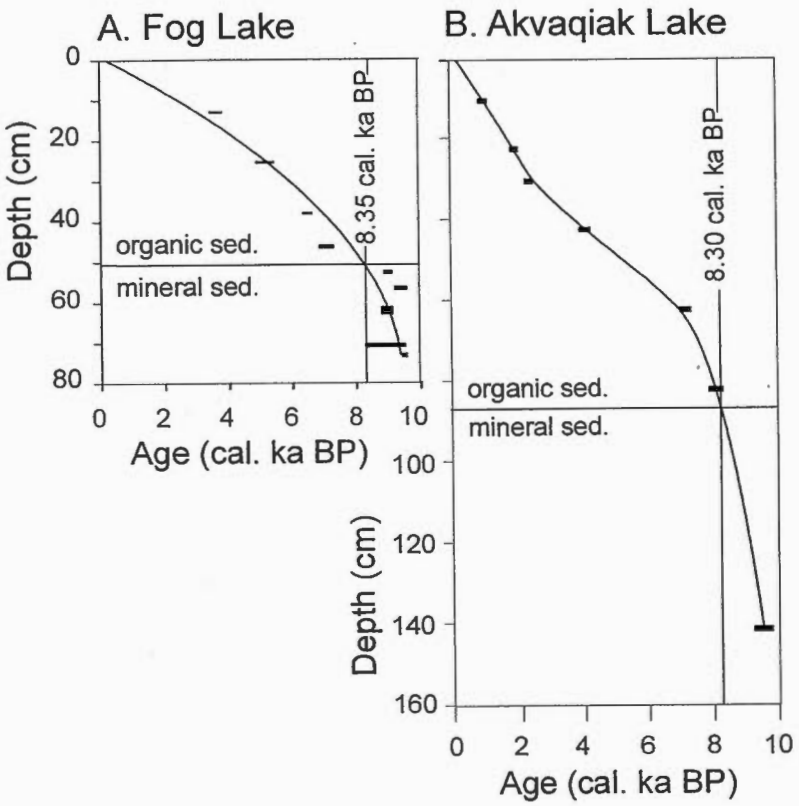

Figure 9. Age-depth curves for the Fog (A) and Akvaqiak (B) lake sediment cores. Fog's model is a polynomial function of order 3 fitted to the available calibrated radiocarbon ages and Akvaqiak's model is a smoothed linear interpolation between the available calibrated radiocarbon ages.

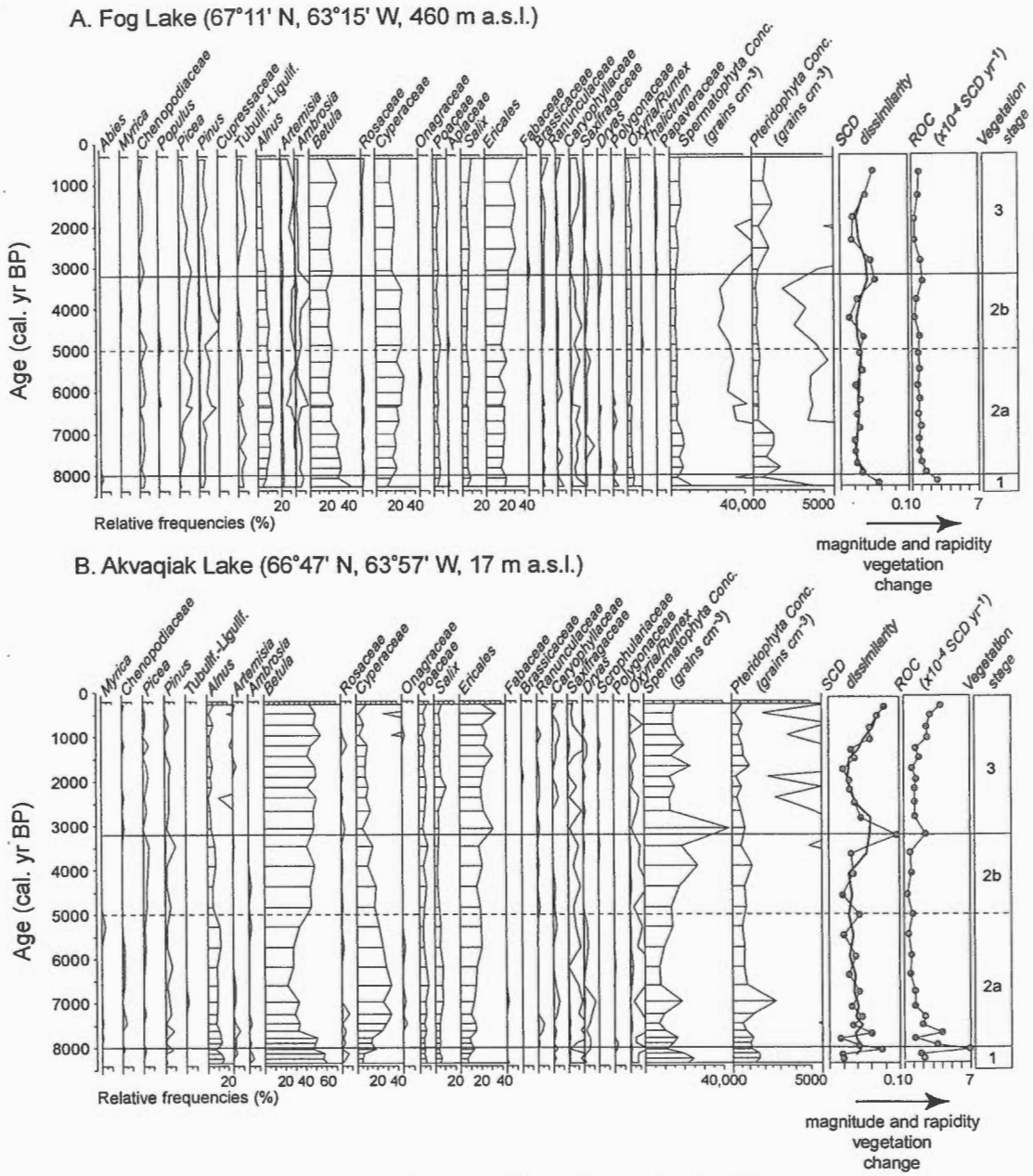

Figure 10. Summary pollen diagrams from Fog (A) and Akvaqiak (B) lakes (analyst: Bianca Fréchette). Hollow curves are 10x exaggerations of pollen relative frequencies. Pollen sums and the ordering of taxa are as in Fig. 5 (warmer on left, colder on right). Spermatophyta concentrations include several taxa outside the 34 principal taxa that form the sum (n = 50 for Fog and 41 for Akvaqiak). Pteridophyta concentrations include all spore types (n = 8 for Fog and 7 for Akvaqiak). SCD between adjacent assemblages are based on percentages of the 34 principal taxa, as are ROC values. Thickened lines for SCD are 3-point moving averages. Horizontal lines delimit major (solid) and minor (dashed) pollen assemblage zones.

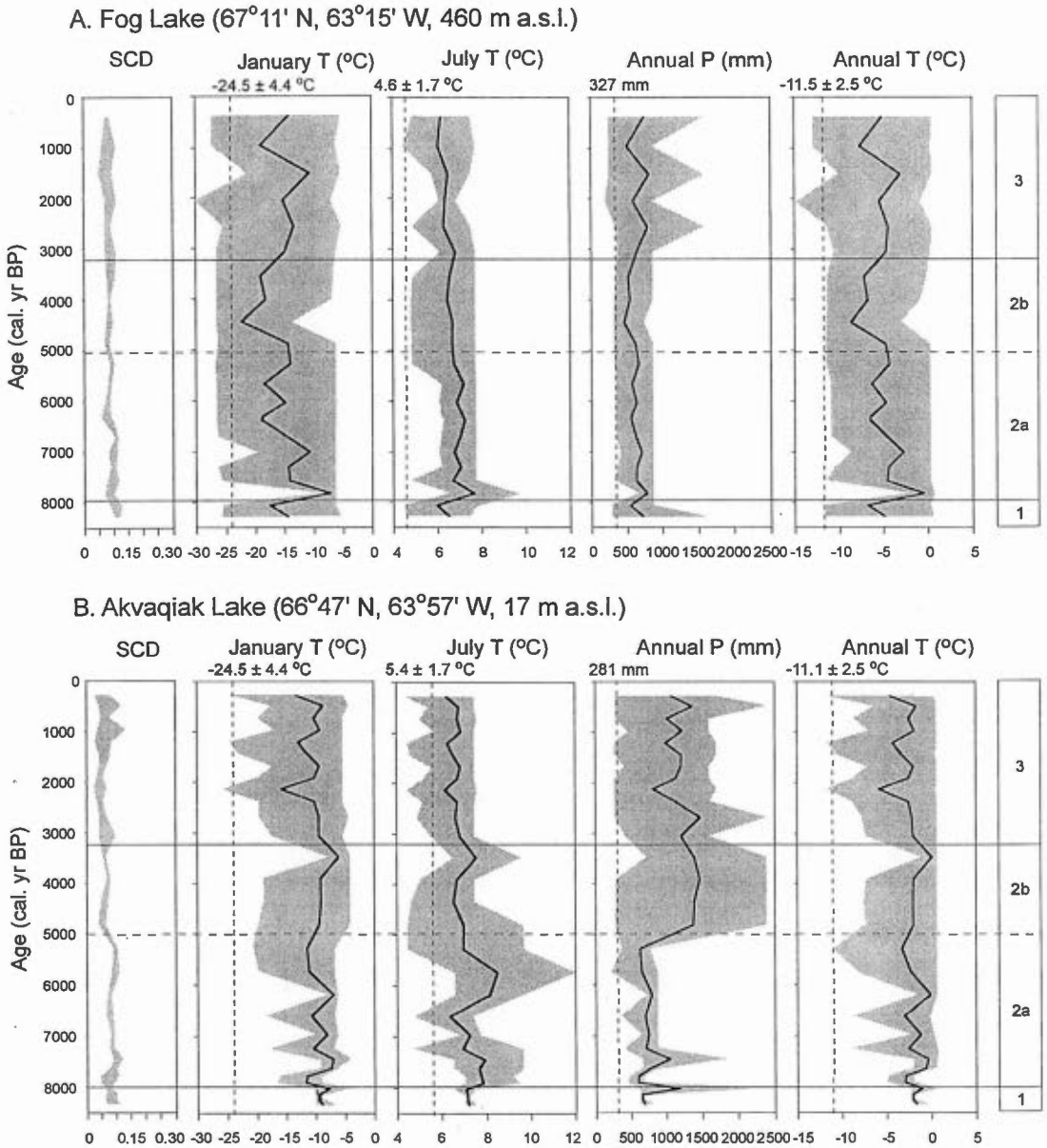

Figure 11. Climate reconstructions from pollen assemblages in Fog (A) and Akvaqiak (B) lake cores, using the best modern analogue (BMA) technique. Dashed vertical lines indicate modern values interpolated for each site, and values are given above the curves. Confidence intervals for each parameter correspond to the five best analogues in the modern data base, and are shown by gray shading. The SCD of the best analogues is given on the left of the diagram, indicating that all reconstruction fall well-within the adopted SCD threshold of 0.31. Horizontal lines delimit pollen zones as in Fig 10. RMSE for January air temperature is ±2.91°C, ±1.02°C for July air temperature, ±1.45 °C for mean annual air temperature, and ±198.17 mm for annual precipitation.

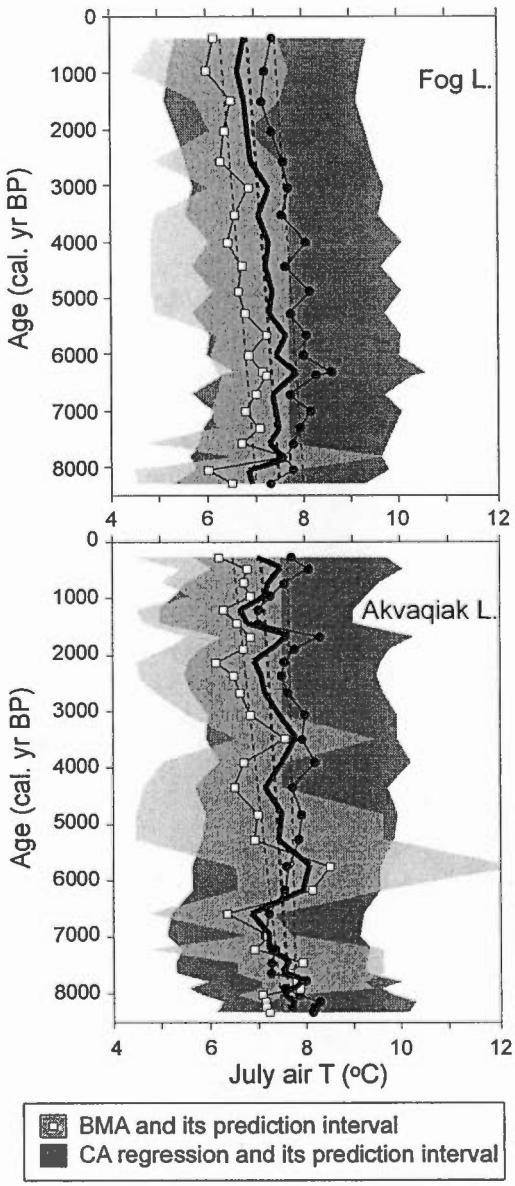

Figure 12. Reconstruction of July air temperatures by correspondence analysis (CA) regression (black circle) and comparison with the same quantity reconstructed by the BMA method (white square) for Fog and Akvaqiak lake cores. The CA regression used is: July air temperature = 10.28-(6.54xCA axis1 sample score). The thick black lines represent consensus curves constructed by averaging the CA and BMA reconstructions from each sample. The dark gray envelope is the confidence intervals for the CA-based reconstruction, representing ±1.98°C. The lighter envelope corresponds to the BMA reconstruction's confidence interval as given in Fig. 11, corresponding to the five best analogues. Since each of these reconstructions reveals a progressive Holocene cooling trend, linear fits for each have been fitted (dashed lines) from 8000 to ~300 cal. year BP. This amounts to July cooling in the order of 0.7°C (BMA), 0.6°C (CA), and 0.7°C (consensus) for Fog Lake, and 1.0°C (BMA), 0.1°C (CA), and 0.6°C (consensus) at Akvaqiak Lake.

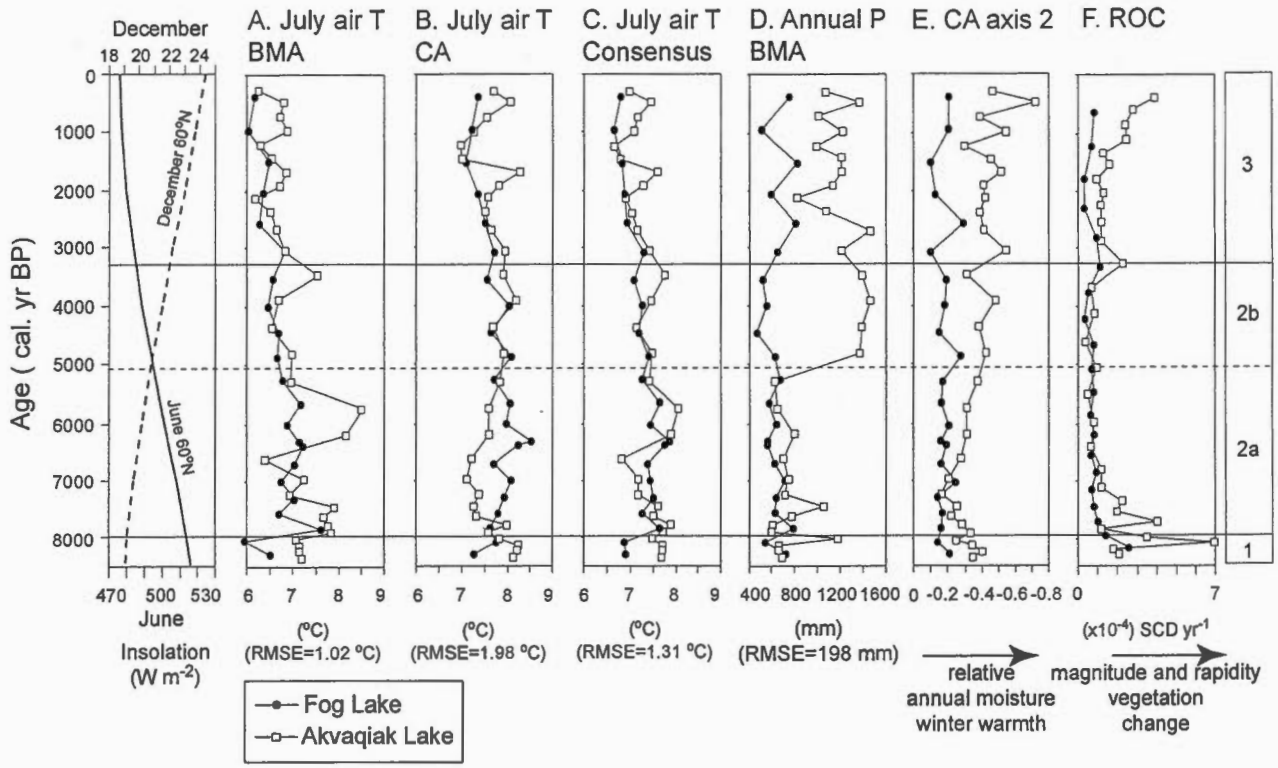

Figure 13. Time-series summarizing Holocene climate amd vegetational development inferred from the Fog (black circles) and Akvaqiak (white squares) lake pollen records. July air temperatures reconstructed by BMA (A), CA regression (B), and consensus (C) methods. RMSE values for each are given. D. Annual precipitation reconstructed by the BMA method. E. Stratigraphic plot of CA axis 2 sample scores, which translates qualitatively the variability in annual moisture and/or winter temperature (cf. Fig. 7B). F. ROC in the two pollen records showing an intial postglacial deceleration in the rates of palynological change prior to 7000 cal. year BP, a subsequent period of relative stability until ~ 4000 cal. year BP, and increased late-Holocene palynological variability, which likely reflects a destabilization of local vegetation dynamics with Neoglacial climate deterioration. In the left panel are Holocene June and December insolation values at 60°N (Berger and Loutre, 1991).

Table 1. List of pollen taxa retained in the 400 site modern lake-sediment pollen database, and their four-letter codes. Some of these taxa result from groupings and deletions (Appendix A), resulting in a 34 taxa total used throughout this study, for which summary statistics are also reported. Taxa that are exotic to the tundra biomes (low to high Arctic) in arctic Canada and Greenland are indicated by *.

Taxa	Code	Range of %	Mean % ± SD	N
Woody plants: trees + shrubs				
*Abies**	PABI	0 - 1.91	0.05 ± 0.20	47
*Alnus**	BALN	0 - 58.20	12.67 ± 11.99	391
Betula	BBET	0 - 71.20	16.80 ± 13.39	396
Cupressaceae	CUPR	0 - 2.46	0.17 ± 0.37	125
Dryas	RDRY	0 - 4.97	0.21 ± 0.51	99
Ericales	ERIC	0 - 49.90	5.50 ± 8.67	322
*Larix**	PLAR	0 - 1.55	0.10 ± 0.24	92
*Myrica**	MMYR	0 - 2.94	0.13 ± 0.34	112
*Picea**	PPIC	0 - 88.72	18.30 ± 20.44	372
*Pinus**	PPIN	0 - 86.86	8.48 ± 15.39	372
*Populus**	SPOP	0 - 1.34	0.06 ± 0.16	70
Salix	SSAL	0 - 61.25	5.15 ± 6.67	376
*Shepherdia**	ESHE	0 - 1.15	0.03 ± 0.13	38
Herbs				
*Ambrosia**	CAMB	0 - 15.04	0.54 ± 1.21	192
Apiaceae	APIA	0 - 1.69	0.02 ± 0.13	20
Artemisia	CART	0 - 40.24	1.70 ± 3.27	326
Brassicaceae	BRAS	0 - 11.18	0.43 ± 1.15	133
Caryophyllaceae	CARY	0 - 3.93	0.34 ± 0.62	185
Chenopodiaceae*	CHEN	0 - 32.39	0.55 ± 2.78	157
Crassulaceae	CRAS	0 - 1.17	0.01 ± 0.09	13
Cyperaceae	CYPE	0 - 89.00	16.61 ± 14.30	398
Fabaceae	FABA	0 - 5.16	0.12 ± 0.37	94
Onagraceae	ONAG	0 - 1.09	0.03 ± 0.12	42
Oxyria/Rumex	POXR	0 - 35.56	2.09 ± 4.33	220
Papaveraceae	PPAV	0 - 7.69	0.15 ± 0.71	46
Plantago	PPLA	0 - 1.32	0.04 ± 0.15	46
Poaceae	POAC	0 - 44.83	6.82 ± 7.30	383
Polygonaceae	POLY	0 - 1.72	0.06 ± 0.22	44
Ranunculaceae	RANU	0 - 12.24	0.36 ± 1.25	145
Rosaceae	ROSA	0 - 6.92	0.53 ± 0.87	250
Saxifragaceae	SAXI	0 - 13.86	0.99 ± 2.09	168
Scrophulariaceae	SCRO	0 - 1.72	0.04 ± 0.18	40
Thalictrum	RTHA	0 - 20.66	0.27 ± 1.73	51
Tubuliflorae/Liguliflorae	TULI	0 - 12.89	0.42 ± 0.90	230

Table 2. AMS ^{14}C dates from Fog and Akvaqiak lake cores used for developing the age-depth model.

Lake	Depth (cm)	Laboratory no.	Material	AMS ^{14}C date (yr BP)	Corr. date (yr BP)	Cal. date (yr BP)	Range of solution at 95.4% (2 σ)
Fog	12.5 - 13.0	CAMS-30531	Humic acids	3600 ± 70*	3430	3655	3868 - 3475
	25.0 - 25.5	CAMS-30532	Humic acids	4690 ± 70*	4520	5140	5447 - 4874
	37.5 - 38.0	CAMS-30533	Humic acids	5910 ± 50*	5740	6499	6716 - 6408
	45.5 - 46.5	CAMS-30535	Macroflora	6150 ± 70*	-	7133	7248 - 6801
	45.5 - 46.5	CAMS-30534	Humic acids	6320 ± 50*	-	-	-
	52.0 - 53.0	CAMS-34298	Macroflora	8130 ± 50*	-	9028	9263 - 8999
	56.0 - 57.0	CAMS-28649	Macroflora	8370 ± 60*	-	9428	9525 - 9149
	61.0 - 63.0	CAMS-30536	Macroflora	8030 ± 50*	-	9000	9028 - 8661
	66.0 - 67.0	CAMS-34299	Humic acids	14,630 ± 60*#	-	-	-
	70.0 - 71.0	OS-26222	Chitin	7950 ± 240	-	8887	9473 - 8219
	71.0 - 72.5	CAMS-31806	Humic acids	16,040 ± 70*#	-	-	-
	72.5 - 73.5	OS-25733	Macroflora	8530 ± 70	-	9529	9600 - 9431
	75.0 - 76.0	CAMS-34300	Humic acids	15,690 ± 70*#	-	-	-
Akvaqiak	11.0 - 12.0	NSRL-11345	Macroflora	1000 ± 50	-	929	790 - 1046
	11.0 - 12.0	NSRL-11346	Humic acids	1700 ± 45	-	-	-
	23.0 - 24.0	NSRL-10621	Humic acids	2510 ± 45	1973	1908	1822 - 2035
	31.0 - 32.0	NSRL-11347	Macroflora	2270 ± 60	-	2329	2124 - 2356
	31.0 - 32.0	NSRL-11348	Humic acids	2840 ± 55	-	-	-
	43.0 - 44.0	NSRL-10622	Humic acids	4290 ± 50	3753	4122	3931 - 4251
	63.0 - 64.0	NSRL-10623	Humic acids	6810 ± 55	6273	7217	7012 - 7311
	82.5 - 83.5	NSRL-10624	Humic acids	7670 ± 60	-	-	-
	82.5 - 83.5	NSRL-10176	Macroflora	7330 ± 95	-	8116	7945 - 8352
	142.0 - 143.0	NSRL-10139	Macroflora	8560 ± 100	-	9533	9331 - 9885
	159.5 - 160.5	NSRL-13332	Humic acids	21,590 ± 75#	-	-	-

* Wolfe et al. (2000)

Date excluded (assumed to contain reworked humic material; Wolfe et al., 2004)

Table 3. Environmental characteristics of the modern lake sediment sites, given by summary statistics for each of the represented regions. Grassland, boreal, and subarctic sites include WC-1, WC-2, JB, NQ, and FCD. Arctic tundra sites include WC-3, G, B, A.

Region and Statistic	Altitude m asl	Annual P mm	Annual T °C	January T °C	July T °C
WC-1 (n = 47)					
Min	180	283.82	-4.68	-27.69	13.17
Max	2000	603.85	5.05	-6.24	18.18
Mean	802	453.88	1.44	-14.99	15.79
SD	386	78.01	2.62	6.17	1.07
WC-2 (n = 73)					
Min	10	121.71	-11.56	-27.69	7.45
Max	620	327.78	-4.14	-24.33	15.95
Mean	162	209.88	-8.96	-26.61	11.51
SD	137	43.10	1.76	0.81	2.25
WC-3 (n = 38)					
Min	35	148.19	-13.57	-29.61	6.75
Max	610	167.68	-11.49	-27.49	8.20
Mean	279	160.49	-12.48	-28.66	7.65
SD	153	4.57	0.65	0.79	0.30
JB (n = 18)					
Min	130	726.85	-2.18	-21.89	13.44
Max	340	868.73	0.72	-17.75	16.49
Mean	234	821.33	-0.26	-19.02	15.63
SD	60	42.40	0.89	1.18	0.81
NQ (n = 51)					
Min	84	945.96	0.67	-17.47	16.38
Max	579	556.86	-6.06	-24.15	10.61
Mean	305	780.22	-2.43	-20.95	13.74
SD	155	109.59	2.31	2.49	2.00
FCD (n = 25)					
Min	50	454.83	-8.30	-25.14	8.75
Max	512	866.55	-0.89	-18.90	15.06
Mean	222	664.34	-4.63	-22.68	12.09
SD	99	124.37	2.35	1.88	2.03
G (n = 58)					
Min	0	151.21	-16.19	-29.01	3.45
Max	400	2470.11	0.88	-4.11	10.19
Mean	73	1046.44	-1.21	-8.00	7.28
SD	70	583.54	3.54	5.01	1.57
B (n = 67)					
Min	0	193.07	-15.05	-32.24	4.37
Max	755	543.76	-8.06	-24.15	8.59
Mean	231	320.23	-11.78	-26.74	5.92
SD	208	80.30	1.71	2.26	1.07
A (n = 23)					
Min	16	81.22	-19.54	-36.83	4.41
Max	305	190.06	-12.47	-30.62	9.05
Mean	135	139.83	-16.17	-33.43	6.23
SD	77	32.20	2.04	1.85	1.29

Table 3. (suite)

Region and Statistic	Altitude m asl	Annual P mm	Annual T °C	January T °C	July T °C
All (n = 400)					
Min	0	81.22	-19.54	-36.83	3.45
Max	2000	2470.11	5.05	-4.11	18.18
Mean	271	498.25	-6.34	-21.85	10.30
SD	278	390.69	5.92	8.03	3.93
Grassland, boreal and subarctic sites (n = 214)					
Min	10	121.71	-11.56	-27.69	7.45
Max	2000	945.96	5.05	-6.24	18.18
Mean	350	503.91	-3.88	-21.61	13.40
SD	326	258.16	4.61	5.43	2.56
Arctic sites (n = 186)					
Min	0	81.22	-19.54	-36.83	3.45
Max	755	2470.11	0.88	-4.11	10.19
Mean	180	491.74	-9.17	-22.12	6.74
SD	170	502.39	6.01	10.25	1.38

Table 4. Summary of CA and CCA results on the 400 modern pollen assemblages.

	Axes		
	1	2	3
CA (34 taxa)			
Eigenvalues (λ)	0.242	0.122	0.084
% variance explained	24.1	12.1	8.4
CCA (34 taxa, 7 environmental predictors)			
Eigenvalues (λ)	0.208	0.062	0.052
% variance explained (taxa data)	20.7	6.16	5.17
% variance explained (taxa-environment)	55.1	16.4	13.7
Species-environment correlation	0.933	0.758	0.748
p-value (999 Monte Carlo permutations with Bonferroni adjustement)	0.001	0.001	0.001
Sum of all unconstrained λ (total inertia): 1.006			
Sum of all canonical λ: 0.377			

Table 5. Ranking of the 7 environmental variables in terms of the importance by their marginal and conditional effects derived from forward selection in CCA. The series of CCAs used each environmental variable as the sole constraining variable (marginal effect). July temperature and latitude produced the highest canonical eigenvalues, annual precipitation the lowest. After forward selection of the best environmental variable (July temperature), remaining environmental variables are ranked through a further series of CCAs with each being alternately chosen as the sole additional variable, thereby yielding the variables conditional effect beyond that already accounted for by July temperature. In this configuration, latitude falls from second to fourth, because a large part of its effect is already explained by July temperature.

Marginal effects		Conditional effects			
Variable	λ_1	Variable	λ_a	p-value	cum(λ_a)
July T	0.182	July T	0.182	0.001	0.182
Latitude	0.136	January T	0.056	0.001	0.238
Annual T	0.107	Altitude	0.052	0.001	0.290
Altitude	0.086	Latitude	0.038	0.001	0.328
Longitude	0.064	Longitude	0.024	0.001	0.352
January T	0.057	Annual P	0.017	0.001	0.369
Annual P	0.048	Annual T	0.008	0.001	0.377

λ_1: fit (eigenvalue with variable j only)

λ_a: additional fit (increase in eigenvalue)

cum(λ_a): cumulative total eigenvalues λ_a

p-value: significance level of the effect obtained from Monte Carlo permutations under the reduced model with 999 random permutations

Table 6. Intra-set correlation matrix between CCA axes 1-3 and the 7 environmental variables, for the 400 sites - 34 taxa of the modern pollen database.

Variable	Environment axis 1	Environment axis 2	Environment axis 3
Annual P	-0.123	-0.811	0.028
January T	-0.127	-0.795	0.500
July T	-0.927	-0.127	-0.015
Annual T	-0.584	-0.683	0.357
Longitude	0.321	-0.706	0.205
Latitude	0.728	0.542	-0.366
Altitude	-0.490	0.372	0.715

Table 7. A simple validation test of the BMA method conceived to assess the extent of spatial autocorrelation and its potential implications with regards to overestimating confidence in BMA-inferred climate reconstructions. All 16 estimates are based on the 5 best analogues and on modern data, but for 4 configurations: 400 reference sites (N) producing 400 inferences (n), 300 reference sites (N) producing 100 inferences (n), 200 reference sites (N) producing 200 inferences (n) and 100 reference sites (N) yielding 300 inferences (n). Although RMSE values increase as N is lowered, correlation coefficients do not decline dramatically.

Parameter	*r*	RMSE
First configuration: N = 400, n = 400		
July T	0.97	1.02 °C
Annual T	0.95	1.86 °C
January T	0.93	2.91 °C
Annual P	0.86	197.93 mm
Second configuration: N = 300, n = 100		
July T	0.97	0.89 °C
Annual T	0.95	1.85 °C
January T	0.93	2.93 °C
Annual P	0.84	219.61 mm
Third configuration: N = 200, n = 200		
July T	0.96	1.03 °C
Annual T	0.94	1.99 °C
January T	0.93	3.09 °C
Annual P	0.85	213.92 mm
Fourth configuration: N = 100, n = 300		
July T	0.96	1.12 °C
Annual T	0.92	2.37 °C
January T	0.88	3.78 °C
Annual P	0.80	232.34 mm

Table 8. Correlation matrices between the interpolated climate variables estimated for the complete suite of sites, as well as for the 2 major phytogeographic subdivisions considered separately.

Variable	Annual P	January T	July T	Annual T	Longitude	Latitude
All vegetation zones (400 sites)						
Annual P	1.000					
January T	0.755	1.000				
July T	0.160	0.254	1.000			
Annual T	0.678	0.868	0.674	1.000		
Longitude	0.654	0.508	-0.294	0.305	1.000	
Latitude	-0.605	-0.674	-0.692	-0.899	-0.334	1.000
Altitude	-0.059	0.196	0.417	0.347	-0.238	-0.432
Grassland, boreal and subarctic zones (212 sites)						
Annual P	1.000					
January T	0.529	1.000				
July T	0.525	0.707	1.000			
Annual T	0.681	0.933	0.852	1.000		
Longitude	0.917	0.311	0.246	0.459	1.000	
Latitude	-0.817	-0.861	-0.685	-0.924	-0.694	1.000
Altitude	0.160	0.771	0.398	0.637	-0.026	-0.565
Arctic tundra zone (186 sites)						
Annual P	1.000					
January T	0.831	1.000				
July T	0.135	0.292	1.000			
Annual T	0.805	0.986	0.404	1.000		
Longitude	0.651	0.751	-0.176	0.706	1.000	
Latitude	-0.731	-0.833	-0.260	-0.870	-0.734	1.000
Altitude	-0.324	-0.358	0.081	-0.320	-0.365	0.199

CHAPITRE II

VEGETATION AND CLIMATE OF THE LAST INTERGLACIAL ON BAFFIN ISLAND, ARCTIC CANADA

Bianca Fréchette[a], Alexander P. Wolfe[b], Gifford H. Miller[c], Pierre J.H. Richard[d], Anne de Vernal[a]

[a] GEOTOP, Université du Québec à Montréal, P.O. Box 8888, Succ. Centre-Ville, Montréal, QC H3C 3P8, Canada

[b] Department of Earth and Atmospheric Sciences, University of Alberta, Edmonton, AB T6G 2E3, Canada

[c] INSTAAR and Department of Geological Sciences, University of Colorado, Boulder, CO 80309-0450, USA

[d] Département de géographie, Université de Montréal, P.O. Box 6128, Succ. Centre-Ville, Montréal, QC H3C 3J7, Canada

Publié

Fréchette, B., Wolfe, A.P., Miller, G.H., Richard, P.J.H. et de Vernal, A, 2006. Vegetation and climate of the last interglacial on Baffin Island, Arctic Canada. *Palaeogeography, Palaeoclimatology, Palaeoecology* 236, 91-106.

Résumé

Les séquences sédimentaires de trois lacs du moyen arctique de la péninsule de Cumberland sur la Terre de Baffin dans l'Arctique canadien montrent deux unités de sédiments organiques (gyttja) inégalement superposées. L'unité supérieure représente la sédimentation holocène. L'unité inférieure est d'âge pré-Holocène. Des mesures radiocarbones obtenues sur des macrofossiles aquatiques indiquent un âge > 50 ka BP pour l'unité inférieure. Des mesures par luminescence sur deux des trois séquences permettent de préciser le moment de sa sédimentation, qui a eu lieu entre 90 et 130 ka BP, i.e. lors du dernier interglaciaire. Les spectres polliniques de ces séquences sédimentaires ont servi à reconstituer la végétation et le climat de l'Holocène et du dernier interglaciaire. Pour chacune des séquences, les sédiments interglaciaires montrent de très fortes concentrations polliniques ainsi qu'une représentation élevée du pollen d'arbustes (*Betula* et *Alnus*) par rapport aux sédiments holocènes sus-jacents. Des comparaisons entre les assemblages polliniques fossiles et 400 assemblages polliniques modernes de sédiments de lacs des hautes latitudes révèlent le caractère bas arctique de la végétation du dernier interglaciaire dans le centre-est de la Terre de Baffin, comparable à celui de la végétation actuelle du sud-ouest du Groenland. L'application de deux méthodes de reconstitution climatique, soit une régression linéaire issue d'une analyse factorielle des correspondances et la technique des meilleurs analogues modernes, permet de retracer des températures de juillet du dernier interglaciaires de 4 à 5°C plus élevées que les températures actuelles sur la côte est de la Terre de Baffin. De telles conditions furent sans doute plus chaudes que celles de tout l'Holocène. Nous associons ainsi l'unité organique inférieure de ces trois lacs à l'optimum climatique du dernier interglaciaire, ca. 117 à 130 ka BP (stade isotopique marin 5e).

Abstract

Sediment cores recovered from three mid-arctic lakes on Cumberland Peninsula, eastern Baffin Island, Arctic Canada, contained two units of unconformably superimposed organic sediment (gytjja), the upper of which represented sedimentation during the Holocene. Radiocarbon ages on aquatic macrofossils from the lower gyttja suggested it to be >50 ka BP, while luminescence ages from two cores constrained the age of this sediment to >90 ka BP and <130 ka BP, that is, encompassing the last interglacial. Pollen spectra from these cores were used to reconstruct past vegetation and climate of the Holocene and last interglacial. In each core, last interglacial sediments yielded remarkably high pollen concentrations, and included far greater percentages of shrub (*Betula* and *Alnus*) grains than did overlying Holocene sediments. Numerical comparisons of fossil pollen assemblages to a data-set of 400 modern high-latitude lake sediment samples revealed that the last interglacial vegetation of east-central Baffin Island was Low Arctic in character, comparable to present-day southwest Greenland. From applications of both correspondence analysis regression and best modern analogue methodologies, we infer July air temperatures of the last interglacial to have been 4 to 5°C warmer than present on eastern Baffin Island, which was warmer than any interval within the Holocene. On these grounds, we ascribe the lower lacustrine unit in these lakes to the climatic optimum of the last interglacial, ca. 117 to 130 ka BP (Marine Isotopic Stage 5e).

Keywords: Arctic, Pollen, Last interglacial, Paleoclimate, Baffin Island

2.1. Introduction

The Arctic is both highly responsive to climate variability, and directly involved in several key processes that mediate climate change. Consequently, there is a need to refine our understanding of arctic climate dynamics, including a quantitative assessment of past intervals of relative warmth. Pollen grains preserved in lake sediments are a useful proxy for reconstructing vegetation and climate. Lakes situated at sensitive ecotonal boundaries, such as the Low to Mid Arctic bioclimatic zone, are of particular interest because small changes in climate can induce relatively large vegetational changes that are discernible in the pollen record (e.g., Barbour et al., 1998).

The last interglacial period *sensu lato* (Marine Isotope Stage 5; MIS 5), 75-130 ka before present, is considered an interval of relative warmth throughout the circum-Arctic region. A compilation of qualitative climate proxies from deep-sea sediments, ice cores, and terrestrial near-shore sequences (LIGA members, 1991) revealed conditions about 4°C warmer than present in northeastern Canada and Greenland for the early warmest portions of the last interglacial (*sensu stricto*), ca. 115-130 ka BP (MIS 5e). Plant macrofossil and fossil insects from east-central Greenland indicate that mean summer air temperatures were about 5°C above present (Bennike and Böcher, 1994). The NorthGrip ice core in Greenland reveals the most detailed arctic climate history for the last interglacial, indicating mean temperatures 5°C warmer than present (NGRIP members, 2004). A quantitative pollen-based climate reconstruction from Bol'shoy Lyakhovsky Island in the Laptev Sea (Siberia), suggests that mean July air temperatures were 4 to 5°C higher than present during the Eemian climatic optimum (Andreev et al., 2004a). However, similar analyses are currently lacking for the eastern Canadian Arctic.

Over the last decade, pre-Holocene lacustrine sediments have been raised from a number of lakes on Baffin Island, Arctic Canada (Wolfe and Härtling, 1996; Steig et al., 1998; Miller et al., 1999; Wolfe et al., 2000). Although a handful of studies have qualitatively addressed the climate of Baffin Island during the last interglacial using pollen, diatoms, and sediment lithostratigraphy (Miller et al., 1977; Miller et al., 1999; Wolfe et al., 2000), the present investigation is a first attempt to quantitatively reconstruct last interglacial July air temperatures for this region. We report detailed last interglacial pollen records from three lakes on Cumberland Peninsula, eastern Baffin Island, situated close to the Low-Mid Arctic ecotonal boundary. We then compare Holocene and last interglacial vegetation and climate histories, revealing that a northward expansion of Low Arctic vegetation occurred over the Cumberland Peninsula during the last interglacial, but was not repeated at any time in the Holocene.

2.2. Study area

Several small upland lakes on Cumberland Peninsula (Baffin Island, Nunavut Territory, Canada) contain weakly-stratified, organic-rich lacustrine sediments that underlie Holocene gyttja, and are at or beyond the range of radiocarbon dating (Wolfe, 1994; Steig et al., 1998; Wolfe et al., 2000; Miller et al., 2002; Wolfe et al., 2004). The two organic (gyttja) units are commonly, but not universally, separated by more strongly stratified and dominantly minerogenic sediments. Cores from three of these lakes (Fig. 1) were selected for pollen analysis based on the overall length and quality of their pre-Holocene organic sediments. Amarok Lake (66° 16'N, 65° 45'W, 848 m altitude, 700 m x 100 m, 14.5 m water depth at coring site) is on southwestern Cumberland Peninsula immediately north of Pangnirtung Fiord. Fog Lake (67° 11'N, 63° 15'W , 460 m altitude, ca. 170 x 140 m, 9.5 m water depth at coring site) and neighbouring Brother-of-Fog Lake 11 km to the northwest (67° 11.5'N; 63° 08'W; 360 m altitude, ca. 350 x 500 m, 16.0 m water depth at coring

site), are situated on the peninsula between Kangert and Padle fiords on northern Cumberland Peninsula, about 145 km from Amarok Lake (Fig. 1).

The nearest community to Amarok Lake, Pangnirtung, has a mean annual air temperature of –8.9°C (July mean: 7.5°C; January mean: -26.3°C), and a mean annual precipitation of 396 mm, of which 56% falls as snow (Maxwell, 1980). Because of its altitude, Amarok Lake experiences colder and moister conditions, and consequently the vegetation around the lake is limited to a sparse *Cassiope tetragona-Salix*-lichen tundra. *Betula* is locally absent. The estimated mean July air temperature at Amarok lake is approximately 5-6°C.

The climate of northern Cumberland Peninsula is more severe. At Broughton Island (North Warming Station Fox 5; 67° 32'N, 63° 47'W, 584 m altitude), 40 km northwest of Fog and Brother-of-Fog lakes, mean annual air temperature is -11.8°C (July mean: 4.4°C; January mean: -24.8°C), and mean annual precipitation is 262 mm, 85% falling as snow. Precipitation increases dramatically eastward along the coast so that at Cape Dyer (66° 34'N, 61° 37'W, 393 m altitude), 100 km east of the lakes, mean annual precipitation is 603 mm (94% as snow, mean annual air temperature: -11.0°C; July mean: 5.3°C; January mean: -24.2°C) (Environment Canada, 2004). Vegetation around Fog and Brother-of-Fog lakes is typical of the Middle Arctic Zone (Young, 1971), with sparse vascular plant cover and few woody taxa. *Betula* is currently absent from the local vegetation. However, at the heads of Padle and Kangert fiords, 50 km to the west of the lakes, isolated outlier populations of prostrate dwarf birches (*Betula nana*, *B. glandulosa*) occur in the valley floor. Green alder (*Alnus crispa*) does not occur on Baffin Island today, nor does it appear to have at any time in the Holocene. We estimate mean July air temperature at Fog and Brother-of-Fog lakes to be similar to the one at Broughton Island, which is 4 to 5°C.

2.3. Methods

2.3.1. Sediment coring and chronology

The three lake sediment cores (7 cm diameter) were obtained in May of 1996 and 1998 from lake ice using a sledge-mounted percussion coring system capable of penetrating dense inorganic sediments (Nesje, 1992). Whole-core magnetic susceptibility (MS) was measured with a portable Bartington loop in the field and again prior to core splitting, logging, and sub-sampling in the laboratory.

The geochronology of Fog Lake sediments was discussed by Wolfe et al. (2000), that of Brother-of-Fog Lake by Miller et al. (2002), and that of Amarok Lake by Wolfe (1996). However, many of these results were provisional and are supplemented by data reported here. For accelerator mass spectrometry (AMS) ^{14}C dates, we targeted either bryophyte macrofossils (principally *Warnstorfia exannulata* leaves and stems), or sediment humic acid extracts. Miller et al. (1999) demonstrated that the average ^{14}C activity of mosses living in non-carbonate Baffin Island lakes was indistinguishable from that of the contemporary atmosphere, implying atmospheric equilibration with respect to carbon and suitability for ^{14}C dating. The accuracy of humic acid dates in this region depends principally on sources of ancient dissolved organic carbon in lake catchments (Wolfe et al. 2004).

However, because the lower gyttja in these lakes has proven close to, or beyond, the interpretable range of AMS ^{14}C dates (Table 1), we also applied luminescence dating of the fine-grain polymineral fraction to estimate the age of these sediments in Fog and Brother-of-Fog lakes. In Fog Lake, sections of ^{14}C-dated Holocene gyttja were also dated by luminescence to verify the completeness of solar resetting of minerals present in organic-rich sediments.

2.3.2. Pollen analysis

The cores (Amarok Lake, 205 cm; Fog Lake, 137 cm; and Brother-of-Fog Lake, 187 cm) were sub-sampled at intervals ranging from 0.5 to 10 cm, with the densest sampling applied to the lower organic sediments. This resulted in 71, 49, and 27 pollen samples from Fog, Amarok and Brother-of-Fog lakes, respectively. Holocene sediments were not analyzed from Brother-of-Fog Lake. From each level, 2.0 cm^3 of fresh sediment were processed for pollen using standard techniques including dispersion with KOH, digestion with HF and HCl, and acetolysis (Faegri and Iversen, 1975). Residues were stained with fuschin, mounted in glycerine, and examined microscopically using at 400x and 1000x. Pollen concentrations were determined by spiking with *Eucalyptus* pollen grains prior to processing (Benninghoff, 1962). The basic sum used for relative frequency calculations included all spermatophyte taxa. Although pteridophyte spores were excluded from the basic sum, their representations were expressed as relative frequencies in relation to the basic sum. Pollen and spores were identified with reference to the keys of Richard (1970), McAndrews et al. (1973), and Moore et al. (1991), as well as modern pollen slides archived at the Laboratoire Jacques-Rousseau, Université de Montréal.

The palynological richness of fossil samples was estimated by means of rarefaction analysis (Birks and Line, 1992), using the 3Pbase software (Guiot and Goeury, 1996). Rarefaction analysis provides unbiased estimates of taxonomic richness for a standardized sample size (i.e. grain count), using a random selection without replacement strategy. The method produces robust estimates of the expected number of taxa ($E(T_n)$) for the smallest pollen sum (n) in the studied sequence. Rarefaction analysis was performed on the raw counts of total assemblages, including both spermatophyte and pteridophyte taxa.

The equatorial diameter of *Betula* pollen grains was measured systematically in order to ascertain whether they originated from shrub or tree species involved (Birks, 1968; Richard, 1970; Prentice, 1981; Mäkelä, 1996; Caseldine, 2001). Diameters were measured in polar view as the distance between the outer layer of the exine and the bottom of the opposite pore. For most samples, at least 100 non-folded *Betula* grains were measured. Because glycerine-mounted slides induce swelling of pollen grains (Andersen, 1978), these measurements were done as soon as possible following sample preparation (i.e., within one month). For reference, *Betula* pollen from surface sediments of a lake surrounded by luxuriant populations of *B. nana* and *B. glandulosa* had diameters in the 17-21 μm range.

2.3.3. Paleoclimate reconstruction

2.3.3.1. Modern pollen database

In North America and Greenland, modern pollen assemblages from Low Arctic shrub tundra are typically dominated by *Betula*, Ericales, *Alnus*, *Picea* and *Pinus* (Fredskild, 1973, 1983, 1992; Gajewski et al., 1993, 2000; Kerwin et al., 2004; Richard, 1981; Ritchie and Lichti-Federovich, 1967; Short et al., 1985). In the eastern Canadian Arctic, the latter three taxa are exotic and thus represent long-distance wind-borne transport from southern source areas. However, shrub *Alnus* currently grows in south-western Greenland, north-western and north-central Canada, and on the Alaskan north slope (Fredskild, 1996; Ritchie et al., 1987; Oswald et al., 2003). Middle Arctic herb tundra vegetation is characterized by Ericales, Cyperaceae and *Salix* (Fredskild, 1973, 1983, 1985; Gajewski, 2002; Kerwin et al., 2004; Richard, 1981; Ritchie and Lichti-Federovich, 1967; Short et al., 1985). Sparser high arctic herb tundra and polar desert are characterized by Poaceae, *Salix* and minor contributions from diverse herb pollen such as Caryophyllaceae, Papaveraceae, Ranunculaceae and Saxifragaceae (Fredskild, 1973; Gajewski, 1995, 2002;

Hyvärinen, 1985; Kerwin et al., 2004; Short et al., 1985; Gajewski and Frappier, 2001).

Although these relationships have been known for some time, they have not been formalized adequately for paleoclimatic reconstructions of the last interglacial on Baffin Island. To this end, modern pollen assemblages from 400 sites north of 50°N latitude were collated, representing north-western Canada (n=120), northern Québec (n=94), the Canadian Arctic Archipelago (n=128), and Greenland (n=58). This provided a new modern pollen database restricted entirely to lake surface sediments. Raw data originated from both published (Fredskild, 1973, 1983, 1985, 1992; Gajewski, 1991, 2002; Kerwin, 2000; Kerwin et al., 2004; Richard, 1979; 1981; Ritchie, 1974; MacDonald and Ritchie, 1986; Ritchie et al., 1987; Richard et al., 1991; Sandgren and Fredskild, 1991) and unpublished sources (B. Fréchette; B. Fredskild; J.C. Ritchie).

Among the 159 pollen taxa reported by these authors, several taxonomic groups were harmonized to ensure a standardized and consistent taxonomic resolution. This resulted in a sub-total of 63 taxa. Thereafter, all taxa that never exceeded 1% of the sum in any one sample were also omitted, resulting in the final inclusion of 34 taxa in the modern database (Table 2). These taxa may all be unambiguously associated with fossil representatives preserved in lake sediments.

Ideally, when using pollen data for paleoclimatic inferences, one assumes that most of the observed pollen originates from plants living in proximity to the lake. However, long-distance wind-blown pollen produced by boreal taxa are consistently, and at times strongly, registered in arctic assemblages in proportions that are functions of both the distance from the source and the degree of dilution by locally-produced pollen. Because both of these factors potentially relate to climate, long-distance taxa were included in the modern database. Furthermore, for the crucial taxa

Betula and *Alnus*, it is difficult to differentiate palynologically the local presence of scattered individuals from dense distant populations.

2.3.3.2. Climate interpolations for the modern reference sites

A major hindrance to developing a pollen database for paleoclimatic reconstructions is obtaining meaningful estimates of climatic parameters to associate with individual modern pollen samples. This problem is exacerbated in the Arctic, where meteorological stations are few. For this study, climatic parameters for the 400 sites were estimated by weighted-averaging of the closest available meteorological station data, using 3Pbase software (Guiot and Goeury, 1996). Modern climate parameters at the three fossil sites were also estimated this way. The interpolated climatic data originated from averaged measurements at a total of 400 meteorological stations in Alberta (n=146), Yukon (n=19), NWT and Nunavut (n=52), Ontario (n=68), Newfoundland (n=12), Québec (n=79), and Greenland (n=24) (Environment Canada, 2004; Cappelen et al., 2001). The data sets included thirty years of climate measurements. Climate observations of the period 1971-2000 were used for most of the stations (n=361). The period 1961-1990 was used for the remainder (n=39). The duration of these climatic records was directly comparable to the time represented by the surface sediments (typically 0-1 cm) collected from northern lakes, given that low sediment accumulations rates were the norm (Wolfe et al., 2004). Moreover, multi-decadal integrations of both climatic and biological data reduced the effects of short-term variability within both systems, allowing for the reconstruction of average conditions from sediment sample that, similarly, represent several decades of accumulation. The estimated climatic parameter, c_o, for a modern pollen site, o, was given by the weighted-average of all the meteorological stations, k, at a distance, d_{ok}, less than or equal to a radius of 10°, R, from the site (Guiot, 1987), as given by:

$$c_o = (\Sigma_k c_k/d_{ok})/(\Sigma_k 1/d_{ok})$$

and

$$d_{ok} = ((x_o - x_k)^2 + (y_o - y_k)^2)^{1/2}$$

where x_k, y_k and c_k represent the longitude, latitude, and measured climatic variables at each meteorological station, $k = 1$ to m (m=400), respectively. The robustness of these interpolations was assessed by comparisons of observed and estimated values for each meteorological station's locality. Observed versus estimated relationships produced root-mean-squared error of prediction (RMSEP) ±1.25°C (r=0.98) for mean annual air temperature, ±1.22°C (r=0.96) for July air temperature, ±2.13°C (0.95) for January air temperature, and ±119.10 mm (r=0.93) for annual precipitation. Thus, the modern environmental gradients embraced by the 400 modern pollen localities were -19.4 to 5.1°C for mean annual air temperature, 3.5 to 18.2°C for July air temperature, –36.8 to –4.1°C for January air temperature, and 81 to 2470 mm for mean annual precipitation.

2.3.3.3. Correspondence analysis and canonical correspondence analysis

Correspondence and canonical correspondence analyses (CA and CCA) were used to explore the relationships between the 400 modern pollen assemblages and climatic parameters. Both techniques exploit unimodal (Gaussian) ordination, as either indirect (CA) or direct (CCA) gradient analysis (ter Braak and Prentice, 1988). Thus, while the CA is restricted to matrix of 34 taxa and 400 sites, the CCA constrained an identical matrix to linear combinations of the following variables: latitude, longitude, altitude, mean annual air temperature, July air temperature, January air temperature, and mean annual precipitation. Prior to ordination, relative frequencies of the 34 included taxa were square-root transformed, and rare taxa were not down-weighted. On the ordination plot the 400 modern sites were grouped into nine geographical regions: western Canada (WC), James Bay (JB), northern Quebec (NQ), Fort Chimo – Diana Bay (FCD), Baffin Island (B), Arctic islands (A), and Greenland (G). Following initial ordinations restricted to modern samples, fossil assemblages were

entered passively, that is, projected onto the ordination space defined by the modern samples without influencing the analysis in any other way. This allowed the fossil samples to be viewed graphically alongside the most similar assemblages from the modern database. CA and CCA were implemented with CANOCO v. 4 (ter Braak and Šmilauer, 1998).

2.3.3.4. Best modern analogues

The best modern analogue (BMA) technique assumes that modern samples with a pollen assemblage similar to a fossil assemblage were produced by similar vegetation and, by inference, under similar climatic regimes (Overpeck et al., 1985; Guiot et al., 1989; Anderson et al., 1989; Guiot, 1990; Andreev et al., 2003, 2004b; Jackson and Williams, 2004). Similarity between fossil and modern assemblages was assessed using the squared-chord-distance (SCD) dissimilarity metric (Overpeck et al., 1985; Gavin et al., 2003). The SCD (d) between fossil (t) and modern (i) pollen assemblages were calculated based on differences in the relative frequencies (p) of each taxon (j = 1 to m; m=34) as follows:

$$d_{it} = \Sigma_j((p_{ij})^{1/2} - (p_{tj})^{1/2})^2$$

Values of SCD can vary between 0 and 2, with larger values indicating grater dissimilarity. Overpeck et al. (1985), using 1618 sites with alternately 15 and 40 taxa, showed that an SCD below 0.12 indicates that a modern analogue exists, but that an SCD of 0.15 remains applicable in situations where poorer analogues are found. Anderson et al. (1989), using 303 modern sites and 25 taxa, proposed SCD thresholds of 0.095, 0.185 and 0.400 for 'good analogues', 'analogues', and 'possible analogues', repsectively. The threshold SCD produced by 3Pbase software (Guiot and Goeury, 1996) was different because it exploited Monte Carlo simulations of the modern data, whereby modern assemblages were successively extracted at random from the population with replacement, and the best-fitting assemblage is obtained (Guiot et al., 1989; Guiot, 1990). This was repeated s times, providing s best

analogues from which confidence intervals are calculated. Here, we retained the five best analogues for each fossil assemblage. The distance between pairs randomly taken in the modern database averaged 0.62, with an average deviation of 0.31. The average minus average deviation gave the adopted threshold for SCD of 0.31 for the 400 modern sites and 34 taxa. The reconstructed July air temperature for a fossil assemblage t (r_t) (Guiot et al., 1989) was indexed by the July air temperature of the 5 best modern analogues:

$$r_t = (\Sigma_i c_i / d_{ti}^2) / \Sigma_i (1/d_{ti}^2)$$

The accuracy of reconstructions was given by the SCD values of the first and the fifth analogues, which were fitted around the reconstructed July air temperature curve. If the distance of the closest analogues was higher than the threshold, no reconstruction is attempted.

The overall reliability of the BMA approach was evaluated by estimating the modern climate of the reference sites based on their own pollen assemblages. Observed versus estimated modern July air temperature produced root-mean-squared error of prediction (RMSEP) of ±1.02°C (r=0.97), which was lower than the RMSEP for the climatic data themselves. This high degree of accuracy suggested that the inclusion of long-distance pollen taxa in the modern pollen database was entirely justified and likely advantageous.

2.4.0. Results and interpretation

2.4.1. Sediment stratigraphy and chronology

The lithostratigraphy of the three cores revealed broad similarities (Figs. 2A, 3A, 4A). Although the basal minerogenic units differed slightly between lakes, from diamict in the Fog Lake core to stony lacustrine sediment in the other cores, in all cases these facies related to deglaciation of the uplands prior to the last interglacial

(Steig et al. 1998). These deglacial sediments were overlain by compacted, de-watered gyttja with low magnetic susceptibility signatures. Aquatic mosses were common in this material. In the Fog and Brother-of-Fog lake cores, this lower gyttja was capped by a stratified minerogenic unit, which in turn was overlain by Holocene gyttja. In the Amarok Lake core, Holocene gyttja unconformably overlay the older organic sediments directly. In both the Brother-of-Fog and Amarok lake cores, the lowermost Holocene gyttja was black with distinctive laminations of siderite ($FeCO_3$), implying a chemically-reducing sedimentary environment (Wolfe and Smith 2004). These reduced zones were in turn overlain by faintly stratified to massive olive gyttja.

Relevant radiocarbon dating results are reported in uncalibrated ^{14}C years BP. The finite dates from the lower gyttja reported in Table 1 must be viewed, conservatively, as minimum ages. This is because finite dates in the 37-60 ka BP range have been obtained on both Baffin Island lake sediments that are demonstrably older on the grounds of luminescence ages (Miller et al., 1999), as well as on ^{14}C free alanine blanks (Wolfe et al., 2004). Stratigraphic and palynologic correlations strongly implied that the lower gyttja was broadly coeval in each of the lakes, so that, given the non-finite ^{14}C results from Fog Lake (Table 1), it was safely assumed that each of these units (A-I, F-III, B-III) was deposited prior to 50 ka BP.

Infrared-stimulated luminescence dates from the lower gyttja in Fog Lake (Unit F-III) produced ages of 94±8 to 96±8 ka BP (n=4), which were possibly minimum ages (Wolfe et al. 2000). Adequate zeroing of the luminescence signal was suggested by comparisons to lithologically-similar sediments of Holocene age. However, further luminescence ages from the lower gyttja in Brother-of-Fog Lake (Unit B-III) yielded maximum limiting ages of <122 ka BP and <145 ka BP, rather than clear finite ages. In contrast to Fog Lake, there was clear evidence of incomplete solar resetting in the

sediments of Brother-of-Fog Lake, indicating the presence of a population of charges stored in deep, thermally-stable, electron traps that were not reset during sediment transport and deposition (S.L. Forman, personal communication, 2003).

Dating the minerogenic unit separating the two organic units in Fog and Brother-of-Fog lake cores also proved challenging because of reworked organic matter, in particular the humic acid fraction, which produced erroneous ^{14}C ages in the 14-16 ka BP range (Wolfe et al., 2000). Subsequent dates on mosses and chironomid head capsules from these sediments provided early Holocene ages (Wolfe et al., 2004), suggesting a prolonged depositional hiatus likely representing most or all of MIS 4, 3 and 2. In Fog and Brother-of-Fog lakes, the minerogenic sediments that separated the last interglacial and Holocene organic sediments probably reflected rapid deposition associated with erosion of largely unvegetated catchments, as climate began to warm in the earliest Holocene.

Despite these various chronological complexities, what can be stated with a certain degree of confidence is that: (1) the basal organic units (A-I, F-III and B-III) were deposited within MIS 5 and appeared to be neither older than ~145 ka BP, nor younger than ~90 ka BP; (2) based on their low magnetic susceptibility, overall thickness, and low bulk density, these sediments represented intervals of deposition of comparable duration to the Holocene; (3) there were prolonged intervals of non-deposition between the formation of MIS 5 and Holocene gyttjas; and (4) the re-initiation of sedimentation in the early Holocene reworked organic matter of last interglacial age, contaminating both pollen assemblages and sediment humic acid pools. Because both pollen and chironomid assemblages in these sediments indicated summer conditions warmer than the Holocene, we tentatively ascribed them to the last interglacial *sensu stricto* (MIS 5e).

2.4.2. Pollen analysis of the fossil sequences

Pollen sums of at least 500 grains were attained in all samples except unit A-II, where sums ranged from 200-500 grains. Over 45 spermatophyte taxa were identified, as well as 11 pteridophyte and 3 algal taxa. Simplified relative frequency pollen diagrams for each of the three lakes are presented (Figs. 2B, 3B, 4B), with taxa ordered according to their CCA axis 1 scores (Birks, 1993). Because CCA axis 1 was negatively correlated with July air temperature, taxa with low (negative) scores were more characteristic of 'warm' environments (left side of diagrams), whereas those with positive scores were characteristic of 'cold' environments (right side).

2.4.2.1. Pollen concentrations

The last interglacial sediment in Amarok and Fog lakes yielded strikingly higher pollen concentrations than Holocene gyttja. In Amarok Lake, the mean pollen concentration in the lower gyttja (A-I) was 84,800±29,200 gr/cm^3, in comparison to 4000±2700 gr/cm^3 in Holocene gyttja (A-III) (Fig. 2B). In Fog lake, the mean concentration in the lower gyttja was 30,000±13,000 gr/cm^3 (F-III), and 4300±1400 gr/cm^3 in the Holocene (F-V) (Fig. 3B). Last interglacial gyttja of Brother-of-Fog Lake (B-III) had a mean pollen concentration of 25,000±8000 gr/cm^3 (Fig. 4B). The higher concentration of pollen in the lower gyttja was in part due to dewatering and compaction of the sediment. However, bulk densities of the last interglacial gyttja were only slightly less than Holocene sediments, and so density differences may have accounted only for a small fraction of the differences in pollen concentrations. We conclude that pollen influxes must have been significantly higher during the interglacial relative to the Holocene.

In Fog Lake, the early Holocene minerogenic unit (F-IV) that overlay last interglacial sediment also produced extremely high mean pollen concentrations (30,300±13,300

gr/cm^3) (Fig. 3B). These were due to redeposition of last interglacial pollen from surrounding soils, before local vegetation became sufficient to stabilize the catchment. The mean pollen concentration in the correlative minerogenic unit in Brother-of-Fog Lake was significantly lower (B-IV: 7700±1050 gr/cm^3). Here too, we infer that much of this pollen was reworked from last interglacial soils at the onset of the Holocene, based on the similarity of assemblages with interglacial deposits. No paleoclimatic inferences were derived from these reworked assemblages.

2.4.2.2. Pollen assemblages

Last interglacial pollen assemblages of all three sequences were strongly dominated by shrubs (*Betula* and *Alnus*), with secondary contributions from arctic herb and boreal taxa (*Picea*, *Pinus* and *Artemisia*, among others) (Figs. 2B, 3B, 4B). *Betula* grains in the last interglacial gyttja (units F-III and A-I) were 2-3 times more abundant than in Holocene counterparts (units F-V and A-III). Furthermore, *Betula* grain diameters in these sediments ranged from 19-24 μm (mean 21 μm), confirming that they originated from shrub and not tree forms (Wolfe et al., 2000). In the Fog Lake core, *Alnus* pollen was 1.5 times more abundant in last interglacial sediments than anytime during the Holocene (Fig. 3B). However, in Amarok Lake relative frequencies of *Alnus* were similar in MIS 5 and Holocene gyttjas (Fig. 2B).

In the last interglacial sediments of Fog Lake, there was evidence for a local succession from a colonizing herb tundra to a denser shrub tundra (units F-II and F-III) (Fig. 3B). The lower unit (F-II) depicted an early postglacial vegetation dominated by herbs (e.g., *Oxyria*, Cyperaceae and *Salix herbacea*-type), and the upper unit (F-III) one dominated by *Betula* and *Alnus* with a low representations of long-distance and high arctic herb taxa. This suggested that relatively dense low arctic shrub tundra with *Betula* populations grew locally, although birch does not

grow near the site today. Within this zone, two decreases in the relative frequency of *Alnus* were noted (108-104 cm and 89-87 cm) (Fig. 3B). These were both associated with concomitant increases in Cyperaceae, *Salix* and Ericales pollen, as well as pteridophyte spores, and were interpreted as episodes of herb tundra alternating with shrub tundra vegetation. Sediments at the base of the last interglacial gyttja from Amarok Lake showed similar subtle changes in pollen assemblages, with arctic herbs, *Salix* and boreal trees better represented here, and *Alnus* less abundant. This palynological change corresponds to elevated magnetic susceptibility, suggesting an unstable catchment (Figs. 2A, 2B).

The pollen content of units B-I and B-II of Brother-of-Fog Lake also reflected local vegetation changes during the last interglacial (Fig. 4B). Higher relative frequencies of Cyperaceae, Ericales and *Salix* were observed in units B-I and B-II, relative to overlying interglacial gyttja (unit B-III) (Fig. 4B), but representation of shrub taxa (*Betula*, *Alnus*) remained high by comparison to Fog Lake units F-II and F-III (Fig. 3B).

The pollen content of the minerogenic units separating last interglacial and Holocene gyttjas in Fog and Brother-of-Fog lakes (F-IV and B-IV) contained high relative frequencies of *Betula*, but lower representations of *Alnus* (Figs. 3B, 4B). In unit B-IV, Cyperaceae, Poaceae, Ericales and *Salix* were more abundant than in the last interglacial gyttja, whereas only Ericales showed higher relative frequency in Fog Lake unit F-IV. The pollen content observed in units F-IV and B-IV was an admixture of reworked MIS 5 and early Holocene pollen grains, with the early Holocene component better registered in Brother-of-Fog Lake.

In the Holocene sediments of Amarok Lake, there was evidence for a local succession from a colonizing herb tundra dominated by Poaceae, *Oxyria* and Cyperaceae (unit A-II), to a more stable herb tundra (unit A-III) (Fig. 2B). The mid-Holocene *Alnus*

rise registered in Amarok and Fog lakes is a common feature in Baffin Island pollen diagrams (e.g. Short et al., 1985; Mode and Jacobs, 1987; Miller et al., 1999), associated with a higher boreal pollen taxa representation derived from long-distance transport. The pollen content of the Holocene gyttja of Fog Lake (unit F-V) is typical of a mid Arctic herb tundra vegetation with high relative frequencies of Cyperaceae, Ericales and *Betula* (Fig. 3B). Further details of the Fog Lake pollen diagram are presented elsewhere (Wolfe et al., 2000).

2.4.2.3. Palynological richness

Stratigraphic profiles of rarefaction-estimated palynological richness are presented for each core on Figs. 2C, 3C, and 4C. In general, palynological richness was lowest in last interglacial sediments dominated by shrubs (A-I, F-III, B-III), and higher whenever shrub pollen representation decreased (F-II, B-II). These intervals of elevated richness correspond with local herb tundra expansions. Indeed, closed yet productive shrub tundra is expected to produce lower palynological richness than more open and less productive shrub tundra (Moore et al., 1991). Furthermore, fewer long-distance pollen grains are represented in productive shrub tundra assemblages relative to more locally impoverished herb tundra. Thus, palynological richness of Baffin Island lake sediments appeared higher for open herb tundra than for denser shrub tundra vegetation.

2.4.2.4. Summary

Palynological results from the last interglacial sediments of all three investigated lakes showed the following characteristics: (1) very high pollen concentrations relative to the Holocene; (2) prolonged intervals dominated by the shrub taxa *Betula* and *Alnus* with relatively few arctic herbs and long-distance pollen grains; (3) low palynological richness of these intervals as the product of dense shrub-dominated

tundra vegetation; and (4) occasional intervals of herb tundra, particularly at the onset of the last interglacial.

In comparison, Holocene pollen assemblages exhibited higher richness as the product of sparser and less productive herb tundra. From these results, we conclude that shrub tundra dominated by *Betula*, perhaps including the local presence of *Alnus*, colonized Cumberland Peninsula during the last interglacial.

2.4.3. Climate-vegetation relationship

Correspondence analysis (CA) of the 400 modern reference sites was used to explore the main pattern of taxonomic variation across the Arctic North America (Figs. 5A, 5B). The first CA axis accounted for 24.1% of total variance (λ_1=0.242), whereas the second CA axis represented 12.1% (λ_2=0.122). The third CA axis accounted for 8.4% (λ_3=0.084) and was not considered further. A biplot of CA sample scores in the low-dimensional space defined by axes 1 and 2 confirmed that a strong spatial (latitudinal) structure was preserved by the modern pollen assemblages (Fig. 5B). Sites from Low, Mid, and High Arctic phytogeographical zones produced positive scores on CA axis 1, whereas sites from forest tundra and boreal forest resulted in negative scores. Furthermore, among the tundra sites, CA axis 2 faithfully differentiated herb tundra vegetation (positive scores) from shrub tundra (negative scores).

Because the CA revealed a clear latitudinal pattern, axis 1 had a significant negative correlation (r=-0.86) with July air temperature (Fig. 5C). Furthermore, the CA allowed clear differentiation between Low Arctic and forest tundra (boreal forest) vegetation as represented by their corresponding pollen assemblages, indicating that this transition occured at a July air temperature of ~10°C (Fig. 5C). It is independently established that the boreal forest-tundra ecotone (or treeline), which

reflects the average position of the Arctic Front, coincides with the 10°C mean July air temperature isotherm (e.g., Bonan et al., 1992; Foley et al., 1994; Pielke and Vidale, 1995).

A canonical correspondence analysis (CCA) constraining the 34 pollen taxa to 7 environmental variables (Fig. 5D) was also conducted. The first two CCA axes explained 26.8% of the variance in the pollen assemblage data (λ_1=0.208; λ_2=0.062; total inertia: 1.006), with pollen-environment correlations of 0.933 for axis 1 and 0.758 for axis 2. This corresponded to 71.5% of the total pollen-environment relationship being explained (55.1% and 16.4% for axis 1 and 2, respectively). Monte Carlo permutation tests indicated that the canonical correlation between the pollen and environmental matrices was highly significant (p=0.001 after 999 permutations). As suspected from the CA results, axis 1 in CCA was strongly correlated with July air temperature, whereas axis 2 was negatively correlated with both annual precipitation (r=-0.61) and January air temperature (r=-0.60) and (Fig. 5D). For the 400 lakes above 50°N latitude in northwestern Canada, northern Québec, the Canadian Arctic Archipelago, and Greenland, the weighted correlation between annual precipitation and January air temperatures was 0.76, and that between annual precipitation and July air temperatures was 0.16.

2.4.4. Paleoclimate reconstructions from pollen assemblages

2.4.4.1. Inferences from Correspondence Analysis

Fossil assemblages were passively entered in the CA of the 400-lake modern assemblages (Figs. 6A and 6B). All samples from Fog, Brother-of-Fog, and Amarok lakes produced positive CA axis 1 scores. Last interglacial samples (units A-I, F-III, B-III) had more negative scores than those representing the Holocene (units F-V, A-III), suggesting consistently higher July air temperatures (see Figs. 5C, 5D). The last

interglacial samples also had negative scores on axis 2 (units A-I, F-III, B-III) (Fig. 6B), implying moister precipitation regimes.

The palynological similarity of last interglacial samples from all three lakes (units A-I, F-III and B-III) suggested that they collectively reflected the widespread development of shrub tundra vegetation with local *Betula* populations on Cumberland Peninsula. In comparison, the pollen content of Holocene gyttja from Amarok and Fog lakes was considerably more site specific (units A-III and F-V). This type of specificity appeared more characteristic of herb tundra vegetation.

The linear correlation between CA axis 1 modern sample scores and July air temperature (Fig. 5C) was given by equation: July T (°C) = 10.28 – 6.54 (CA axis 1 sample score). Applying this relationship to the fossil samples entered passively in the ordination enabled a first-order appreciation of the July air temperatures associated with interglacial pollen assemblages. The quantitative reconstruction of July air temperature based on this method suggested that last interglacial July air temperatures were 4 to 6°C warmer than present at all three lakes, that is, between 7.5 and 10°C (Figs. 2D, 3D, 4D).

2.4.4.2 Quantitative July air temperatures from best modern analogues

Pollen-based reconstructions of July air temperature using the best modern analogue method are also presented on Figs. 2E, 3E, 4E. The modern database contained close analogues for both Holocene and last interglacial assemblages, with SCD for the 5 best analogues well within threshold values adopted by 3Pbase software (0.31) and proposed by Overpeck et al. (1985) (0.15) (Figs. 2F, 3F, 4F). However, reconstructions of modern July air temperatures from core tops from Amarok and Fog lakes resulted in overestimates (by 1.5°C; Figs. 2E, 3E). These discrepancies were of the same order as interpolated July air temperature RMSEP (±1.02°C), and were

within the standard deviation of measured July air temperatures for Cumberland Peninsula (4.6±1.7°C for 1971-2000; Environment Canada, 2004). For the last interglacial sediments, July air temperatures reconstructed by best modern analogues were 4 to 5°C warmer than present for Amarok and Fog lakes, producing values ranging from 8 to 10°C (Figs. 2E, 3E). Results from Brother-of-Fog Lake were slightly cooler (between 7 and 8°C) (Fig. 4E).

However, the very beginning of the last interglacial at Fog Lake (unit F-II), where herb pollen taxa was dominant, was ~1.5°C colder than late Holocene reconstructions. Furthermore, the two subsequent episodes of herb tundra reappearance within the last interglacial at Fog Lake (unit F-III) also produced July air temperatures comparable to the late Holocene. Pollen from units B-I and B-II in Brother-of-Fog Lake, which combined abundant herb pollen while maintaining strong representations of *Betula* and *Alnus*, produced July air temperatures 1°C warmer than the episodic herb tundra phases noted in Fog Lake, and may have represented July air temperatures comparable to, or slightly warmer, than those of the late Holocene. The lower portion of the last interglacial in Amarok Lake, with abundant *Salix*, arctic herbs, and boreal tree pollen (but fewer *Betula*), contained an interval of cool reconstructed July air temperatures (Figs. 2B, 2E).

2.4.4.3. Summary

Last interglacial pollen assemblages from the three investigated sites on Baffin Island were most comparable to modern assemblages from southwestern Greenland between 60-64°N and 44-40°W. In this region, green alder (*Alnus crispa*), shrub birch (*Betula nana, B. glandulosa*) and dwarf tree birch (*B. pubescens*) grow locally (Fredskild and Ødum, 1990; Fredskild, 1996). July air temperature is currently 7.4±1.8°C (Cappelen et al., 2001).

From both methods of quantitative reconstruction applied here, July air temperatures of the last interglacial on eastern Baffin Island attained between 8 and 10°C (Table 3), significantly warmer than present. For example, the current mean July air temperature for Cumberland Peninsula is 4.6±1.7°C (Environment Canada, 2004). At the optimum of the last interglacial, summer temperatures were high enough to allow the establishment of dense shrub tundra vegetation, comparable to that of modern southwestern Greenland, as far north as Cumberland Peninsula on Baffin Island. This implies a 300-500 km northward migration of the Low Arctic phytogeographical zone. We do not question the presence of shrub *Betula* in the immediate vicinities of the lakes studied here during the last interglacial, in part because local populations occur within 100 km. Although our reconstructed summer temperatures could have allowed for the presence of *Alnus* locally, we remain unable to confirm the latter's presence in absolute terms on Cumberland Peninsula in the last interglacial.

2.5. Conclusion

Pollen analysis of three lacustrine sediment sequences from Cumberland Peninsula provided a basis for comparing interglacial vegetation and climate of east-central Baffin Island with that of the Holocene. The vegetation of the last interglacial period on east-central Baffin Island was primarily Low-Arctic in character. Shrub birch-dominated tundra expanded considerably, driven by summer temperatures significantly warmer than present. The northward expansion of birch may also have been favoured by deeper snow cover associated with warmer winters and enhanced precipitation (see Fig. 6B).

The exact paleoenvironmental and paleoclimatic dynamics throughout the last interglacial on Cumberland Peninsula remain partially compromised by the problems presented by lake sediment chronology. Nonetheless, our data suggested strong regional coherence within the palynological signature of the last interglacial, more

than during the Holocene, in which vegetational histories were more site-specific. Based on the clear evidence of terrestrial summer warmth greater than at any time in the Holocene, we equate the interglacial sediment with the last interglacial *sensu stricto,* ca. 117 to 130 ka BP (MIS 5e).

Results that emerge from the application of the correspondence analysis and best modern analogue techniques indicated that July air temperatures of the last interglacial were warmer by as much as 4 to 5°C on eastern Baffin Island (Table 3). Our quantitative July air temperature reconstructions are thus directly comparable to both earlier qualitative estimates (LIGA Members, 1991; Bennike and Böcher, 1994), as well as more recent quantifications from ice core (NGRIP Members, 2004) and pollen (Andreev et al., 2004a) analyses. Because the warmest millennia of the last 200 ka appear to have occurred at this time, the associated biotic communities foreshadow possible future community shifts that may be associated with anthropogenic warming.

Acknowledgments

We thank Joël Guiot (CEREGE-France) and Maryse Henry (GEOTOP) for their help with the data analysis, Nicole Morasse (Université de Montréal) for her help with pollen analysis, Bent Fredskild (University of Copenhagen) and Michael Kerwin (University of Denver) for providing modern pollen data, three anonymous reviewers for their critical comments on the manuscript, and Rachel Jones for improving the english. This study was supported by the Natural Science and Engineering Council of Canada (NSERC), the Fonds québécois de la Recherche sur la Nature et les Technologies, the Climate Foundation for Climate and Atmosphere Sciences (project no GR-240), and NSF-PALE/PARCS programs (USA). Steven Forman (University of Illinois, Chicago) provided luminescence dates. Access to field sites was granted by the Inuit of Pangnirtung and Qikiqtarjuaq (formerly Broughton Island), who also

provide logistical assistance and welcome advice. The Nunavut Research Institute (Nunavummi Qaujisaqtulirijikkut) provided logistical support in Iqaluit.

References

Andersen, S.T., 1978. On the size of *Corylus avellana* L. pollen mounted in silicon oil. Grana 17, 5-13.

Anderson, P.M., Bartlein, P.J., Brubaker, L.B., Gajewski, K., Ritchie, J.C., 1989. Modern analogues of late-Quaternary pollen spectra from the western interior of North America. J. Biogeogr. 16, 573-596.

Andreev, A.A., Tarasov, P.E., Siegert, C., Ebel, T., Klimanov, V.A., Melles, M., Bobrov, A.A., Dereviagin, A.Y., Lubinski, D.J., Hubberten, A-W., 2003. Late Pleistocene and Holocene vegetation and climate on the northern Taymyr Peninsula, Arctic Russia. Boreas 32, 484-505.

Andreev, A.A., Grosse, G., Schirrmeister, L., Kuzmina, S.A., Novenko, E.Y., Bobrov, A.A., Tarasov, P.E., Ilyashuk, B.P., Kuznetsova, T.V., Krbetschek, M., Meyer, H., Kunitsky, V.V., 2004a. Late Saalian and Eemian paleoenvironmental history of the Bol'shoy Lyakhovsky Island (Laptev Sea Region, Arctic Siberia). Boreas 33, 319-348.

Andreev, A., Tarasov, P., Schwamborn, G., Ilyashuk, B., Ilyashuk, E., Bobrov, A., Klimanov, V., Rachold, V., Hubberten, H-W., 2004b. Holocene paleoenvironmental records from Nikolay Lake, Lena River Delta, Arctic Russia. Palaeogeogr. Palaeoclimatol. Palaeoecol. 209, 197-217.

Barbour, M.G., Burk, J.H., Pitts, W.D., Gilliam, F.S., Schwartz, M.W., 1998. Terrestrial plant ecology. 3rd edition. Addison Wesley Longman, Inc. Menlo Park, California.

Bennike, O., Böcher, J., 1994. Land biotas of the last interglacial/glacial cycle on Jameson Land, East Greenland. Boreas 23, 479-487.

Benninghoff, W.S., 1962. Calibration of pollen and spore density in sediments by addition of exotic pollen in known quantities. Pollen et Spores 4, 232-233.

Birks, H.J.B., 1968. The identification of *Betula nana* pollen. New Phytologist 67, 309-314.

Birks, H.J.B., 1993. Quaternary palaeoecology and vegetation science – current contributions and possible future developments. Rev. Palaeobot. and Palynol. 79, 153-177.

Birks, H.J.B., Line, J.M., 1992. The use of rarefaction analysis for estimating palynological richness from Quaternary pollen-analytical data. The Holocene 2, 1-10.

Bonan, G.B., Pollard, D., Thompson, S.L., 1992. Effects of boreal forest vegetation on global climate. Nature 359, 716-718.

Cappelen, J., Jørgensen, B., Laursen, E., Stanius, L., Thomsen, R., 2001. The observed climate of Greenland – with climatological normals, 1961-90. DMI Technical Report No. 00-18.

Caseldine, C., 2001. Changes in *Betula* in the Holocene record from Iceland – a palaeoclimatic record or evidence for early Holocene hybridisation? Rev. Palaeobot. Palynol. 117, 139-152.

Environment Canada, 2004. http://climate.weatheroffice.ec.gc.ca/climate_normals.

Faegri, K., Iversen, J., 1975. Textbook of Pollen Analysis, 3rd Edition. Blackwell Scientific Publications, Oxford.

Foley, J.A., Kutzbach, J.E., Coe, M.T., Levis, S., 1994. Feedbacks between climate and boreal forests during the Holocene epoch. Nature 371, 52-54.

Fredskild, B., 1973. Studies in the vegetational history of Greenland. Palaeobotanical investigations of some Holocene lake and bog deposits. Meddr Grønland 198 (4), 245 pp.

Fredskild, B., 1983. The Holocene vegetational development of the Godhåbsfjord area, West Greenland. Meddr Grønland, Geosci. 10, 28 p.

Fredskild, B., 1985. The Holocene vegetational development of Tugtuligssuaq and Qeqertat, Northwest Greenland. Meddr Grønland, Geosci. 14, 20 p.

Fredskild, B., 1992. Erosion and vegetational changes in South Greenland caused by agriculture. Geogr. Tidsskr. 92, 14-21.

Fredskild, B., 1996. A phytogeographical study of the vascular plants of West Greenland (62°20'-74°00'). Meddr Grønland, Biosci. 45, 157 pp.

Fredskild, B., Ødum, S., 1990. The Greenland Mountain birch zone, an introduction. Meddr Grønland, Biosci. 33, 3-7.

Gajewski, K., 1991. Représentation pollinique actuelle à la limite des arbres au Nouveau Québec. Can. J. Earth Sci. 28, 643-648.

Gajewski, K., 1995. Modern and Holocene pollen assemblages from some small Arctic lakes on Somerset Island, N.W.T., Canada. Quat. Res. 44, 228-236.

Gajewski, K., 2002. Modern pollen assemblages in lake sediments from the canadian Arctic. Arct. Antarct. Alp. Res. 34, 26-32.

Gajewski, K., Frappier, M., 2001. A Holocene lacustrine record of environmental change in northeastern Prince of Wales Island, Nunavut, Canada. Boreas 30, 285-289.

Gajewski, K., Mott, R.J., Ritchie, J.C., Hadden, K., 2000. Holocene vegetation history of Banks Island, Northwest Territories, Canada. Can. J. Bot. 78, 430-436.

Gajewski, K., Payette, S., Ritchie, J.C., 1993. Holocene vegetation history at the boreal-forest – shrub-tundra transition in north-western Québec. J. Ecol. 81, 433-443.

Gavin, D.G., Oswald, W.W., Wahl, E.R., Williams, J.W., 2003. A statistical approach to evaluating distance metrics and analog assignments for pollen records. Quat. Res. 60, 356-367.

Guiot, J., 1987. Late Quaternary climatic change in France estimated from multivariate pollen time series. Quat. Res. 28, 100-118.

Guiot, J., 1990. Methodology of the last climatic cycle reconstruction in France from pollen data. Palaeogeography 80, 49-69.

Guiot, J., Goeury, C., 1996. 3Pbase – a software for statistical analysis of paleoecological and paleoclimatological data. Dendrochronologia 14, 123-135.

Guiot, J., Pons, A., de Beaulieu, J.-L., Reille, M., 1989. A 140,000-year continental climate reconstruction from two European pollen records. Nature 338, 309-313.

Hyvärinen, H., 1985. Holocene pollen stratigraphy of Baird Inlet, east-central Ellesmere Island, arctic Canada. Boreas 14, 19-32.

Jackson, S.T., Williams, J.W., 2004. Modern analogs in Quaternary paleoecology: here today, gone yesterday, gone tomorrow? Annu. Rev. Earth Planet. Sci. 32, 495-537.

Kerwin, M.K., 2000. Quantifying and modeling Holocene climate variability based on modern and fossil pollen records from the Eastern Canadian Arctic and subarctic. Unpublished PhD thesis, University of Colorado, Boulder, U.S.A.

Kerwin, M.K., Overpeck, J.T., Webb, R.S., Anderson, K.H., 2004. Pollen-based summer temperature reconstructions for the Eastern Canadian Boreal forest, Sub-Arctic and Arctic. Quat. Sci. Rev. 23, 1901-1924.

Legendre, P., Legendre, L., 1998. Numerical ecology, 2nd English edition. Elsevier Science BV, Amsterdam.

LIGA Members, 1991. Report of the 1st discussion group: The last interglacial in high latitudes of the northern hemisphere: terrestrial and marine evidence. Quat. Int. 10-12, 9-28.

MacDonald, G.M., Ritchie, J.C., 1986. Modern pollen spectra from the western interior of Canada and the interpretation of late Quaternary vegetation development. New Phytol. 102, 245-268.

Mäkelä, E.E., 1996. Size distributions between *Betula* pollen types – A review. Grana 35, 248-256.

Maxwell, J.B., 1980. The climate of the Canadian Arctic Islands and adjacent waters. Atmospheric Environment Services, Downsview.

McAndrews, J.H., Berti, A.A., Norris, G., 1973. Key to the Quaternary pollen and spores of the great Lakes region. Life Science Miscellaneous Publications, Royal Ontario Museum, Toronto, Canada.

Miller, G.H., Andrews, J.T., Short, S.K., 1977. The last interglacial-glacial cycle, Clyde Foreland, Baffin Island, N.W.T.: stratigraphy, biostratigraphy, and chronology. Can. J. Earth Sci. 14, 2824-2857.

Miller, G.H., Mode, W.N., Wolfe, A.P., Sauer, P.E., Bennike, O., Forman, S.L., Short, S.K., Stafford Jr., T.W., 1999. Stratified interglacial lacustrine sediments from Baffin Island, Arctic Canada: chronology and paleoenvironmental implications. Quat. Sci. Rev. 18, 789-810.

Miller, G.H., Wolfe, A.P., Steig, E.J., Sauer, P.E., Kaplan, M.R., Briner, J.P., 2002. The Goldilocks dilemma: big ice, little ice, or 'just-right' ice in the Eastern Canadian Arctic. Quat. Sci. Rev. 21, 33-48.

Mode, W.N., Jacobs, J.D., 1987. Surficial geology and palynology, inner Frobisher Bay. In J.T. Andrews (Eds.), Cumberland sound and Frobisher Bay, southeastern Baffin Island, N.W.T. (pp. 53-62). XIIth INQUA Congress Field Excursion Guidebook C-2. Ottawa: National Research Council of Canada.

Moore, P.D., Webb, J.A., Collinson, M.E., 1991. Pollen analysis, 2nd edition. Blackwell Scientific Publications, Oxford.

Nesje, A., 1992. A piston corer for lacustrine and marine sediments. Arct. Alp. Res. 24, 257-259.

NGRIP Members, 2004. High-resolution record of Northern Hemisphere climate extending into the last interglacial period. Nature 431, 147-151.

Oswald, W.W., Anderson, P.M., Brubaker, L.B., Hu, F.S., Engstrom, D.R., 2003. Representation of tundra vegetation by pollen in lake sediments of northern Alaska. J. Biogeogr. 30, 521-535.

Overpeck, J.T., Webb, T., III, Prentice, I.C., 1985. Quantitative interpretation of fossil pollen spectra: dissimilarity coefficients and the method of modern analogs. Quat. Res. 23, 87-108.

Pielke, R.A., Vidale, P.L., 1995. The boreal forest and the polar front. J. Geophys. Res. 100, 755-758.

Prentice, I.C., 1981. Quantitative birch (*Betula* L.) pollen separation by analysis of size frequency data. New Phytol. 89, 145-157.

Richard, P.J.H., 1970. Atlas pollinique des arbres et de quelques arbustes indigènes du Québec. Nat. Can. 97, 1-34, 97-161, 241-306.

Richard, P.J.H., 1979. Contributions à l'histoire postglaciaire de la végétation au nord-est de la Jamésie, Nouveau-Québec. Géogr. Phys. Quat. 33, 93-112.

Richard, P.J.H., 1981. Paléophytogéographie postglaciaire en Ungava par l'analyse pollinique. Collection Paléo-Québec 13, Université du Québec à Trois-Rivières, Trois-Rivières.

Richard, P.J.H., Bouchard, M.A., Gangloff, P., 1991. The significance of pollen-rich inorganic lake sediments in the Cratère du Nouveau-Québec area, Ungava, Canada. Boreas 20, 135-149.

Ritchie, J.C., 1974. Modern pollen assemblages near the arctic treeline, Mackenzie Delta region, Northwest Territories. Can. J. Bot. 52, 381-396.

Ritchie, J.C., Hadden, K.A., Gajewski, K., 1987. Modern pollen spectra from lakes in arctic western Canada. Can. J. Bot. 65, 1605-1613.

Ritchie, J.C., Lichti-Federovitch, S., 1967. Pollen dispersal phenomena in Arctic-Subarctic Canada. Rev. Paleobot. Palynol. 3, 255-266.

Sandgren, P., Fredskild, B., 1991. Magnetic measurements as recorders of Late Holocene man-induced erosion in the interior of South Greenland. Boreas 20, 315-331.

Short, S.K., Mode, W.N., Davis, P., 1985. The Holocene record from Baffin Island: modern and fossil pollen studies. In J.T. Andrews (Ed.), Quaternary environments: Eastern Canadian Arctic, Baffin Bay and Western Greenland (pp. 608-642). Boston, Allen and Unwin.

Steig, E.J., Wolfe, A.P., Miller, G.H., 1998. Wisconsinan refugia and the late glacial history of eastern Baffin Island, Arctic Canada: Coupled evidence from cosmogenic isotopes and lake sediments. Geology 26, 835-838.

ter Braak, C.J.F., Prentice, I.C., 1988. A theory of gradient analysis. Adv. Ecol. Res. 18, 271-317.

ter Braak, C.J.F., Šmilauer, P., 1998. CANOCO for windows: software for Canonical Community Ordination (version 4). Microcomputer Power, Ithaca, NY, USA.

Wolfe, A.P., 1994. Late Wisconsinan and Holocene diatom stratigraphy from Amarok Lake, Baffin Island, N.W.T. J. Paleolimnol. 10, 129-139.

Wolfe, A.P., 1996. A high resolution late-glacial and early Holocene diatom record from Baffin Island, eastern Canadian Arctic. Can. J. Earth Sci. 33, 928-937.

Wolfe, A.P., Fréchette, B., Richard, P.J.H., Miller, G.H., Forman, S.L., 2000. Paleoecology of a >90,000-year lacustrine sequence from Fog Lake, Baffin Island, Arctic Canada. Quat. Sci. Rev. 19, 1677-1699.

Wolfe, A.P., Härtling, J.W., 1996. The late Quaternary development of three ancient tarns on southwestern Cumberland Peninsula, Baffin Island, Arctic Canada: Paleolimnological evidence from diatoms and sediment chemistry. J. Paleolimnol. 15, 1-18.

Wolfe, A.P., Miller, G.H., Olsen, C.A., Forman, S.L., Doran, P.T., Holmgren, S.U., 2004. Geochronology of high latitude lake sediments. In R. Pienitz, M.S.V. Douglas and J.P. Smol (Eds). Long-term Environmental Change in Arctic and Antartic Lakes. Developments in Paleoenvironmental Research, vol. 8, Springer, Dordrecht, p.19-52.

Wolfe, A.P., Smith, I.R., 2004. Paleolimnology of the Canadian Arctic Archipelago. In R. Pienitz, M.S.V. Douglas and J.P. Smol (Eds). Long-term Environmental Change in Arctic and Antartic Lakes. Developments in Paleoenvironmental Research, vol. 8, Springer, Dordrecht, p.241-268.

Young, S.B., 1971. The vascular flora of St-Lawrence Island with special reference to floristic zonation in the arctic region. Contribution of the Herbarium of Harvard University 201, 11-115.

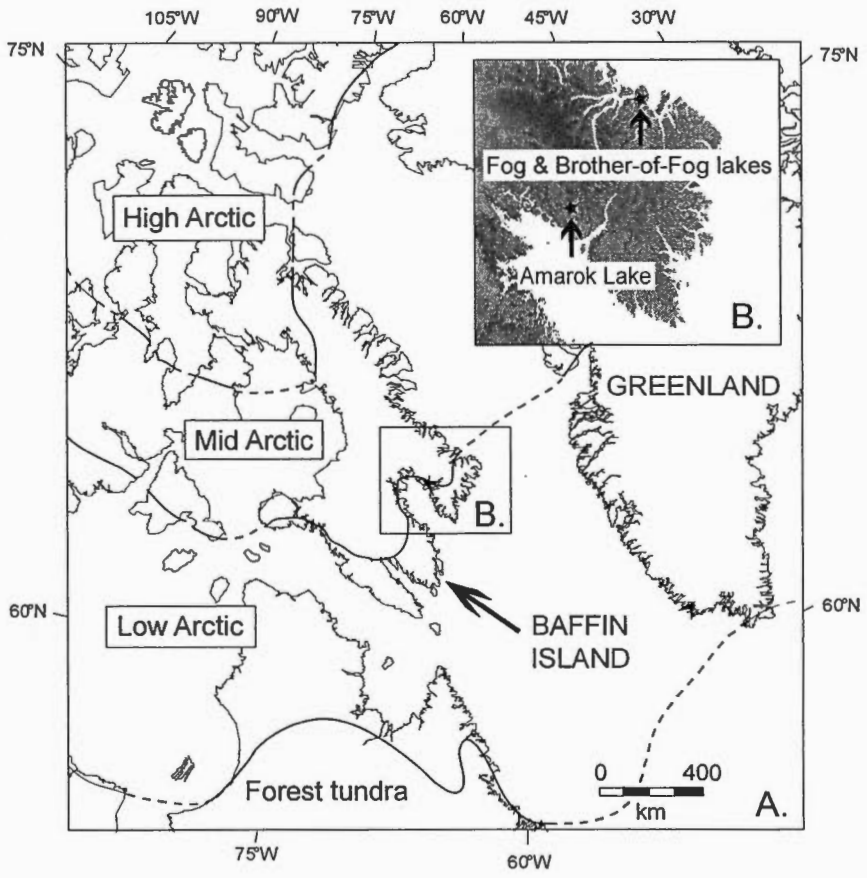

Figure 1. Locations of the study lakes on northern Cumberland Peninsula, Baffin Island, and approximate limits of Low, Middle, and High Arctic vegetation zones after Young (1971).

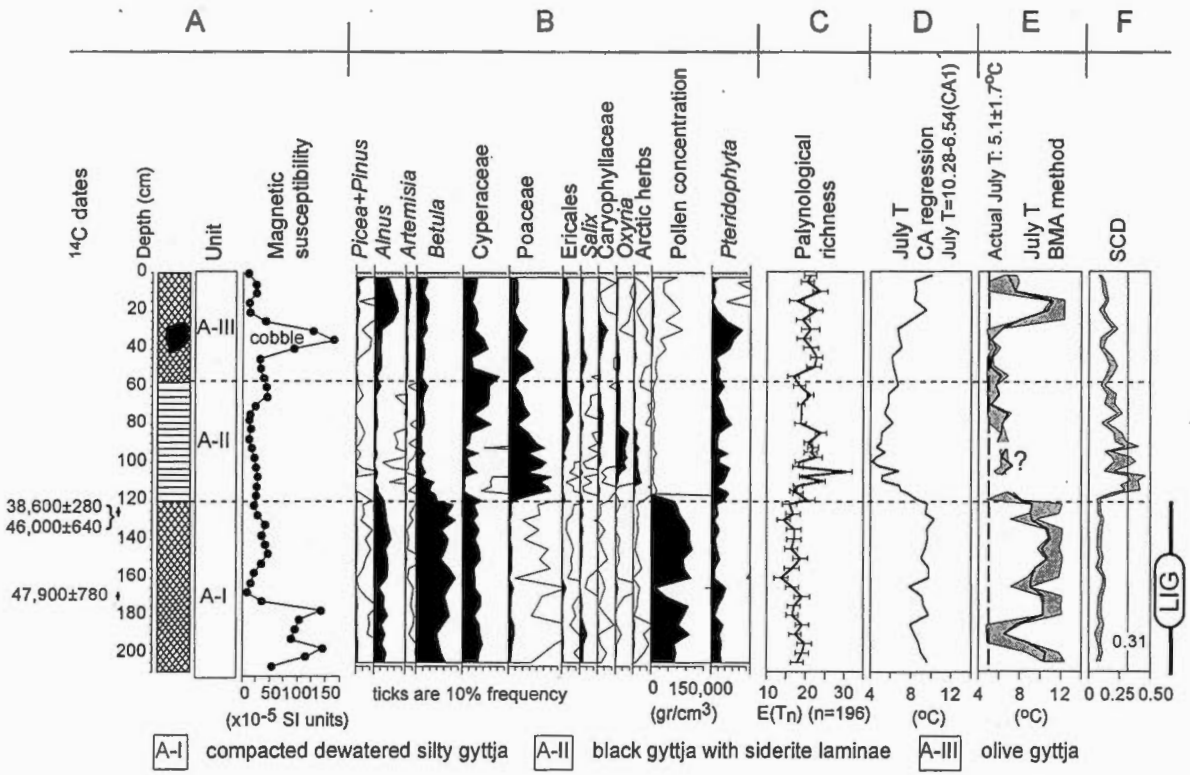

Figure 2. Amarok Lake (66°16'N, 65°45'W, 848 m asl) summary lithology, pollen stratigraphy, and July air temperature reconstructions. A. Summarized sediment stratigraphy, magnetic susceptibility, and uncalibrated radiocarbon dates. Horizontal dashed lines delineate lithological units. B. Simplified percentage pollen diagram. Unshaded curves are 10x exaggerations of pollen relative frequencies. Taxa are ordered according to their scores on the first axis of CCA in the modern reference data set. The Arctic herbs category includes the following taxa: Ranunculaceae, Brassicaceae, Saxifragaceae, *Dryas*, Papaveraceae, Rosaceae, other Polygonaceae. C. Expected taxonomic richness (E(Tn)) as estimated by rarefaction analysis, with 95% confidence intervals shown as horizontal bars (Birks and Line, 1992). D. July air temperature reconstructions based on the CA regression (see Fig. 5C). E. July air temperature reconstructions based on closest modern analogues. The thick curve is the weighted mean July air temperature associated with the five closest analogues. The grey area represents the confidence interval. The vertical dashed line shows the actual July air temperature (Environment Canada, 2004). F. The squared-chord distance (SCD) of the first and the fifth analogue with each fossil spectrum. The vertical line shows the adopted threshold value (0.31). LIG: last interglacial interval.

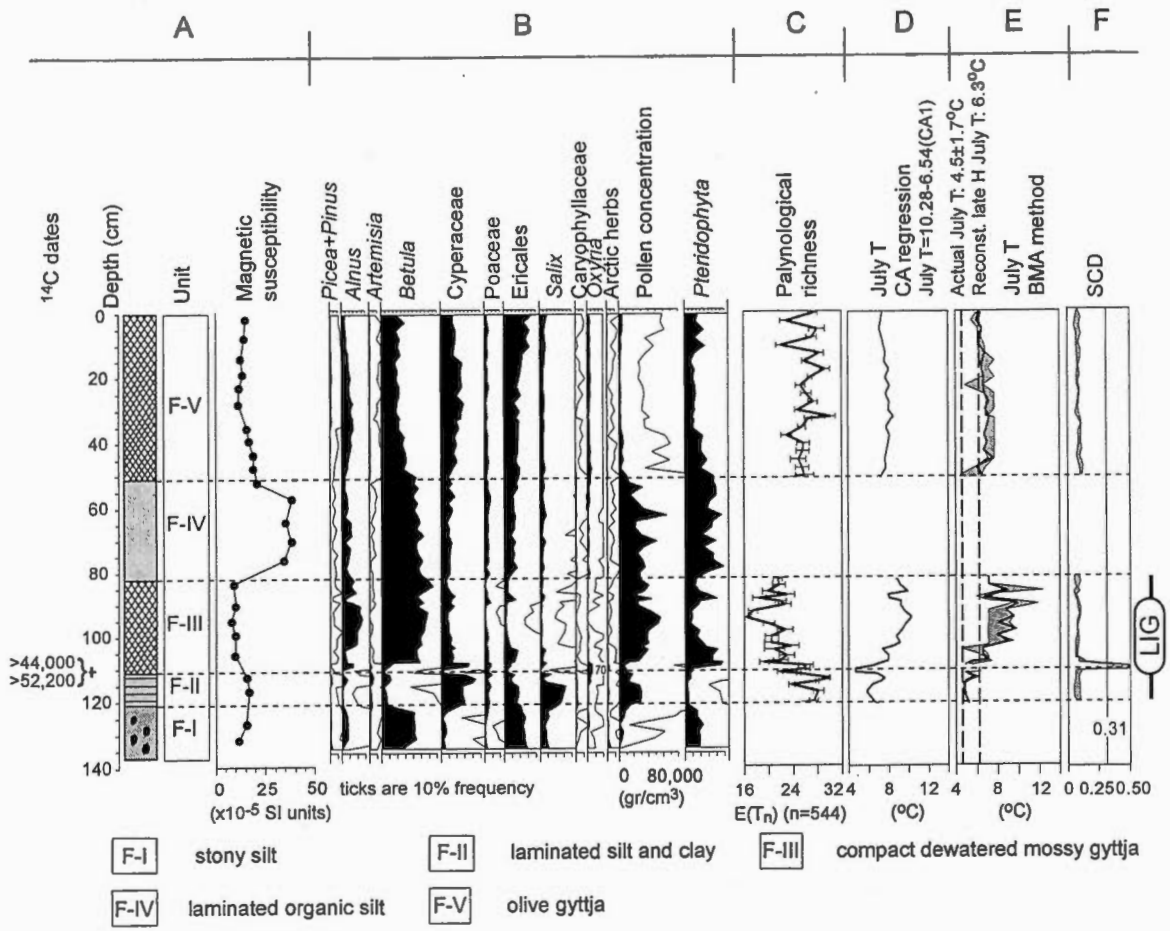

Figure 3. Fog Lake (67°11'N, 63°15'W, 460 m asl) summary lithology, pollen stratigraphy, and July air temperature reconstructions. Legends for A-F are as for Fig. 2. Note that the *Oxyria* pollen curve is truncated at 110 and 112 cm. At these levels, *Oxyria* pollen frequency reaches 70%.

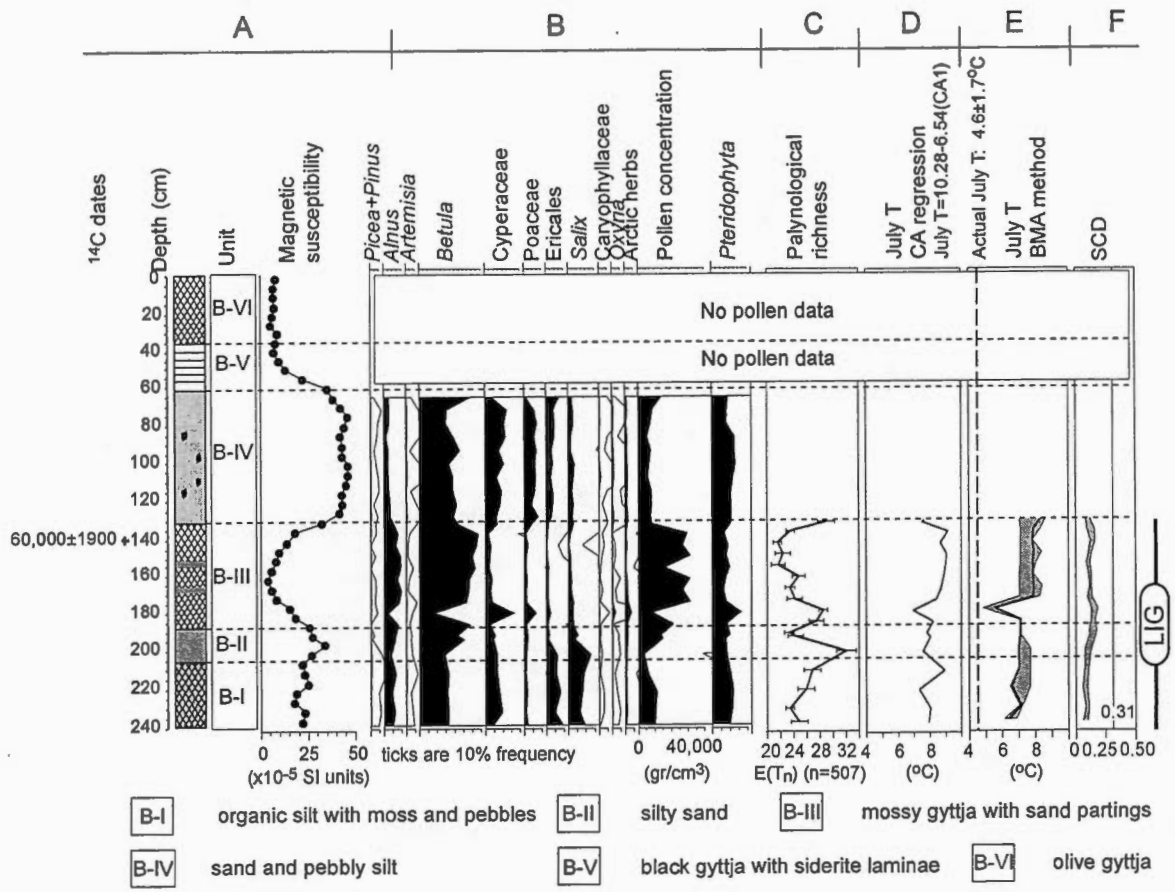

Figure 4. Brother-of-Fog Lake (67°11'N, 63°15'W, 380 m asl) summary lithology, pollen stratigraphy, and July air temperature reconstructions. Legends for A-F are as for Figs. 2 and 3.

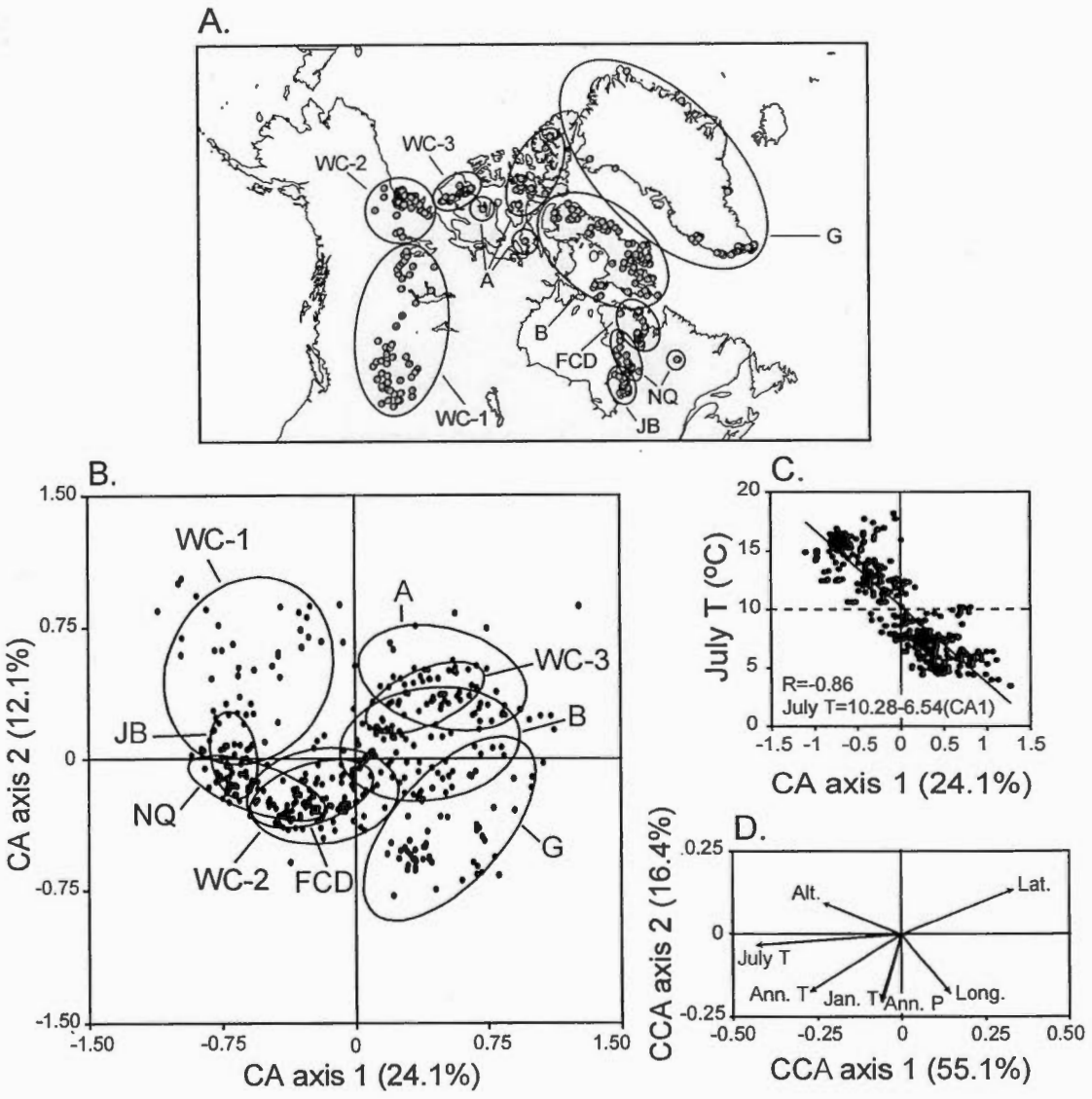

Figure 5. A. Locations of the 400 lake sediment surface samples used to construct the modern pollen database. The 400 sites have been grouped in nine geographical regions: Western Canada (WC), James Bay (JB), northern Québec (NQ), Fort Chimo - Diana Bay (FCD), Baffin Island (B), Arctic islands (A) and Greenland (G). B. Results of Correspondence Analysis (CA) ordination showing sample scores from the 400 modern sites. A 95% ellipse is drawn around the reference sites of each region. C. Plot of CA axis 1 sample scores against interpolated July air temperature. The horizontal dashed line delineates sites in the Low Arctic from those occupying forest tundra. D. Canonical Correspondence Analysis (CCA) plot of environmental gradients associated with the 400 modern sites.

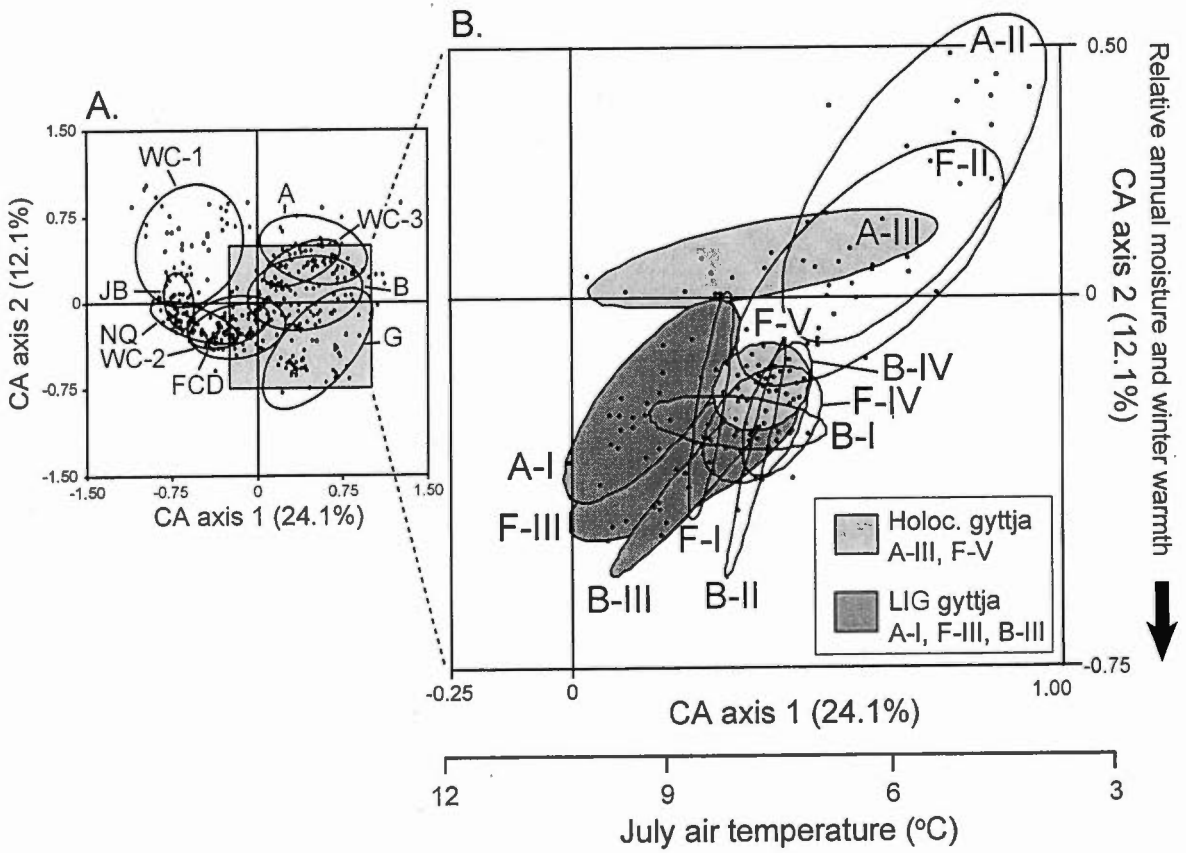

Figure 6. A. Correspondence Analysis (CA) ordination diagram of sample scores from the 400 modern assemblages. A 95% ellipse is drawn around the reference sites of each region. B. Projection of fossil assemblages from Amarok, Fog, and Brother-of-Fog lakes in the ordination spaces defined by the 400 modern assemblages. A 95% ellipse is drawn around the fossil assemblages of each unit. The July air temperature scale has been calculated with the CA regression: July air T = 10.28-6.54(CA1) (see Fig. 5C).

Table 1. AMS ^{14}C dates pertaining to the lower organic units of the cores investigated here.

Core	Depth (cm)	Unit	^{14}C ages (yr BP)	Lab number	Material
98AKL-02	124-125	A-I	38,600±280	OS-17676	Humic acid extract
98AKL-02	124-125	A-I	46,000±640	OS-18067	Bryophyte macrofossil
98AKL-02	170-171	A-I	47,900±780	OS-18066	Bryophyte macrofossil
96FOG-05	110.0-111.5	F-III	>44,400	CAMS-31808	Humic acid extract
96FOG-05	110.0-111.5	F-III	>52,200	CAMS-28652	Bryophyte macrofossil
98BRO-05	134.5-135.5	B-III	60,000±1900	OS-18064	Bryophyte macrofossil

Table 2. Pollen taxa retained in the modern database for paleoclimate reconstructions. Taxa that do not grow on Baffin Island today are indicated by *.

Woody plants	Herbs
*Abies**	*Ambrosia**
Betula	Apiaceae*
Cupressaceae*	*Artemisia*
*Larix**	Brassicaceae
*Picea**	Caryophyllaceae
*Pinus**	Chenopodiaceae*
*Populus**	Crassulaceae
*Alnus**	Cyperaceae
Dryas	Fabaceae
Ericales	Onagraceae
*Myrica**	*Oxyria/Rumex*
Salix	Papaveraceae
*Shepherdia**	*Plantago*
	Poaceae
	Polygonaceae
	Ranunculaceae
	Rosaceae
	Saxifragaceae
	Scrophulariaceae
	*Thalictrum**
	Tubuliflorae/Liguliflorae

Table 3. Summary of pollen-based July air temperature reconstructions (in °C) from the three studied lakes.

Site	Method [a]	LIG [b]	Max LIG	Early Holocene [c]	Late Holocene [d]
Amarok	CA	9.5±0.4	10.3	6.4±1.3	9.0±0.9
Amarok	BMA	9.9±0.8	11.0	6.6±1.8	7.1±0.4
Amarok	Concensus	9.7±0.7	n.a.	6.5±1.5	8.1±1.2
Fog	CA	9.0±0.8	10.3	7.8±0.4	7.6±0.3
Fog	BMA	8.2±1.2	10.0	6.7±0.4	6.5±0.3
Fog	Consensus	8.6±1.1	n.a.	7.2±0.6	7.0±0.6
Brother-of-Fog	CA	8.8±0.3	9.2	n.a.	n.a.
Brother-of-Fog	BMA	7.8±0.3	7.9	n.a.	n.a.
Brother-of-Fog	Consensus	8.3±0.6	n.a.	n.a.	n.a.

[a] CA: correspondence analysis regression, BMA: best modern analogue, Consensus: CA and BMA together

[b] last interglacial

[c] > 5 cal ka BP

[d] < 5 cal ka BP

CHAPITRE III

REGIONALISM OF CLIMATE CHANGES IN SOUTHWEST GREENLAND AND EASTERN BAFFIN ISLAND AREAS SINCE 7000 YEARS

Bianca Fréchette[a], Anne de Vernal[a], Gifford H. Miller[b],
Alexander P. Wolfe[c],

[a] GEOTOP, Université du Québec à Montréal, P.O. Box 8888, Succ. Centre-Ville, Montréal, QC H3C 3P8, Canada
[b] INSTAAR and Department of Geological Sciences, University of Colorado, Boulder, CO 80309-0450, USA
[c] Department of Earth and Atmospheric Sciences, University of Alberta, Edmonton, AB T6G 2E3, Canada

En préparation pour être soumis à la revue scientifique
Science

Résumé

Le stabilité du climat de l'Holocène, jadis bien acceptée parmi la communauté scientifique, est actuellement remise en question. Ce doute découle de la découverte d'inégalités dans son évolution climatique, dans le temps et l'espace, et d'oscillations millénaires depuis ca. 11 500 ans BP. L'hypothèse de l'existence d'un régionalisme dans les changements climatiques au cours de l'Holocène semble de plus en plus éprouvée. Les relevés disponibles sont toutefois peu nombreux, en particulier pour les hautes latitudes. À partir de relevés polliniques de séquences sédimentaires lacustres, nous montrons qu'au cours des dernières 7000 années, le refroidissement estival fut davantage prononcé sur la côte sud-ouest du Groenland (3,0-3,5°C) que sur la côte est de la Terre de Baffin (0,5-1,0°C). Ce régionalisme dans l'évolution du climat, de l'Holocène moyen à l'Holocène supérieur, est cohérent avec les relevés marins. En effet, la température estivale des masses d'eau de surface a très peu changé dans la secteur ouest de la mer du Labrador alors qu'au large, dans la région centrale de l'Atlantique nord, plus précisément dans la région de la Ride de Reykjanes, un refroidissement de plus de 6°C a été enregistré. Les résultats soulignent l'étroit lien entre la circulation océanique de surface et le climat atmosphérique des marges est canadiennes et du Groenland. Par ailleurs, les résultats suggèrent une diminution, avec le temps, de l'influence du flux d'eau chaude nord-atlantique sur les conditions hydro-climatiques du sud du Groenland, alors que la Terre de Baffin et les marges est canadiennes seraient vraisemblablement demeurées sous l'influence des courants froids de Baffin et du Labrador.

Abstract

The Holocene climate that has been considered "stable" for a long time in the scientific literature is now the subject of debate with respect to trends and millennial oscillations. There is growing evidence for regionalism in the climate changes, but the records are still scattered, especially at high latitudes. Here, we show from terrestrial records that the last 7000 years have been marked by a trend of cooling in southwest Greenland (3.0-3.5°C), much larger in amplitude than in eastern Baffin Island (0.5-1.0°C). Such regionalism in the mid- to late Holocene climate trend is consistent with marine core data indicating no significant changes of sea-surface temperature (SST) in the northwest Labrador Sea, whereas cooling of up to 6°C is recorded offshore in the central North Atlantic, in the Reykjanes Ridge area. The results illustrate strong linkages between ocean circulation pattern and terrestrial climate along eastern Canadian margins and Greenland. They also point to the decreasing influence of North Atlantic water inflow as moisture and heat source over southern Greenland, whereas Baffin Island and eastern Canadian margins apparently remained under Arctic influence through the Baffin Land and Labrador currents.

3.1. Principal text

Present-day climate conditions across the subpolar North Atlantic are by no means uniform, and regional scale differences need to be taken into account in paleoclimate studies and for climate and paleoclimate modelling (Wohlfahrt et al., 2004; Renssen et al., 2005). Over the past few years, paleoclimate studies from both marine and terrestrial records at high latitudes of the North Atlantic and adjacent lands have reported different regional trends in climate changes during the Holocene (e.g. Kaufman et al., 2004; de Vernal and Hillaire-Marcel, 2006). Of particular importance is the mid- to late Holocene summer sea-surface temperature (SST) cooling which shows significant differences in the western and eastern North Atlantic, suggesting important changes in surface ocean circulation pattern (e.g., Marchal et al., 2002; Andersen et al., 2004a; Moros et al., 2004). In addition to variations in SST distribution in space, some records suggest changes in the annual amplitude of temperature, notably in the northeast North Atlantic (e.g. Solignac et al., 2006; de Vernal and Hillaire-Marcel, 2006). Thus, the mid-late Holocene climate history is more complex than previously thought (e.g. Steig, 1999). Large uncertainties remain concerning the regional response of terrestrial and marine environments to changes in insolation and ocean circulation. Here we use palynological data from marine and lacustrine sediment cores collected in the northwest North Atlantic and adjacent lands (Baffin Island and southern Greenland) to derive climate records spanning about 8000 years for terrestrial and marine ecosystems.

Pollen grains and dinocysts are two biogenic proxies currently used in paleoclimatology and paleoceanography to reconstruct air and sea-surface paleotemperatures, respectively (e.g., Davis et al., 2003; de Vernal et al., 2005). In order to establish paleoclimate records of terrestrial environments, we analysed the

pollen content of two lacustrine sedimentary sequences. One is from eastern Baffin Island (Akvaqiak Lake; 66°47'N, 63°57'W; 45 m a.s.l.) and the other is from southwest Greenland (Qipisarqo Lake; 61°00'N, 47°45'W; 7 m a.s.l.) (Fig. 1). Both lakes are from low elevations, in protected valleys or lowlands located at the extremity of fjords. The climate conditions at both sites show important contrast, especially in winter. The present-day July and January air temperatures average respectively 4.6 ± 1.7°C and -24.8 ± 4.4°C on eastern Baffin Island (Environment Canada, 2004) and 6.4 ± 0.7°C and -6.5 ± 0.8°C in southwest Greenland (Cappelen et al., 2001). Annual precipitation is about 332 mm on eastern Baffin Island and 753 mm in southwest Greenland. The higher winter temperature and annual precipitation in southern Greenland are related to oceanic circulation patterns. The relatively warm West Greenland Current (WGC), which is formed from the mixing of the cold East Greenland Current (EGC) and a westward branch of the North Atlantic Current (NAC), drives relatively mild conditions along the southwest Greenland coast, whereas the outflow of cold, low-salinity surface waters from the Arctic Ocean through the Baffin Land Current (BLC) and dense winter sea-ice cover drives cold winter conditions on eastern Baffin Island.

In parallel to pollen from lake cores, the dinocyst content of deep-sea cores is used to document changes in offshore sea-surface conditions (Fig. 1). Core HU021 (58°22.06'N, 57°30.42'W) was collected on the continental slope of the Canadian margin, at the vicinity of the center of deep Labrador Sea Water (LSW) formation. The core is located close to a front between the Labrador Current (LC) formed from the BLC and outflow from the Hudson Strait, and the WGC. At site HU021, modern sea-surface temperature (SST) and salinity (SSS) in summer are 6.7°C and 34.3 psu, respectively, and sea-ice cover develops for about 2 months per year (2.0±1.05) during winter (cf. de Vernal and Hillaire-Marcel, 2006). Core HU085 was collected in the northwest North Atlantic (53°58.51'N, 38°38.25'W), along the axis of the warm NAC, where SST is at 10.3°C and 5.3° C in summer and winter respectively

and where salinity ranges from 34.5 to 34.8 psu (de Vernal and Hillaire-Marcel, 2006).

The respective location of the terrestrial and marine sedimentary sequences appears thus suitable to address the question of changes in ocean circulation patterns and its impact on continental climates, since they lie in the trajectory of surface ocean currents that play a major role in northward heat fluxes (the North Atlantic Current and its westward branch making the West Greenland Current) and southward Arctic water flow (Baffin Land, Labrador and East Greenland currents).

The chronology of the lake sequences has been established from calibrated ^{14}C dates on organic matter, which were used to derive an age model from smoothed linear interpolation (see Table S1 and Fig. S1 in Supporting Material). For the last 8000 cal. years, sediment accumulation rates average 11.35 ± 4.41 cm/ka at Akavaqiak Lake and 26.77 ± 16.84 cm/ka at Qipisarqo Lake. Palynological analyses performed at 3 to 5 cm interval yield a multi-centennial resolution, which permits us to identify Holocene trends, but makes difficult to identify millennial oscillations. At Qipisarqo Lake, the pollen fluxes are 438 ± 212 grains/cm^2/year and the assemblages are dominated by *Betula* (birches) and Ericales (heaths) (see Fig. S2 in Supporting Material). At Akavaqiak Lake, the pollen fluxes are 156 ± 76 grains/cm^2/year and the assemblages are dominated by *Betula* (birches) and Ericales (heaths) (see Fig. S2 in Supporting Material). Given the modern vegetation and pollen content in surface sediments, the assemblages reflect local and regional influxes with minor contributions from long-distance transport.

The chronology of the deep-sea cores has been established from ^{14}C dates on planktonic foraminifers corrected by 400 years to account for the air-sea reservoir differences and calibrated to calendar years to derive an age model from smoothed linear interpolation (see Supporting Material). For the last 8000 cal. years,

sedimentation rates average 17.61 cm/ka in core HU021 and in core HU085 they are 6.22 cm/ka. Palynological analyses performed at 1 to 2 cm intervals yield a centennial resolution, which permits identification of Holocene and possibly millennial oscillations. In cores HU021 and HU085, the dinocyst fluxes are of the order of 50,000 and 2000 cysts/ka, respectively, which indicate relatively high productivity at both sites. In core HU021, the assemblages are characterized by the increase of the subpolar taxa *Nemotosphaeropsis labyrinthus* and temperate taxon from the early to late Holocene. In core HU085, the dinocyst assemblages are dominated by temperate taxa and characterized by maxima of thermophilic species (*Spiniferites mirabilis*, *Impagidinium* spp.) in the early Holocene (see Fig. 3 in Supporting Material). These dinocyst assemblages are consistent with the more temperate conditions in the axis of the NAC than off the Canadian margins

Principal component analysis (PCA) is used to summarize the middle to late Holocene succession and variability in pollen and dinocyst assemblages. The first PCA in both lake and marine cores shows strong linear trends in assemblages since 8000 cal. years BP (Fig. 2) (see Table S2 in Supporting Material for details on PCA loadings). The first eigenvalue (λ_1) of eastern sites (Qipisarqo and HU085) is two times higher than western sites (Akvaqiak and HU021) indicating much higher amplitude of change in pollen and dinocyst assemblages in southwest Greenland and central North Atlantic than in eastern Baffin Island and along the Canadian margin. At all sites there is a pronounced change around the mid-late Holocene transition (i.e., at about 5000 cal. years BP). The transition is abrupt in the central North Atlantic (HU085), whereas it appears more gradual westward, in eastern Baffin Island (Akvaqiak). An abrupt mid to late Holocene transition has been also reported from coccolith and dinocyst data in marine cores from the central North Atlantic, south of Iceland (Giraudeau et al., 2000) and on the northern Iceland shelf (Solignac et al., 2006). Such an abrupt mid to late Holocene transition, which is documented from

different proxies in the central part of the North Atlantic, near the main axis of the NAC, is a robust feature in the regional paleoceanography.

In order to examine the change in ocean conditions and its relationship with terrestrial climate, we reconstructed sea-surface and air temperatures from dinocyst and pollen assemblages, respectively (see Method section in Supporting Material). Akvaqiak and Qipisarqo lakes show a progressive decrease in July air temperature since 7000 cal. years BP (Fig. 3). However, the amplitude of the cooling at Qipisarqo Lake (3.5°C) is much more pronounced than at Akvaqiak Lake, where the cooling trend does not exceed 1°C (Figs. 3c, 3d, 4b). The east to west contrast in the amplitude of the mid to late Holocene trend is also observed in the marine record: the central North Atlantic site (HU085) shows a progressive decrease in August SST of about 6°C, whereas the Canadian margin site (HU021) does not show a significant trend (Figs. 3b, 3e, 4c). Such east to west gradients in the amplitude of the Holocene cooling trend seems to be a consistent feature across the mid to high latitudes of the central and western North Atlantic (de Vernal and Hillaire-Marcel, 2006).

Beyond trends in temperature, the marine data permit reconstruction of salinity. In the context of the Canadian margins, low salinity anomalies can be associated with the outflow of Arctic ocean water and often correspond to enhanced winter sea ice. Interestingly, the summer SSS estimates at HU021 show three short-term oscillations at 2-3, 5-5.5 and 6.8-7.2 cal. ka BP (Fig. 3a). Despite uncertainties in the absolute chronology of the terrestrial vs. marine sequences, the salinity oscillations have a terrestrial counterpart in the July air temperature estimates at the Baffin Island site (Fig. 3c). The consistency of the two independent records suggests that short-term cooling events may relate to pulses of freshwater/meltwater exported from the Arctic through the BLC and LC, which may have contributed to lower air temperatures in eastern Baffin Island, episodically from mid-Holocene to today.

In addition to reconstruction of July air temperature, the pollen record permits semi-quantitative inferences about winter temperature and precipitation. These two parameters that covary in the modern database are strongly related to the second axis derived from correspondence analyses (CA). The mid to late Holocene is characterized by a gradual trend of decreasing scores for the CA axis 2 at both Qipisarqo and Akvaqiak lakes, which would correspond to a gradual increase in winter warmth and annual moisture (Fig. 4e) (see Methods in the Supporting Material for details on calculations). These results suggest a trend towards enhanced oceanic influence on climate of eastern Baffin Island and southwest Greenland from the early to the late Holocene. Our results showing a trend toward milder winters and/or enhanced snow fall appear consistent with the results of other studies at high latitudes of the Northern Hemisphere. Pollen data from western Europe led to the reconstruction of increasing winter temperature throughout the Holocene (Fig. 4f) (Davis et al., 2003), and various paleoceanographical data also suggest slight winter temperature increase in the subpolar North Atlantic (Moros et al., 2004; Solignac et al., 2006). Moreover, a late-Holocene increase in annual precipitation was also proposed to explain the limited eolian deflation and dust transport to the Penny ice cap on Baffin Island (Zdanowicz et al., 2000) and glacier expansion in Scandinavia (Dahl and Nesje, 1996; Nesje et al., 2001).

Our reconstructions show a Holocene summer cooling trend that is particularly pronounced in southern Greenland. They also suggest a slight winter warming from the middle to late Holocene, which would indicate a decrease in the seasonal contrast of temperatures. Decreased seasonality applies to both terrestrial and marine environments, and is supported by paleoecological data from Scandinavia (e.g. Hammarlund et al., 2002) and paleoceanographic records from the northern North Atlantic (Solignac et al., 2006; de Vernal and Hillaire-Marcel, 2006) and is consistent with reduced seasonal contrasts in insolation (Fig. 4g) (Berger and Loutre, 1991).

The middle to late Holocene insolation change (Berger and Loutre, 1991) certainly accounts for a large part in the cooling recorded and the decreasing winter to summer temperature contrast. However, differences if the amplitude of the cooling trend (lower in the western North Atlantic than in the eastern North Atlantic; Figs. 4b, 4c) most probably reflect changes in the ocean circulation pattern. We suggest that the strong mid-Holocene east to west thermal gradient could have been generated by stronger and/or warmer NAC, i.e. enhanced poleward penetration of warm North Atlantic waters (e.g. Koç et al., 1993; Kerwin et al., 1999; Duplessy et al., 2001; Birks and Koç, 2002; de Vernal and Hillaire-Marcel, 2006), and enhanced freshwater/meltwater export from the Arctic (e.g. Andersen et al., 2004b; de Vernal and Hillaire-Marcel, 2006). These hydrographic conditions during the middle Holocene may have promoted summer temperatures higher in central North Atlantic and southwest Greenland than along the eastern Canadian margins, including Baffin Island. During the late Holocene, a weakening of the NAC strength northeastward concomitant with reduced freshwater/meltwater export from the Arctic through the EGC (Solignac et al., 2006), BLC and LC (de Vernal and Hillaire-Marcel, 2006) would have resulted in the diminution of the west to east gradient of temperature, both in surface waters and inland. Reduced freshwater export from the Arctic balanced by an enhanced westward component of the NAC could have favoured milder winters and increased snow fall during late-Holocene in the eastern Baffin Bay area.

In summary, our terrestrial climate reconstructions and the paleoceanographical records from northwest North Atlantic region illustrate the sensitivity of the climate system during a warm interglacial interval and provide evidence for strong linkages between terrestrial climate and oceanic conditions in the subpolar North Atlantic during the middle to late Holocene (e.g., Chapman and Shackleton, 2000; Jiang et al., 2002; Hall et al., 2004; Moros et al., 2004; Maddy et al., 2005).

References for principal text

Alley, R.B., Agustsdottir, A.M., Fawcwtt, P.J., 1999. Ice-core evidence of Late Holocene reduction in North Atlantic Ocean heat transport. Geophysical Monograph 112, 301-312.

Andersen, C., Koç, N., Jennings, A., Andrews, J.T., 2004a. Non uniform response of the major surface currents in the Nordic Seas to insolation forcing: implications for the Holocene climate variability. Paleoceanography 19, PA2003, doi: 10.1029/2002PA000873.

Andersen, C., Koç, N., Moros, M, 2004b. A highly unstable Holocene climate in the subpolar North Atlantic: evidence from diatoms. Quaternary Science Reviews 23, 2155–2166.

Berger, A., Loutre, M.F., 1991. Insolation values for the climate of the last 10 million years. Quaternary Science Reviews 10, 297-318.

Birks, C.J.A., Koç, N., 2002. A high-resolution diatom record of late-Quaternary sea-surface temperatures and oceanographic conditions from the eastern Norwegian Sea. Boreas 31, 323-344.

Cappelen, J., Jørgensen, B., Laursen, E., Stanius, L., Thomsen, R., 2001. The observed climate of Greenland – with climatological normals, 1961-90. DMI Technical Report No. 00-18.

Chapman, M.R., Shackleton, N.J., 2000. Evidence of 550-year and 1000-year cyclicities in North Atlantic circulation patterns during the Holocene. The Holocene 10, 287-291.

Dahl, O.S., Nesje, A., 1996. A new approach to calculating Holocene winter precipitation by combining glacier equilibrium-line altitudes and pine-tree limits: a case study from Hardangerjokulen, central southern Norway. The Holocene 6, 381-398.

Davis, B.A.S., Brewer, S., Stevenson, A.C., Guiot, J., Data Contributors, 2003. The temperature of Europe during the Holocene reconstructed from pollen data. Quaternary Science Reviews 22, 1701-1716.

de Vernal, A., Hillaire-Marcel, C., 2006. Provincialism in trends and high frequency changes in the northwestern North Atlantic during the Holocene. Global and Planetary Changes 54, 263-290.

de Vernal, A., Eynaud, F., Henry, M., Hillaire-Marcel, C., Londeix, L., Mangin, S., Matthiessen, J., Marret, F., Radi, T., Rochon, A., Solignac, S., Turon, J.-L., 2005. Reconstruction of sea-surface conditions at middle to high latitudes of the Northern Hemisphere during the Last Glacial Maximum (LGM) based on dinoflagellates cyst assemblages. Quaternary Science Reviews 24, 897-924.

Duplessy, J.-C., Ivanova, E., Murdmaa, I., Paterne, M., Labeyrie, L., 2001. Holocene paleoceanography of the northern Barents Sea and variations of the northward heat transport by the Atlantic Ocean. Boreas 30, 2-16.

Environment Canada, 2004. http://climate.weatheroffice.ec.gc.ca/climate_normals

Giraudeau, J., Cremer, M., Manthé, S., Labeyrie, L., Bond, G., 2000. Coccolith evidence for instabilities in surface circulation south of Iceland during Holocene times. Earth and Planetary Science Letters 179, 257-268.

Hall, I.R., Bianchi, G.G., Evans, J.R., 2004. Centennial to millennial scale Holocene climate-deep water linkage in the North Atlantic. Quaternary Science Reviews 23, 1529-1536.

Hammarlund, D., Barnekow, L., Birks, H.J.B., Buchardt, B., Edwards, T.W.D., 2002. Holocene changes in atmospheric circulation recorded in the oxygen-isotope stratigraphy of lacustrine carbonates from northen Sweden. The Holocene 12, 339-351.

Jiang, H., Seidenkrantz, M.-S., Knudsen, K.L., Eiríksson, J., 2002. Late-Holocene summer sea-surface temperatures based on a diatom record from the north Icelandic shelf. The Holocene 12, 137-147.

Kaplan, M.R., Wolfe, A.P., Miller, G.H., 2002. Holocene environmental variability in southwestern Greenland inferred from lake sediments. Quaternary Research 58, 149-159.

Kaufman, D.K., Ager, T.A., Anderson, N.J., Anderson, P.M., Andrews, J.T., Bartlein, P.J., Brubaker, L.B., Coats, L.L., Cwynar, L.C., Duvall, M.L., Dyke, A.S., Edwards, M.R., Eisner, W.R., Gajewski, K., Geirsdottir, A., Hu, F.S., Jennings, A.E., Kaplan, M.R., Kerwin, M.W., Lozhkin, A.V., MacDonald, G.M., Miller, G.H., Mock, C.J., Oswald, W.W., Otto-Bliesner, B.L., Porinchu, D.F., Ruhland, K., Smol, J.P., Steig, E.J., Wolfe, B.B., 2004. Holocene thermal maximum in the western Arctic (0–180°W). Quaternary Science Reviews 23, 529–560.

Kerwin, M.W., Overpeck, J.T., Webb, R.S., de Vernal, A., Rind, D.H., Healy, R.J., 1999. The role of oceanic forcing in mid-Holocene Northern Hemisphere climate change. Paleoceanography 14, 200-210.

Koç, N., Jansen, E., Haflidason, H., 1993. Paleoceanographic reconstructions of surface ocean conditions in the Greenland, Iceland and Norwegian Seas through the last 14 ka based on diatoms. Quaternary Science Reviews 12, 115-140.

Maddy, D., Long, A.J., Bridgland, D.R., 2005. Quaternary land-ocean correlation: A tribute to Professor David Q. Bowen. Quaternary Science Reviews 24, 1543-1546.

Marchal, O., Cacho, I., Stocker, T.F., Grimalt, J.O., Calvo, E., Martrat, B., Shackelton, N., Vautravers, M., Cortijo, E., Van Kreveld, S., Andersson, C., Koç, N., Chapman, M., Sbaffi, L., Duplessy, J.-C., Sarnthein, M., Turon, J.-L., Duprat, J., Jansen, E., 2002. Apparent cooling of the sea surface in the northeast Atlantic and Mediterranean during the Holocene. Quaternary Science Reviews 21, 455-483.

Meincke, J., 2002. Climate dynamics of the North Atlantic and NW-Europe: An observation-based overview. In: Wefer, G., Berger, W.H., Behre, K.-E., Jansen, E. (Eds.), Climate Development and History of the North Atlantic Realm. Springer, Berlin, pp. 25-40.

Moros, M., Emeis, K., Risebrobakken, B., Snowball, I., Kuijpers, A., McManus, J., Jansen, E., 2004. Sea surface temperatures and ice rafting in the Holocene North Atlantic: climate infuences on northern Europe and Greenland. Quaternary Science Reviews 23, 2113–2126.

Moros, M., Jensen, K.G., Kuijpers, A., 2006. Mid- to late-Holocene hydrological and climatic variability in Disko Bugt, central West Greenland. The Holocene 16, 357-367.

Nesje, A., Matthews, J.A., Dahl, S.O., Berrisford, M.S., Andersson, C., 2001. Holocene glacier fluctuations of Flatebreen and winter-precipitation changes in the Jostedalsbreen region, western Norway, based on glaciolacustrine sediment records. The Holocene 11, 267-280.

NODC- National Oceanographic Data Center, 2001. World Ocean Database 2001, Scientific Data Sets, Observed and Standard Level Oceanographic Data [CD-Rom], National Oceanic and Atmospheric Administration, Silver Spring, Md.

Renssen, H., Goose, H., Fichefet, T., Brovkin, V., Driesschaert, E., Wolk, F., 2005. Simulating the Holocene climate evolution at northern high latitudes using a coupled atmospheric-sea ice-ocean-vegetation model. Climate Dynamics 24, 23-43.

Solignac, S., Giraudeau, J., de Vernal, A., 2006. Holocene sea surface conditions in the western North Atlantic: Spatial and temporal heterogeneities. Paleoceanography 21, PA2004, doi:10.1029/2005PA001175.

Steig, E.J., 1999. Mid-Holocene climate change. Science 286, 1485-1487.

Wohlfahrt, J., Harrison, S.P., Braconnot, P., 2004. Synergistic feedbacks between ocean and vegetation on mid- and high-latitude climates during the mid-Holocene. Climate Dynamics 22, 223-238.

Zdanowicz, C.M., Zielinski, G.A., Wake, C.P., Fisher, D.A., Koerner, R.M., 2000. A Holocene record of atmospheric dust deposition on the Penny ice cap, Baffin Island, Canada. Quaternary Research 53, 62-69.

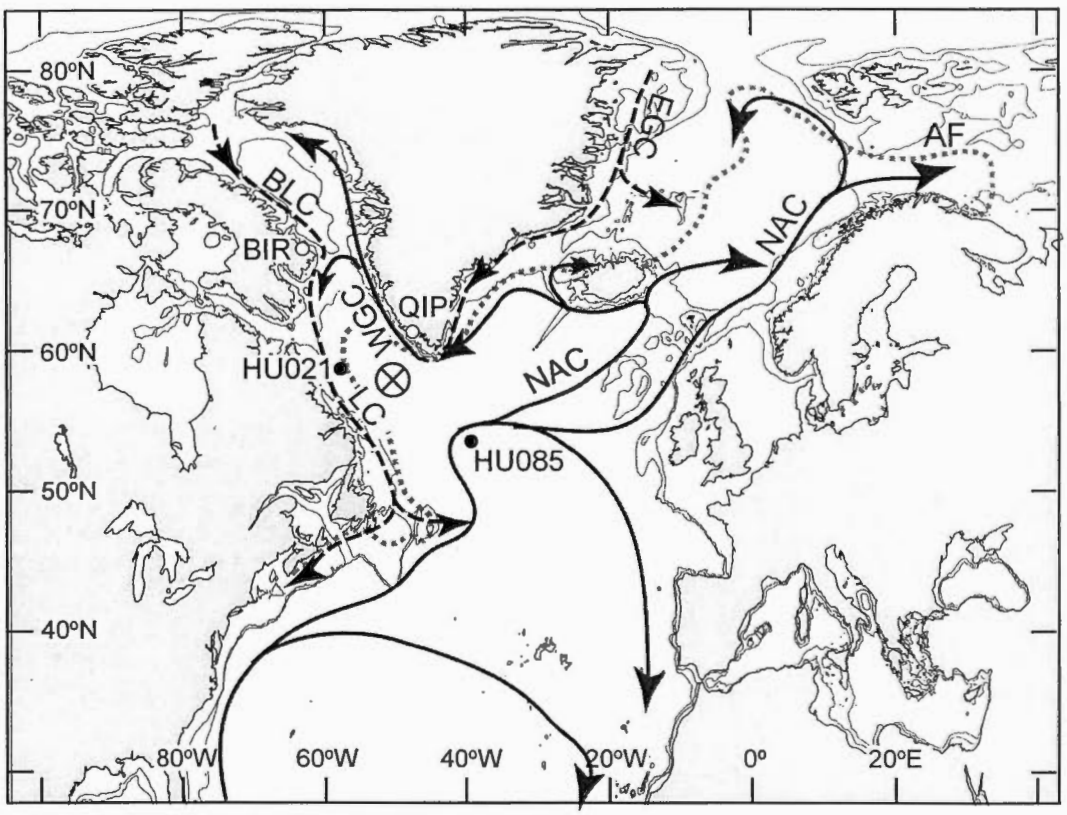

Figure 1. Map of the northern North Atlantic showing the location of the study sites and major ocean currents. The isolines correspond to the 200 m and 1000 m isobaths. The arrows illustrate schematically the surface circulation of the North Atlantic (redrafted after Meincke, 2002). The thick dark grey arrows correspond to the poleward flow of the North Atlantic Current (NAC), and its western branch, the West Greenland Current (WGC). The dashed black arrows correspond to southward flow of Arctic ocean waters through the East Greenland Current (EGC), the Baffin Current (BLC) and the Labrador Current (LC). Circled cross corresponds to the center of deep Labrador Sea Water (LSW) formation. The dashed grey line corresponds to the maximum extent of sea-ice cover in winter. The vegetation around both Akvaqiak (BIR; 66°47'N, 63°57'W; 45 m above sea-level) and Qipisarqo (QIP; 61°00'N, 47°45'W; 7 m above sea-level) lakes is moderately lush shrub tundra dominated by shrub birch (Betula) and heaths (Ericales). Deep snow cover around Akvaqiak Lake is critical to the survival of Betula. Core HU84-030-021TWC (HU021 ; 58°22.06'N, 57°30.42'W; water depth = 2853 m) was collected on the continental slope at the vicinity of the center of deep Labrador Sea Water formation. Core HU-91-045-085TWC (HU085; 53°58.51'N, 38°38.25'W; water depth = 3603 m) was collected in the area of the Charlie Gibbs Fracture Zone in the central part of the North Atlantic.

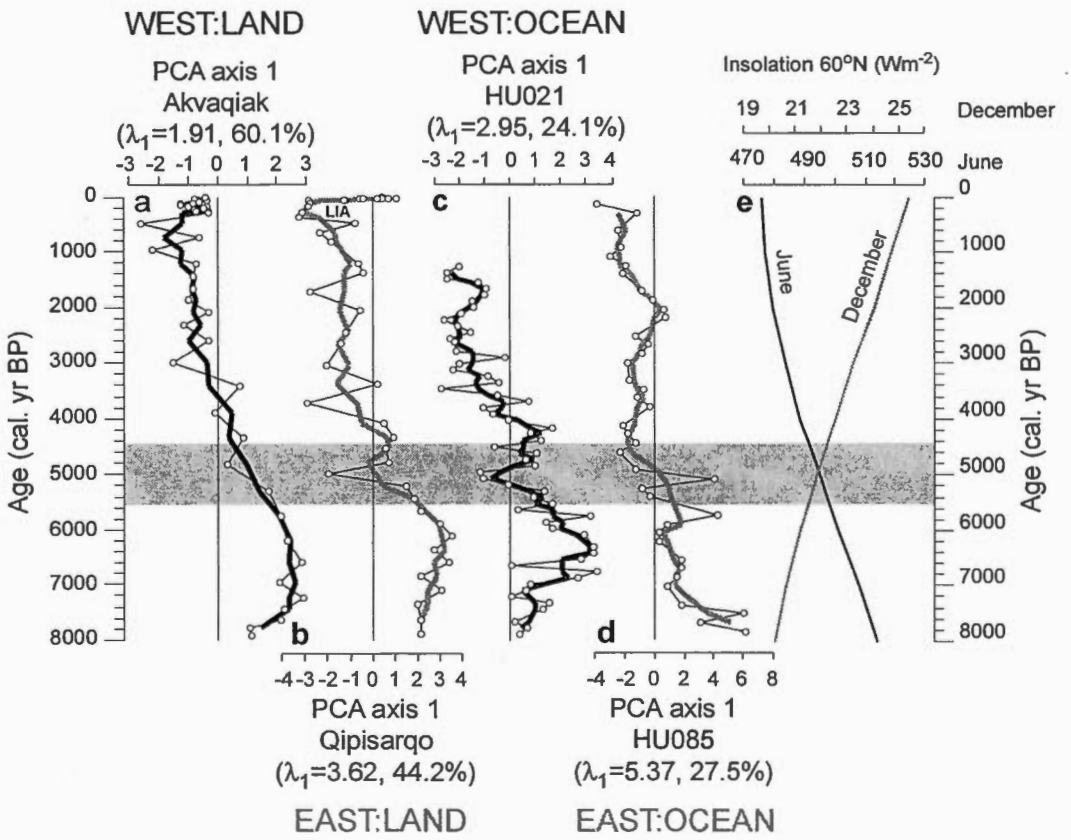

Figure 2. Result of principal component analysis (PCA). Stratigraphic plot of PCA axis 1 sample scores of (a) Akavqiak Lake, (b) Qipisarqo Lake, (c) core HU021, (d) core HU085. The thick grey and black lines correspond to 3-point moving averages. The first eigenvalue (1) and percentage of variance are given for each sequence. See Method section in Supporting Material for details on PCA calculations and PCA loadings. WEST: western sector of northwestern North Atlantic. EAST: eastern sector of northwestern North Atlantic. (e) Northern Hemisphere high-latitude (60°N) June and December insolation curves (Berger and Loutre, 1991). The shaded horizontal zone marks the mid-late Holocene transition, which occurred at ca. 5000 cal. year BP. LIA: Little Ice Age.

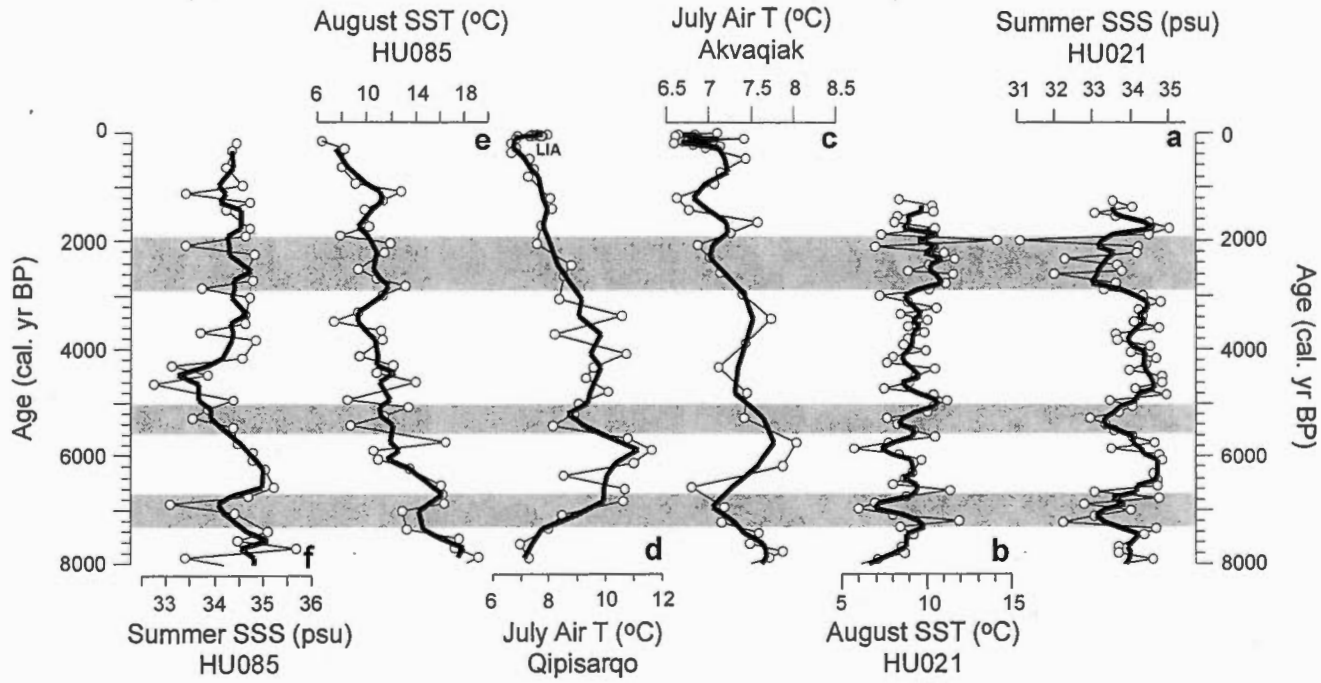

Figure 3. Time series of climatic and sea-surface conditions. The July air temperature estimates are based on an average between the results obtained from the modern analogue technique (MAT) and regression based on correspondence analysis (CA) (RMSE = 1.30°C, r = 0.94). The reconstructions of August sea-surface temperature (SST) (RMSE = 1.68°C, r = 0.97) and summer sea-surface salinity (SSS) (RMSE = 2.53 psu, r = 0.85) are based on MAT (de Vernal et al., 2006). See Method section in Supporting Material for more details on calculations. (a) Summer sea-surface salinity (SSS) at core HU021 (de Vernal and Hillaire-Marcel, 2006). Modern value: 34.31 ± 0.16 psu (NODC, 2001). (b) August sea-surface temperature (SST) at core HU021 (de Vernal and Hillaire-Marcel, 2006). Modern value: 6.70 ± 0.93°C (min: 5.8°C; max: 9.7°C) (NODC, 2001). (c) July air temperature at Akvaqiak Lake. Modern value: 5.6 ± 1.7°C (Environment Canada, 2004). (d) July air temperature at Qipisarqo Lake. Modern value: 7.2 ± 1.8°C (Cappelen et al., 2001). (e) August SST at core HU085 (de Vernal and Hillaire-Marcel, 2006). Modern value: 10.55 ± 0.80°C (min: 9.4°C; max: 11.4°C) (NODC, 2001). (f) Summer SSS at core HU085 (de Vernal and Hillaire-Marcel, 2006). Modern value: 34.31 ± 0.16 psu (NODC, 2001). The tree vertical shaded zones mark short-term episodes of decreasing summer SSS in core HU021. On each curves the thick black lines correspond to 3-point moving averages. LIA: Little Ice Age.

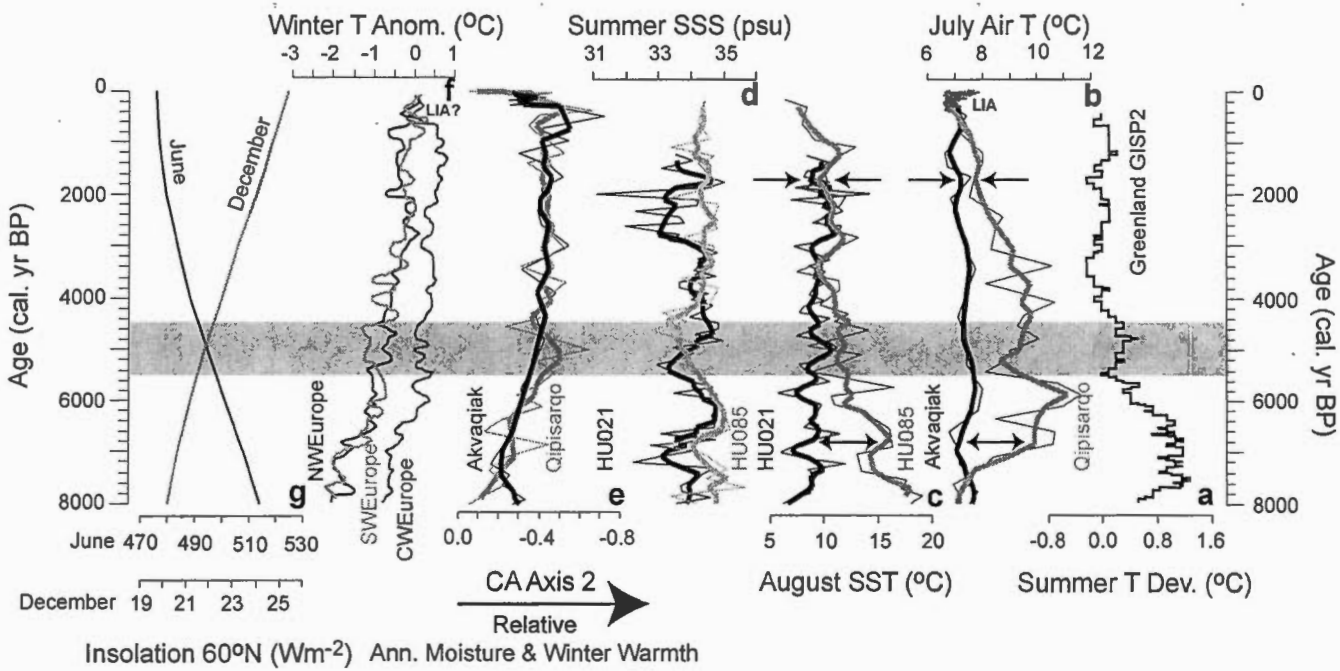

Figure 4. Comparison of paleoclimate reconstructions. (a) Summer temperature deviation at Greenland GISP2 core (Alley et al., 1999). (b) July air temperature reconstruction at Akvaqiak (black) and Qipisarqo (grey) lakes. The thick black and grey lines correspond to 3-point moving averages. The arrows illustrate the diminution of the west to east gradient of temperature from middle to late Holocene. (c) August SST reconstructionfrom cores HU021 (black) and HU085 (grey) (de Vernal and Hillaire-Marcel, 2006). The thick black and grey lines correspond to 3-point moving averages. The arrows illustrate the diminution of the west to east gradient of temperature from middle to late Holocene. (d) Summer SSS reconstruction curve at cores HU021 (black) and HU085 (grey) (de Vernal and Hillaire-Marcel, 2006). The thick black and grey lines correspond to 3-point moving averages. (e) Stratigraphic plot of CA axis 2 scores at Akvaqiak (black) and Qipisarqo (grey) lakes. The thick black and grey lines correspond to 3-point moving averages. This curve represents a semi-quantitative estimate of the January air temperature and annual precipitation, which are co-variant parameters . (f) Winter temperature anomaly for Western Europe (Davis et al., 2003). CWEurope: Centre West Europe, SWEurope: South West Europe, NWEurope: North West Europe. (g) Northern Hemisphere high-latitude (60°N) June and December insolation curves (Berger and Loutre, 1991). The shaded horizontal zone marks the mid-late Holocene transition, which occurred at ca. 5000 cal. year BP. LIA: Little Ice Age.

3.2 Supporting material

3.2.1. Lacustrine sediment cores chronology

Akvaqiak (98BIR-02, 98BIR-G01) and Qipisarqo (98QIP-02, 98QIP-G01) lake cores were collected in May 1998 from the frozen lake surface. At the two lakes, piston and gravity (Glew) cores were used for the establishment of composite records, in which the Glew cores provide the upper part of the sedimentary sequences (Table S1). The geochronology of the Akavqiak Lake record is based on seven accelerator mass spectrometry (AMS) ^{14}C dates on bryophyte macrofossils and humic acid extracts (for discussion, see Fréchette et al., submitted). The geochronology of the Qipisarqo Lake record is based on six AMS- ^{14}C dates on bryophyte macrofossils and humic acid extracts (for discussion, see Kaplan et al., 2002). Paired macrofossil and humic acid dates have been obtained at three levels in the Akvaqiak Lake core and one level in the Qipisarqo Lake core, producing humic acid ages that are older than adjacent macrofossils. This has led to age correction of 537 and 230 years for humid acid dates in Akvaqiak and Qipisarqo lakes, respectively. All corrected (humic acid) and uncorrected (bryophyte) dates have been calibrated to calendar years using the CALIB program (version 5.0.2) (Stuiver and Reimer, 1993) updated with the Intcal04c14 dataset (Reimer et al., 2004). Age models were then derived from smoothed linear interpolation between calibrated ages (Figure S1). For the last 8000 cal. years, sediment accumulation rates average 11.35 ± 4.41 cm/ka at Akavaqiak lake and 26.77 ± 16.84 cm/ka at Qipisarqo lake.

3.2.2. Marine sediment cores chronology

Core HU021 (HU-84-030-021TWC) and core HU085 (HU-91-045-085TWC) were collected during expeditions of the CSS-Hudson. The chronology was established on

the basis of AMS ^{14}C dates on planktic foraminifera. For core HU021 three dates are available and for core HU085 two dates are available. The conventional ^{14}C ages have been calibrated into calendar years using the CALIB Rev 5.0.1 program (Stuiver and Reimer, 1993) and the marine calibration dataset (Marine04.14C) of Hughen et al. (2004). The marine calibration was made with a global ocean reservoir correction of 400 years, but no further correction of reservoir age (delta R) was used to account for local effects. The age models were established from linear interpolation between calibrated ages. For the last 8000 cal. years, sediment accumulation rates average 17.61 cm/ka at HU021 core and 6.22 cm/ka at HU085 core.

3.2.3. Pollen analysis

Standard pollen preparation techniques, including dispersion with KOH, digestion with HF and HCl, and acetolysis (Faegri and Iversen, 1975), were applied to 1.0 or 2.0 cm^3 samples of fresh (wet) sediment. Pollen and spores were identified using the taxonomic keys of Richard (1970), McAndrews et al. (1973) and Moore et al. (1991), as well as reference to modern collection archived at the Laboratoire Jacques-Rousseau, Université de Montréal. For consistency, the pollen sum used for computing relative frequencies from the fossil assemblages includes only the 34 pollen types contained in the modern database (cf. Table 2 in Fréchette et al., 2006). The basic sums average 555 ± 48 grains for Akvaqiak lake, and 516 ± 44 grains for Qipisarqo lake. The diagram of pollen assemblages of Akvaqiak and Qipisarqo lacustrine sediment cores is given on Figure S2.

3.2.4. Fossil dinoflagellate analysis

Palynological preparation for the analyses of dinocysts have made following standardized laboratory procedure that include sieving at 10 μm to eliminate fine silt and clays, in addition to repeated HCl (10%) and HF (52%) treatments to dissolve

carbonate and silica particles. No oxidation treatment was done. For consistency, the dinoflagellate cysts sum used for computing relative frequencies from the fossil assemblages includes only the 60 dinoflagellate cysts contained in the modern database (cf. Table 1 in de Vernal et al., 2005). The basic sums average 345 ± 70 grains for core HU021, and 256 ± 87 grains for core HU085. The diagram of dinoflagellate cyst assemblages of HU021 and HU085 marine sediment cores is given on Figure S3.

3.2.5. Methods for continental climate reconstruction

The transfer functions used for continental climate reconstruction rely on a database that includes 34 pollen types and 400 reference sites from Canada (north of 50°N) and Greenland (Fréchette et al., 2006; submitted). For the modern analogue technique (MAT), similarity between fossil and modern pollen assemblages is based on the squared chord distance (SCD) dissimilarity metric (Birks, 1977; Prentice, 1980; Overpeck et al., 1985; Gavin et al., 2003), which is an euclidean distance calculated on the square-root transformed pollen types abundances expressed in percent. Values of SCD vary between zero and 200, with larger values indicate greater dissimilarity. The adopted SCD threshold for the present study is of 31. The climate estimates rely on a set of 5 modern analogues. Close analogues for the Akvaqiak and Qipisarqo lakes fossil pollen assemblages exist in the 400 sites modern database, with SCD values lower than 13 and 19 for Akavqiak and Qipisarqo lakes, respectively. Reconstructions of the July air temperature were performed with the 3Pbase software (Guiot and Goeury, 1996), and the error of prediction (RMSE) is ±1.02°C

Correspondence analysis (CA) ordination of the 400 modern reference sites (34 pollen types) demonstrates that the first CA axis ($\lambda_1 = 0.242$; 24.1% of total variance)

negatively correlates with July air temperature (r = -0.86) (Fréchette et al., 2006). Based on this relationship, a linear regression equation between CA axis 1 modern sample scores and July air temperature was derived (July air T (°C) = 10.28-6.54 (CA axis 1 sample score)) (Figure S4). Fossil pollen assemblages of Akvaqiak and Qipisarqo lakes were projected passively onto the ordination space, without influencing the CA analysis in any other way. The CA linear regression was applied to fossil sample scores to quantitatively reconstruct the July air temperature, with an estimated RMSE = 1.98°C (r = 0.86). Canonical correspondence analysis (CCA) ordination of the 400 modern reference sites (34 pollen types, 7 environmental variables) demonstrates that CA axis 2 is negatively correlated to the annual precipitation (r = -0.61) and covaries with the January air temperature (r = -0.60) (correlation between annual precipitation and January air temperature is of 0.76) (Figure S4). Therefore, the scores of Akavaqik and Qipisarqo spectra projected on CA axis 2 of the 400-site modern assemblages allow semi-quantitative estimates of annual precipitation and January air temperature. For CA and CCA ordinations the frequencies of the 34 pollen types, square-root transformation was made and rare taxa were not down-weighted. CA and CCA were performed with CANOCO version 4.0 (ter Braak and Šmilauer, 1998). The quantitative July air temperature reconstructed in the present study is based on an average between MAT and CA regression. This approach has an estimation error of RMSE = 1.30°C (r = 0.94). It is of note that this error is close to the actual standard deviation around the mean for the July air temperature, which average 1.7°C and 1.8°C, respectively in eastern Baffin Island and southern Greenland (Environment Canada, 2004; Cappelen et al., 2001).

3.2.6. Methods for the reconstruction of hydrographic conditions

The transfer functions used for quantitative past sea-surface conditions is based on MAT applied to dinocyst assemblages and using the software of Guiot and Goeury (1996). The reference database includes 60 taxa and 1054 reference sites from mid-

to high latitude North Atlantic, North Pacific and Arctic oceans, and adjacent sub-polar seas (de Vernal and Hillaire-Marcel, 2006). The dissimilarity metric used is the euclidean distance calculated on neperian logarithmic transformed dinocysts abundance, expressed in per mil (de Vernal et al., 2001; 2005). Unlike the SCD used with the pollen database, the dissimilarity metric used with the dinocyst database has no upper limit. The adopted dissimilarity threshold for the present study is of 74. The hydrographic estimates rely on a set of 5 modern analogues. The error of prediction (RMSE) for the summer sea-surface salinity (SSS) and sea-surface temperature (SST) is estimated to be ±1.6°C for the winter and summer SSTs, and ±1.2 psu for the salinity. It is of note that these errors are close to the actual standard deviation around the mean for the summer temperature and salinity data, which average 1.6°C and 1.1 psu, respectively in the modern hydrographical database (NODC, 2001). Relatively close analogues for dinocyst assemblages exist in the 1054 sites modern database, with distances lower than 44 and 78 for cores HU021 and HU085, respectively.

3.2.7. Methods for the principal component analysis

Detrended correspondence analysis (DCA) was first used to estimate the compositional gradient lenghts along the first few DCA axes in the lacustrine and marine records (Gauch, 1982; ter Braak and Prentice, 1988; Birks, 1995). For DCA calculations we used the pollen types and the dinoflagellates cysts selected for the quantitative climate and hydrographic reconstructions. Among the 34 pollen types, 25 were present at Akvaqiak Lake and 32 at Qipisarqo Lake. Among the 60 dinoflagellate cysts, 25 were present at HU021 core and 21 at HU085 core. The length of gradient of DCA axis 1 is 0.87 and 1.01 SD (standard deviation) units for Akvaqiak and Qipisarqo lakes, respectively, and 1.09 and 1.41 SD units for HU021 and HU085, respectively, which indicates linear responses of both pollen and dinoflagellate cysts data to the underlying environmental gradient and, therefore,

linear ordination (principal component analysis) was applied. Principal component analysis (PCA) was used to detect the major gradient among the fossil pollen and dinoflagellate cysts spectra. Because the variables are dimesionally homogeneous, a dispersion (variance/covariance) matrix was used (Birks, 1995; Legendre and Legendre, 1998). The number of pollen and dinoflagellate cysts was lowered. We selected taxa with a value $\geq 1\%$ in at least one sample and created a collective category among the pollen types (*Picea+Pinus*). This selection resulted in 10 pollen types for Akvaqiak Lake, 17 pollen types for Qipisarqo Lake, 15 dinoflagellate cysts for HU021 core and 17 dinoflagellate cysts for HU085 core. For PCA, as for the quantitative climate and hydrographic reconstructions, the relative frequencies (in percent) of the pollen types was square-root transformed and the relative frequencies (in per mil) of the dinoflagellate cysts was logarithmic transformed. These transformations were done in an attempt to optimize the signal-to-noise ration and stabilize the variances. DCA was implemented with CANOCO version 4.0 (ter Braak and Šmilauer, 1998) with rare taxa not down-weighted and PCA calculations were performed using the computer program Progiciel R (version 4) (Legendre and Legendre, 1998). Informations on PCA results (first three eigenvalues, % variance and loadings) are given on Table S2.

References for supporting material

Birks, H.J.B., 1977. Modern pollen rain and vegetation of the St. Elias Mountains, Yukon Territory. Canadian Journal of Botany 55, 2367-2382.

Birks, H.J.B., 1995. Quantitative palaeoenvironmental reconstructions. In Maddy, D. & J.S. Brew (eds), Statistical Modelling of Quaternary Science Data. Technical guide 5. Quaternary Research Association, Cambridge, 161-254.

de Vernal, A., Eynaud, F., Henry, M., Hillaire-Marcel, C., Londeix, L., Mangin, S., Matthiessen, J., Marret, F., Radi, T., Rochon, A., Solignac, S., Turon, J.-L., 2005. Reconstruction of sea-surface conditions at middle to high latitudes of the Northern Hemisphere during the Last Glacial Maximum (LGM) based on dinoflagellates cyst assemblages. Quaternary Science Reviews 24, 897-924.

de Vernal, A., Henry, M., Matthiessen, J., Mudie, P.J., Rochon, A., Boessenkool, K.P., Eynard, F., Grøsfjeld, K., Guiot, J., Hamel, D., Harland, R., Head, M.J., Kunz-Pirrung, M., Levac, E., Loucheur, V., Peyron, O., Pospelova, V., Radi, T., Turon, J.-L., Voronina, E., 2001. Dinoflagellate cyst assemblages as tracers of sea-surface conditions in the northern North Atlantic, Arctic and sub-Arctic seas: the new 'n = 677' data base and its application for quantitative palaeoceanographic reconstruction. Journal of Quaternary Science 16, 681-698.

de Vernal, A., Hillaire-Marcel, C., 2006. Provincialism in trends and high frequency changes in the northwestern North Atlantic during the Holocene. Global and Planetary Changes 54, 263-290.

Faegri, K., Iversen, J., 1975. Textbook of Pollen Analysis, 3rd Edition. Blackwell Scientific Publications, Oxford.

Fréchette, B., de Vernal, A., Guiot, J., Wolfe, A.P., Miller, G.H., Fredskild, B., Kerwin, M.W., Richard, P.J.H., Gajewski, K., submitted. Quantitative paleoclimate reconstruction in the Canadian Arctic from pollen assemblages preserved in lake sediments: methodology and application to Holocene sequences from eastern Baffin Island. Quaternary Science Reviews.

Fréchette, B., Wolfe, A.P., Miller, G.H., Richard, P.J.H., de Vernal, A., 2006. Vegetation and climate of the last interglacial on Baffin Island, Arctic Canada. Palaeogeography, Palaeoclimatology, Palaeoecology 236, 91-106.

Gauch, H.G.Jr., 1982. Multivariate analysis in community ecology. Cambridge University Press, Cambridge, 298 p.

Gavin, D.G., Oswald, W.W., Wahl, E.R., Williams, J.W., 2003. A statistical approach to evaluating distance metrics and analog assignments for pollen records. Quaternary Research 60, 356-367.

Guiot, J., Goeury, C., 1996. 3Pbase – a software for statistical analysis of paleoecological and paleoclimatological data. Dendrochronologia 14, 123-135.

Hughen, K.A., Baillie, M.G.L., Bard, E., Bayliss, A., Beck, J.W., Bertrand, C., Blackwell, P.G., Buck, C.E., Burr, G., Cutler, K.B., Damon, P.E., Edwards, R.L., Fairbanks R.G., Friedrich, M., Guilderson, T.P., Kromer, B., McCormac, F.G., Manning, S., Bronk Ramsey, C., Reimer, P.J., Reimer, R.W., Remmele, S., Southon, J.R., Stuiver, M., Talamo, S., Taylor, F.M., van der Plicht, J., Weyhenmeyer C.E., 2004. Marine04 Marine Radiocarbon Age Calibration, 0–26 cal. kyr BP. Radiocarbon 46, 1059-1086.

Kaplan, M.R., Wolfe, A.P., Miller, G.H., 2002. Holocene environmental variability in southwestern Greenland inferred from lake sediments. Quaternary Research 58, 149-159.

Legendre, P., Legendre, L., 1998. Numerical ecology, 2nd English edition. Elsevier Science BV, Amsterdam.

McAndrews, J.H., Berti, A.A., Norris, G., 1973. Key to the Quaternary pollen and spores of the great Lakes region. Life Science Miscellaneous Publications, Royal Ontario Museum, Toronto, Canada.

Moore, P.D., Webb, J.A., Collinson, M.E., 1991. Pollen analysis, 2nd edition. Blackwell Scientific Publications, Oxford.

NODC- National Oceanographic Data Center, 2001. World Ocean Database 2001, Scientific Data Sets, Observed and Standard Level Oceanographic Data [CD-Rom], National Oceanic and Atmospheric Administration, Silver Spring, Md.

Overpeck, J.T., Webb, T., III, Prentice, I.C., 1985. Quatitative interpretation of fossil pollen spectra: dissimilarity coefficients and the method of modern analogs. Quaternary Research 23, 87-108.

Prentice, I.C., 1980. Multidimensional scaling as a research tool in Quaternary palynology: a review of theory and methods. Review of Palaeobotany and Palynology 31, 71-104.

Reimer, P. J., Baillie, M. G. L., Bard, E., Bayliss, A., Beck, J. W., Bertrand, C. J. H., Blackwell, P. G., Buck, C. E., Burr, G. S., Cutler, K. B., Damon, P. E., Edwards, R. L., Fairbanks, R. G., Friedrich, M., Guilderson, T. P., Hogg, A. G., Hughen, K. A., Kromer, B., McCormac, F. G., Manning, S. W., Ramsey, C. B., Reimer, R. W., Remmele, S., Southon, J. R., Stuiver, M., Talamo, S., Taylor, F. W., van der Plicht, J., and Weyhenmeyer, C. E., 2004. IntCal04 Terrestrial radiocarbon age calibration, 26 - 0 ka BP. Radiocarbon 46, 1029-1058.

Richard, P.J.H., 1970. Atlas pollinique des arbres et de quelques arbustes indigènes du Québec. Naturaliste Canadien 97, 1-34, 97-161, 241-306.

Stuiver, M., and Reimer, P.J., 1993. Extended 14C database and revised CALIB radiocarbon calibration program. Radiocarbon 35, 215-230.

ter Braak, C.J.F, Prentice, I.C., 1988. A theory of gradient analysis. Advances in ecological research 18, 271-317.

ter Braak, C.J.F., Šmilauer, P., 1998. CANOCO for windows: software for Canonical Community Ordination (version 4). Microcomputer Power, Ithaca, NY, USA.

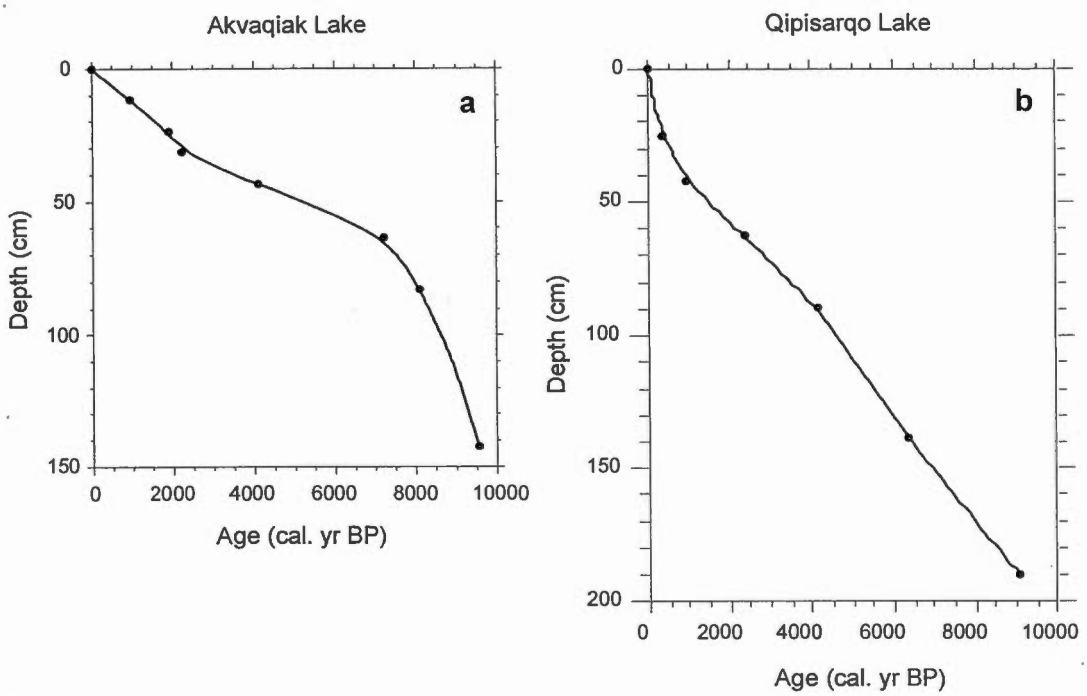

Figure S1. Age-depth curves for the Akvaqiak (a) and Qipisarqo (b) lake composite sediment cores. Akvaqiak's and Qipisarqo's models are a smoothed linear interpolation between the available calibrated radiocarbon ages.

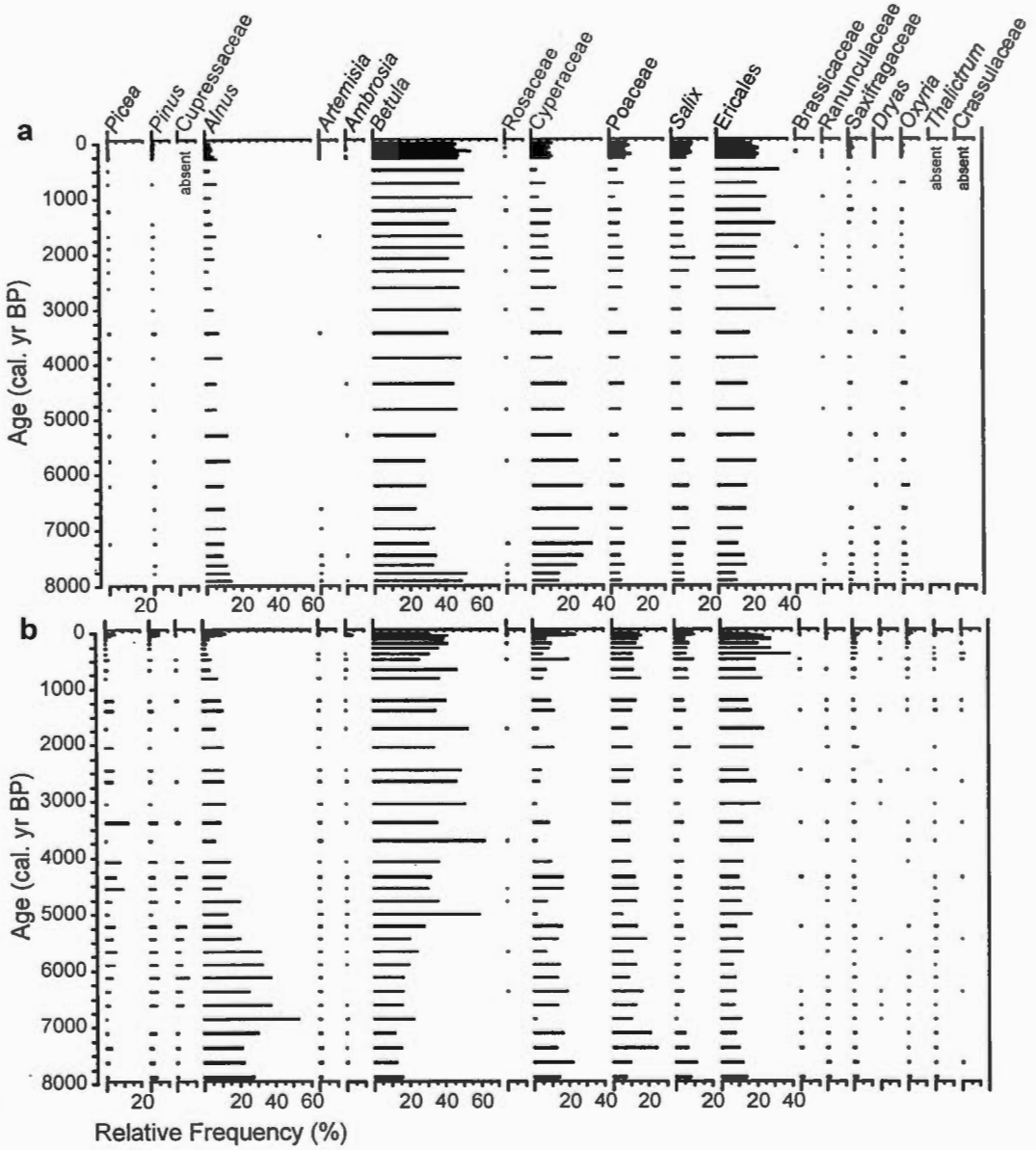

Figure S2. Summary pollen diagrams from Akvaqiak (a) and Qipisarqo (b) composite lake sediment cores for the past 8000 calibrated years. Only taxa with a value = 1% in at least one sample are illustrated. The following taxa are not illustrated: *Abies*, *Myrica*, Chenopodiaceae, *Populus*, Tubuliflorae-Liguliflorae, *Plantago*, Onagraceae, Apiaceae, Fabaceae, Caryophyllaceae, Scrophulariaceae, Polygonaceae, Papaveraceae. They were however included in the basic sum used to compute the relative frequencies. The taxa are ordered from those typical of warmer (Sub-Arctic shrub tundra) environments on the left, to those characterizing sites that are increasingly polar (high Arctic herb tundra) to the right. To allow a better between-core comparison we used the same upper limit scales for each taxa.

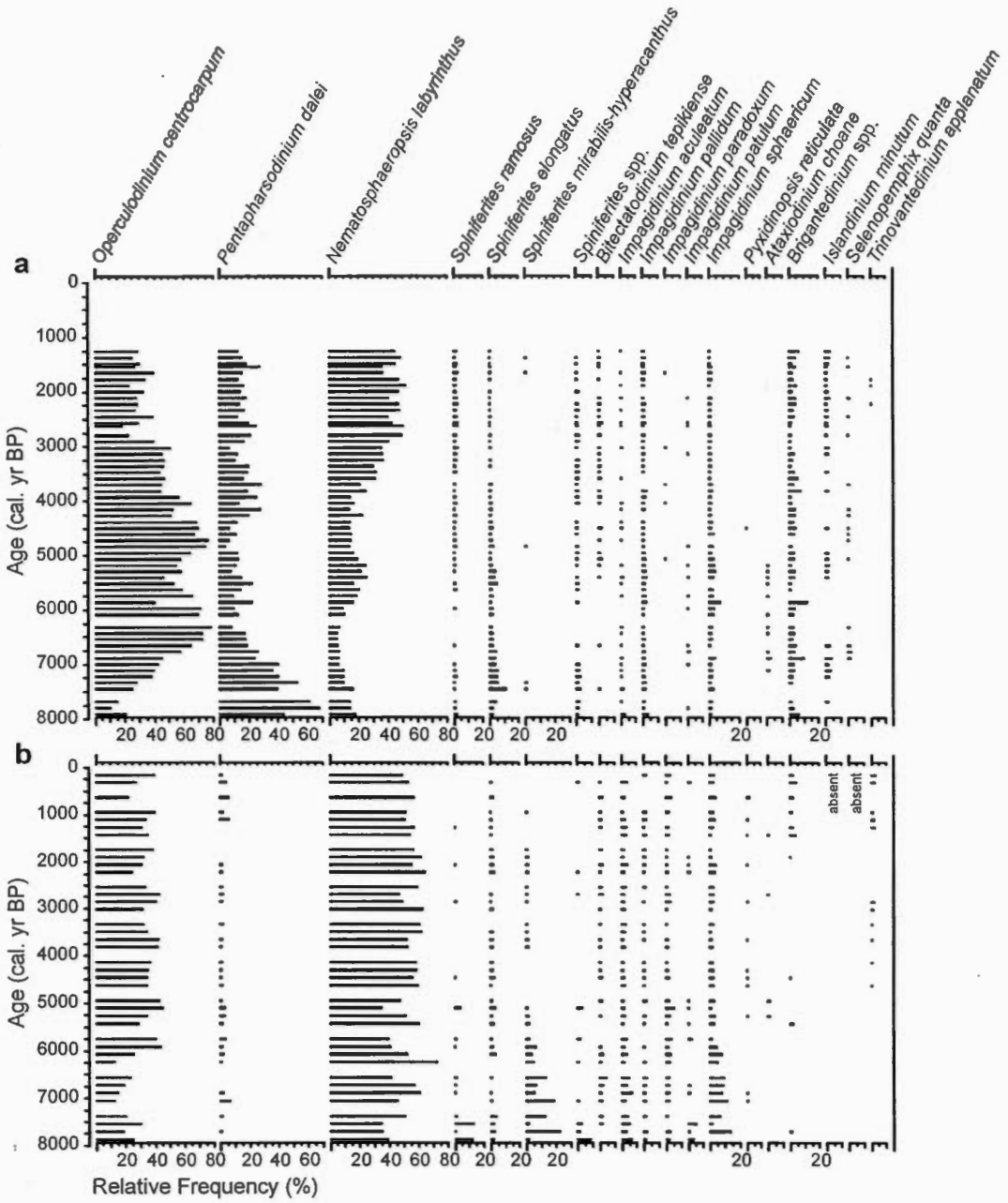

Figure S3. Summary dinocyst diagrams of core HU021 (a) and HU085 (b) marine sediment cores for the past 8000 calibrated years. Only taxa with a value = 1% are illustrated. The following taxa are not illustrated: *Impagidinium strialatum*, *Impagidinium* spp., cyst of cf. *Scrippsiella trifida*, *Operculodinium israelianum*, *Spiniferites lazus*, Protoperidinioids, cyst of *Polykrikos schwartzii*, *Echinidinium* cf. *karaense*. They were however included in the basic sum used to compute the relative frequencies. To allow a better comparison between the two diagrams, we used the same upper limit scales for each taxa.

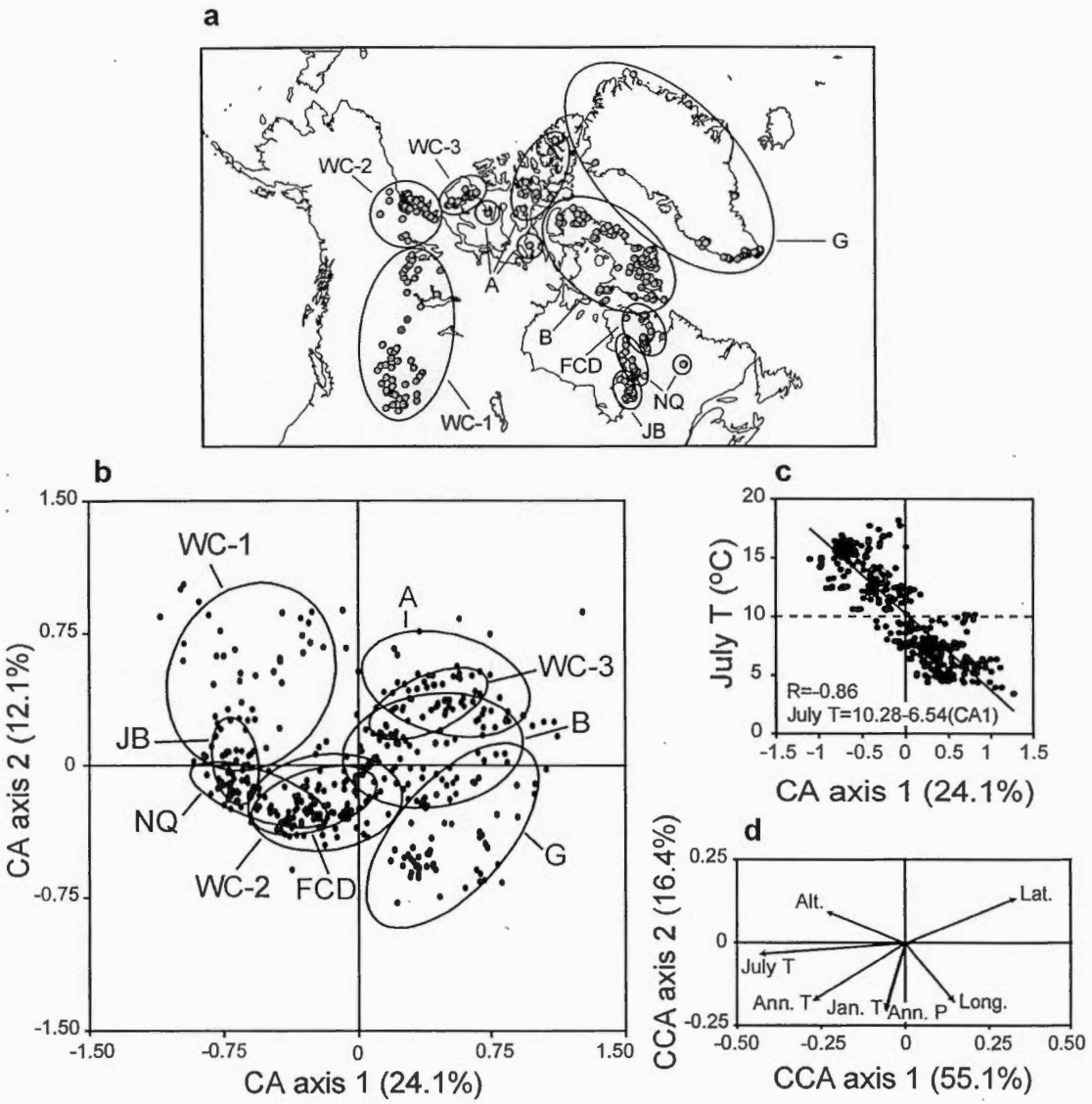

Figure S4. (a) Locations of the 400 lake sediment surface samples used to construct the modern pollen database. The 400 sites have been grouped in nine geographical regions: Western Canada (WC), James Bay (JB), northern Québec (NQ), Fort Chimo - Diana Bay (FCD), Baffin Island (B), Arctic islands (A) and Greenland (G). (b) Results of Correspondence Analysis (CA) ordination showing sample scores from the 400 modern sites. A 95% ellipse is drawn around the reference sites of each region. (c) Plot of CA axis 1 sample scores against interpolated July air temperature. The horizontal dashed line delineates sites in the Low Arctic from those occupying forest tundra. (d) Canonical Correspondence Analysis (CCA) plot of environmental gradients associated with the 400 modern sites. Note that Jan.T (January air T) and Ann. P (mean annual precipitation) are nearly perfectly superimposed. Figure from Fréchette et al. (2006).

Table S1. AMS ^{14}C dates from Akvaqiak and Qipisarqo lake cores used for developing the age-depth model. Indications on the construction of the composite cores are also given.

Lake	Raw Depth (cm)	Composite Depth (cm)[a]	Laboratory No.	Material	AMS ^{14}C date (yr BP)	Corrected Date (yr BP)[b]	Calibrated Date (yr BP)[c]	Range of solution at 95.4% (1s)
(A) Akvaqiak	8.5	11.5	NSRL-11345	Macroflora	1000±50	-	933	902-963
piston core	8.5	11.5	NSRL-11346	Humic acids	1700±45	-	-	-
98BIR-02	20.5	23.5	NSRL-10621	Humic acids	2510±45	1973	1915	1879-1951
	28.5	31.5	NSRL-11347	Macroflora	2270±60	-	2211	2177-2245
	28.5	31.5	NSRL-11348	Humic acids	2840±55	-	-	-
	40.5	43.5	NSRL-10622	Humic acids	4290±50	3753	4117	4076-4158
	60.5	63.5	NSRL-10623	Humic acids	6810±55	6273	7214	7158-7270
	80	83	NSRL-10624	Humic acids	7670±60	-	-	-
	80	83	NSRL-10176	Macroflora	7330±95	7330	8113	8020-8205
	139.5	142.5	NSRL-10139	Macroflora	8560±100	8560	9550	9466-9634
	157	160	NSRL-13332	Humic acids	21,590±75	-	-	-
(B) Qipisarqo	20	22.5	CURL-4475	Humic acids	1240±35	1010±35	937	910-964
piston core	23	25.5	CURL-3036	Humic acids	530±40	300±40	394	357-431
98QIP-02	40	42.5	CURL-4486	Humic acids	1330±40	1100±40	989	963-1014
	60	62.5	CURL-4476	Humic acids	2570±35	2340±35	2346	2327-2365
	86.5	89	CURL-3037	Humic acids	3970±40	3740±40	4114	4076-4151
	136	138.5	CURL-4487	Humic acids	5840±60	5610±60	6377	6317-6437
	136	138.5	CURL-4488	Macroflora	5610±60	5610±60	6377	6317-6437
	187.5	190	CURL-3038	Humic acids	8400±40	8170±40	9079	9023-9135
	264	266.5	CURL-4914	Macroflora	8560±50	8560±50	9524	9498-9549

[a] Depth added to correct for offset between piston and gravity (Glew) core depths (see text)

[b] Years subtracted from humic acid ages to correct for offset measured between paired macrofossil and humic acid dates (see text).

[c] Calibration using the CALIB program (version 5.0.2) (Stuiver et Reimer, 1993) updated with the Intcal04c14 (Remier et al., 2004)

Table S1 (suite)

(A) Akvaqiak Lake (98BIR-G01; 98BIR-02)				**(B)** Qipisarqo Lake (98QIP-G01; 98QIP-02			
Core	Raw Depth (cm)	Composite Depth (cm)	Calibrated Age (yr BP)	Core	Raw Depth (cm)	Composite Depth (cm)	Calibrated Age (yr BP)
gravity	0.125	0.125	10	gravity	0.625	0.625	8
gravity	0.375	0.375	30	gravity	0.875	0.875	11
gravity	0.625	0.625	51	gravity	1.125	1.125	14
gravity	0.875	0.875	71	gravity	1.375	1.375	17
gravity	1.125	1.125	91	gravity	1.625	1.625	20
gravity	1.375	1.375	111	gravity	1.875	1.875	23
gravity	1.625	1.625	131	gravity	2.125	2.125	26
gravity	1.875	1.875	152	gravity	2.375	2.375	29
gravity	2.125	2.125	172	gravity	2.625	2.625	33
gravity	2.375	2.375	192	gravity	2.875	2.875	36
gravity	2.625	2.625	212	gravity	3.125	3.125	39
gravity	2.875	2.875	233	gravity	3.375	3.375	42
gravity	3.125	3.125	253	gravity	3.875	3.875	49
gravity	3.375	3.375	273	piston	1.5	4	50
piston	0.5	3.5	283	piston	5.5	8	106
piston	3	6	486	piston	10.5	13	182
piston	6	9	730	piston	15.5	18	270
piston	9	12	974	piston	20.5	23	370
piston	12	15	1213	piston	24.5	27	467
piston	15	18	1444	piston	30.5	33	656
piston	18	21	1667	piston	34.5	37	812
piston	21	24	1882	piston	42.5	45	1207
piston	24	27	2085	piston	45.5	48	1388
piston	27	30	2310	piston	50.5	53	1709
piston	30	33	2613	piston	55.5	58	2041
piston	33	36	3002	piston	61.5	64	2446
piston	36	39	3430	piston	64.5	67	2648
piston	39	42	3883	piston	70.5	73	3052
piston	42	45	4350	piston	75.5	78	3384
piston	45	48	4824	piston	80.5	83	3707
piston	48	51	5294	piston	86.5	89	4071
piston	51	54	5754	piston	91.5	94	4341
piston	54	57	6195	piston	95.5	98	4539
piston	57	60	6607	piston	100.5	103	4772
piston	60	63	6969	piston	105.5	108	4995
piston	63	66	7237	piston	110.5	113	5215
piston	66	69	7449	piston	115.5	118	5435
piston	69	72	7626	piston	120.5	123	5659
piston	72	75	7775	piston	125.5	128	5887
piston	75	78	7906	piston	130.5	133	6120
				piston	135.5	138	6358
				piston	140.5	143	6602
				piston	145.5	148	6849
				piston	150.5	153	7101
				piston	155.5	158	7357
				piston	160.5	163	7616
				piston	165.5	168	7880

Table S2. Summary of PCA results on the fossil assemblages of Akvaqiak Lake, Qipisarqo Lake, HU021 marine core and HU085 marine core.

(A) Alkvaqiak Lake composite core

	PCA axis		
	1	2	3
Eigenvalues (λ)	1.9065	0.4287	0.2998
% variance	60.12	13.52	9.46
Sum of all λ (total variance): 3.1708			
Mean of the λ's: 0.3171			
	Eigenvector (variable loadings)		
	axis 1	axis 2	axis 3
Betula	-0.3807	-0.1679	0.5014
Ericales	-0.3229	-0.2485	-0.7237
Salix	-0.0740	0.5523	0.0786
Poaceae	-0.0151	0.5502	-0.0149
Picea + Pinus	-0.0016	0.2265	-0.0941
Saxifragaceae	0.0104	0.1705	0.2461
Dryas	0.1031	0.0368	0.1272
Oxyria	0.1970	0.0637	-0.0885
Alnus	0.4365	-0.4502	0.2768
Cyperaceae	0.7106	0.1179	-0.2201

(B) Qipisarqo Lake composite core

	PCA axis		
	1	2	3
Eigenvalues (λ)	3.615	2.109	0.7266
% variance	44.19	25.78	8.88
Sum of all λ (total variance): 8.1800			
Mean of the λ's: 0.4812			
	Eigenvector (variable loadings)		
	axis 1	axis 2	axis 3
Betula	-0.4699	0.2898	-0.4240
Ericales	-0.3720	-0.0345	0.2529
Salix	-0.0523	-0.4109	0.1639
Crassulaceae	-0.0304	-0.0584	0.0412
Saxifragaceae	-0.0104	-0.1859	0.1061
Dryas	-0.0039	-0.0465	0.0453
Ambrosia	0.0107	-0.1772	-0.0075
Oxyria	0.0190	-0.1327	0.0710
Poaceae	0.0356	-0.0978	0.1085
Brassicaceae	0.0361	-0.0322	0.0574
Thalictrum	0.0816	-0.0346	-0.0297
Artemisia	0.0855	0.0974	0.0055
Ranunculaceae	0.1008	-0.0278	0.0602
Cupressaceae	0.2140	0.0517	-0.3716
Picea + Pinus	0.2538	-0.1435	-0.6926
Cyperaceae	0.2644	-0.6364	-0.0727
Alnus	0.6555	0.4545	0.2581

Table S2 (suite)

(C) Core HU021

	PCA axis		
	1	2	3
Eigenvalues (λ)	2.9506	1.9136	1.643
% variance	24.12	15.65	13.43
Sum of all λ (total variance): 12.2310			
Mean of the λ's: 0.8154			
	Eigenvector (variable loadings)		
	axis 1	axis 2	axis 3
Spiniferites ramosus	-0.4545	0.2226	-0.0544
Islandinium minutum	-0.4219	-0.6318	-0.3691
Bitectatodinium tepikiense	-0.4153	-0.0885	0.0363
Nemotosphaeropsis labyrinthus	-0.3309	0.0587	0.0735
Spiniferites ssp.	-0.2106	0.3964	-0.4881
Brigantedinium spp.	-0.0601	-0.3956	0.2001
Impagidinium pallidum	-0.0502	-0.0502	-0.2882
Pentapharsodinium dalei	0.0216	0.0356	-0.1812
Impagidinium patulum	0.0771	-0.0632	-0.0802
Selenopemphix quanta	0.0842	-0.3219	0.2360
Impagidinium sphaericum	0.0872	-0.1363	-0.0861
Impagidinium aculeatum	0.1002	-0.1716	-0.3943
Operculodinium centrocarpum	0.1236	-0.0192	0.1154
Ataxiodinium choane	0.2407	-0.2579	-0.1369
Spiniferites elongatus	0.4226	-0.0019	-0.4505

(D) Core HU085

	PCA axis		
	1	2	3
Eigenvalue (λ)	5.3704	3.6884	2.2308
% variance	27.52	18.90	11.43
Sum of all λ (total variance): 19.5172			
Mean of the λ's: 1.1481			
	Eigenvector (variable loadings)		
	axis 1	axis 2	axis 3
Trinovantedinium applanatum	-0.2447	-0.2177	0.1256
Brigantedinium spp.	-0.1857	-0.2063	0.2297
Pyxidinopsis reticulata	-0.1164	0.0762	0.2236
Impagidinium pallidum	-0.0947	0.1458	-0.3004
Pentapharsodinium dalei	-0.0909	0.1862	0.7666
Bitectatodinium tepikiense	-0.0523	0.2676	-0.0144
Impagidinium sphaericum	-0.0509	0.4109	0.1548
Nemotosphaeropsis labyrinthus	-0.0485	0.0114	-0.0283
Operculodinium centrocarpum	-0.0403	-0.0959	-0.0184
Impagidinium paradoxum	0.0656	0.1243	0.2800
Spiniferites elongatus	0.1493	-0.0865	0.0840
Impagidinium aculeatum	0.1633	0.0342	-0.0141
Impagidinium spp.	0.3147	-0.2465	0.0976
Impagidinium patulum	0.3658	-0.1943	0.1194
Spiniferites ssp.	0.3832	-0.2068	0.2495
Spiniferites mirabilis-hyperacanthus	0.4543	0.6352	-0.0623
Spiniferites ramosus	0.4756	-0.1722	-0.0520

CONCLUSION GÉNÉRALE

Dans cette thèse, par une analyse détaillée des assemblages polliniques modernes et fossiles, nous avons exploré le potentiel paléoenvironnemental (végétation et climat) des grains de pollen et de spores contenus dans les sédiments lacustres des hautes latitudes de l'Hémisphère nord. L'analyse des assemblages polliniques modernes de 400 sites lacustres du Canada (>50°N) et du Groenland, répartis de la forêt boréale au désert arctique, et leur comparaison avec les conditions climatiques actuelles, nous a permis de mieux cerner la relation pollen – climat. La reconnaissance d'un lien entre les assemblages polliniques et le climat nous a encouragé à reconstituer les climats passés de la Terre de Baffin et du Groenland. Les reconstitutions climatiques présentées s'appuient sur la méthode des meilleurs analogues modernes (BMA) et sur une régression issue d'une analyse factorielle des correspondances (CA).
L'application de ces deux techniques, aux sédiments fossiles de la Terre de Baffin et du Groenland, nous a permis d'isoler un facteur pouvant interférer dans les reconstitutions paléoclimatiques de la région circum-arctique, soit la ressemblance entre les assemblages polliniques de sites à température hivernale et précipitation annuelles très différentes. Néanmoins, si elles sont utilisées avec prudence, les techniques de reconstitution developpées dans cette thèse sont encourageantes et méritent d'être exploitées. Effectivement, nous avons montré qu'en dépit des difficultés inhérentes à la palynologie des hautes latitudes, comme celles découlant de la faible productivité des plantes arctiques et du type de pluie pollinique enregistré dans le sédiment (régional ou extra-régional), il est possible de reconstituer quantitativement les températures estivales et d'illustrer l'évolution de la précipitation moyenne annuelle et de la température hivernale au cours d'une période donnée, permettant ainsi une estimation de la saisonnalité. La cohérence entre nos reconstitutions de la température estivale, et celles issues d'autres relevés paléoclimatiques terrestres, marins et même glaciaires, des environs de la baie de Baffin et de la mer du Labrador (e.g. Kerwin et al., 2004 ; NGRIP Members, 2004 ;

de Vernal et Hillaire-Marcel, 2006), éprouve en quelque sorte la technique de reconstitution développée dans cette thèse.

La relation entre les assemblages polliniques et le climat

L'analyse des données modernes a fait ressortir le lien étroit existant entre les assemblages polliniques de surface et la température actuelle de juillet (r = -0,86). Elle a, de plus, démontré la covariance existant entre la précipitation moyenne annuelle et la température de janvier. L'analyse a également montré que la corrélation entre ces deux variables climatiques est plus importante dans la toundra arctique (r = 0,83) qu'à travers la forêt boréale et la toundra subarctique (r = 0,53). Dans cette dernière région, la précipitation moyenne annuelle est également liée à la température de juillet (r = 0,53) alors que dans la toundra arctique, la relation entre la précipitation moyenne annuelle et la température du juillet est négligeable (r = 0,14). Ainsi, pour l'archipel de l'Arctique canadien et le Groenland, la reconstitution de la précipitation annuelle est intimement liée à la reconstitution de la température hivernale.

Les exemples d'application ont fait ressortir une limite aux reconstitutions climatiques des sites de la Terre de Baffin et du Groenland. Cette limite s'applique à la reconstitution de leur précipitation moyenne annuelle (PANN), de leur température de janvier (TJAN) et de leur température moyenne annuelle (TANN). Les reconstitutions de la température de juillet sont réalistes. Pour les sites de la Terre de Baffin, les valeurs reconstituées de la PANN, de la TJAN et de la TANN de l'Holocène sont grandement sur-estimées. Cette sur-estimation s'explique par la très forte ressemblance (SCD bien souvent inférieure à 0,10) entre les assemblages polliniques de la Terre de Baffin et du Groenland, deux endroits à température hivernale et précipitation annuelle bien contrastées (cf. Tableau 3, Chapitre I). En effet, des analogues modernes du sud-ouest du Groenland ont été retenus pour le

calcul des reconstitutions des sites de la Terre de Baffin, basées sur la BMA. Cette limitation est sérieuse et mérite notre attention, car elle touche à la théorie même des reconstitutions climatiques basées sur les assemblages polliniques. Elle nous indique que deux régions à température hivernale et précipitation annuelle très différentes peuvent produire des assemblages polliniques « identiques ». Notre savons que ceci est valable pour les sites de la toundra. Nous ignorons toutefois si cela s'applique également aux autres formations végétales.

Afin de bien reconstituer ces paramètres (PANN, TJAN, TANN) sur la Terre de Baffin, nous pourrions omettre de la base de données de référence les sites modernes du Groenland. En effet, le Groenland en raison de sa calotte glaciaire et d'un courant océanique chaud de surface, longeant ses côtes sud et ouest, constitue un environnement particulier et distinct de celui de l'archipel de l'Arctique canadien. Il y a toutefois un obstacle à cette avenue : que devrions-nous penser alors des reconstitutions de la PANN, de la TJAN et de la TANN du tardiglaciaire et de l'Holocène inférieur des régions englacées. Pour ces régions, le tardiglaciaire et l'Holocène inférieur représentent deux périodes où les calottes glaciaires sont parfois encore présentes et où l'insolation estivale est maximum ? Il s'agit aussi, comme au Groenland, d'un environnement particulier. Il arrive souvent qu'il n'y ait pas d'analogues modernes pour ces périodes, mais pour d'autres sites, des analogues existent. Nous nous pencherons bientôt sur ce problème lié à la reconstitution de la PANN, TJAN et TANN des sites de la Terre de Baffin en espérant y trouver une solution. Nous pourrions, par exemple, calibrer les taxons en fonction de la variable environnementale à l'aide d'une analyse canonique des correspondances. Malgré tout, nous avons montré dans notre travail de recherche qu'il est possible d'estimer, semi-quantitativement, ces paramètres climatiques à l'aide de l'analyse factorielle de correspondances.

Le dernier interglaciaire

Lors du dernier interglaciaire, une toundra arbustive relativement dense colonisait les sols de la péninsule de Cumberland, alors qu'aujourd'hui cette région abrite une toundra herbacée clairsemée. Les bouleaux colonisaient alors les sols de la région avec peut-être quelques aulnes isolés. Contrairement à l'Holocène, la végétation du dernier interglaciaire était plus homogène sur la péninsule de Cumberland. Le caractère de la végétation du dernier interglaciaire est typique de la végétation de la zone bioclimatique du bas Arctique, plus précisément de la végétation actuelle du sud-ouest du Groenland entre les latitudes 60-64°N et les longitudes 44-50°W. À cet endroit la température estivale est de 7,4 ± 1,8°C (Cappelen et al., 2001). La présence d'une toundra arbustive sur la péninsule de Cumberland, lors du dernier interglaciaire, implique une extension, de quelques centaines de kilomètres, de la zone bioclimatique du bas Arctique sur la côte est de la Terre de Baffin.

Les températures estivales du dernier interglaciaire sur la péninsule de Cumberland ont atteint des sommets de 8 à 10°C, ce qui est substantiellement plus chaud que les températures actuelles. La température de juillet actuelle sur la péninsule de Cumberland est de 4,6 ± 1,7°C (Environnement Canada, 2004). Nos reconstitutions ont également indiqué une température hivernale plus chaude que celle de l'actuel ainsi qu'une précipitation annuelle plus abondante durant cette période, sans doute principalement sous forme de neige. Par ailleurs, nous savons qu'un couvert de neige est nécessaire à la protection des racines du bouleau arbustif (cf. Fredskild, 1973 ; 1991). En regard de ces résultats, nous croyons que le climat du dernier interglaciaire sur la Terre de Baffin était plus océanique que l'actuel.

Le climat du dernier interglaciaire, sur la côte est de la Terre de Baffin, était donc de 4-5°C plus chaud qu'actuellement. Ces données sont cohérentes avec d'autres reconstitutions disponibles pour la portion ouest des hautes latitudes de l'Hémisphère

nord (LIGA Members, 1991 ; Bennike and Böcher, 1994 ; NGRIP Members, 2004 ; CAPE Last Interglacial Project Members, 2006, Otto-Bliesner et al., 2006). Une augmentation des précipitations annuelles sur la péninsule de Cumberland sous-entend une diminution de l'étendue du couvert de glace de mer dans la baie de Baffin et le détroit de Davis (cf. Williams et Bradley, 1985). Un rétrécissement du couvert de glace de mer et de la calotte groenlandaise, lors du dernier interglaciaire, a dernièrement été suggéré par Otto-Bliesner et al. (2006) et Overpeck et al. (2006).

La présence d'une végétation de toundra arbsutive sur la côte est de la Terre de Baffin a sans doute, tout comme la faible étendue de glace de mer dans la région, diminué l'albédo du territoire et amplifié le réchauffement (e.g. Chapin et al., 2005). Le remplacement d'une végétation de toundra herbacée, par une végétation de toundra arbustive, sur la Terre de Baffin est une information pertinente aux changements climatiques, tout comme l'intégration de nos données, dans une perspective circum-arctique (CAPE Last Interglacial Project Members, 2006 ; Otto-Bliesner et al., 2006), peuvent l'être aux simulations numériques visant à transcrire la répartition du réchauffement à travers les hautes latitudes de l'Hémisphère nord en cas d'un réchauffement planétaire substantiel (e.g. Overpeck et al., 2006).

L'Holocène

Les techniques de reconstitution (BMA et CA) appliquées aux séquences de sédiments lacustres holocènes de la Terre de Baffin et du Groenland montrent un refroidissement progressif estival, de l'Holocène moyen à l'Holocène supérieur, lequel est cohérent avec la diminution de l'insolation estivale (Berger et Loutre, 1991). Les reconstitutions montrent également une augmentation de la température hivernale, en accord avec l'augmentation progressive de l'isolation hivernale. Nos reconstitutions transcrivent ainsi une diminution de la saisonnalité de l'Holocène moyen à aujourd'hui. Elles indiquent également une augmentation de la précipitation

annuelle lors de l'Holocène supérieur. Par ailleurs, une augmentation des précipitations annuelles à l'Holocène supérieur a été suggérée par Dahl et Nesje (1996) et Nesje et al. (2001) pour expliquer l'avancée des glaciers scandinaviens au cours de cette époque. L'augmentation de la précipitation annuelle et de la température de janvier suggèrent un climat davantage océanique sur les côtes adjacentes à la baie de Baffin et au détroit de Davis depuis ca. 5000 ans BP.

Que ce soit sur la côte est de la Terre de Baffin ou la côte sud-ouest du Groenland, la transition entre l'Holocène moyen et l'Holocène supérieur, à ca. 5000 ans BP, est marquée par une augmentation notable de la représentation du pollen de bouleau (cf. Annexe B). Il s'agit de bouleau arbustif ; sans doute de *Betula glandulosa*. Le bouleau glanduleux est une espèce de bouleau océanique, auquel un certain niveau d'humidité est nécessaire à la survie (Fredskild, 1973 ; 1991). Son développement régional à l'Holocène supérieur peut avoir été favorisé par le climat « océanique » de l'époque.

Le refroidissement estival, de l'Holocène moyen à l'Holocène supérieur, a été de l'ordre de 0,5 à 1,0°C sur la côte est de la Terre de Baffin alors que sur la côte sud-ouest du Groenland, il fut beaucoup plus important, i.e. de l'ordre de 3,0 à 3,5°C. Une évolution climatique contrastante entre la côte est de la Terre de Baffin et la côte sud-ouest du Groenland sous-entend l'existence d'un régionalisme du climat à travers la baie de Baffin et le détroit de Davis et par le fait même, entre les eaux des marges est canadiennes et celles plus au large. En effet, de Vernal et Hillaire-Marcel (2006) ont montré que le refroidissisement des eaux du surface du talus du Labrador a été quasi-nul au cours de cette période alors que celui des eaux de l'Atlantique central, plus précisément à proximité de la Ride de Reykjanes fut de plus de 6°C. Ce contraste climatique d'ouest en est ainsi que la diminution de son intensité de l'Holocène moyen à l'Holocène supérieur suggèrent une diminution progressive de l'influence du flux d'eau chaude nord Atlantique le long de la côte sud, sud-ouest du

Groenland, alors que l'est de la Terre de Baffin et les marges est canadiennes seraient vraisemblablement demeurées sous l'influence des courants froids de Baffin et du Labrador. Les résultats de notre recherche s'ajoutent ainsi à plusieurs autres études (e.g. Bond et al., 1997 ; CAPE Project Members, 2001 ; Hammarlund et al., 2002 ; Davis et al., 2003 ; Kaufman et al., 2004 ; Solignac et al., 2004 ; de Vernal et Hillaire-Marcel, 2006) et confortent le caractère instable du climat de l'Holocène, à travers le temps et l'espace.

Épilogue

Au terme de ce travail de recherche, nous pouvons affirmer que l'analyse pollinique de sédiments lacustres arctiques s'avère un excellent outil pour reconstituer la végétation de toundra à long et moyen terme et préciser l'histoire climatique des hautes latitudes de l'Hémisphère nord. Il serait maintenant intéressant de préciser le délai de réaction de la végétation arctique à un changement climatique. Pour ce genre d'étude toutefois la reconstitution climatique devra être faite à l'aide d'un proxy climatique indépendant, comme par exemple les chironomides. De même, l'étude d'autres sédiments interglaciaires nous permettrait de préciser l'étendue de la toundra arbustive sur la Terre de Baffin et peut-être ainsi d'élucider le mystère planant toujours sur la présence locale de l'aulne à cette époque et même en des temps plus récents.

BIBLIOGRAPHIE GÉNÉRALE

Andersen, C., Koç, N., Jennings, A., Andrews, J.T., 2004. Non uniform response of the major surface currents in the Nordic Seas to insolation forcing: implications for the Holocene climate variability. Paleoceanography 19, PA2003, doi: 10.1029/2002PA000873.

Arctic Climate Impact Assessment, 2005. Impacts of a warming Arctic: Arctic Climate Impact Assessment. Cambridge University Press, New York, 144pp.

Barbour, M.G., Burk, J.H., Pitts, W.D., Gilliam, F.S., Schwartz, M.W., 1998. Terrestrial plant ecology. 3e édition. Addison Wesley Longman, Inc. Menlo Park, California.

Bennike, O., Böcher, J., 1994. Land biotas of the last interglacial/glacial cycle on Jameson Land, East Greenland. Boreas 23, 479-487.

Berger, A., Loutre, M.F., 1991. Insolation values for the climate of the last 10 million years. Quaternary Science Reviews 10, 297-318.

Berger, A.L., 1983. Approche astronomique des variations paléoclimatiques: les variations mensuelles et en latitude de l'insolation de ~130 000 à ~100 000 et de ~30 000 à aujourd'hui. Bulletin de l'Institut de géologie du bassin d'Aquitaine, 1-29.

Bigelow, N.H., Brubaker, L.B., Edwards, M.E., Harrison, S.P., Prentice, I.C., Anderson, P.M., Andreev, A.A., Bartlein, P.J., Christensen, T.R., Cramer, W., Kaplan, J.O., Lozhkin, A.V., Matveyeva, N.V., Murray, D.F., McGuire, A.D., Razzhivin, V.Y., Ritchie, J.C., Smith, B., Walker, D.A., Gajewski, K., Wolf, V., Holmqvist, B.H., Igarashi, Y., Kremenetskii, K., Paus, A., Pisaric, M.F.J., Volkova, V.S., 2003. Climate change and Arctic ecosystems: 1. Vegetation changes north of 55°N between the last glacial maximum, mid-Holocene, and present. Journal of Geophysical Research 108, doi:10.1029/2002JD002558.

Bond, G.C., Showers, W., Cheseby, M., Lotti, R., Almasi, P., deMenocal, P., Priore, P., Cullen, H., Hajdas, I. and Bonani, G., 1997. A pervasive millennial-scale cycle in North Atlantic Holocene and glacial climates. Science 278, 1257-1266.

Boulton, G.S., Dickson, J.H., Nichols, H., Nichols, M., Short, S., 1976. Late Holocene glacier fluctuations and vegetation changes at Maktak Fiord, Baffin Island, NWT, Canada. Arctic and Alpine Research 8, 343-356.

CAPE Last Interglacial Project Members, 2006. Last Interglacial Arctic warmth confirms polar amplification of climate change. Quaternary Science Reviews 25, 1383-1400.

CAPE Project Members , 2001. Holocene paleoclimate data from the Arctic: testing models of global climate change. Quaternary Science Reviews 20, 1275-1287.

Cappelen, J., Jørgensen, B., Laursen, E., Stanius, L., Thomsen, R., 2001. The observed climate of Greenland – with climatological normals, 1961-90. DMI Technical Report No. 00-18.

Chapin III, F.S., Sturm, M., Serreze, M.C., McFadden, J.P., Key, J.R., Lloyd, A.H., McGuire, A.D., Rupp, T.S., Lynch, A.H., Schimel, J.P., Beringer, J., Chapman, W.L., Epstein, H.E., Euskirchen, E.S., Hinzman, L.D., Jia, G., Ping, C.-L., Tape, K.D., Thompson, C.D.C., Walker, D.A., Welker, J.M., 2005. Role of land-surface changes in Arctic summer warming. Science 310, 657-660.

Chapman, M.R., Shackleton, N.J., 2000. Evidence of 550-year and 1000-year cyclicities in North Atlantic circulation patterns during the Holocene. The Holocene 10, 287-291.

CLIMAP Project Members, 1984. The Last Interglacial ocean. Quaternary Research 21, 123-224.

Dahl, O.S., Nesje, A., 1996. A new approach to calculating Holocene winter precipitation by combining glacier equilibrium-line altitudes and pine-tree limits: a case study from Hardangerjokulen, central southern Norway. The Holocene 6, 381-398.

Davis, B.A.S., Brewer, S., Stevenson, A.C., Guiot, J., Data Contributors, 2003. The temperature of Europe during the Holocene reconstructed from pollen data. Quaternary Science Reviews 22, 1701-1716.

Davis, P.T., 1980. Late Holocene glacial, vegetational, and climatic history of Pangnirtung and Kingnait Fiord area, Baffin Island, Canada. PhD Thesis, Department of Geological Sciences, University of Colorado, 366pp.

de Vernal, A., Hillaire-Marcel, C., 2006. Provincialism in trends and high frequency changes in the northwestern North Atlantic during the Holocene. Global and Planetary Changes 54, 263-290.

Environment Canada, 2004. http://climate.weatheroffice.ec.gc.ca/climate_normals

Foley, J.A., 2005. Tipping points in the tundra. Science 310, 627-628.

Fréchette, B., 2004. Le maximum thermique de l'Holocène a-t-il été uniforme dans l'espace et synchrone à travers les hautes latitudes (>60°) de l'hémisphère nord ? De quelle manière et comment cela s'explique-t-il ? Rapport de synthèse environnementale, Université du Québec à Montréal.

Fredskild, B., 1973. Studies in the vegetational history of Greenland. Palaeobotanical investigations of some Holocene lake and bog deposits. Meddelelser om Grønland 198 (4), 245 pp.

Fredskild, B., 1991. The genus Betula in Greenland – Holocene history, present distribution and synecology. Nordic Journal of Botany 11, 393-412.

Gajewski K., Garneau M., Bourgeois J.C., 1995. Paleoenvironments of the Canadian High Arctic derived from pollen and plant macrofossils: problems and potentials. Quaternary Science Reviews 14, 609-629.

Gajewski, K., Mott, R.J., Ritchie, J.C., Hadden, K., 2000. Holocene vegetation history of Banks Island, Northwest Territories, Canada. Can. J. Bot. 78, 430-436.

Gajewski, K., Frappier, M., 2001. A Holocene lacustrine record of environmental change in northeastern Prince of Wales Island, Nunavut, Canada. Boreas 30, 285-289.

Gajewski, K., MacDonald, G.M., 2004. Palynology of North American Arctic lakes. In R. Pienitz, M.S.V. Douglas and J.P. Smol (Eds). Long-term Environmental Change in Arctic and Antartic Lakes. Developments in Paleoenvironmental Research, vol. 8, Springer, The Netherlands, pp 89-116.

Gajewski, K., 1995. Modern and Holocene pollen assemblages from some small Arctic lakes on Somerset Island, N.W.T., Canada. Quat. Res. 44, 228-236.

Hammarlund, D., Barnekow, L., Birks, H.J.B., Buchardt, B., Edwards, T.W.D., 2002. Holocene changes in atmospheric circulation recorded in the oxygen-isotope stratigraphy of lacustrine carbonates from northen Sweden. The Holocene 12, 339-351.

Holland, M.M., Bitz, C.M., 2003. Polar amplification of climate change in coupled models. Climate Dynamics 21, 221-232.

Hyvärinen, H., 1985. Holocene pollen stratigraphy of Baird Inlet, east-central Ellesmere Island, Arctic Canada. Boreas 14, 19-32.

Jiang, H., Seidenkrantz, M.-S., Knudsen, K.L., Eiríksson, J., 2002. Late-Holocene summer sea-surface temperatures based on a diatom record from the north Icelandic shelf. The Holocene 12, 137-147.

Kaplan, M.R., Wolfe, A.P., Miller, G.H., 2002. Holocene environmental variability in southwestern Greenland inferred from lake sediments. Quaternary Research 58, 149-159.

Kaplan, M.R., Wolfe, A.P., 2006. Spatial and temporal variability of Holocene temperature trends in the North Atlantic sector. Quaternary Research 65, 223-231.

Kaufman, D.K., Ager, T.A., Anderson, N.J., Anderson, P.M., Andrews, J.T., Bartlein, P.J., Brubaker, L.B., Coats, L.L., Cwynar, L.C., Duvall, M.L., Dyke, A.S., Edwards, M.R., Eisner, W.R., Gajewski, K., Geirsdottir, A., Hu, F.S., Jennings, A.E., Kaplan, M.R., Kerwin, M.W., Lozhkin, A.V., MacDonald, G.M., Miller, G.H., Mock, C.J., Oswald, W.W., Otto-Bliesner, B.L., Porinchu, D.F., Ruhland, K., Smol, J.P., Steig, E.J., Wolfe, B.B., 2004. Holocene thermal maximum in the western Arctic (0–180°W). Quaternary Science Reviews 23, 529–560.

Kerwin, M.K., Overpeck, J.T., Webb, R.S., Anderson, K.H., 2004. Pollen-based summer temperature reconstructions for the Eastern Canadian Boreal forest, Sub-Arctic and Arctic. Quaternary Science Reviews 23, 1901-1924.

LIGA Members, 1991. Report of the 1st discussion group: The last interglacial in high latitudes of the northern hemisphere: terrestrial and marine evidence. Quat. Int. 10-12, 9-28.

Maslin, M., 2004. Ecological versus climatic threshold. Science 306, 2197-2198.

Meincke, J., 2002. Climate dynamics of the North Atlantic and NW-Europe: An observation-based overview. In: Wefer, G., Berger, W.H., Behre, K.-E., Jansen, E. (Eds.), Climate Development and History of the North Atlantic Realm. Springer, Berlin, pp. 25-40.

Mode, W.N., 1980. Quaternary stratigraphy and palynology of the Clyde Foreland, Baffin Island, NWT, Canada. PhD Thesis, Department of Geological Sciences, University of Colorado, 219pp.

Moreno, A., Cacho, I., Canals, M., Grimalt, J.O., Sánchez-Goñi, M.F., Shackleton, N., Sierro, F.J., 2005. Links between marine and atmospheric processes oscillating on a millennial time-scale. A multi-proxy study of the last 50,000 yr from the Alboran Sea (Western Mediterranean Sea). Quaternary Science Reviews 24, 1623-1636.

Nesje, A., Matthews, J.A., Dahl, S.O., Berrisford, M.S., Andersson, C., 2001. Holocene glacier fluctuations of Flatebreen and winter-precipitation changes in the Jostedalsbreen region, western Norway, based on glaciolacustrine sediment records. The Holocene 11, 267-280.

NGRIP Members, 2004. High-resolution record of Northern Hemisphere climate extending into the last interglacial period. Nature 431, 147-151.

Otto-Bliesner, B.L., Marshall, S.J., Overpeck, J.T., Miller, G.H., Hu, A., CAPE Last Interglacial Project Members. Simulating Arctic climate warmth and icefield retreat in the last interglaciation. Science 311, 1751-1753.

Overpeck, J.T., Otto-Bliesner, B.L., Miller, G.H., Muhs, D.R., Alley, R.B., Kiehl, J.T., 2006. Paleoclimatic evidence for future ice-sheet instability and rapid sea-level rise. Science 311, 1747-1750.

Overpeck, J.T., Hughen, K.A., Hardy, D., Bradley, R.S., Case, R., Douglas, M.S.V., Finney, B., Gajewski, K., Jacoby, G., Jennings, A.E., Lamoureux, S., Lasca, A., MacDonald, G.M., More, J.J., Retelle, M., Wolfe, A.P. et Zielinski, G. (1997). Arctic environmental change of the last four centuries. Science 278: 1251-1256.

Prentice, I.C., 1986. Vegetation responses to past climatic variation. Vegetatio 67, 131-141.

Ritchie, J.C., 1986. Climate change and vegetation response. Vegetatio 67, 65-74.

Serreze, M.C., Francis, J.A., 2006. The Arctic amplification debate. Climatic Change 76, 241-264.

Short, S.K., Mode, W.N., Davis, P., 1985. The Holocene record from Baffin Island: modern and fossil pollen studies. In J.T. Andrews (Ed.), Quaternary environments: Eastern Canadian Arctic, Baffin Bay and Western Greenland (pp. 608-642). Boston, Allen and Unwin.

Solignac, S., de Vernal, A., Hillaire-Marcel, C., 2004. Holocene sea-surface conditions in the North Atlantic – contrasted trends and regimes in the western and easrtern sectors (Labrador Sea vs. Iceland Basin). Quaternary Science Reviews 23, 319-334.

Webb III, T., 1986. Is vegetation in equilibrium with climate? How to interpret late-Quaternary pollen data. Vegetatio 67, 75-91.

Williams, L.D., Bradley, R.S., 1985. Paleoclimatology of the Baffin Bay region. In J.T. Andrews (Ed.), Quaternary environments: Eastern Canadian Arctic, Baffin Bay and Western Greenland (pp. 741-772). Boston, Allen and Unwin.

Wolfe, A.P., Fréchette, B., Richard, P.J.H., Miller, G.H., Forman, S.L., 2000. Paleoecology of a >90,000-year lacustrine sequence from Fog Lake, Baffin Island, Arctic Canada. Quaternary Science Reviews 19, 1677-1699.

Young, S.B., 1971. The vascular flora of St-Lawrence Island with special reference to floristic zonation in the arctic region. Contribution of the Herbarium of Harvard University 201, 11-115.

ANNEXE A

LA BASE DE DONNÉES POLLINIQUES DE RÉFÉRENCE

Le matériel de cette annexe est présenté sur un disque CD.
Il s'agit de sept tableaux en format Excel.
Le texte sur les tableaux est rédigé en anglais.

A1. Les données climatiques des stations météorologiques du Canada et du Groenland utilisées pour estimer par interpolation le climat des sites de référence.
A2. La source des données polliniques de la base de référence.
A3. Les données climatiques et bioclimatiques des sites de référence.
A4. Le nom des taxons polliniques répertoriés parmi les 400 sites de référence et l'information concernant leur groupement (harmonisation taxonomique).
A5. Le dénombrement des données polliniques brutes (159 taxons).
A6. Le dénombrement des données polliniques après harmonisation taxonomique (63 taxons).
A7. Le dénombrement des données polliniques retenues pour les reconstitutions climatiques (34 taxons).

ANNEXE B

DIAGRAMMES POLLINIQUES COMPLETS DES SITES À L'ÉTUDE

Page

La localisation des régions (A, B, FCD, NQ, JB, G, WC-3, WC-2, WC-1) indiquées sur le diagramme des sites de référence est donnée à la figure 1 du Chapitre I.

La somme de base utilisée pour le calcul des pourcentages ne comprend que les spermatophytes. Le pourcentage des spores de ptéridophytes, bryophytes (*Sphagnum*) et des plantes aquatiques a été calculé en fonction de la somme de base définie par les spermatophytes.

La localisation des sites polliniques à l'étude est donnée à la figure 1 de l'introduction.

L'information concernant les mesures radiocarbones indiquées sur les diagrammes polliniques des sites à l'étude est donnée à l'Annexe C.

Appendix B1

Modern Pollen Spectra; see Fig. 1 (Chapiter I) for location of the regions (A, B, FCD, NQ, JB, G, WC)

400 sites, 34 taxa

Relative frequency diagram

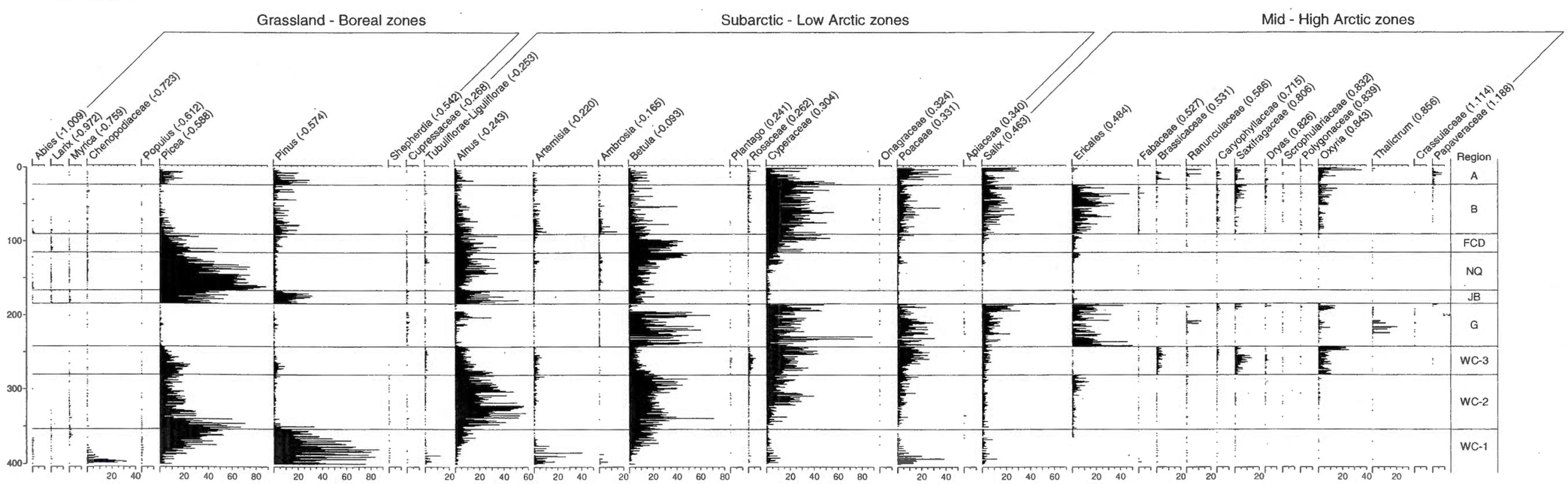

Taxa are ordered according to their scores on the primary CCA axis (Fig. 7B, Chapter I), which appear in brackets

Appendix B2
Fog Lake (96FOG-05), piston core
67°11' N, 63°15' W, altitude: 460 m asl
Relative frequency diagram

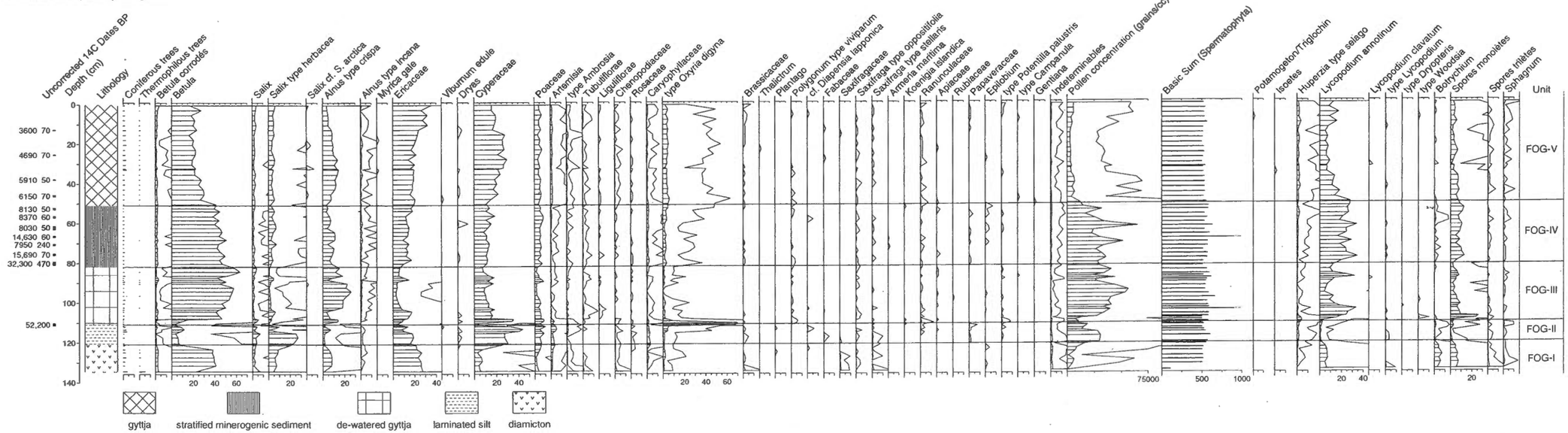

Appendix B3
Brother of Fog Lake (98BRO-05), piston core
67°11' N, 63°15' W, altitude: 380 m asl
Relative frequency diagram

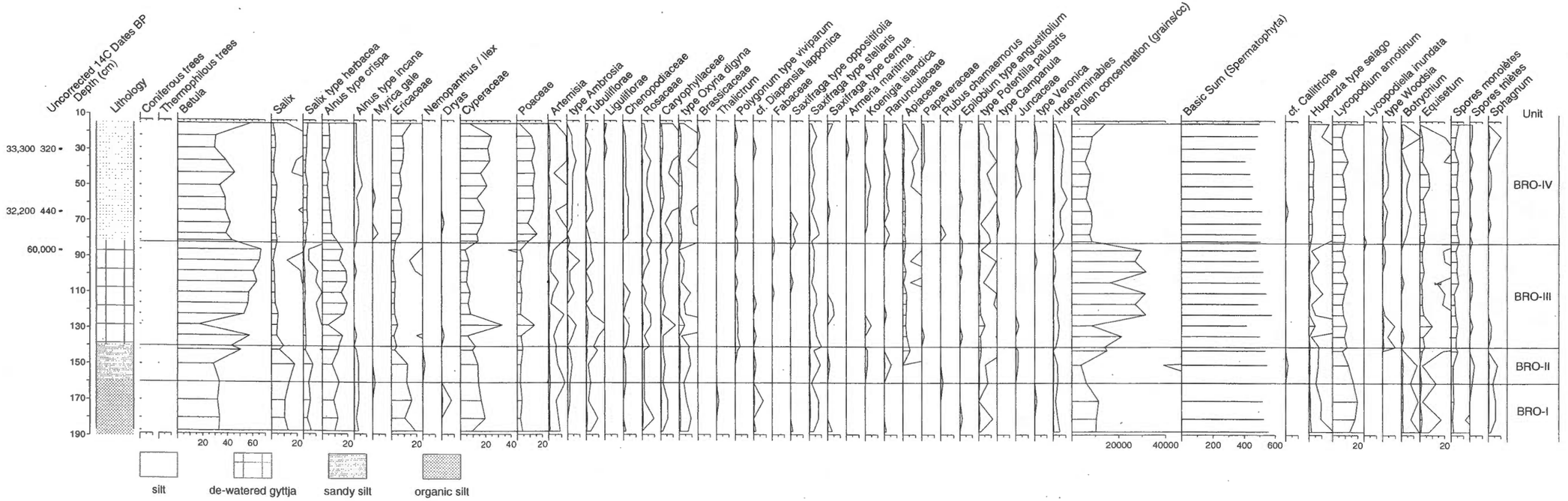

Appendix B4

Amarok Lake (98AKL-02), piston core
66°16' N, 65°45' W, altitude: 848 m asl
Relative frequency diagram

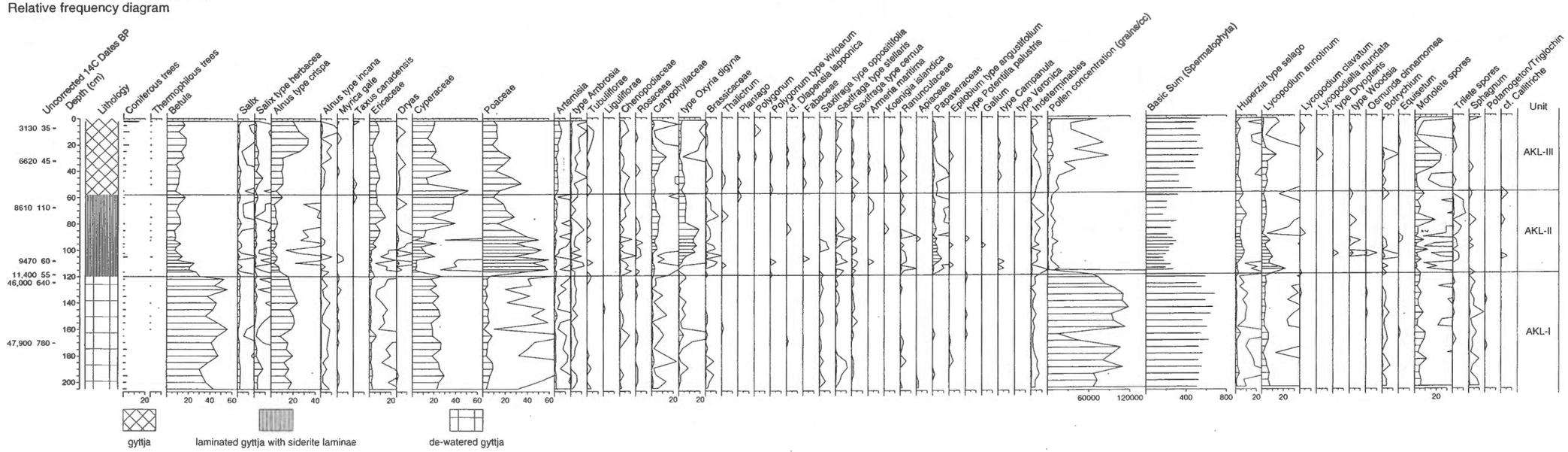

Appendix B5
Akvaqiak Lake (98BIR-02), piston core
66°47' N, 63°57' W, 45 m asl
Relative Frequency Diagram

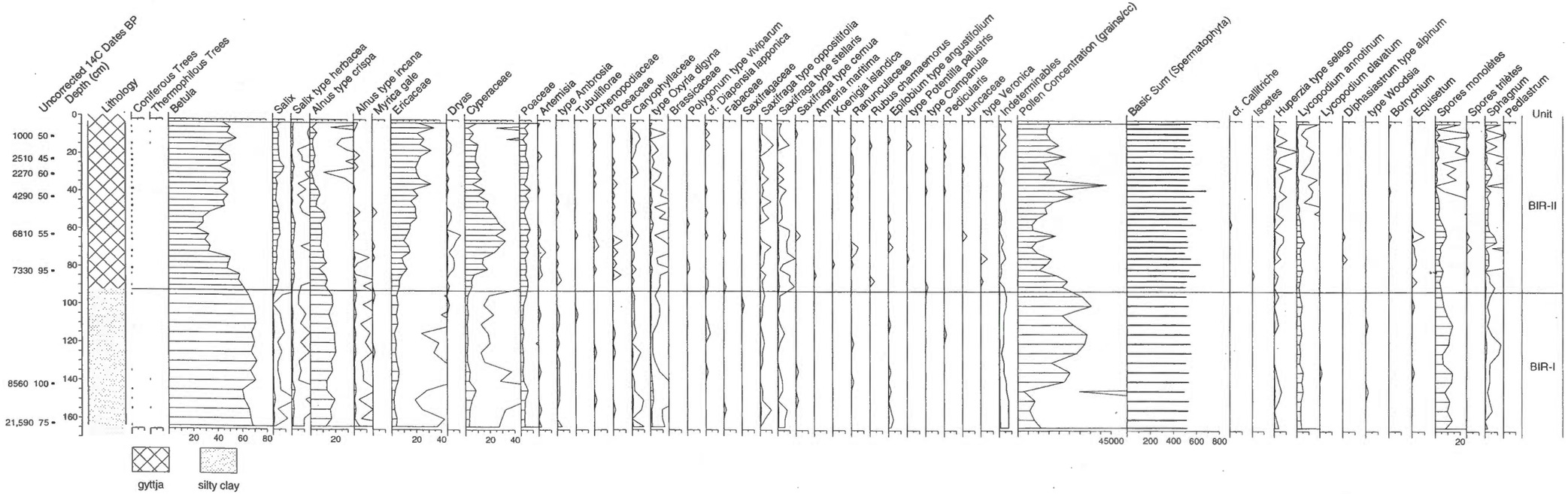

Appendix B6
Akvaqiak Lake (98BIR-G01), gravity (Glew) core
66°47' N, 63°57' W, 45 m asl

Relative Frequency Diagram

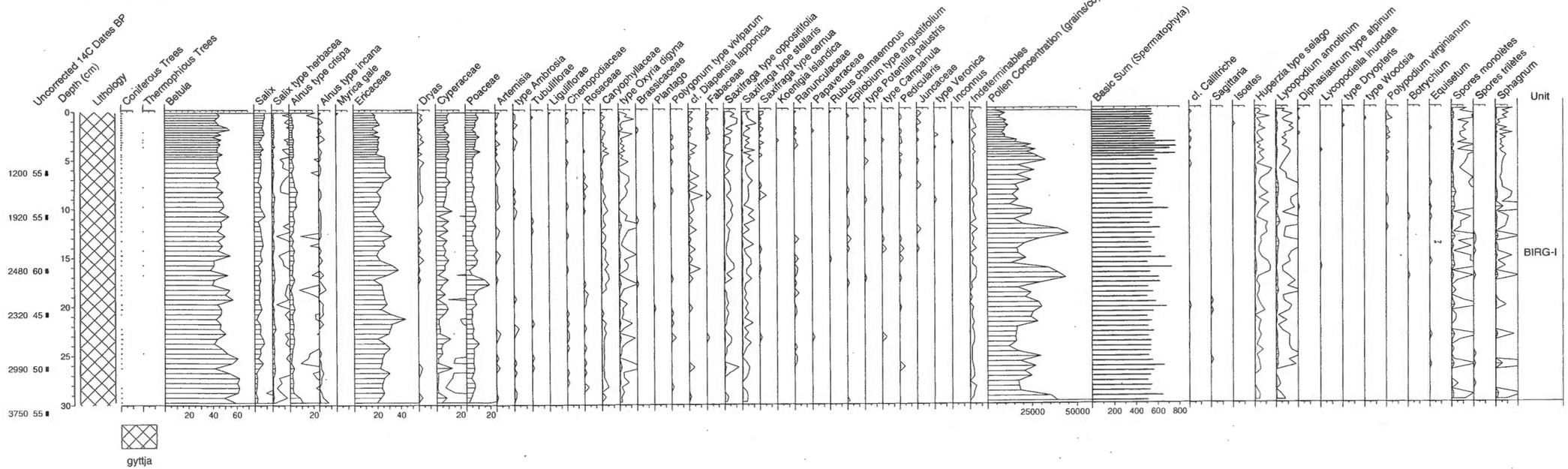

Appendix B7
Qipisarqo Lake (98QIP-02), piston core
61°00' N, 47°45' W, 7 m asl
Relative Frequency Diagram

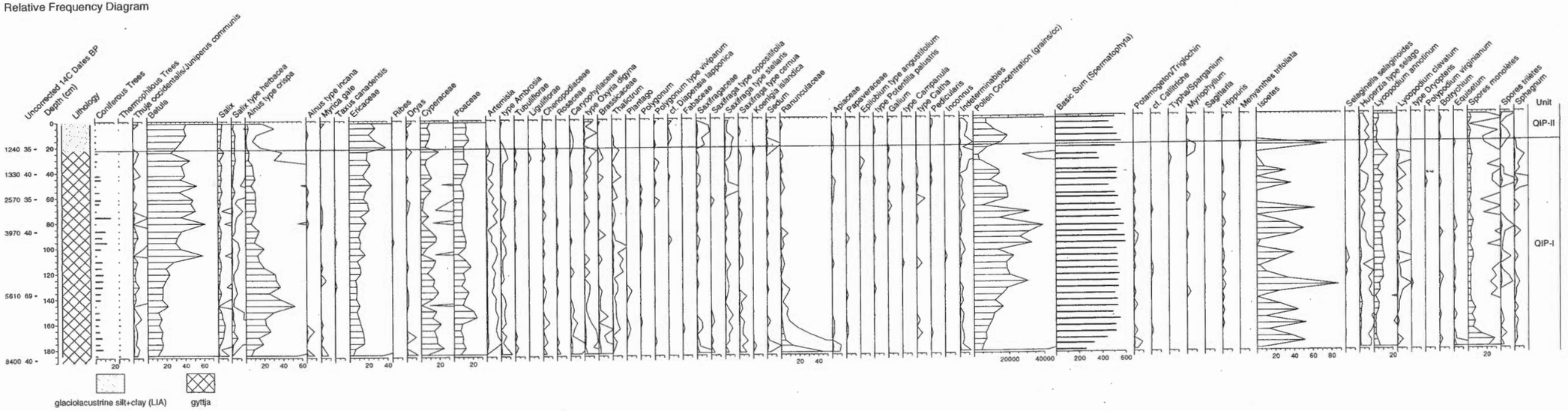

Appendix B8
Qipisarqo Lake (98QIP-G01), gravity (Glew) core; sediment post-LIA
61°00' N, 47°45' W, 7 m asl
Relative Frequency Diagram

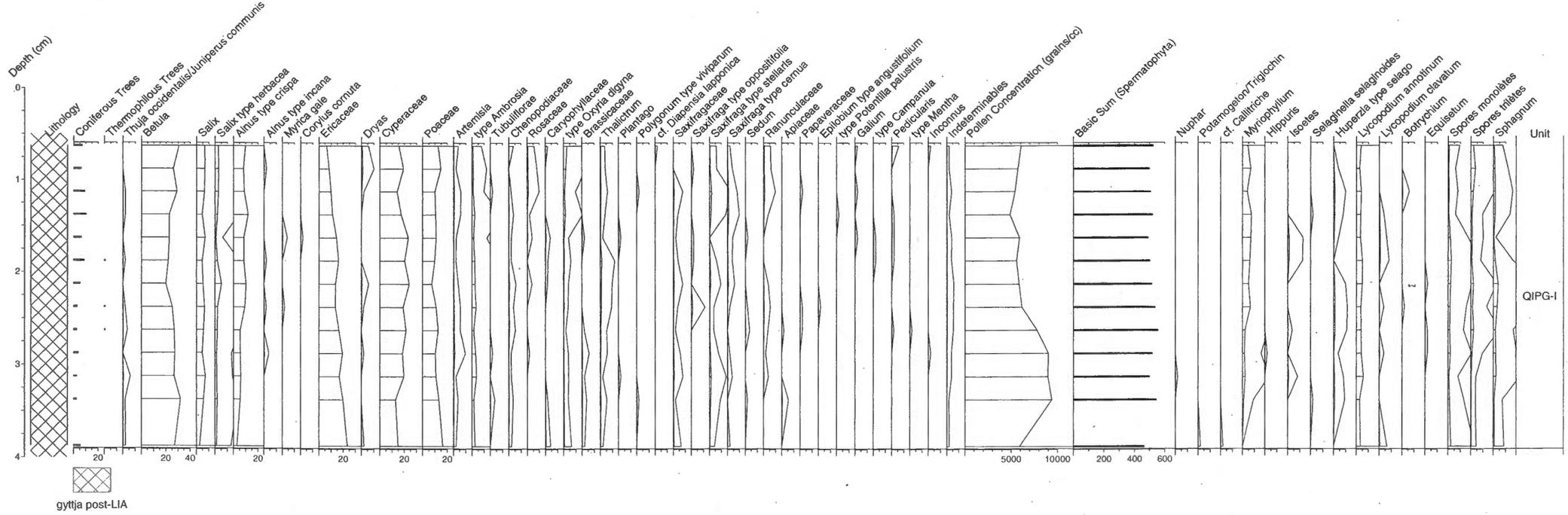

ANNEXE C

DONNÉES CHRONOLOGIQUES DES SITES À L'ÉTUDE

Page

Appendix C

Depth (cm)	Unit	Laboratory No.	Material	Uncorrected ^{14}C date (yr BP)
C1. Fog Lake (96FOG-05), piston core				
12.5 - 13.0	FOG-V	CAMS-30531	Humic acids	3600 ± 70
25.0 - 25.5	FOG-V	CAMS-30532	Humic acids	4690 ± 70
37.5 - 38.0	FOG-V	CAMS-30533	Humic acids	5910 ± 50
45.5 - 46.5	FOG-V	CAMS-30535	Macroflora	6150 ± 70
45.5 - 46.5	FOG-V	CAMS-30534	Humic acids	6320 ± 50
52.0 - 53.0	FOG-IV	CAMS-34298	Macroflora	8130 ± 50
56.0 - 57.0	FOG-IV	CAMS-28649	Macroflora	8370 ± 60
61.0 - 63.0	FOG-IV	CAMS-30536	Macroflora	8030 ± 50
66.0 - 67.0	FOG-IV	CAMS-34299	Humic acids	14,630 ± 60
70.0 - 71.0	FOG-IV	OS-26222	Chitin	7950 ± 240
75.0 - 76.0	FOG-IV	CAMS-34300	Humic acids	15,690 ± 70
79.0 - 81.0	FOG-IV	CAMS-30537	Macroflora	32,300 ± 470
110.0-111.5	FOG-III	CAMS-28652	Macroflora	>52,200
C2. Brother-of-Fog Lake (98BRO-05), piston core				
30.0 - 31.0	BRO-IV	NSRL-10617	Humic acids	33,300 ± 320
65.0 - 66.0	BRO-IV	NSRL-10618	Humic acids	32,200 ± 440
86.5 - 87.5	BRO-III	NSRL-10131	Macroflora	60,000 ± 1900
C3. Amarok Lake (98AKL-02), piston core				
6.5 - 7.5	AKL-III	NSRL-13451	Macroflora	3139 ± 35
31.5 - 32.5	AKL-III	NSRL-13452	Macroflora	6620 ± 45
67.0 - 68.0	AKL-II	?	?	8610 ± 110
85.5 - 86.5	AKL-II	NSRL-13453	Humic acids	9470 ± 60
107.5 - 108.5	AKL-II	NSRL-13454	Humic acids	11,400 ±55
124-125	AKL-I	OS-18067	Macroflora	46,000 ± 640
170-171	AKL-I	OS-18066	Macroflora	47,900 ± 780

Appendix C (suite)

Depth (cm)	Unit	Laboratory No.	Material	Uncorrected ^{14}C date (yr BP)
C4. Akvaqiak Lake (98BIR-02), piston core attention				
11.0 - 12.0	BIR-II	NSRL-11345	Macroflora	1000 ± 50
11.0 - 12.0	BIR-II	NSRL-11346	Humic acids	1700 ± 45
23.0 - 24.0	BIR-II	NSRL-10621	Humic acids	2510 ± 45
31.0 - 32.0	BIR-II	NSRL-11347	Macroflora	2270 ± 60
31.0 - 32.0	BIR-II	NSRL-11348	Humic acids	2840 ± 55
43.0 - 44.0	BIR-II	NSRL-10622	Humic acids	4290 ± 50
63.0 - 64.0	BIR-II	NSRL-10623	Humic acids	6810 ± 55
82.5 - 83.5	BIR-II	NSRL-10624	Humic acids	7670 ± 60
82.5 - 83.5	BIR-II	NSRL-10176	Macroflora	7330 ± 95
142.0 - 143.0	BIR-I	NSRL-10139	Macroflora	8560 ± 100
159.5 - 160.5	BIR-I	NSRL-13332	Humic acids	21,590 ± 75
C5. Akvaqiak Lake (98BIR-G01), gravity (Glew) core				
6.0-6.5	BIRG-I	NSRL-11342	Humic acids	1200 ± 65
10.5-11.0	BIRG-I	NSRL-10625	Humic acids	1920 ± 55
16.0-16.5	BIRG-I	NSRL-11343	Humic acids	2480 ± 60
20.5-21.0	BIRG-I	NSRL-10626	Humic acids	2320 ± 45
26.0-26.5	BIRG-I	NSRL-11344	Humic acids	2990 ± 50
30.5-31.0	BIRG-I	NSRL-10627	Humic acids	3750 ± 55
C6. Qipisarqo Lake (98QIP-02), piston core				
19.5 - 20.5	QIP-I	CURL-4475	Humic acids	1240 ± 35
39.5 - 40.5	QIP-I	CURL-4486	Humic acids	1330 ± 40
59.5 - 60.5	QIP-I	CURL-4476	Humic acids	2570 ± 35
86.0 - 87.0	QIP-I	CURL-3037	Humic acids	3970 ± 40
135.5 - 136.5	QIP-I	CURL-4487	Humic acids	5840 ± 60
135.5 - 136.5	QIP-I	CURL-4488	Macroflora	5610 ± 60
187.0 - 188.0	QIP-I	CURL-3038	Humic acids	8400 ± 40

ANNEXE D

COPIE DE L'ARTICLE DES
CAPE LAST INTERGLACIAL PROJECT MEMBERS
PUBLIÉ EN 2006 DANS LA REVUE *QUATERNARY SCIENCE REVIEWS*

ELSEVIER

Quaternary Science Reviews 25 (2006) 1383–1400

QSR

Last Interglacial Arctic warmth confirms polar amplification of climate change

CAPE-Last Interglacial Project Members*,[1]

Received 15 June 2005; accepted 23 January 2006

Abstract

The warmest millennia of at least the past 250,000 years occurred during the Last Interglaciation, when global ice volumes were similar to or smaller than today and systematic variations in Earth's orbital parameters aligned to produce a strong positive summer insolation anomaly throughout the Northern Hemisphere. The average insolation during the key summer months (M, J, J) was ca 11% above present across the Northern Hemisphere between 130,000 and 127,000 years ago, with a slightly greater anomaly, 13%, over the Arctic. Greater summer insolation, early penultimate deglaciation, and intensification of the North Atlantic Drift, combined to reduce Arctic Ocean sea ice, allow expansion of boreal forest to the Arctic Ocean shore across vast regions, reduce permafrost, and melt almost all glaciers in the Northern Hemisphere. Insolation, amplified by key boundary condition feedbacks, collectively produced Last Interglacial summer temperature anomalies 4–5 °C above present over most Arctic lands, significantly above the average Northern Hemisphere anomaly. The Last Interglaciation demonstrates the strength of positive feedbacks on Arctic warming and provides a potentially conservative analogue for anticipated future greenhouse warming.

1. Introduction

Planetary warm times in the recent geological past inform the debate over Earth's response to the continuing build up of radiatively active atmospheric trace gases. Strong positive feedbacks in the Arctic are expected to amplify future greenhouse warming (Holland and Bitz, 2003), but the cumulative effect of these feedbacks remains debated (Serreze and Francis, 2006). Past planetary warm times provide a testing ground for the debate over polar amplification of climate change. During the Last Interglaciation (LIG) Earth was warmer than at any time in at least the past 250,000 years, with global temperatures 0–2 °C above present (e.g., CLIMAP Project Members, 1984; Bauch and Erlenkeuser, 2003). Circum-Arctic warming is recognized to have been substantial during the LIG (Lauritzen and Anderson, 1995), but quantitative reconstructions for this region are lacking.

Here we present quantitative estimates of circum-Arctic LIG summer air and sea-surface temperatures reconstructed from proxy records preserved in terrestrial and marine archives. These reconstructions demonstrate that Arctic summer air temperatures averaged ca 4–5 °C above present for most of the Arctic, well above the planetary LIG average, although with coherent spatial patterns in the magnitude of warmth. Arctic summers were warm enough to melt all glaciers below 5 km elevation except the Greenland Ice Sheet, which was reduced by ca 20–50% (Cuffey and Marshall, 2000; Otto-Bliesner et al., 2006). In addition, the margins of permanent Arctic Ocean sea ice retracted well into the Arctic Ocean basin and boreal forests advanced to the Arctic Ocean coast across vast regions of the Arctic currently occupied by tundra, although the central Arctic Ocean basin remained covered by permanent sea ice (Spielhagen et al., 2004). These boundary condition changes reduced Earth's albedo and altered the exchange of heat, moisture and trace gases between the land, ocean and atmosphere, collectively amplifying insolation-driven (Fig. 1) circum-Arctic interglacial warmth.

*Corresponding author. G.H. Miller. Tel.: +1 303 492 6962.
E-mail address: gifford.miller@colorado.edu.
[1]A full list of authors appears in Appendix A.

0277-3791/$ - see front matter © 2006 Elsevier Ltd. All rights reserved.
doi:10.1016/j.quascirev.2006.01.033

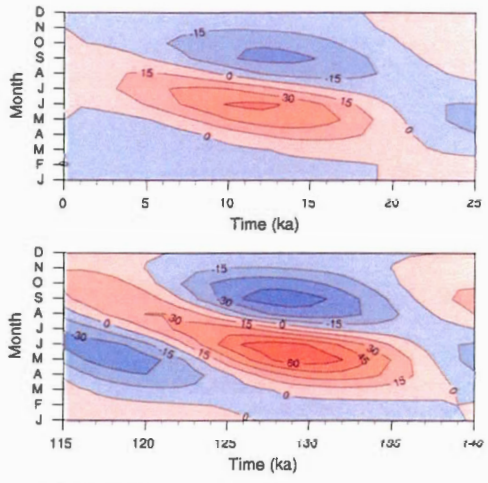

Fig. 1. Monthly insolation anomalies (deviations from the present) for the time periods from 25 ka to present (upper panel) and from 140 to 115 ka (lower panel) at 65°N, showing the larger insolation anomaly for the Last Interglaciation relative to the present interglaciation. Anomalies are expressed as W m^{-2}; time is in thousands of years before present.

2. The Last Interglaciation

The LIG was recognized more than a century ago in northern Europe (Harting, 1875). Subsequently, it was defined from pollen records as the Eemian, a time of deciduous forests bounded by periods of tundra (Jessen and Milthers, 1928). A half-century later, the Eemian was correlated with marine isotope stage (MIS) 5 (Emiliani, 1955), and eventually with the much shorter MIS 5e (Shackleton, 1969; Mangerud et al., 1979; Shackleton et al., 2002). The LIG was securely placed in an absolute time frame when correlated to coral terraces on stable platforms that were amenable to high-precision uranium-series dating (Broecker and Van Donk, 1970; Gallup et al., 2002). We define the LIG temporally as the penultimate interval of minimum global ice volume, when sea level was at or above present. It is now widely accepted that sea level reached modern levels 130±2 ka (thousands of years ago), and remained at or above this level until the inception of the last glaciation, as ice grew on the continents ca 116 ka (Stirling et al., 1998; Henderson and Slowey, 2000; Mcculloch and Esat, 2000; Gallup et al., 2002; Muhs et al., 2002). Although we use the term LIG as broadly correlative with both the Eemian and MIS 5e, we recognize that these intervals are not precisely correlative. The first half of the LIG coincides with an unusually strong Northern Hemisphere positive summer insolation anomaly, whereas summer insolation receipts are relatively low through the later half of the marine highstand (Fig. 1). Peak Eemian warmth may have occurred slightly before sea level reached present, and certainly was over long before sea level fell below present ca 116 ka (Zagwijn, 1996; Grøsfjeld et al., 1996). Despite these modest temporal differences, sea level provides a powerful tool for correlating the LIG across much of the globe, and associated coral reefs offer the most secure dating of the LIG.

The LIG has received less attention in the Arctic than at mid-latitudes, largely because of difficult access and paucity of sites. A decade ago, a circum-Arctic summary confirmed that the LIG was warmer than present (Lauritzen and Anderson, 1995), although quantitative estimates of warmth were not then possible. In the intervening decade, many new sites have been described from both marine and terrestrial archives, systematic recovery of sea-floor sediment from the Arctic Ocean has provided new evidence for the state of the polar ocean during the LIG, and new training sets, coupled to improved statistical tools, allow more precise quantification of many climate proxies (ter Braak and Juggins, 1993; Birks, 1998). For many Arctic regions, reliable transfer functions for summer temperatures are now available for pollen, chironomids, diatoms, dinoflagellates, planktonic and benthonic foraminifera, alkenones, and several ice-core parameters. Consequently, it is now possible to describe quantitatively at least some aspects of the LIG climate in the Arctic.

3. Methods

3.1. Dating the Last Interglaciation

We capitalize on the uniqueness of the Late Quaternary climate record and recent advances in geochronology to define LIG sites with reasonable certainty. Arctic sites with continuous accumulation since the LIG demonstrate that only the LIG shows evidence of summer temperatures comparable to, or higher than the Holocene. Materials suitable for high-precision U/Th analyses are rare in the Arctic, but advances in trapped-charge dating (optically stimulated luminescence, infra-red-stimulated luminescence, thermoluminescence) provide independent verification of LIG ages for many sites, although the dates often lack sufficient precision to subdivide the interglaciation (Berger and Anderson, 2000; Murray and Funder, 2003). Diagnostic tephra, especially in Alaska and the Nordic Seas, provide additional temporal constraint (Haflidason et al., 2000; Begét and Keskinen, 2003; Rasmussen et al., 2003a, b). LIG sites (Tables 1 and 2) are identified with moderate to high certainty by a combination of stratigraphic position, climate proxies, absolute dating, and relationship to stratigraphic marker horizons (e.g. diagnostic tephra).

3.2. Quantifying Last Interglacial summer temperatures

At high northern latitudes, summer temperatures exert the dominant control on glacier mass balance, unless

Table 1
Published sites with quantitative summer temperature estimates for peak LIG warmth from terrestrial sites around the circum-Arctic. Details of site location and reconstruction techniques are provided in the references cited. Some key cites with important qualitative LIG summer or winter temperature or precipitation are also included

	Proxy	ΔT (°C) Summer	ΔT (°C) Winter	Ppt	Reference	Comments
Scandinavia						
Finland	Treeline position reconstructed from pollen	Warmer			(Saarnisto et al., 1999)	Boreal forest north of present limit; birch at Arctic Ocean shore.
Russia						
European Russia	Pollen, plant macrofossils		4		(Devyatova, 1982) (Grichuk, 1984)	Boreal forest north of present limit.
West central Siberia	Pollen, plant macrofossils	6 to 8	5 to 7	Wetter	(Gudina et al., 1983) (Grichuk, 1984)	Boreal forest 800 km north of present limit.
NE Siberia	Pollen	4 to 8	4	Wetter	(Lozhkin and Anderson, 1995)	Treeline (boreal forest) ~600 km farther north and west of modern range limits. Range extensions up to 1000 km for primary tree species.
NE Siberia Lake Elgygytgyn	Pollen	⩾3	⩾4	Wetter	(Lozkhin et al., 2006)	Northern extension of treeline by at least 150 km.
Siberia	Pollen	4 to 5		Wetter	(Andreev et al., 2004)	Some plant taxa suggest even warmer summers.
Alaska						
NW Alaska Squirrel Lake, SW Brooks Range	Pollen, plant macrofossils	1 to 2	−1 to −3	Wetter	(Berger and Anderson, 2000) (Anderson, 2005)	Continuous high-resolution pollen record. Currently near treeline. Black spruce boreal forest at LIG, analogous to fully developed modern forests located ~300 km to the southeast. Unpublished pollen analogue-derived temperature estimates.
NW Alaska Ahaliorak Lake, North Slope	Pollen	1 to 2	−1 to −2	Wetter	(Brubaker et al., 1996) (Anderson and Brubaker, 1986) (Brubaker, 2005)	Continuous record. Currently in tundra of Brooks Range. In LIG forest extended north of Brooks Range (at least 50 km). Unpublished pollen-Panalogue-derived temperature estimates.
NW Alaska Imuruk Lake, Seward Pen.	Pollen	1 to 2	−1 to −2		(Shackleton, 1982) (Colinvaux, 1964)	Continuous low-resolution record. Old Crow tephra. Tundra today, boreal forest in LIG; westward expansion beyond present limits.
NW Alaska Noatak Valley	Pollen, beetles, plant macrofossils	0 to 2			(Edwards et al., 2003)	Tundra today. OC tephra reworked into LIG sediment. Treeline in Brooks Range of north present limit in LIG

Table 1 (*continued*)

	Proxy	ΔT (°C) Summer	ΔT (°C) Winter	Ppt	Reference	Comments
Interior Alaska Eva Creek	Pollen. spores, soils	0 to 2		Wetter	(Muhs, et al. 2001)	
Interior Alaska KY-11, Koyukuk River, Southern Brooks Range	Pollen, tephra	0 to −2	0 to 1		(Hamilton and Brigham-Grette, 1991) (Schweger, 2002)	Contains Old Crow tephra; partial record of LIG. Unpublished pollen analog-derived temperature estimates.
Interior Alaska Palisades of the Yukon	Pollen, spruce needles, tephra				(Begét, et al., 1991)	Contains Old Crow tephra
Western Alaska Nome	Pollen,	Warmer			(Brigham-Grette and Hopkins, 1995)	Pollen in Pelukian (LIG) marine deposits indicates boreal forest beyond Holocene limits
NW Alasaka Deering	Spruce macrofossils,	Warmer			(Brigham-Grette and Hopkins, 1995)	Macrofossils in Pelukian (LIG) marine deposits indicate spruce was beyond Holocene spruce limit.
NW Alaska Baldwin Peninsula	Spruce macrofossils	Warmer			(Brigham-Grette and Hopkins, 1995)	Macrofossils in Pelukian (LIG) marine deposits indicate spruce was beyond Holocene spruce limit.
Interior Alaska Birch Creek	Pollen	0 to −2	0 to 3	Wetter	(Edwards and McDowell, 1991) (Edwards, 2005)	Lake sediments; contains Old Crow Tephra. Unpublished pollen analog-derived temperature estimates.
Canada						
Tuktoyaktuk, NW Canada	Plant macrofossils	2			(Rampton, 1988)	Boreal forest at coast
Old Crow Basin, northern Yukon	plant macrofossils, beetles	Warmer			(Matthews et al., 1990)	Extra-limital taxa currently restricted to southern Yukon and northern British Columbia
Hudson Bay	Plant macrofossils	Warmer			(Dredge et al., 1990)	Boreal forest farther north
Banks Island, Arctic Canada	Pollen, plant macrofossils, insects	Warmer			(Matthews et al., 1986)	
Ellesmere Is	Pollen	Warmer			(Evans and Mott, 1993)	Possible LIG; organics between till
Robinson Lake, SE Baffin Island.	Pollen	5			(Miller et al., 1999) (Fréchette, 2005)	Stratified LIG lacustrine sediment below till. Correspondence analysis regression; Best modern analogue
Amarok Lake, S. Cumberland Peninsula, Baffin Is.	Pollen	5 to 6			(Fréchette et al., 2006)	Stratified LIG lacustrine sediment Correspondence analysis regression; Best modern analogue
Fog Lake, N. Cumberland Peninsula, Baffin Is.	Pollen	3 to 4			(Fréchette et al., 2006)	Stratified LIG lacustrine sediment. Correspondence analysis regression; Best modern analogue
Fog Lake, N. Cumberland Peninsula, Baffin Is.	Chironomids	7±2			(Francis et al., 2006)	Stratified LIG lacustrine sediment. Weighted averaging

Table 1 (*continued*)

	Proxy	ΔT (°C) Summer	ΔT (°C) Winter	Ppt	Reference	Comments
Brother of Fog Lake N. Cumberland Pen Baffin Is.	Pollen	4			(Fréchette et al., 2006)	Stratified LIG lacustrine sediment. Correspondence analysis regression; Best modern analogue
Brother of Fog Lake N. Cumberland Pen Baffin Is.	Chironomids	8±2			(Francis et al., 2006)	Stratified LIG lacustrine sediment. Weighted averaging
Flitaway Beds, Isortoq Beds, Central Baffin Is.	Insects, plant remains	4 to 5			(Morgan et al., 1993)	Originally thought to be LIG, then assigned to Plio-Pleistocene because estimated temperatures so warm; now likely to be LIG
Greenland						
NGRIP, Central Greenland	$\delta^{18}O$, δD	5			(North Greenland Ice Core Project members, 2004)	Ice core, Greenland Ice Sheet
Renland, E Greenland	$\delta^{18}O$, δD	5			(Johnsen et al., 2001)	Ice core, Renland Ice Cap
Jameson Land, East Greenland	Pollen, plant macrofossils, beetles, other invertebrates	5			(Bennike and Böcher, 1994) (Funder et al., 1998) (Bennike and Weidick, 2001)	Birch woodland present; none today.
Thule, NW Greenland	Pollen, chironomids	4			(Kelly et al., 1999)	
Labrador Sea	Pollen, spores				(Hillaire-Marcel et al., 2001)	ODP site 646: Pollen in LIG Lab Sea sediments indicate that southern Greenland must have been free of inland ice

accompanied by dramatic precipitation changes (Koerner, 2006). Summer temperature is also the most effective predictor for most biological processes, although seasonality and moisture availability may influence phenomena such as evergreen vs. deciduous biotic dominance (Kaplan et al., 2003). For these reasons, we focus our reconstructions on peak summer warmth during the LIG, a strategy adopted for other time periods in the Arctic (e.g the Holocene (Kaufman et al., 2004), and the past 400 years (Overpeck et al., 1997)). Terrestrial climate is reconstructed from diagnostic assemblages of biotic proxies preserved in lacustrine, peat, alluvial, and marine archives and isotopic changes preserved in ice cores and marine and lacustrine carbonates. Quantitative reconstructions of climatic departures from the present-day are derived from range extensions of individual taxa, mutual climatic range estimations based on groups of taxa, and analogue techniques. Estimated winter temperatures, and hence seasonality are well constrained for Europe, but poor for most sectors; likewise, precipitation estimates are limited to qualitative estimates in most cases, and are not available for most regions.

4. Regional summaries (Tables 1 and 2)

4.1. NW Europe

Although well outside of the Arctic, we include the LIG in NW Europe because it has the most detailed terrestrial record of the LIG (see Kaspar et al., 2005 for a review of sites), where a characteristic and remarkably uniform vegetational succession characterizes most of the region (Zagwijn, 1996; Guiter et al., 2003; Kühl and Litt, 2003). Annually laminated lacustrine sediments in Germany suggest that the LIG persisted for 10,000–12,000 years (Müller, 1974; Frenzel and Bludau, 1987; Hahne et al., 1994; Caspers, 1997). Mean July temperatures were 2–3 °C above present in the UK, and about 2 °C above present on the continent, with considerable spatial variability (Aalbersberg and Litt, 1998; Kaspar et al., 2005) . The widespread occurrence of *Hippopotamus* and the water tortoise *Emys orbicularis* in Britain supports these reconstructions (Turner, 2000). Boreal spruce forest spread north of its Holocene limit, and birch forest likely reached to the shores of the Arctic Ocean in Finish Lapland

Table 2
Published sites with quantitative summer sea surface temperature estimates for peak LIG warmth from marine sites around the circum-Arctic. Details of site location and reconstruction techniques are provided in the references cited. Some key cites with important qualitative summer SST information are also included

Site	Proxy	ΔT (°C) Smr SST	ΔT (°C) Wntr SST	Ppt	Reference	Temp. reconstruction technique	Comments
Svalbard	Mollusks, foraminifera	2 to 2.5			(Mangerud et al., 1998) (Miller et al., 1989) (Sejrup et al., 2004)	Faunal range extensions	
North Atlantic	Foraminifera				(McManus et al., 2002)		
JPC8: 61°N	Planktic forams	3 to 4			(Cortijo et al., 1999)	Modern analog	
NA87-25 52°N	Planktic forams	1 to 2			(Cortijo et al., 1999)	Modern analog	
CH69-K9 41°N	Planktic forams	-1			(Cortijo et al., 1999)	Modern analog	
SU90-03 40°N	Planktic forams	0±1			(Cortijo et al., 1999)	Modern analog	
M23414 53.5°N	Planktic forams; Mg/Ca	up to 2			(Kandiano et al., 2004)	Mg/Ca & Faunal	
European Russia	Mollusk, foraminifera	3 to 4			(Funder et al., 2002) (Grøsfjeld, et al., 1996, and references in Svendsen et al., 2004)		LIG "Boreal Transgression" brought Atlantic water along Russian coast from White Sea to eastern Taimyr.
West and central Siberia	Mollusk, foraminifera,		4 to 8		(Troitsky, 1964) (Funder et al., 2002)		
North coast Alaska	Mollusks in beaches, isotopes in mollusks, ostracodes in off shore marine sediments; Beach morphology	3			(Brigham-Grette and Hopkins, 1995) (Brigham-Grette et al., 2001) (Khim et al., 2001)		Sea ice reduction by 800 km; Atlantic water at much shallower depths (30 to 50 m) than in the Holocene (>200 m).
Bering Sea	Mollusks, beach morphology				(Brigham-Grette and Hopkins, 1995)		Sea ice did not occur South of Kotzebue
Arctic Ocean Gateways/Marginal Seas PS2138: 81°N PS2741: 81°N PS2471: 79°N PS2757: 81°N	Coccoliths, dinocysts, benthic forams				(Matthiessen et al., 2001a, b) (Matthiessen and Knies, 2001) (Svendsen et al., 2004)		High influx of Atlantic water through the Nordic Seas into the Arctic Ocean; At least as warm or warmer than present. Boreal mollusks along Russian Arctic coast to Taimyr.
Nordic Seas	Planktic foraminifera				(Sejrup et al., 1995)		
North Nordic Seas	Planktic forams	<0			(Bauch et al., 1999)		
Denmark Shelf	Benthic forams	1.5 to 2			(Seidenkrantz, et al., 2000) (Rasmussen et al., 2003b)		
SW Norway	Benthic forams	1 to 2 greater			(Sejrup et al., 2004)	WA-PLS	
Heat flux to Nordic Seas					(Fronval et al., 1998)		
Central Arctic Ocean	Foraminifera, nanofossils				(Spielhagen et al., 2004)		Abundant planktic fossils in Lomonosov

Table 2 (*continued*)

Site	Proxy	ΔT (°C) Smr SST	ΔT (°C) Wntr SST	Ppt	Reference	Temp. reconstruction technique	Comments
					(Jakobsson et al., 2003) (Svendsen et al., 2004)		Ridge cores imply seasonally open waters or common leads in the eastern and central Arctic Ocean.
Labrador Sea	Foramifera				(Rasmussen et al., 2003a)		Continuous ventilation through LIG
Labrador Sea	Dinocysts, foraminifera				(Hillaire-Marcel et al., 2001)		No ventilation in LIG
Thule, West Greenland	Mollusks, foraminifera	Warmer			(Funder, 1990) (Kelly et al., 1999)		Shallow-water raised marine sediment.
Jameson Land, East Greenland	Mollusks, foraminifera	2 to 3			(Funder et al., 1998)		Vigorous advection of Atlantic water into coastal regions

(Saarnisto et al., 1999). LIG January anomalies were small over most of Europe, but increased to the east and north, where temperatures 4–7 °C higher than present are reconstructed for the LIG (Kaspar et al., 2005).

4.2. Russia

Syntheses of fossil pollen data and other proxy evidence have been used to produce continental-scale reconstructions of vegetation, soils, and climate during the LIG in the Russian Federation (Grichuk, 1984; Velichko et al., 1991; Lozhkin and Anderson, 1995; Velichko et al., 1998; Zelikson et al., 1998). A difficulty with many of the sites used in these syntheses is that sedimentary deposition from LIG to present is not continuous, and a LIG age for a specific horizon is largely derived from stratigraphic position. Nevertheless, we can surmise with reasonable confidence that the northern forest ecosystems underwent dramatic poleward expansions (Fig. 2).

Forests reached the Arctic Ocean coast across most of the European sector (Grichuk, 1984; Morozova et al., 1998). In western Siberia, the boreal forest (e.g., Siberian spruce (*Picea obovata*), Siberian fir (*Abies sibirica*), Siberian stone pine (*Pinus sibirica*)) was displaced northward by as much as 400 km, and arctic tundra and forest-tundra was likely eliminated from the landscape (Arkhipov and Volkova, 1994). Southern areas of the conifer-dominated forest included broadleaf species (e.g., linden (*Tilia*), elm (*Ulmus*), oak (*Quercus*)), which are characteristic of more southern boreal forest today.

LIG sites are rare in Eastern Siberia; consequently, the character of LIG climate in this region is not well documented. Grichuk (1984) suggested that dark coniferous forest possibly extended from the Yenisei valley eastward to the middle Lena and Aldan basins during the LIG. Light coniferous forest occupied areas north of ~64 °N, extending nearly to the coast. A narrow band of coastal forest-tundra was limited to the vicinity of the Lena delta, continuing slightly to the west.

Forest dominated the vegetation of northeastern Siberia during the peak of the LIG (Lozhkin and Anderson, 1995). Light coniferous forest migrated ~600 km northward, eliminating coastal tundra. The forest also moved a similar distance eastward into areas of Chukotka that are now shrub tundra. Tree birch formed forests in parts of Chukotka, representing northward range extensions of ~1000 (*Betula ermani*) to ~600 km (*Betula cajanderi*). Like today, the interior of Northeast Siberia supported Dahurian larch (*Larix dahurica*) forest, but in contrast to the modern forest, Siberian spruce, Siberian stone pine, and tree alder (*Alnus hirsuta*) were also present. The establishment of Siberian spruce and pine in the upper Kolyma and Indigirka drainages suggest range extensions of 700–800 km. As compared to the modern vegetation, the LIG forests along the northern coast of the Okhotsk Sea contained more tree birch and temperate trees, representing range extensions of up to 1000 km.

The LIG is well represented in the pollen spectra extracted from a sediment core from Lake El'gygytgyn, northern Siberia, within a continuous record of vegetation change over the past 300,000 years (Lozkhin et al., 2006). Although larch pollen is absent in the LIG spectra, climate reconstructions based on statistical comparisons to modern pollen assemblages suggest that summer temperatures were sufficiently warm to support this tree, which is greatly under-represented in pollen records. Such an interpretation is consistent with other studies that suggest an extensive northward displacement of boreal taxa, with open *Betula* forest-tundra and *Larix-Pinus pumila* forest established in northeastern Chukotka (Lozhkin and Anderson, 1995).

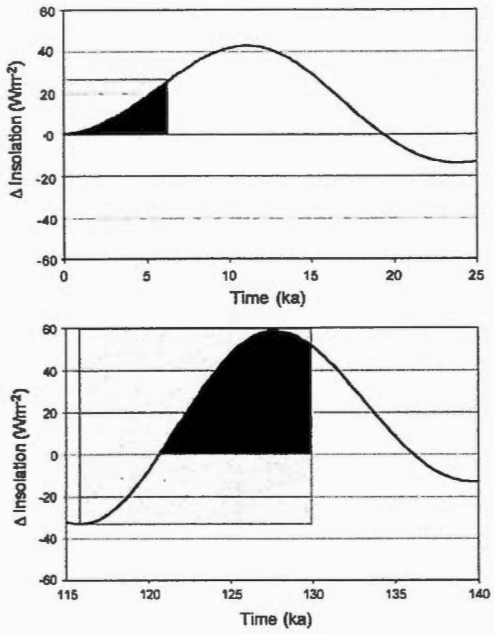

Fig. 2. Mean summer (M, J, J) insolation anomalies ($W m^{-2}$) expressed as the departure from present at 65°N from 25 ka to present (upper panel) and from 140–115 ka (lower panel). The region where summer insolation was above present and sea level at or above present is shown by solid black fill, whereas the duration of the interglacial, defined as the time when sea level is at or above present, is shown by the hachured box. The larger magnitude and duration of the LIG insolation anomaly relative to the Holocene anomaly results from the combination of a greater LIG insolation anomaly and early penultimate deglaciation.

Furthermore, it is likely that *Betula*, *Alnus*, and possibly *Salix* occurred in large growth forms (trees or tree-sized shrubs).

In summary, the LIG plant communities represent individual range extensions of as much as 1000 km.The western boreal forest contained considerably more birch than does the present-day boreal forest and broadleaf taxa such as hornbeam (*Carpinus*) were found north and east of their modern distributions in European Russia. Dahurian-larch dominated northern boreal forests in northeastern Siberia as is the case today, but in some regions Siberian stone pine, Siberian spruce, and tree alder were important constituents of the light coniferous forest.

Climate estimates based on these floristic differences suggest summer temperatures 0–2 °C above present along the present southern boreal forest belt, 5–8 °C higher than present across central Siberia, and 4–8 °C above present in NE Siberia. Where winter temperatures can be reconstructed, almost all sites indicate milder temperatures, despite reduced winter insolation, suggesting reduced sea ice more than compensated for lower winter insolation. The Lake El'gygytgyn pollen data suggest that maximum summer warmth was 2–4 °C above present and winters were warmer than present (Lozhkin et al., 2006). The Lake El'gygytgyn record also suggests a rapid increase in tree and shrub taxa during the early part of the LIG, where the proportion of tree and shrub pollen rises from 10% to over 90% in a period of what appears to be a few centuries based upon the current chronological control.

4.3. Alaska

Several stratified sites north and west of modern tree line in Alaska document the extension of forest into regions dominated by tundra throughout the Holocene, although LIG ecotonal shifts were not as great as for the Eurasian north. Summer warmth during the LIG is estimated to have been 0–2 °C above present, but winters were 1–3 °C below present. There is a consistent signal for greater moisture at Alaskan sites, but summer temperature increases over present were small compared with other sectors; spatial gradients between the interior and the north and west may have been shallower.

Continuous lacustrine sections through the LIG and fossils in other LIG deposits show establishment of spruce forest at sites in the north and west of Alaska that lie beyond spruce limits characteristic of the Holocene, although tree line displacements were not as great as for the Eurasian north (Brigham-Grette and Hopkins, 1995). Sedimentation at Squirrel Lake, NW Alaska, was continuous from MIS 6 through to the present. Temperature estimates using the modern analogue technique on pollen assemblages in LIG beds at Squirrel Lake indicate a modest (1–2 °C) increase in mean July temperature (Anderson, 2005). The temporal sequence indicates that warming occurred early and rapidly and that high moisture levels were attained early in the interglacial. Pollen from LIG levels in Ahaliorak Lake suggests that mean January temperatures were 1–3 °C cooler and annual precipitation slightly higher than modern (Eisner and Colinvaux, 1990). Fossil beetle assemblages from NW Alaska suggest summer temperatures similar to, or 1–2 °C warmer than present, and winter temperatures similar to, or 1–2 °C colder than present (Edwards et al., 2003). In interior Alaska, LIG deposits are related to the stratigraphic marker of the Old Crow tephra (Hamilton and Brigham-Grette, 1991). A LIG forest bed and paleosol near Fairbanks that contains spruce needles and pollen indicating summers as warm as present also contains spores and chemical weathering characteristics suggesting conditions considerably wetter than present (Péwé et al., 1997; Muhs et al., 2001).

4.4. Arctic Canada

Although tundra remained dominant over much of far northern Canada during the LIG, pollen, macrofossil and

insect data indicate warmer-than-present summers in the Queen Elizabeth Islands (Matthews et al., 1986). Boreal forest advanced to the Arctic Ocean coast in the NW of mainland Canada (Rampton, 1988) and north of its present position in the Hudson Bay region (Nielsen et al., 1986; Dredge et al., 1990; Mott and Dilabio, 1990; Wyatt, 1990), changes that require only modest warming. In contrast, four stratified LIG lacustrine sequences from the eastern Canadian Arctic that capture the LIG document summer temperatures 4–8 °C above present (Table 1). For two nearby lakes (Fog, Brother-of-Fog), LIG summer temperatures are independently reconstructed from pollen and chironomid analyses from the same sediment cores. From Fog Lake, pollen indicates peak LIG summer temperatures 3–5 °C above present, whereas chironomids indicate 7 ± 2 °C above present. At Brother-of-Fog Lake, pollen indicates 3–4 °C warmer, and chironomids indicate 8 ± 2 °C warmer than present (Francis et al., 2006; Fréchette et al., 2006). Collectively, the proxy data indicate a LIG summer temperature 4–7 °C above present. Pollen data are also available from two other LIG lakes (Amarok (Fréchette et al., 2006) and Robinson (Miller et al., 1999; Fréchette, 2005) lakes), both suggesting LIG summers ca 5 °C warmer than present. A probable LIG site in central Baffin Island contains plant and insect remains indicating summer temperatures 4–5 °C above present (Morgan et al., 1993). Shallow-water marine records of probable LIG age are common along the Baffin Island coast, and contain extralimital southern invertebrates indicative of a greater flux of Atlantic Water into Baffin Bay and reduced summer sea ice (Miller, 1985), although the chronologies for the marine sites are less certain than for the terrestrial sites and SSTs have not been quantified.

The absence of any ice older than the LIG at the base of the larger Canadian ice caps indicates they melted completely during the LIG, only to reappear when climate deteriorated during the transition into the ensuing glacial period (Koerner and Fisher, 2002). Many of these ice caps survived the warm early Holocene period but have negative balances today and would again disappear if the present warm period persisted. However, the time to melt all ice in Arctic Canada (several millennia) almost certainly is longer than that which could be maintained by the effects of anthropogenically produced greenhouse gases.

4.5. Greenland

Terrestrial LIG conditions over Greenland are defined from ice-core and biological proxies. A rich and diverse assemblage of bryophytes, vascular plants, beetles and other invertebrates from terrestrial and shallow marine LIG localities along central East Greenland indicate summers 5 °C warmer than present (Bennike and Böcher, 1994). Extensive birch forests are inferred, suggesting an ice-free southern Greenland. Pollen and spores from LIG levels in a core from the Labrador Sea off SW Greenland also suggest that adjacent southern Greenland was free of inland ice, with a sub-arctic or even temperate climate (Hillaire-Marcel et al., 2001). Extralimital southern taxa found in LIG beds at Thule, NW Greenland, require summer temperatures at least 4 °C warmer than present (Bennike and Böcher, 1992; Kelly et al., 1999).

Two ice cores from Greenland capture undisturbed LIG layers, NorthGRIP (North Greenland Ice Core Project members, 2004) and Renland (Johnsen et al., 2001), although neither extends through the LIG and into the preceding glacial period. Ice-isotopes in LIG layers from both cores indicate that the LIG was 5 °C warmer than present. The impact of warmer summers on the dimensions of the Greenland Ice Sheet remains debated. The absence of a continuous record of undisturbed ice through the LIG, and the discordance between ice isotopes in the older portions of cores from DYE-3 and Camp Century relative to the benchmark Summit and NorthGRIP cores, suggest that significant reduction in the ice sheet may have occurred, with both Camp Century and DYE-3 ice free in the LIG (Koerner, 1989; Koerner and Fisher, 2002). Total gas evidence from Eemian ice in the GRIP ice core indicates that the Summit region may have been up to 500 m lower than present at some time in the LIG (Raynaud et al., 1997). Ice-sheet modeling (Cuffey and Marshall, 2000; Otto-Bliesner et al., 2006) suggests that the Greenland Ice Sheet may have been reduced by as much as half its current volume during the LIG, including the loss of its southern dome, whereas the northern dome is modeled to remain within 700 m vertically of its current elevation (Otto-Bliesner et al., 2006), implying an ice sheet with a much steeper profile.

The ice core data has also been used to make a case for a relatively stable Greenland Ice Sheet through the LIG. LIG ice is present in all deep ice cores from Greenland, and this ice has $\delta^{18}O$ values ca 3‰ heavier than typical Holocene $\delta^{18}O$ values in the same cores (except DYE-3; North Greenland Ice Core Project members, 2004). This constant isotopic offset has been used to suggest that the ice sheet was not dramatically smaller in the LIG than in the Holocene, with the southern dome remaining intact through the LIG, although somewhat thinner (North Greenland Ice Core Project members, 2004). Regardless of the exact configuration of the Greenland Ice Sheet, all interpretations of the ice core data indicate LIG temperatures 5 °C above present.

4.6. Arctic ocean

The Arctic Ocean remains the least understood ocean basin; access is difficult and many standard climate proxies are compromised by dissolution and meltwater overprinting, especially in the central Arctic Ocean basin where even the development of reliable geochronologies has been a challenge (Jakobsson et al., 2003; Backman et al., 2004). The LIG is usually identified by a combination of coccoliths, low IRD, and increased biological productivity.

Direct solar insolation, river runoff, sea level, and the intensity and pattern of North Atlantic Drift (NAD) inflow are expected to be the dominant determinants of surface water characteristics in the Arctic Ocean during the LIG. Concerted efforts over the past decade have led to the recovery of high-quality sediment cores from the Arctic Ocean, and improvements in their geochronology and the interpretation of environmental proxies extracted from the sediment. This has led the way to an emerging consensus view of the LIG, especially in the marginal seas, with significant improvements in our understanding of the central interior (Spielhagen et al., 2004).

A stronger flux of warm, salty Atlantic water into the Arctic Ocean started early in the LIG (Matthiessen et al., 2001b; Wollenburg et al., 2001). This influx led to greatly reduced sea ice in the marginal seas (Knies and Vogt, 2003), although not all core sites support this interpretation. Site-to-site differences in LIG surface water characteristics may indicate changing trajectories of Atlantic Water currents between the Holocene and the LIG, and even within the LIG; Additional uncertainties may be related to changes in carbonate dissolution rates (see discussions in Matthiessen et al., 2001b). Seasonal increases in primary productivity in ice-free areas and along extensive leads supported a more diverse and abundant nano- and micro-fauna (Gard and Backman, 1990; Matthiessen et al., 2001a; Matthiessen and Knies, 2001; Wollenburg et al., 2001). The increased flux of Atlantic water reduced the vertical stratification over many of the marginal seas, allowing Atlantic water to remain closer to the surface than in the Holocene. Atlantic surface water characterized the Arctic coast of Russia from the White Sea to eastern Taimyr, 2000 km farther east and 3–4 °C warmer than in the Holocene (Funder et al., 2002; Grøsfjeld et al., in review; Svendsen et al., 2004). Delayed winter sea ice formation along the Eurasian coast would have led to significant warming of the winter atmosphere, despite negative winter insolation anomalies at that time. This may help to explain the maintenance of boreal forest far north of its current position across Eurasia during the LIG. Conifer trees are sensitive to extreme winter cold, which would have been mitigated by reduced coastal-zone sea ice.

LIG beaches along northern Alaska contain southern extralimital mollusk taxa indicative of SST 3 °C above present, and extensive storm beaches that require sea ice reduction by 800 km in winter (Brigham-Grette and Hopkins, 1995).

Although the status of sea ice over much of the central Arctic Basin is still debated, the available data suggest that sea ice remained through the summer in the central basin, possibly as far as NE Svalbard throughout the LIG (Spielhagen et al., 2004). On the other hand, relatively high concentrations of planktonic foraminifera and the presence of coccoliths in LIG levels of cores from the Lomonosov Ridge, central Artic Ocean, suggest that seasonally open waters or extensive leads characterized the eastern and central Arctic Ocean during portions of the LIG (Svendsen et al., 2004).

4.7. Nordic seas

Identification of the LIG is more secure for the Nordic Seas than for the Arctic Ocean. Standard marine isotope stages can be recognized by diagnostic patterns of $\delta^{18}O$ in benthic foraminifera, although with some meltwater overprinting during the deglaciations (Bauch et al., 1996; Fronval et al., 1998), supported by the occurrence of Icelandic tephra during the LIG (Sjoholm et al., 1991), low levels of IRD, and increased concentrations of sub-polar faunal and floral species reflecting a northward displacement of the Polar Front. During the past 150 ka, only the Holocene and the LIG show evidence of a strong and sustained incursion of Atlantic Water into the Nordic Seas (Kellogg, 1980). Higher LIG SST characterize the Scandinavian coast well into Arctic Russia (Mangerud et al., 1981; Raukas, 1991; Velichko et al., 1991; Funder et al., 2002), suggesting warm North Atlantic current close to the coast of Norway, extending well into the Eurasian coast of the Arctic Ocean. Cores from the southwestern Nordic Seas, along the coast of E. Greenland and western Svalbard, south of Jan Mayen, and in northern Baffin Bay indicate LIG SST above those of the Holocene (Miller et al., 1989; Mangerud and Svendsen, 1992; Sejrup et al., 1995; Funder et al., 1998; Bauch et al., 1999; Kelly et al., 1999), but this difference is not reflected in many cores from the eastern Nordic Seas. An alternative position is that Eeman SSTs in the Nordic Seas were lower than during the Holocene (Bauch et al., 1999). Conflicting interpretations of SSTs in the Nordic Seas during the Eemian and Holocene could be related to the manner by which different proxies respond to changing water masses, within-interglacial variability at millennial- to submillennial-scales that complicates the interpretation of low-resolution records, or changes in the precise thread of warm, salty North Atlantic water as it moved through the Nordic Seas into the Arctic Ocean. Although some Atlantic surface water was routed through the Baltic into the White Sea early in the LIG, the capacity of this connection was not sufficient to have an impact on the general surface circulation, and isostatic emergence severed the passage ca 3000 yr into the LIG (Funder et al., 2002). The evidence from the Arctic Ocean (above) necessitates a greater dominance of Atlantic water at the surface of the Arctic Ocean. This could be accomplished by some combination of intensified NAD, stronger surface water mixing in the Arctic Ocean, or reduced freshwater runoff; an intensified flux of Atlantic water into the Arctic Ocean must have come through the Nordic Seas.

4.8. Sub-polar North Atlantic

Conditions in the sub-polar North Atlantic are relevant to the transfer of energy between low and high latitudes.

North Atlantic SSTs were stable and similar to, or up to 2 °C higher than present throughout the LIG (Bauch et al., 2000); SSTs warmer than for the Holocene are most apparent in the eastern North Atlantic at ca 50 °N. The strength of deepwater production appears to have been similar to present (Adkins et al., 1997; Hall et al., 1998; Lehman et al., 2002; McManus et al., 2002; Backman et al., 2004), although there are few reliable quantitative proxies of past deep-water production rates.

5. Discussion

5.1. The Arctic at peak LIG warmth

All sectors of the Arctic register summers warmer than present during the LIG, but the magnitude of warming exhibits spatial variability (Fig. 3). The greatest positive summer temperature anomalies occur around the currently arctic regions of the Atlantic sector, where summer warming was typically 4–6 °C. This anomaly extends into Siberia, where summer temperature anomalies were 4–8 °C, presumably due to the impact of strong insolation forcing over a large continent supplemented by the penetration of Atlantic water well into the Arctic Ocean along the Russian coast. The anomalies decrease from Siberia westward to the European sector (0–2 °C), and eastward toward Beringia (2–4 °C). The Arctic coast of Alaska indicates warmer SST (3 °C) and considerable summer sea ice reduction, but much of interior Alaska registers small anomalies (0–2 °C) that probably extend into western Canada, although quantitative data to evaluate this trend is scarce. In contrast, northeastern Canada and Greenland register summer temperature anomalies of at least 5 °C. The Arctic Ocean records greater advection of warm, salty Atlantic water through the Nordic Seas, although Atlantic water did not dominate surface waters of the central Arctic Ocean. Surface waters were warmer in the LIG than at any time in the Holocene in Baffin Bay and along the north coast of Alaska, where sea ice was also much retracted.

Precipitation and winter temperatures are more difficult to reconstruct for the LIG than are summer temperatures. In northeast Europe, the later part of the LIG was characterized by a marked increase in winter temperatures. A large positive winter temperature anomaly is seen also in Russia and western Siberia, although the timing is not as well constrained (Troitsky, 1964; Gudina et al., 1983; Funder et al., 2002). Precipitation is more difficult to quantify, but most sectors with qualitative estimates indicate wetter conditions than in the Holocene.

Despite some uncertainty in the SSTs of the Nordic Seas during the LIG, the general consensus is that there must have been a greater flux of Atlantic water through the Nordic Seas into the Arctic Ocean. The precise path this flow followed may have differed from the present route, especially early during the LIG when the marginal shelves had yet to recover from isostatic depression under the MIS 6 ice sheets. From the pattern of LIG SSTs, the eastern branch of the Norwegian Current intensified and reached

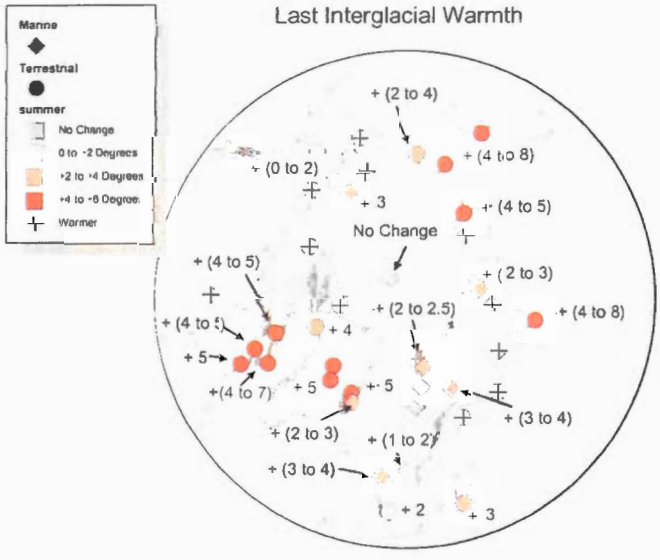

Fig. 3. Polar projection showing regional maximum LIG summer temperature anomalies relative to present derived from paleotemperature proxies (derived from Tables 1 and 2). Terrestrial sites in circles, marine sites in squares.

the White Sea region already a few centuries into the LIG (Mangerud et al., 1998; Grøsfjeld et al., in review). The western branch may have followed a path different than present, but reached the East Greenland coast early in the LIG (Funder et al., 1998). As isostatic recovery progressed, the trajectory of the NAD likely evolved through the LIG. The increased poleward transfer of Atlantic water implies a larger production of deepwater, currently estimated to be about 15 Sv ($10^6 m^3 s^{-1}$), but no quantitative LIG estimates are available. Alternatively, the greater influx of Atlantic water may have been countered by a greater outflow of surface water from the Arctic Ocean, which could have changed the position of the Polar Front in the Nordic Seas (Fronval et al., 1998).

Several sites suggest that the transition into the LIG was rapid, with peak warmth early in the interglaciation. Although not all Arctic LIG sites offer sufficient resolution to evaluate the pattern of warming during the LIG, those that do exhibit rapid warming to a peak temperature near the beginning of the LIG. The pattern of rapid initial warming, followed by slow cooling is mirrored in all four Antarctic ice cores that sample the LIG (Byrd, Vostok, Dome Fuji, and Dome C (Johnsen et al., 1972; Petit et al., 1999; Watanabe et al., 2003; EPICA Community Members, 2004), despite negative summer insolation forcing in the Southern Hemisphere at this time. The apparent concordance of Antarctic ice core and Northern Hemisphere summer temperature records suggests that the oceans may have transferred Northern Hemisphere warmth into the Southern Hemisphere.

5.2. *Why was the LIG in the Arctic so warm?*

Arctic summers during peak LIG warmth were 5 °C above present over most of the region, considerably higher than during the Holocene thermal maximum (Kaufman et al., 2004). The pattern and magnitude of LIG summer temperature anomalies in the Arctic is largely related to four phenomena: (1) strong summer insolation forcing, (2) optimal phasing of penultimate deglaciation in relation to the orbitally controlled insolation maximum, (3) increased meridional heat transport through the Nordic Seas into the Arctic Ocean, and (4) strong positive feedbacks associated with changes in sea ice, land ice and snow cover, and the poleward expansion of boreal forests.

A strong positive summer insolation anomaly across the Northern Hemisphere through the first half of the LIG is the dominant forcing that explains the observed Arctic warmth. Average LIG summer (M, J, J) insolation anomalies are positive in the Arctic from ca 138 until ca 121 ka, with anomalies between 131 and 127 ka much larger than at any time in the Holocene (Fig. 1). Peak LIG summer insolation at the top of the atmosphere across the Arctic (60–90 °N) was ca 13% higher than present, whereas it was ca 9% higher at the peak Holocene anomaly, 11 ka (Fig. 4). In most regions, LIG summer temperatures were well above those of the Holocene thermal maximum, consistent with greater LIG insolation forcing. However, the reconstructed thermal response of the Arctic at peak Holocene insolation forcing 11 ka (CAPE Project Members, 2001), and at the ice-volume minimum 6 ka (Bigelow et al., 2003) was, by comparison, muted. Tree line advances were modest and relatively short-lived in most sectors, and temperature anomalies at the Holocene thermal maximum were also modest (ca 1.6 °C; Kaufman et al., 2004).

The weaker thermal response of the Arctic in the Holocene is only partly explained by the insolation anomaly differences; phasing of deglaciation also must be important. A rigorous evaluation of all uranium-series dates on corals from stable platforms confirms that sea level reached modern levels (global ice volume similar to present) by 130±2 ka (summarized in Overpeck et al., 2006). LIG summer (M, J ,J) insolation at the top of the atmosphere peaked between 131 and 127 ka (Fig. 1). Because the penultimate (MIS 6) ice sheets disappeared (sea level at or above present) by 130 ka, the full magnitude of the summer insolation anomaly was available to heat the Northern Hemisphere, rather than to melt residual ice sheets. This contrasts with the Holocene, when peak Northern Hemisphere insolation occurred 5 ka before the Northern Hemisphere ice sheets had melted and sea level attained modern levels (6 ka; Fig. 2). Consequently, during early Holocene peak summer insolation, much of the insolation anomaly was consumed in the melting of residual ice sheets, rather than heating the land/ocean/atmosphere, dampening the climate response to insolation forcing (Koerner, 1989; Bigelow et al., 2003; Kaplan et al., 2003; Vavrus and Harrison, 2003). By the time sea level reached present in the Holocene (6 ka), the high latitude Northern Hemisphere summer (M, J, J) insolation anomaly was ca 15 Wm^{-2}, whereas at the comparable time in the LIG (130 ka) it was ca 45 Wm^{-2}, three times as large.

Changes in oceanic surface currents may explain some of the LIG spatial variability across the Arctic. Although the insolation anomaly is symmetric about the Arctic, the expansion of forest ecotones north of their northernmost Holocene limits is most pronounced in Eurasia, and less so in Alaska, and central and northwestern Canada. A plausible explanation for this asymmetry is the increased flux of warm Atlantic surface waters northward around the Eurasian Arctic. Atlantic water along the Arctic coast of Russia would have limited the formation of sea ice, minimizing extreme winter cold, which is a strong deterrent to poleward expansion of evergreen trees. The flux of Atlantic water may have also influenced climate by steering relatively warm air masses into the Eurasian North.

The magnitude of LIG summer warmth observed across the Arctic is not mirrored by comparable warmth at lower Northern Hemisphere latitudes, despite similar forcing. Peak LIG summer insolation anomalies averaged only slightly below the Arctic (60–90 °N) values at low (0–30 °N; 20% less) and mid (30–60 °N; 10% less) latitudes. Although hemispheric summaries of LIG summer temperature anomalies have not been compiled, the available

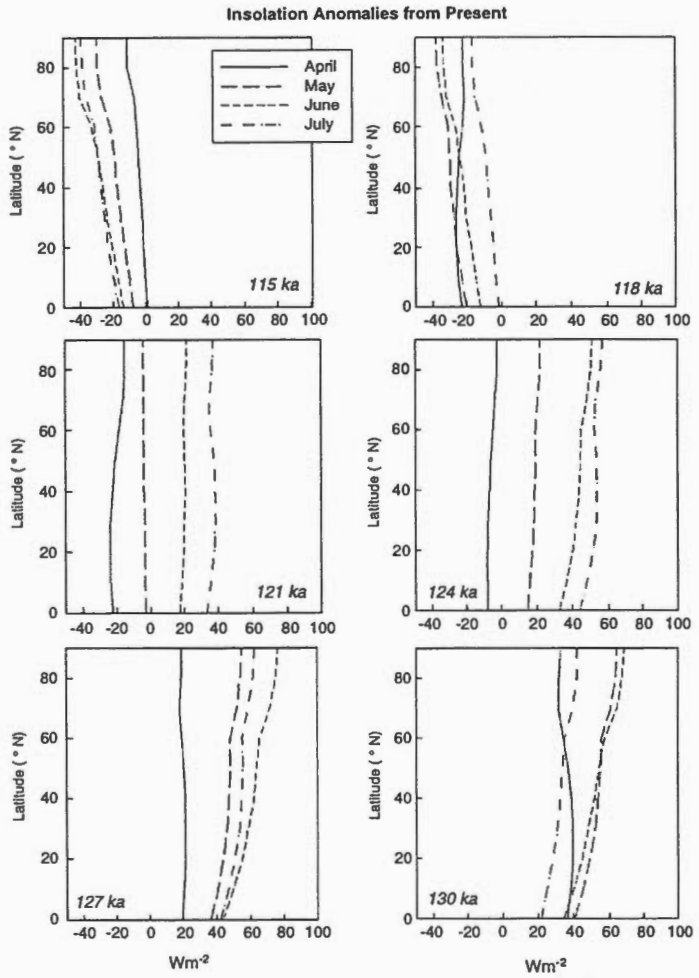

Fig. 4. Insolation anomalies expressed as a percentage deviation from present for the months of April (blue), May (red), June (yellow), and July (green), plotted against Northern Hemisphere latitude every 3 ka from 130–115 ka, showing the evolution of the insolation anomaly through the LIG, and its latitudinal gradient (data from Berger and Loutre, 1991).

records suggest that peak LIG warmth at mid- and low-latitudes in the Northern Hemisphere was between 0–2 °C above present.

The greater thermal response of the Arctic in the LIG than at lower latitudes cannot be explained easily by the modest latitudinal gradients of LIG summer insolation forcing (Fig. 4). The most likely explanation for this discrepancy is the strong positive feedbacks associated with reduced sea ice/snow cover and the expansion of boreal forests. Increased summer insolation and the poleward transport of heat by ocean currents led to reduced sea ice in the Arctic Ocean and its marginal seas. Positive feedbacks associated with reduced sea ice in both summer and winter would have amplified primary insolation forcing. The replacement of tundra with boreal forest across much of the Arctic landscape would have decreased its albedo, providing another strong positive feedback that would amplify Arctic warming (Chapin et al., 2005; Serreze and Francis, 2006).

We postulate that the cumulative effect of positive feedbacks from reduced sea ice, reduced permanent land ice, reduced seasonal snow cover and the expansion of

boreal forests northward, coupled with increased meridional heat transport by oceanic surface currents and the atmosphere, amplified the modest LIG summer insolation gradient to produce the substantially stronger thermal response seen in the Arctic relative to lower latitudes in the Northern Hemisphere. Climate modeling of the LIG also underscores the importance of snow, ice and vegetation feedbacks that amplify insolation-driven Arctic warmth (Crucifix and Loutre, 2002; Otto-Bliesner et al., 2006).

6. Conclusions

Quantitative reconstructions of LIG summer temperatures suggest that much of the Arctic was 5 °C warmer during the LIG than at present, and that this warming occurred rapidly and reached peak warmth during the earliest portion of the interglaciation. Arctic sea ice was reduced to a greater extent in the LIG than during the early Holocene due to both greater summer insolation and the larger flux of relatively warm Atlantic surface water into the Arctic Ocean during the LIG than at any time in the Holocene. Changes in surface ocean characteristics influenced the planetary energy balance through ice-albedo feedback; reduced winter sea ice and increased ventilation rates impacted climate over adjacent lands, especially in winter. The magnitude and spatial gradients of LIG Arctic summer temperature anomalies are related to the timing and magnitude of the orbitally controlled summer insolation anomaly in conjunction with optimal phasing of penultimate deglaciation, increased meridional heat transport through the Nordic Seas into the Arctic Ocean, and strong positive feedbacks associated with reduced land ice and snow, retraction of sea ice and expansion of boreal forests.

Polar amplification of climate change is predicted by most climate models. However, the observational records of 20th century warming are not in perfect accord with model projections, an observation that has fed a lively debate (Serreze and Francis, 2006). During the 20th century, the planetary temperature increased 0.7 °C, whereas most regions of the Arctic record warming of 1–3 °C over the same interval (Serreze et al., 2000). But, most of the warming occurred in summer months, whereas model projections indicate winter warming should dominate. The paleoclimate record is more direct. The average planetary temperature depression during the peak of the last glacial maximum (ca 20 ka) is generally estimated to be 6 to 8 °C, whereas Arctic cooling, as measured by borehole temperatures in the Greenland Ice Sheet, was ca 25 °C (Cuffey et al., 1995; Dahl-Jensen et al., 1998). Our reconstructions of LIG Arctic warmth show similar anomalies, with summers averaging 5 °C warmer than present across most of the Arctic, whereas the Northern Hemisphere average summer temperature is estimated to be only 0–2 °C warmer than present, despite similar insolation forcing. These discrepancies are consistent with strong positive feedbacks in the Arctic that amplify primary insolation forcing.

A quantitative assessment of LIG Arctic summer temperatures informs projections of future greenhouse warming. Although LIG summer warmth is primarily the result of a peak summer insolation anomaly, the responses of land and sea ice, and vegetation, may have provided feedbacks that not only amplified summer warmth, but also contributed to winter warmth, counteracting, in part, negative forcing from negative winter insolation anomalies (Fig. 1). In contrast, projected greenhouse forcing does not exhibit seasonality and is predicted to increase both winter and summer temperatures. Warmer winters would contribute to the poleward migration of coniferous forest, and via earlier spring melting, accelerate summer snow and ice melting (Guetter and Kutzbach, 1986; Chapin et al., 2005). Thus, the pattern of warming may differ in the coming decades from those observed in the LIG. However, the strong thermal response of the Arctic to primary summer insolation forcing during the LIG suggests that future Arctic changes related to the continuing build up of greenhouse gases are likely to be much larger than at lower latitudes.

Acknowledgements

CAPE (Circum-Arctic PaleoEnvironments) is an activity within PAGES, a core program of the International Geosphere-Biosphere Program (IGBP), with a mandate to facilitate international syntheses of Arctic records of past environments. The CAPE Last Interglacial Workshop was held in coastal Maine, USA, in October 2002, at facilities operated by Bates College, Lewiston, Maine. We thank M. Retelle for facilitating local arrangements. Support for the workshop was provided by the US NSF through the PARCS (Paleoenvironmental Arctic Science) Program funded by OPP-ARCSS and ESH, as well as various national and international funding agencies that assisted in travel support for the participants. Critical reviews by Norbert Kuhl and an unidentified referee significantly helped to clarify the manuscript.

Appendix A. : CAPE Last Interglacial Project Members

Pat Anderson, Quaternary Research Center, University of Washington, Seattle, WA 98195-1310, USA.

Ole Bennike, Geological Survey Denmark, Copenhagen, Denmark.

Nancy Bigelow, Alaska Quaternary Center, University of Alaska, Fairbanks, AK, USA.

Julie Brigham-Grette, Department of Geosciences, University of Massachusetts, Amherst, MA 01003, USA.

Matt Duvall, Bates College, Lewiston, ME, USA.

Mary Edwards, School of Geography, University of Southampton, Southampton SO17 1BJ, UK.

Bianca Fréchette, GEOTOP, Université du Québec à Montréal, C.P. 8888, Succursale Centre-Ville, Montréal, Qué, Canada H3C 3P8.

Svend Funder: Geological Museum, University of Copenhagen, Ostervoldgade 5-7, Copenhagen, Denmark.

Sigfus Johnsen, University of Copenhagen, Copenhagen, Denmark.

Jochen Knies, Geological Survey of Norway, Trondheim, Norway.

Roy Koerner, Geological Survèy of Canada, Ottawa, Canada.

Anatoly Lozhkin, Far East Branch, Russian Academy of Sciences, 16 Portovaya St., Magadan 685000, Russia.

Shawn Marshall, Department Geography, University of Calgary, Calgary Canada T2N 1N4.

Jens Matthiessen, Alfred Wegener Institute for Polar and Marine Research, Columbusstrasse, Bremerhaven, 27568, Germany.

Glen Macdonald, Department of Geography, UCLA, Los Angeles, CA 90095-1524, USA.

Gifford Miller, INSTAAR, University of Colorado, Boulder, CO 80309-0450, USA.

Marisa Montoya, Potsdam Institute for Climate Impact Research, Potsdam, D-14412, Germany.

Daniel Muhs, U.S. Geological Survey, MS 980, Federal Center, Denver, CO 80225, USA.

Bette Otto-Bliesner: Climate Change Research, NCAR, Boulder, Colorado 80307, USA.

Jonathan Overpeck, Institute for the Study of Planet Earth, University of Arizona, Tucson, AZ 85721, USA.

Niels Reeh, Danish Technical University, Copenhagen, Denmark.

Hans Petter Sejrup, Department of Earth Science, University of Bergen, Allegt. 41, 5007 Norway.

Robert Spielhagen, GEOMAR, Department of Paleoceanology, Wischhofstrasse 1-3, 24148 Kiel, Germany.

Charles Turner, Department of Earth Sciences, The Open University, Milton Keynes, MK76AA, UK.

Andrei Velichko, Laboratory of Evolutionary Geography, Institute of Geography, Russian Academy of Sciences, Moscow 109017 Russia.

References

Aalbersberg, G., Litt, T., 1998. Multiproxy climate reconstructions for the Eemian and Early Weichselian. Journal Quaternary Science 13, 367–390.

Adkins, J.F., Boyle, E.A., Keigwin, L., Cortijo, E., 1997. Variability of the North Atlantic thermohaline circulation during the Last Interglacial period. Nature 390, 154–156.

Anderson, P.M., Brubaker, L.B., 1986. Modern pollen assemblages from northern Alaska. Review of Palaeobotany and Palynology 46, 273-291.

Andreev, A.A., et al., 2004. Late Saalian and Eemian paleoenvironmental history of the Bol'shoy Lyakhovsky Island, Laptev Sea region, Arctic Siberia. Boreas 33, 319–348.

Arkhipov, S.A., Volkova, V.S., 1994. Geological history, Pleistocene landscapes and climate in West Siberia. Russian Academy of Sciences, Siberian Branch: United Institute of Geology, Geophysics and Mineralogy, Novosibirsk (in Russian).

Backman, J., Jakobsson, M., Lovlie, R., Polyak, L., Febo, L.A., 2004. Is the central Arctic Ocean a sediment starved basin? Quaternary Science Reviews 23, 1435–1454.

Bauch, H.A., Erlenkeuser, H., 2003. Interpreting glacial-interglacial changes in ice volume and climate from subarctic deep water foraminiferal $\delta^{18}O$. In: Droxler, A.W., Poore, R.Z., Burckle, L.H. (Eds.), Earth's Climate and Orbital Eccentricity: The Marine Isotope Stage 11 Question. American Geophysical Union Monograph Series, Washington, DC, pp. 87–102.

Bauch, H.A., Erlenkeuser, H., Grootes, P.M., Jouzel, J., 1996. Implications of stratigraphic and paleoclimatic records of the Last Interglaciation from the Nordic Seas. Quaternary Research 46, 260–269.

Bauch, H.A., Erlenkeuser, H., Fahl, K., Spielhagen, R.F., Weinelt, M.S., Andruleit, H., Henrich, R., 1999. Evidence for a steeper Eemian than Holocene sea surface temperature gradient between Arctic and sub-Arctic regions. Palaeogeography, Palaeoclimatology, Palaeoecology 145, 95–117.

Bauch, H.A., Erlenkeuser, H., et al., 2000. Surface and deep water changes in the subpolar North Atlantic during termination II and the last Interglaciation. Paleoceanography 15, 76–84.

Begét, J.E., Keskinen, M.J., 2003. Trace-element geochemistry of individual glass shards of the Old Crow tephra and the age of the Delta glaciation, central Alaska. Quaternary Research 60, 63–69.

Begét, J.E., Edwards, M.E., Hopkins, D., Keskinen, M., Kukla, G., 1991. Old Crow tephra found at the Palisades of the Yukon, Alaska. Quaternary Research 35, 291–297.

Bennike, O., Böcher, J., 1992. Early Weichselian interstadial land biotas at Thule, Northwest Greenland. Boreas 21, 111–117.

Bennike, O., Böcher, J., 1994. Land biotas of the Last Interglacial/glacial cycle on Jameson Land, East Greenland. Boreas 23, 479–487.

Bennike, O., Weidick, A., 2001. Late Quaternary history around Nioghalvfjerds-fjorden og Jøkelbugten, North-East Greenland. Boreas 30, 205–227.

Berger, A., Loutre, M.F., 1991. Insolation values for the climate of the last 10 million years. Quaternary Science Reviews 10, 297–317.

Berger, G.W., Anderson, P.M., 2000. Extending the geochronometry of arctic lake cores beyond the radiocarbon limit by using thermoluminescence. Journal Geophysical Research-Atmospheres 105, 15439–15455.

Bigelow, N.H., et al., 2003. Climate change and Arctic ecosystems: 1. Vegetation changes north of 55°N between the last glacial maximum, mid-Holocene, and present. Journal of Geophysical Research 108, 11-1–11-25.

Birks, H.J.B., 1998. Numerical tools in quantitative paleolimnology—progress, potentialities and problems. Journal of Paleolimnology 20, 301–332.

Brigham-Grette, J., Hopkins, D.M., 1995. Emergent marine record and paleoclimate of the Last Interglaciation along the northwest Alaskan coast. Quaternary Research 43, 159–269.

Broecker, W.S., Van Donk, J., 1970. Insolation changes, ice volumes, and the O18 record in deep-sea cores. Reviews of Geophysics and Space Physics 8, 169–198.

Brubaker, L.B., Anderson, P.M., Oswald, W.W., 1996. A new pollen record from Ahaliorak Lake, North Slope, Alaska. Third Annual PALE Abstracts Volume, Boulder, CO, pp. 54–57.

CAPE Project Members, 2001. Holocene paleoclimate data from the Arctic: testing models of global climate change. Quaternary Science Reviews 20, 1275–1287.

Caspers, G., 1997. Die eem- und weichselzeitliche Hohlform von Gross Todtshorn (Kr. Harburg; Niedersachsen)—Geologische und palynologische Untersuchungen zu Vegetation und Klimaverlauf der letzten Kaltzeit. In: Freund, H., Caspers, G. (Eds.), Vegetation und Paläoklima der Weichsel-Kaltzeit im nördlichen Mitteleuropa—Ergebnisse paläobotanischer, -faunistischer und geologischer Untersuchungen. Schriftenreihe der Deutschen Geologischen Gesellschaft, pp. 7–59.

Chapin, F.S.I., et al., 2005. Role of land-surface changes in Arctic summer warming. Science 310, 657–660.

CLIMAP Project Members, 1984. The Last Interglacial ocean. Quaternary Research 21, 123–224.

Colinvaux, P.A., 1964. The environment of the Bering Land Bridge. Ecological Monographs 34, 297–329.

Cortijo, E., Lehman, S.J., Keigwin, L.D., Chapman, M., Paillard, D., Labeyrie, L., 1999. Changes in meridional temperature and salinity gradients in the North Atlantic Ocean (30 3 to 723N) during the Last Interglacial Period. Paleoceanography 14, 23–33.

Crucifix, M., Loutre, M.F., 2002. Transient simulations over the last interglacial period (126–115 ka BP): feedback and forcing analysis. Climate Dynamics 19, 417–433.

Cuffey, K.M., Marshall, S.J., 2000. Substantial contribution to sea-level rise during the last interglacial from the Greenland ice sheet. Nature 404, 591–594.

Cuffey, K.M., et al., 1995. Large Arctic temperature change at the Wisconsin-Holocene glacial transition. Science 270, 455–458.

Dahl-Jensen, D., et al., 1998. Past temperatures directly from the Greenland ice sheet. Science 282, 268–271.

Devyatova, E.I., 1982. Prirodnaya sreda pozdnego pleistotcena i yeyo vliyanie na razvitie cheloveka v Severodvinskom basseine i v Karelii. (Late Pleistocene environments as related to human migrations in the Severnaya Dvina basin and in Karelia). Petrozavodsk, Karelia 156pp. (in Russian).

Dredge, L.A., Morgan, A.V., Nielsen, E., 1990. Sangamon and pre-Sangamon interglaciations in the Hudson Bay Lowlands of Manitoba. Geographie Physique et Quaternaire 44, 319–336.

Edwards, M.E., McDowell, P.F., 1991. Interglacial deposits at Birch Creek, northeast interior Alaska. Quaternary Research 35, 41–52.

Edwards, M.E., Hamilton, T.D., Elias, S.A., Bigelow, N.H., Krumhardt, A.P., 2003. Interglacial extension of the boreal forest limit in the Noatak Valley, northwest Alaska: Evidence from an exhumed river-cut bluff and debris apron. Arctic Antarctic Alpine Research 35, 460–468.

Eisner, W.R., Colinvaux, P.A., 1990. A long pollen record from Ahaliorak Lake, arctic Alaska. Review of Palaeobotany and Palynology 63, 35–52.

Emiliani, C., 1955. Pleistocene temperatures. Journal of Geology 63, 538–578.

EPICA Community Members, 2004. Eight glacial cycles from an Antarctic ice core. Nature 429, 623–628.

Evans, D.J.A., Mott, R.J., 1993. Stratigraphy and paleoecology of a possible interglacial site, northernmost Ellesmere Island, Canada. Journal of Quaternary Science 8, 251–262.

Francis, D.R., Wolfe, A.P., Walker, I.R., Miller, G.H., 2006. Interglacial and Holocene temperature reconstructions based on midge remains in sediments of two lakes from Baffin Island, Nunavut, Arctic Canada. Palaeogeography, Palaeoclimatology, Palaeoecology, in press.

Fréchette, B., Wolfe, A.P., Miller, G.H., Richard, P.J.H., deVernal, A., 2006. Vegetation and climate of the Last Interglacial on Baffin Island, Arctic Canada. Palaeogeography, Palaeoclimatology, Palaeoecology, in press.

Frenzel, B., Bludau, W., 1987. On the duration of the interglacial to glacial transition at the end of the Eemian Interglacial (deep sea stage 5e): botanical and sedimentological evidence. In: Berger, W.H., Labeyrie, L.D. (Eds.), Abrupt Climate Change. Reidel, Doordrecht, pp. 151–162.

Fronval, T., Jansen, E., et al., 1998. Variability in surface and deep water conditions in the Nordic Seas during the Last Interglacial period. Quaternary Science Reviews 17, 963–985.

Funder, S. (Ed.), 1990. Late Quaternary stratigraphy and glaciology in the Thule area, Northwest Greenland, Meddelelser om Grønland—Geoscience 22, 1–63.

Funder, S., Hjort, C., Landvik, J.Y., Nam, S.I., Reeh, N., Stein, R., 1998. History of a stable ice margin—East Greenland during the Middle and Upper Pleistocene. Quaternary Science Reviews 17, 77–125.

Funder, S., Demidov, I., Yelovicheva, Y., 2002. Hydrography and mollusc faunas of the Baltic and the White Sea-North Sea seaway in the Eemian. Palaeogeography, Palaeoclimatology, Palaeoecology 184, 275–304.

Gallup, C.D., Cheng, H., Taylor, F.W., Edwards, R.L., 2002. Direct determination of the timing of sea level change during Termination II. Science 295, 310–313.

Gard, G., Backman, J., 1990. Synthesis of Arctic and Subarctic Coccolith Biochronology and History of North Atlantic Drift Water Influx during the last 500,000 Years. In: Bleil, U., Thiede, J. (Eds.), Geological History of the Polar Oceans: Arctic versus Antarctic. NATO ASI Series C. Kluwer Academic Publishers, Dordrecht, pp. 417–436.

Grichuk, V.P., 1984. Late Pleistocene vegetation history. In: Velichko, A.A. (Ed.), Late Quaternary Environments of the Soviet Union. University of Minnesota Press, Minneapolis, pp. 155–178.

Grøsfjeld, K., Funder, S., Seidenkrantz, M.-S., Glaister; C., 2006. Last Interglacial marine environments in the White Sea region, northern Russia. Boreas, in press.

Gudina, V.I., Kryukov, V.D., Levchuk, L.K., Sudkov, L.A., 1983. Upper-Pleistocene sediments in north-eastern Taimyr. Bulletin of Commission on Quaternary Researches 52, 90–97 (in Russian).

Guetter, P.J., Kutzbach, J.E., 1986. The influence of changing orbital parameters and surface boundary conditions on climate simulations for the past 18,000 years. Journal Atmospheric Sciences 43, 1726–1759.

Guiter, F., et al., 2003. The last climatic cycles in Western Europe: a comparison between long continuous lacustrine sequences from France and other terrestrial records. Quaternary International 111, 59–74.

Haflidason, H., Eiriksson, J., Van Kreveld, S., 2000. The tephrochronology of Iceland and the North Atlantic region during the Middle and Late Quaternary: a review. Journal of Quaternary Science 15, 3–22.

Hahne, J., Kemle, S., Merkt, J., Meyer, K.-D., 1994. Eem-, weichsel- und saalezeitliche Ablagerungen der Bohrung "Quakenbrück GE 2". Geologisches Jahrbuch A 134, 9–69.

Hall, I.R., McCave, I.N., Chapman, M.R., Shackleton, N.J., 1998. Coherent deep flow variation in the Iceland and American basins during the Last Interglacial. Earth and Planetary Science Letters 164, 15–21.

Hamilton, T.D., Brigham-Grette, J., 1991. The Last Interglaciation in Alaska: stratigraphy and paleoecology of potential sites. Quaternary International 10–12, 49–71.

Harting, P., 1875. Le système Éemien. Archives Néerlandaises Sciences Exactes et Naturelles de la Societé Hollandaise des Sciences (Harlem) 10, 443–454.

Henderson, G.M., Slowey, N.C., 2000. Evidence from U-Th dating against northern hemisphere forcing of the penultimate deglaciation. Nature 404, 61–66.

Hillaire-Marcel, C., de Vernal, A., Bilodeau, G., Weaver, A.J., 2001. Absence of deep-water formation in the Labrador Sea during the last interglacial period. Nature 410, 1073–1077.

Holland, M.M., Bitz, C.M., 2003. Polar amplification of climate change in coupled models. Climate Dynamics 21, 221–232.

Jakobsson, M., Backman, J., Murray, A., Løvlie, R., 2003. Optically stimulated luminescence dating supports central Arctic Ocean cm-scale sedimentation rates. Geochemistry Geophysics Geosystems 4, 1–11.

Jessen, K., Milthers, V., 1928. Interglacial fresh-water deposits in Jutland and Northwest Germany., 48. Danmarks Geologiske Undersøgelse II, 379pp.

Johnsen, S.J., Dansgaard, W., Clausen, H.B., Langway, C.C.J., 1972. Oxygen isotope profiles through the Antarctic and Greenland ice sheets. Nature 235, 429–434.

Johnsen, S.J., Dahl-Jensen, D., Gundestrup, N., Steffensen, J.-P., Clausen, H.B., Miller, H., Masson-Delmotte, V., Sveinbjornsdottir, A.E., White, J., 2001. Oxygen isotope and palaeotemperature records from six Greenland ice-core stations: Camp Century, Dye-3, GRIP, GISP2, Renland and NorthGRIP. Journal of Quaternary Science 16, 299–307.

Kandiano, E.S., Bauch, H.A., Müller, A., 2004. Sea surface temperature variability in the North Atlantic during the last two glacial-interglacial cycles: comparison of faunal, oxygen isotopic, and Mg/Ca-derived records. Palaeogeography, Palaeoclimatology, Palaeoecology 204, 145–164.

Kaplan, J.O., et al., 2003. Climate change and arctic ecosystems II: Modeling, paleodata-model comparisons, and future projections. Journal of Geophysical Research 108, 12-1–12-17.

Kaspar, F., Kühl, N., Cubasch, U., Litt, T., 2005. A model-data-comparison of European temperatures in the Eemian interglacial. Geophysical Research Letters 32 (11), L11703.

Kaufman, D.S., et al., 2004. Holocene thermal maximum in the western Arctic (0–180°W). Quaternary Science Reviews 23, 529–560.

Kellogg, T.B., 1980. Paleoclimatology and paleoceanography of the Norwegian and Greenland Seas: glacial–interglacial contrasts. Boreas 9, 115–137.

Kelly, M., Funder, S., Houmark-Nielsen, M., Knudsen, K.L., Kronborg, C., Landvik, J., Sorby, L., 1999. Quaternary glacial and marine environmental history of northwest Greenland: a review and reappraisal. Quaternary Science Reviews 18, 373–392.

Khim, B.-K., Krantz, D.E., Brigham-Grette, J., 2001. Stable isotope profiles of Last Interglacial (Pelukian Transgression) mollusks and paleoclimate implications in the Bering Strait Region. Quaternary Science Reviews 20, 463–483.

Knies, J., Vogt, C., 2003. Freshwater pulses in the eastern Arctic Ocean during Saalian and Early Weichselian ice-sheet collapse. Quaternary Research 60, 243–251.

Koerner, R.M., 1989. Ice core evidence for extensive melting of the Greenland Ice Sheet during the last interglacial. Science 244, 964–968.

Koerner, R.M., 2006. Mass Balance of glaciers in the Queen Elizabeth Islands, Nunavut, Canada. Annals Glaciology, in press.

Koerner, R.M., Fisher, D.A., 2002. Ice-core evidence for widespread Arctic glacier retreat in the Last Interglacial and the early Holocene. Annals Glaciology 35, 19–24.

Kühl, N., Litt, T., 2003. Quantitative time series reconstruction of Eemian temperature at three European sites using pollen data. Archaeobotany 12, 205–214.

Lauritzen, S.-E., Anderson, P.M., 1995. The Last Interglaciation in Arctic and Subarctic regions: time frame, structure, and duration. Quaternary Research 43, 115–116.

Lehman, S.J., Sachs, J.P., Crotwell, A.M., Keigwin, L.D., Boyle, E.A., 2002. Relation of subtropical Atlantic temperature, high-latitude ice rafting, deep water formation, and European climate 130,000-60,000 years ago. Quaternary Science Reviews 21, 1917–1924.

Lozhkin, A.V., Anderson, P.M., 1995. The last interglaciation of northeast Siberia. Quaternary Research 43, 147–158.

Lozkhin, A.V., Anderson, P.M., Matrosova, T.V., Minyuk, P., 2006. The pollen record from El'gygytgyn Lake: implications for vegetation and climate histories of northern Chukotka since the late middle Pleistocene. Journal Paleolimnology, in press.

Mangerud, J., Svendsen, J.I., 1992. The last interglacial-glacial period on Spitsbergen, Svalbard. Quaternary Science Reviews 11, 633–664.

Mangerud, J., Sønstegaard, E., Sejrup, H.P., 1979. Correlation of the Eemian (interglacial) Stage and the deep-sea oxygen-isotope stratigraphy. Nature 277, 189–192.

Mangerud, J., Sonstegaard, E., Sejrup, H.P., Haldorsen, S., 1981. A continuous Eemian-Early Weichselian sequence containing pollen and marine fossils at Fjosanger, western Norway. Boreas 10, 137–208.

Mangerud, J., Dokken, T., Hebbeln, D., Heggen, B., Ingolfsson, O., Landvik, J.Y., Mejdahl, V., Svendsen, J.I., Vorren, T.O., 1998. Fluctuations of the Svalbard-Barents Sea Ice Sheet during the last 150,000 years. Quaternary Science Reviews 17, 11–42.

Matthews, J.V., Mott, R.J., Vincent, J.-S., 1986. Preglacial and interglacial environments of Banks Island: Pollen and macrofossils from Duck Hawk bluffs and related sites. Geographie Physique et Quaternaire 40, 279–288.

Matthews, J.V.J., Schweger, C.E., Janssens, J., 1990. The last (Koy-Yukon) interglaciation in the northern Yukon: evidence from unit 4 at Chijee's Bluff, Bluefish Basin. Geographie Physique et Quaternaire 44, 341–362.

Matthiessen, J., Knies, J., 2001. Dinoflagellate cyst evidence for warm interglacial conditions at the northern Barents Sea margin, during marine isotope stage 5. Journal of Quaternary Science 16, 727–737.

Matthiessen, J., Baumann, K.-H., Schroeder-Ritzrau, A., Hass, C., Andruleit, H., Baumann, A., Jensen, S., Kohly, A., Pflauman, U., Samtleben, C., Schafer, P., Thiede, J., 2001a. Distribution of calcareous, siliceous and organic-walled planktic microfossils in surface sediments of the Nordic seas and their relation to surface-water masses. In: Schafer, P., Ritzrau, P., Schluter, M., Thiede, J. (Eds.), The Northern North Atlantic: A Changing Environment. Springer, Berlin, pp. 105–127.

Matthiessen, J., Knies, J., Nowaczyk, N., Stein, R., 2001b. Late Quaternary dinoflagellate cyst stratigraphy along the Eurasian Continental Margin (Arctic Ocean): Indications of Atlantic water inflow in the last 150,000 years. Global and Planetary Change 31, 65–86.

McCulloch, M.T., Esat, T., 2000. The coral record of last interglacial sea levels and sea surface temperatures. Chemical Geology 169, 107–129.

McManus, J.F., Oppo, D.W., Keigwin, L.D., Cullen, J.L., Bond, G.C., 2002. Thermohaline circulation and prolonged interglacial warmth in the North Atlantic. Quaternary Research 58, 17–21.

Miller, G.H., 1985. Aminostratigraphy of Baffin Island shell-bearing deposits. In: Andrews, J.T. (Ed.), Quaternary Environments: Baffin Island, Baffin Bay, and West Greenland. Allen & Unwin, Winchester, MA, pp. 394–427.

Miller, G.H., Sejrup, H.P., Lehman, S.J., Forman, S.L., 1989. Glacial history and marine environmental change during the last interglacial-glacial cycle, western Spitsbergen, Svalbard. Boreas 18, 273–296.

Miller, G.H., Mode, W.N., Wolfe, A.P., Sauer, P.E., Bennike, O., Forman, S.L., Short, S.K., Stafford Jr., T.W., 1999. Stratified interglacial lacustrine sediments from Baffin Island, Arctic Canada: Chronology and paleoenvironmental implications. Quaternary Science Reviews 18, 789–810.

Morgan, A.V., Kuc, M., Andrews, J.T., 1993. Paleoecology and age of the Flitaway and Isortoq interglacial deposits, northcentral Baffin Island, Northwest Territories, Canada. Canadian Journal Earth Sciences 30, 954–974.

Morozova, T.D., Velichko, A.A., Dlussky, K.G., 1998. Organic carbon content in the late Pleistocene and Holocene fossil soils (reconstruction for Eastern Europe). Global and Planetary Change 16–17, 131–151.

Mott, R.J., Dilabio, N.W., 1990. Paleoecology of organic deposits of probable last interglacial age in northern Ontario. Geographie Physique et Quaternaire 44, 309–318.

Muhs, D.R., Ager, T.A., Beget, J.E., 2001. Vegetation and paleoclimate of the last interglacial period, central Alaska. Quaternary Science Reviews 20, 41–61.

Muhs, D.R., Simmons, K.R., Steinke, B., 2002. Timing and warmth of the last interglacial period: new U-series evidence from Hawaii and Bermuda and a new fossil compilation for North America. Quaternary Science Reviews 21, 1355–1383.

Müller, H., 1974. Pollenanalytische Untersuchungen und Jahresschichtenzählungen an der eemzeitlichen Kieselgur von Bispingen/Luhe. Geologisches Jahrbuch A 21, 149–169.

Murray, A.S., Funder, S., 2003. Optically stimulated luminescence dating of a Danish Eemian coastal marine deposit: a test of accuracy. Quaternary Science Reviews 22, 1177–1183.

Nielsen, E., et al., 1986. Stratigraphy, paleoecology, and glacial history of the Gillam area, Manitoba. Canadian Journal Earth Sciences 23, 1641–1666.

North Greenland Ice Core, Project members, 2004. High-resolution record of Northern Hemisphere climate extending into the last interglacial period. Nature 431, 147–151.

Otto-Bliesner, B.L., et al., 2006. Simulating Warm-Arctic Climate and Ice Sheet Sensitivity for the Last Interglaciation. Science, in press.

Overpeck, J., et al., 1997. Arctic environmental change of the last four centuries. Science 278, 1251–1256.

Overpeck, J.T., et al., 2006. Paleoclimatic Evidence for Future Ice Sheet Instability and Rapid Sea Level Rise. Science, in press.

Petit, J.R., et al., 1999. Climate and atmospheric history of the 420,000 years from the Vostok ice core, Antarctica. Nature 399, 429–436.

Péwé, T.L., Berger, G.W., Westgate, J.A., Brown, P.M., Leavitt, S.W., 1997. Eva Interglaciation Forest Bed, Unglaciated East-Central Alaska: Global Warming 125,000 Years Ago. Geological Society of America Special Paper 319.

Rampton, V., 1988. Quaternary geology of the Tuktoyaktuk coastlands, Northwest Territories. Geological Survey of Canada Memoir 423, 1–98.

Rasmussen, T.L., Oppo, D.W., Thomsen, E., S.J., L., 2003a. Deep sea records from the southeast Labrador Sea: Ocean circulation changes and ice-rafting events during the last 160,000 years. Paleoceanography, 18: doi:10.1029/2001PA000736.

Rasmussen, T.L., Wastegård, S., Kuijpers, A., van Weering, T.C.E., Heinemeier, J., Thomsen, E., 2003b. Stratigraphy and distribution of tephra layers in marine sediment cores from the Faeroe Islands, North Atlantic. Marine Geology 188, 165–192.

Raukas, A., 1991. Eemian Interglacial record in the Northwestern European part of the Soviet Union. Quaternary International 10–12, 183–189.

Raynaud, D., Chappellaz, J., Ritz, C., Martinerie, P., 1997. Air content along the Greenland Ice Core Project core: a record of surface climatic parameters and elevation in central Greenland. Journal Geophysical Research 102, 26607–26614.

Saarnisto, M., Eriksson, B., Hirvas, H., 1999. Tepsankumpu revisited—pollen evidence of stable Eemian climates in Finnish Lapland. Boreas 28, 12–22.

Seidenkrantz, M.S., Knudsen, K.L., Kristensen, P., 2000. Marine late Saalian to Eemian environments and climatic variability in the Danish shelf area. Netherlands Journal of Geosciences 79, 335–343.

Sejrup, H.P., Haflidason, H., Kristensen, D., Johnsen, S., 1995. Last interglacial and Holocene climatic development in the Norwegian Sea region: Oceanic front movements and ice core data. Journal of Quaternary Science 10, 385–390.

Sejrup, H.P., Birks, H.J.B., Klitgaard Kristensen, D., Madsen, H., 2004. Benthonic foraminiferal distributions and quantitative transfer functions for the northwest European continental margin. Marine Micropaleontology 53, 197–226.

Serreze, M.C., Francis, J.A., 2006. The arctic amplification debate. Climatic Change, in press.

Serreze, M.C., et al., 2000. Observational evidence of recent change in the northern high-latitude environment. Climatic Change 46, 159–207.

Shackleton, J., 1982. Environmental histories from Whitefish and Imuruk Lakes, Seward Peninsula, Alaska. Institute of Polar Studies Report No. 76, Ohio State University, Columbus, Ohio.

Shackleton, N.J., 1969. The last interglacial in the marine and terrestrial records. Proceedings of the Royal Society of London 174, 135–154.

Shackleton, N.J., Chapman, M., Sánchez-Goni, M.F., Pailler, D., Lancelot, Y., 2002. The classic marine isotope substage 5e. Quaternary Research 58, 14–16.

Sjoholm, J., Sejrup, H.P., Furnes, H., 1991. Quaternary volcanic ash zones on the Iceland Plateau, southern Norwegian Sea. Journal Quaternary Science 6, 159–173.

Spielhagen, R.F., et al., 2004. Arctic Ocean deep-sea record of northern Eurasian ice sheet history. Quaternary Science Reviews 23, 1455–1483.

Stirling, C.H., Esat, T.M., Lambeck, K., McCulloch, M.T., 1998. Timing and duration of the Last Interglacial: Evidence for a restricted interval of widespread coral reef growth. Earth and Planetary Science Letters 160, 745–762.

Svendsen, J.I., et al., 2004. Late Quaternary ice sheet history of Northern Eurasia. Quaternary Science Reviews 23, 1229–1271.

ter Braak, C.J.F., Juggins, S., 1993. Weighted averaging partial least squared regression (WA-PLS): an improved method for reconstructing environmental variables from species assemblages. Hydrobiologica 268, 485–502.

Troitsky, S.L., 1964. Osnoviye zakonomernosti izmeneniya sostava fauny po razrezam morskikh meshmorennykh sloev ust-eniseyskoy vpadiny i nishne-pechorskoy depressii. Akademia NAUK SSSR, Trudy instituta geologii i geofiziki 9, 48–65 (in Russian).

Turner, C., 2000. The Eemian interglacial in the North European Plain and adjacent areas. Netherlands Journal of Geosciences 79, 217–231.

Vavrus, S., Harrison, S.P., 2003. The impact of sea ice dynamics on the Arctic climate system. Climate Dynamics 20, 741–757.

Velichko, A.A., Borisova, O.K., Y.Y., G., Zelikson, E.M., 1991. Climate rhythm of the last interglacial in northern Eurasia. Quaternary International 10–12, 191–213.

Velichko, A.A., et al., 1998. Estimates of methane emission during the last 125,000 years in Northern Eurasia. Global and Planetary Change 16–17, 159–180.

Watanabe, O., et al., 2003. Homogeneous climate variability across East Antarctica over the past three glacial cycles. Nature 422, 509–512.

Wollenburg, J., Kuhnt, W., Mackensen, A., 2001. Changes in Arctic Ocean paleoproductivity and hydrography during the last 145 ka: the benthic foraminiferal record. Paleoceanography 16, 65–77.

Wyatt, P.H., 1990. Amino acid evidence indicating two or more ages of pre-Holocene nonglacial deposits in Hudson Bay Lowland, northern Ontario. Geographie Physique et Quaternaire 44, 389–393.

Zagwijn, W.H., 1996. An analysis of Eemian climate in western and central Europe. Quaternary Science Reviews 15, 451–469.

Zelikson, E.M., Kremenetski, C.V., Borisova, O.K., Velichko, A.A., 1998. Phytomass and carbon storage during the Eemian optimum, late Weichselian maximum and Holocene optimum in Eastern Europe. Global and Planetary Change 16–17, 181–195.